Potential Cosmetic and Therapeutic Applications of North East Origin Silk Sericin

A Thesis

Submitted in Partial Fulfillment of the Requirements for the Degree of

DOCTOR OF PHILOSOPHY

by

JADI PRAVEEN KUMAR

Department of Biosciences and Bioengineering
Indian Institute of Technology Guwahati
Guwahati-781039, Assam, India

February 2019

Potential Cosmetic and Therapeutic Applications of North East Origin Silk Sericin

A Thesis

Submitted in Partial Fulfillment of the Requirements for the Degree of

DOCTOR OF PHILOSOPHY

by

JADI PRAVEEN KUMAR

Department of Biosciences and Bioengineering
Indian Institute of Technology Guwahati
Guwahati-781039, Assam, India

February 2019

Dedicated to my Family and Friends

INDIAN INSTITUTE OF TECHNOLOGY GUWAHATI

DEPARTMENT OF BIOSCIENCES AND BIOENGINEERING

STATEMENT

I do hereby declare that the research findings of this thesis is the result of research work carried out by me in the Department of Biosciences and Bioengineering, Indian Institute of Technology Guwahati, Guwahati, India, under the supervision of Dr. Biman B. Mandal.

As per the general norms of reporting research findings, due acknowledgments have been made, wherever the research findings of other researchers have been cited in this thesis.

Date: **Jadi Praveen Kumar**

INDIAN INSTITUTE OF TECHNOLOGY GUWAHATI

DEPARTMENT OF BIOSCIENCES AND BIOENGINEERING

CERTIFICATE

It is certified that the work described in this thesis entitled " **Potential Cosmetic and Therapeutic Applications of North East Origin Silk Sericin**" by **Mr. Jadi Praveen Kumar** for the award of degree of Doctor of Philosophy is an authentic record of the results obtained from the research work carried out under my supervision in the Department of Biosciences and Bioengineering, Indian Institute of Technology Guwahati, India, and this work has not been submitted elsewhere for the award of any other degree.

CERTIFIED

Jadi Praveen Kumar
(Candidate)
Roll No: 126106004

Biman B. Mandal, Ph.D.
(Thesis Supervisor)
Date:

ACKNOWLEDGEMENT

Firstly, I would like to express my sincere gratitude and appreciation to my Ph.D. supervisor Dr. Biman B. Mandal for his continuous support and encouragement throughout my Ph.D. study. His guidance helped me in conducting all my research work and writing of this thesis. I could not have imagined having a better mentor and supervisor for my Ph.D. study.

In addition to my mentor, I would like to thank my Doctoral committee members Dr. Senthilkumar Sivaprakasam (Chairman), Dr. Manish Kumar, and Professor Kanagaraj, for their great support, valuable suggestion and encouragement for shaping my thesis work. They are also acknowledged for their insightful questions and comments that incented me to widen my research work from different perspectives. I would also like to thank Dr. Piruthivi Sukumar, former Doctoral committee member for his support and encouragement.

I would like to acknowledge Dr. Kausar Mahmood Ansari, CSIR-Indian Institute of Toxicology Research, Lucknow for providing us with animal house facility. I would like to thank Dr. Shamshad Alam and Abhishek Kumar Jain for helping in animal studies.

I would also like to acknowledge Dr. Nandana Bhardwaj, National Institute of Pharmaceutical Education and Research (NIPER), Guwahati for helping in material characterization and providing me valuable inputs to improve my manuscripts throughout this dissertation.

I would like to acknowledge Professor Latha Rangan, Head of the Department of Biosciences and Bioengineering (BSBE), IIT Guwahati and former Head of the Department Professor K. Pakshirajan, Professor V. V. Dasu, and Professor Arun Goyal for providing me the necessary facilities, which helped me to perform my research work at IIT Guwahati.

I am also grateful to all faculty members and staff of Department of BSBE for supporting me throughout my Ph.D. tenure. I would like to acknowledge Department of BSBE for providing the infrastructural facility for my research work. I would also like to acknowledge Central Instrumentation Facility (CIF), IIT Guwahati for providing equipment to execute my experiments.

I am grateful to the Department of Science and Technology (DST) and Department of Biotechnology (DBT), Government of India for supporting my research. I am also grateful

to Ministry of Human Resource Development (MHRD), SCSP and TSP Grant and IIT Guwahati for providing research fellowship.

It is my pleasure to thank my current lab members Dr. Manishekhar, Dimple, Bibhas, Ankit, Shreya, Prerak, Yogendra, Janani, Joseph, Sohenii, Ashutosh, Survo, Triya, Souradeep, Dr. Rajiv, and Dr. Aparajita, for their feedback, co-operation, and stimulating discussion. I am also thankful to my former lab members Salma, Tarishi, Namit, Dr. Rocktotpal, Dr. Biswajeet, Dr. Deepika, Prerna, Garima, Ranjana, Deepak, Smriti, Surodeep, Sween, Korah, and Sonu for their support during my Ph.D. work.

I would like to extend my sincere gratitude to Professor V. V. Dasu, Department of BSBE, IIT Guwahati for the scientific collaborations.

I wish to acknowledge my friends, Sandipan, Dr. Ziauddin, Srikanth, and Bheem for having enriched me as a person. I would like to thank all the individuals who supported me throughout and contributed significantly to the outcome of this dissertation, their time and effort are greatly appreciated.

Last but not least; I would like to thank my family: my grandparents, parents, my brother, and sister, and Jayalakshmi, my wife and daughter for supporting me spiritually throughout this journey and my life in general. Thanks to the Lord, the Almighty for showering his grace to complete the research work successfully.

Jadi Praveen Kumar

CONTENTS

ABBREVIATIONS

UV	Ultraviolet
UVR	Ultraviolet radiation
UVRs	Ultraviolet radiations
RS	Reactive species
ROS	Reactive oxygen species
RNS	Reactive nitrogen species
AO	Antioxidant
AOs	Antioxidants
SOD	Superoxide dismutase
CAT	Catalase
GPX	Glutathione peroxidase
LMWMs	Low molecular weight molecules
Vit. C	Vitamin C
Vit. E	Vitamin E
Vit. A	Vitamin A
CoQ10	Coenzyme Q10
SS	Silk sericin
BM	*Bombyx mori*
BMS	*Bombyx mori* sericin
AM	*Antheraea mylitta*
UVA	Ultraviolet A
UVB	Ultraviolet B
UVC	Ultraviolet C
TEWL	Trans-epidermal water loss
NMF	Natural moisturizing factors
AA	*Antheraea assamensis*
AAS	*Antheraea assamensis* sericin
PR	*Philosamia ricini*
PRS	*Philosamia ricini* sericin
6-4PP	pyrimidine-(6-4)-pyrimidone photoproducts
CPD	cyclobutane pyrimidine dimers
IL-1	Interleukin-1

Abbreviations

IL-6	Interleukin-6
IL-8	Interleukin-8
TNF-α	Tumor necrosis factor-α
COX-2	Cyclooxygenase-2
PGE2	Prostaglandin E2
DOPA	3, 4-dihydroxyphenylalanine
TRP-1	Tyrosinase-related protein-1
TRP-2	Tyrosinase-related protein-2
NF-κB	Nuclear factor-kappa B
AP-1	Activator protein-1
MMP	Matrix metalloproteinase
MMPs	Matrix metalloproteinases
ECM	Extracellular matrix
NMSC	Non-melanoma skin cancer
8-oxodG	8-oxo-deoxyguanine
C	Cytosine
T	Thymine
CpG	5'-Cytosine-phosphate-Guanosine-3'
DNA	Deoxyribonucleic acid
miRNA	Micro-ribonucleic acid
MED	Minimal erythema dose
GSH	Glutathione
GSSG	Glutathione disulfide
GST	Glutathione S-transferase
GSR	Glutathione-disulfide reductase
MnSOD	Manganese superoxide dismutase
CuZnSOD	Copper Zinc Superoxide dismutase
HO	Heme oxygenase
ODC	Ornithine decarboxylase
ALP	Anti-lipid peroxidation
DPPH	2, 2-diphenyl-1-picrylhydrazyl
L929 cells	Mouse fibroblast cells
DMSO	Dimethyl sulfoxide
SDS	Sodium dodecyl sulfate
TCA	Trichloroacetic acid

TPTZ	2, 4, 6-Tris (2-pyridyl)-s-triazine
DCFH-DA	Dichloro-dihydro-fluorescein diacetate
PMSF	Phenylmethylsulfonyl fluoride
TBA	Thiobarbituric acid
LDH	Lactate dehydrogenase
M	Molar
mL	Milliliter
°C	Degree celsius
min	Minute
MWCO	Molecular weight cutoff
kDa	Kilodaltons
h	hours
g	Earth's gravitational force
L	Liter
µL	Microliter
%	Percentage
mJ	Millijoule
J	Joule
cm	Centimeter
s	seconds
µm	Micrometer
nm	Nanometer
θ	Molar ellipticity
mg	Milligram
ddH_2O	Double distilled water
GAE	Gallic acid equivalents
CE	(+)-catechin equivalents
FRAP	Ferric ion reducing antioxidant power
NCCS	National Centre for Cell Science
FBS	Fetal bovine serum
DMEM	Dulbecco's modified Eagle's medium
mM	Millimolar
µg	Microgram
PBS	Phosphate buffer saline
µM	Micromolar

nmol	Nanomoles
rpm	Revolutions per minute
kHz	Kilohertz
W/cm	Watt per centimeter
SDS-PAGE	Sodium dodecyl sulfate-polyacrylamide gel electrophoresis
FTIR	Fourier transform infrared spectroscopy
CD spectroscopy	Circular dichroism spectroscopy
MTT	Thiazolyl blue tetrazolium bromide or 3-(4,5-dimethylthiazol-2-yl)-2,5 diphenyl tetrazolium bromide
MDA	Malondialdehyde
H_2O_2	Hydrogen peroxide
MCF-7 cells	Human breast cancer cells
SAS cells	Human oral cancer cells
A431 cells	Human squamous cancer cells
cyt *c*	Cytochrome *c*
EGF	Epidermal growth factor
RNase A	Ribonuclease A
PI	Propidium iodide
NP-40	nonidet P-40
Annexin V-FITC	Annexin V- Fluorescein isothiocyanate
MCF-10 cells	Non-tumorigenic epithelial cells
HaCaT cells	Human epidermal cells
FACS	Fluorescence-activated cell sorting
DCF	Dichlorofluorescein
DTT	Dithiothreitol
WST-1	water-soluble tetrazolium salt-1
cDNA	Complementary DNA
RT-PCR	Real-time polymerase chain reaction
RIPA buffer	Radio immune precipitation assay buffer
PVDF	Polyvinylidene fluoride or polyvinylidene difluoride
TBST	Tris-buffered saline-Tween
GAPDH	Glyceraldehyde 3-phosphate dehydrogenase
IgG	Immunoglobulin G
ECL	enhanced chemiluminescence
ANOVA	One-way analysis of variance

JNKs	cJun-terminal kinases
w/v	Weight/volume
~	Approximately
MES	4-Morpholine ethane sulfonic acid
EDTA	Ethylenediaminetetraacetic acid
OTM	Olive tail moment
H & E	Haemotoxylin and Eosin
NAC	N-acetylcysteine
HDF	Human dermal fibroblast
Col1α1	Collagen1alpha1
Col1α2	Collagen1alpha2
EGCG	Epigallocatechin gallate
FALGPA	N-[3-(2-furyl) acryloyl]-Leu-Gly-Pro-Ala
OA	Oleanolic acid
BSA	Bovine serum albumin
HA	Hyaluronic acid
U	Units
RH	Relative humidity
KA	Kojic acid
B16F10 cells	Mouse melanoma
SCN	5-S-cysteinyldopa
DHI	5, 6-dihydroxyindole
NADPH	Nicotinamide adenine dinucleotide phosphate
CD36	Cluster of differentiation 36
SR-B1	Scavenger receptor class B member 1
gm	Gram
SIRT1	silent information regulator 1

LIST OF TABLES

CHAPTER 7

LIST OF FIGURES

Chapter 1

Introduction and Literature Review

Introduction and Literature Review

1.1. Introduction

Skin is the largest organ, which covers the entire body with ~1.5 to 2 m^2 surface area and confers protection against physical, chemical, and biological assaults (Kanitakis, 2002; Kolarsick et al., 2011). It also prevents water loss from the body, synthesizes vitamin D, and plays a critical role in thermoregulation (Kolarsick et al., 2011; McLafferty et al., 2012). Skin is constantly exposed to pollutants, ultraviolet radiations (UVRs), chemicals, cigarette smoke, and microbes. Among all these factors, UVRs play an important role in maintaining human health as well as damaging it. Exposure of skin to UVRs triggers the vitamin D synthesis, which is essential for human health (Nair and Maseeh, 2012). However, chronic exposure of skin to ultraviolet radiation (UVR)-induced DNA photoproducts formation and damages the epidermal cells (Verschooten et al., 2006). UVRs also elevates the production of reactive species (RS) [reactive nitrogen species (RNS) and reactive oxygen species (ROS)] in the epidermal and dermal layers of skin (Svobodová and Vostálová, 2010). Elevated levels of RS leads to redox imbalance in the skin and oxidizes the surrounding biomacromolecules; lipids, proteins, and nucleic acids. Oxidation of biomacromolecules causes an alteration in their functions, which leads to inflammation, immunosuppression, hyperpigmentation, moisture loss, aging, wrinkling, and skin cancer (Gil and Kim, 2000; Kulms et al., 2002; Rittié and Fisher, 2002). The thwart of RS is counterbalanced by the endogenous antioxidant (AO) defense system (Godic et al., 2014). Skin is enriched with both enzymatic [superoxide dismutase (SOD), catalase (CAT), and glutathione peroxidase (GPX)] and non-enzymatic [glutathione (GSH), α-tocopherol (vitamin E), and vitamin C (ascorbic acid)] endogenous antioxidants (AOs) (Godic et al., 2014; Svobodová and Vostálová, 2010). The enzymatic AOs convert the ionic RS into stable non-ionic RS (O_2^- to $H_2O_2 + O_2$) and further, they convert them to molecular oxygen and water molecules (H_2O_2 to $H_2O + O_2$). Whereas, non-enzymatic AOs present in the epidermal region of skin reduces the RS by donating their electrons or hydrogen. Non-enzymatic AOs also act as co-substrate for enzymatic AOs during scavenging the elevated levels of RS (Svobodová and Vostálová, 2010). Both enzymatic and non-enzymatic AOs protect the skin from pollutants, UVRs, and cigarette smoke-induced

skin damage by scavenging the elevated levels of RS. However, prolonged exposure of skin to UVRs depletes their levels and activity, which leads to the elevation and accumulation of RS in epidermal and dermal layers of skin (Scharffetter–Kochanek et al., 2000; Tyrrell, 1996). Elevated levels of RS oxidizes the biomacromolecules, which alters signaling pathways and causes mutations. These changes lead to severe skin damage. According to the world health organization (WHO), globally 132,000 people are diagnosed with melanoma skin cancer and 2-3 million people are diagnosed with non-melanoma skin cancer per year. Therefore, there is a need to protect the skin against all the environmental factors.

Low molecular weight molecules (LMWMs) (polyphenols, flavonoids, vitamins, carotenoids, alkaloids etc) produced by plants have the ability to donate their hydrogen or electrons to RS and reduce them (Dinkova-Kostova, 2008; Sharma et al., 2013). These compounds are stored in different parts of the plants; seeds, flowers, leaves, and bark. LMWMs (vitamin C and E, carotenoids, lycopene, and polyphenols) consumed/ supplemented through the diet are transported to the epidermal and dermal layers of skin and protects it from UVR and pollutants-induced oxidative damage (Fernández-García, 2014). However, prolonged exposure of skin to UVRs reduce their levels and activity. Therefore, scientists have extracted LMWMs from different parts of the plants and delivered them topically to protect the skin from the UVRs and pollutants-induced skin damage. Topical delivery of vitamin C (Vit. C) or vitamin E (Vit. E) showed protection against UVR-induced erythema, immunosuppression, photoaging, and photocarcinogenesis. Whereas, topical administration of vitamin A (Vit. A) protected the skin from photoaging. Topical applications of polyphenols (secondary metabolites of plants; green tea, grape seed, and pomegranate polyphenols) enhance endogenous AO activity and reduce inflammation, erythema, and immunosuppression. They also prevent photocarcinogenesis and photoaging. Idebenone an analog of Coenzyme Q10 (CoQ10) acts as an anti-wrinkling molecule. These LMWMs are used in several cosmetic products to improve skin appearance and prevent its damage (Allemann and Baumann, 2008; Chen et al., 2012; Farris, 2014; Stojiljković et al., 2014).

Many LMWMs used in cosmetics lack complete protection or causes skin damage, however, million dollars are spent annually on these products worldwide. For example, potential antioxidant like Vit. C, which is used in various skin care cosmetics become inactive by opening its lactone ring irreversibly and forms diketogulonic acid by exposing to UVRs and air. Whereas, Vit. E get depleted by exposing to UVRs and also

causes various cutaneous side effects, including contact dermatitis. Vit. A also gets deplete by exposing to UVRs. Skin care cream containing idebenone developed contact dermatitis (Allemann and Baumann, 2008; Chen et al., 2012; Farris, 2014; Stojiljković et al., 2014). Green tea polyphenols are used as an ingredient in several cosmetic preparations. However, they are sensitive to light-induced oxidation and have poor penetrating ability into the skin through stratum corneum. Lycopene penetration through stratum corneum is also questionable (Fang et al., 2006; Fernández-García, 2014; Montenegro, 2014). To overcome all these limitations, we have explored silk sericin (SS) as a potent antioxidant to protect the skin against oxidative damage, cancer, and UVR-induced photodamage, hyperpigmentation, photoaging, and wrinkling.

SS is a glycoprotein composed of 18 amino acids; among which, serine (31.99%), aspartic acid (15.74%), glycine (14.20%), and threonine (6%) are predominant (Vaithanomsat and Kitpreechavanich, 2008; Züge et al., 2017). It is produced in the lumen of Lepidoptera insects belonging to the Bombycidae and Saturniidae families. It helps in the cocoon formation and protects the pupa and fibroin from the UVRs, pollutants and microbes-induced damage (Dash et al., 2007; Kaur et al., 2013). SS extracted from the cocoons is known to possess AO activity along with other biomedical application such as anti-lipid peroxidation (ALP), anti-elastase, anti-tyrosinase, anti-coagulation, anti-tumor, and anti-microbial activity (Chlapanidas et al., 2013; Jena et al., 2018; Kaewkorn et al., 2012; Kato et al., 1998; Sarovart et al., 2003). SS extracted from the cocoons of *Antheraea mylitta* (AM) and *Bombyx mori* (BM) protected human keratinocytes and SKH-1 hairless mice from ultraviolet B (UVB) radiation-induced oxidative damage, respectively (Dash et al., 2008; Zhaorigetu et al., 2003). SS extracted from the BM cocoons improved wound healing by enhancing cell attachment, proliferation, and collagen production (Ersel et al., 2016). Constitution of 30% serine makes the SS to hold a high amount of moisture (Nagura et al., 2001). SS extracted from the cocoons of BM are reported in various skin, hair, and nail care cosmetics by blending with other polymers (Padamwar and Pawar, 2004; Zhang, 2002). Sericin gels prepared with carbopol and pluronic prevent trans-epidermal water loss (TEWL) and restore natural moisturizing factor (NMF) of the skin. A mixture of sericin (5-30%) and silk fibroin (70–95%) powder show antistatic features and moisture absorbing ability (Kirikawa et al., 2000). Skin problems like dermatitis can be controlled by the hydrolysate solution of SS (Yasuda et al., 1998). Lotion containing 4% (w/w) D-glucose and 1% (w/w) SS shows moisturizing and conditioning effect (Yamada et al., 2001b).

Low molecular weight sericin hydrolysates are used as conditioners for hair and skin (Padamwar and Pawar, 2004). SS is a potent AO molecule, whose activity does not get alter after continues exposure to UVRs and it is also stable after heating sericin at high temperatures.

The properties of the SS is mainly depended on the amino acid composition and associated polyphenols and flavonoids (secondary metabolites). Hydroxyl groups of serine and threonine and electron donating groups of aromatic amino acids and secondary metabolites contribute to its biomedical applications by chelating trace elements like iron and copper and donating their electrons to free radicals (Fan et al., 2009; Kato et al., 1998). The amino acids composition of SS and associated secondary metabolites vary based on the silk varieties as well as the peptides generated during their extraction from the cocoons. Alteration in the amino acid and secondary metabolite composition determines the properties of SS; AO activity, suppression of tyrosinase and trypsin. (Aramwit et al., 2010a; Aramwit et al., 2010b; Kumar and Mandal, 2017; Kurioka et al., 2004). Despite all these properties, tons [50,000 tons out of 1 million fresh cocoons (Aramwit et al., 2012)] of SS is discarded as a by-product of the textile industry. Tapping such industrial waste into value-added bioresource would open a new portal in the skin care industry. Therefore exploring the antioxidant activity of SS extracted from the cocoons of different silk varieties (mulberry and non-mulberry) would be useful to identify a potent antioxidant that could protect skin from pollutants and UVR-induced damage.

Geographical pockets like North-Eastern region of India is enriched with different silk varieties; mulberry (BM) and non-mulberry [*A. assamensis* (AA; endemic to Assam, India) and *Philosamia ricini* (PR)]. Herein, this thesis presents the extraction of SS from the cocoons of mulberry and non-mulberry silk varieties using five different extraction methods. Extracted SS characterized for their molecular weight distribution, secondary structural confirmation, metal chelating and free radical reducing activity. Silk varieties, which showed free radical scavenging activity was taken further to assess their protective against H_2O_2 induced oxidative damage of mouse fibroblast (L929) cells.

SS extracted from three different silk varieties by alkali-degradation (showed protective activity against H_2O_2 induced oxidative damage) were used to assess for its anti-tumor activity using human breast carcinoma, squamous carcinoma, and oral carcinoma. Further, these silk varieties were assessed for their protective effect against UVA and UVB radiation-induced oxidative damage, photoaging, wrinkling and

hyperpigmentation along with anti-elastase, anti-collagenase, anti-hyaluronidase, and anti-tyrosinase activity.

Alkali-degraded AA sericin (AAS) showed better anti-tumor and protective effect against UVA and UVB radiation-induced skin damage than PR sericin (PRS) and BM sericin (BMS). It was used an ingredient in the skin care preparation and characterized its flow properties by rheological studies.

1.2. Literature Review

1.2.1. Skin anatomy

Skin is the largest organ of the body, which has diverse functions; protects the whole body from physical and biological assaults, maintains bodies temperature, synthesize vitamin D and prevents moisture loss (Kolarsick et al., 2011; Marzulli and Maibach, 1984; McLafferty et al., 2012). The anatomy of the skin shows that it is a complex, integrated and dynamic tissue composed of the epidermis, dermis, and hypodermis (**Fig.1.1**).

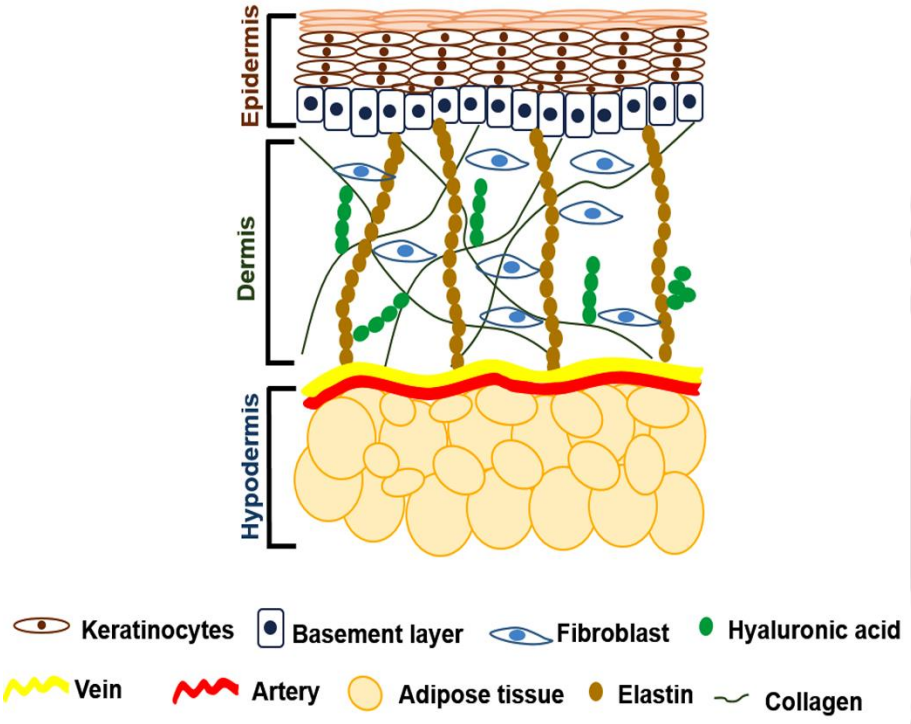

Fig.1.1. *Anatomy of the skin*

1.2.1.1. Epidermis

The epidermis is the outer most region of skin consists of several layers, however, its surface topography and thickness varies based on its location (Schmitt, 1992). The epidermis is enriched with squamous keratinized epithelium with nearly 80% keratinocytes (Monteiro-Riviere, 1996). It also consists of other cell types; melanocytes (synthesis melanin pigment), Merkel cells (receptor function) and Langerhans cells (immunological functions) (Monteiro-Riviere, 1996). The epidermis of skin is made up of 4 to 5 layers based on its body site; stratum corneum, stratum lucidum (palms, soles, and fingertips), stratum granulosum, stratum spinosum, and stratum basale (McLafferty et al., 2012). Stratum basale is the innermost layer of the epidermis made up a single tier

of columnar keratinocytes along with other cell types; Merkel cells and melanocytes (McLafferty et al., 2012). Keratinocytes present in the stratum basale are capable of division. They undergo mitosis and produces two daughter cells among one remains in the stratum basale and another cell emigrates up to other layers and reaches the surface of the epidermis (average of 0.1 mm thickness) within 28 days (Derrickson, 2009). Cells present in the stratum basale obtained nourishment from the dermis, whereas, daughter keratinocytes migrated to the upper layer of the epidermis dies due to lack of nutrients. In the epidermis, there is a balance maintained between the formation of new keratinocytes and the peeling of dead keratinocytes. Stratum basale of epidermis also accounts for one melanocyte in every six cells (McLafferty et al., 2012). Melanocytes produce melanin pigment, which protects the skin from UVR-induced damage. Melanin granules produced by melanocytes transferred to keratinocytes by slender projections, which forms a protective covering across the nucleus and shields against UVR-induced damage. The color of skin also depends on the amount of melanin produced by melanocytes. Merkel cells present in the stratum basale make a connection with the flattening process of a sensory neuron known as Merkel disc. They assess the sensation of touch (McLafferty et al., 2012).

The stratum spinosum (5-12 cells thick) is the second innermost layer of the epidermis. Keratinocytes, which migrated from stratum basale to stratum spinosum losses their capability to divide and turn into rounded and spikier in shape (McLafferty et al., 2012). They join with other keratinocytes by intracellular bridges known as desmosomes. Desmosomes have thorn-like protrusions that draw the adjacent cells close together and impart flexibility and tensile strength to skin. While daughter keratinocytes moving to other layers causes the breakage and reformation of desmosomes. Langerhans cells (produced by the dendritic cells of the immune system) present in stratum spinosum contributes skin protection against microbes by presenting the phagocytized microbes to T lymphocytes and activate them to destroy appropriate microbes (Pringle and Penzer, 2002). They also play a crucial role in assisting other immune cells to identify invading microbes and destroy them.

Keratinocytes move from stratum spinosum to stratum granulosum of the epidermis become longer and flattened horizontally (Derrickson, 2009). Stratum granulosum consist of 3 to 5 layers of flattened keratinocytes. Newly entered cells become metabolically inactive, losses their nucleus and become keratinized and covered throughout with a tough pliable protein known as keratin (Derrickson, 2009; Pringle and

Penzer, 2002). Stratum granulosum also contains Odland bodies, which are membrane-coating lamellar granules produce lipids and releases into spaces between the cells. The released lipids help the cells to stick together and prevent them from drying (Derrickson, 2009; Pringle and Penzer, 2002). The outermost layer of the epidermis is stratum corneum that consists of 25-30 flattened layers of dead keratinocytes arranged as orderly vertical stacks, which are strongly attached to each other (Derrickson, 2009). It is enriched with keratin protein that supports the underlying tissue and protects skin from chemicals, microbes, and heat.

1.2.1.2. Dermis

The dermis is the second innermost layer of skin that lies beneath the epidermis. It provides physical support and supplies nutrients to the epidermis (Burr and Penzer, 2005). The dermis and epidermis are connected by rete ridges (furrows), which stabilizes the connections between them and helps in nutrient exchange (McLafferty et al., 2012). In the dermis, fibroblast cells are the most predominant cell types along with other cell types such as macrophages, mast cells, plasma cells and adipocytes (Svobodová and Vostálová, 2010). Fibroblast cells are spindle-shaped and contain a well-defined rough endoplasmic reticulum. They synthesize ground substance and all types of fibers (collagen and elastin) (Svobodová and Vostálová, 2010).

The dermis is made up of two layers; the papillary and reticular layers. The papillary layer is the outermost region of the dermis, which contains a small and loose distribution of collagen and elastin fibrils. Collagen and elastin fibers present in the papillary layer are vertically arranged and connects with the dermal-epidermal junction. They provide protection to the cells and blood vessels from the mechanical damage. The physiological variation in the content of vascular and water volume of papillary layer effects the whole mechanical properties of skin. The reticular layer is composed of strong connective tissue consisting of elastin and collagen fibers (Pringle and Penzer, 2002). Collagen bundles of the dermis maintain the structural integrity of skin and provide high tensile strength that prevents skin tearing. Collagen bundles constitute nearly 70% of the dry weight of the dermis (Pringle and Penzer, 2002). Elastin fibers produced by the dermal fibroblast cells are thin fibers intertwined among collagen bundles and imparts elasticity to skin. The elastin fibers network also helps to recover architecture and shape of tissue after deformation. The interwoven network of collagen and elastin fibers have a significant tensile strength that provides support and flexibility to skin (Derrickson, 2009).

1.2.1.3. Hypodermis

The hypodermis is the third innermost layer of skin present between the dermis and fasciae of the muscle (Avram et al., 2005). The hypodermis is also known as subcutaneous adipose tissue. It is structurally and functionally connected with the dermis of skin with vascular and nerve network. Thickness of the hypodermis varies based on the anatomical region of skin, race, sex, nutritional and endocrine status of a person. The major portion of the hypodermis is a loose connotation of adipocytes. However, it contains only one-third portion of matured lipid-filled cells (Avram et al., 2005). While remaining portion of the hypodermis is enriched with stromal-vascular cells containing pre-adipocytes, fibroblast cells, macrophages, and leukocytes (Albright and Stern, 1998). The major portion of the adipocytes are stored with lipid droplets (50 µm) and the cytoplasm and nucleus seem like thin rim in the periphery of the cells. They are connected with capillaries, which help in the exchange of metabolites and allows them to function properly.

1.2.2. Skin disorders

The human skin plays an important role in protecting the underlying tissues from the external environmental factors. However, chronic exposure of the skin to UVRs and pollutants (cigarette smoke, smog, car exhaust, dirt, dust, industrial chemicals, and other particulates) causes severe damage to skin. Among them, UVRs play a major role in damaging the skin (**Fig.1.2**). UVRs (200-400 nm) of the electromagnetic spectrum are categorized into ultraviolet A (UVA) (400-320 nm), UVB (320-280 nm) and ultraviolet C (UVC) (280-200 nm) radiations based on their wavelength (Liu et al., 1994). Among total UVRs, UVA (90-98%) and UVB (1-10%) radiations reach the earth, whereas UVC is absorbed by the ozone layer of the stratosphere (Hou et al., 2015). Nearly 80% of the UVA radiations reaches the epidermal-dermal junction of skin and penetrates deeper into the dermal layers and further reaches to the hypodermis (nearly 10%). Whereas, 70% of UVB radiations are blocked by the stratum corneum and the remaining 30% of UVB radiations are absorbed by the epidermis (Verschooten et al., 2006).

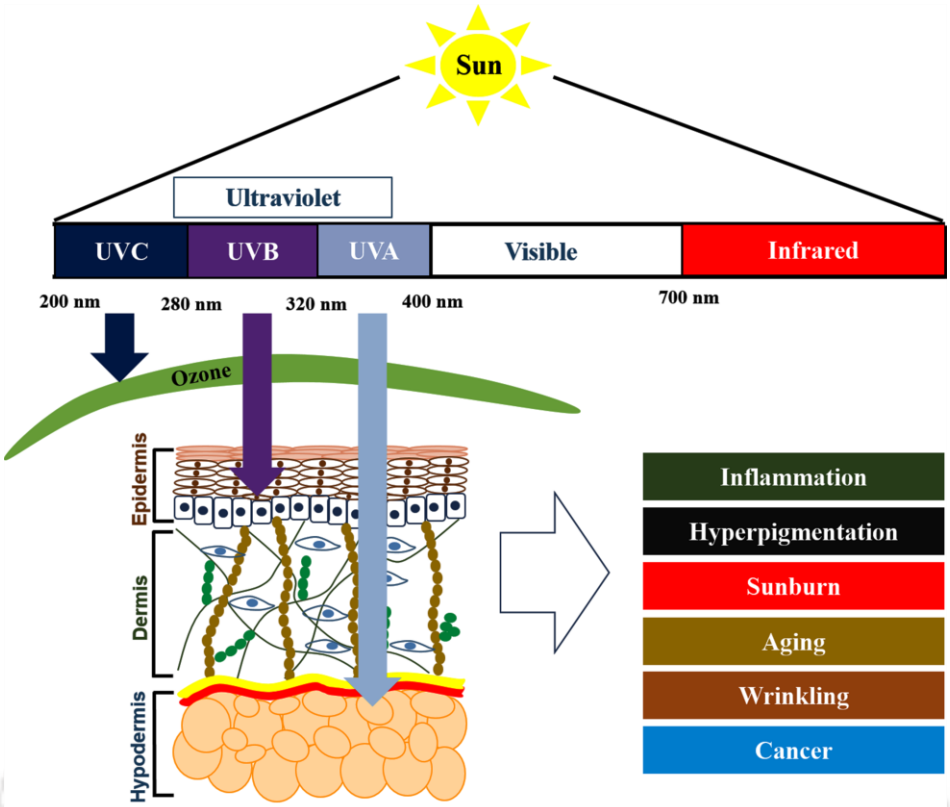

Fig.1.2. *A schematic representation of the effect of UV radiations on skin.*

UVA radiations penetrated into skin and elevate the generation of RS (ROS and RNS; **Table 1.1**) by interacting with endogenous chromophores; NADPH, NADH, flavins, quinones, eumelanin, porphyrins, 7-dehydrocholesterol, urocanic acid and heme (Svobodová and Vostálová, 2010). RS are highly unstable molecules with an odd number of electrons and they steal electrons from various cellular structures (lipids, aromatic amino acids of proteins, nucleic acid bases). Oxidation of biomacromolecules and endogenous chromophores results in various skin disorders. Whereas, UVB radiations absorbed by the epidermal keratinocytes induce DNA damage by initiating the formation of pyrimidine-(6-4)-pyrimidone photoproducts (6-4PP) and cyclobutane pyrimidine dimers (CPD) between the adjacent pyrimidine bases (Verschooten et al., 2006). In addition to the formation of DNA photoproducts, UVB radiations also elevate the generation of RS and oxidize the biomacromolecules. Oxidation of biomacromolecules and formation DNA photoproducts causes inflammation, erythema, hyperpigmentation, skin aging, wrinkle formation and skin cancer (melanoma and non-melanoma) (Gil and Kim, 2000; Kulms et al., 2002; Rittié and Fisher, 2002). The details about the effect of UVR-induced skin disorders are described below.

Table 1.1. *Reactive species generated in the skin by UV irradiation (Svobodová and Vostálová, 2010).*

Reactive oxygen species (ROS)	Reactive nitrogen species (RNS)
Superoxide anion (O_2^-)	
Singlet oxygen ($^1O_2$)	Nitric oxide (NO)
Ozone (O_3)	Peroxynitrite ($ONOO^-$)
Hydroxyl radical (·OH)	Nitrogen dioxide (NO_2)
Hydrogen peroxide (H_2O_2)	

1.2.2.1. Inflammation

Prolonged exposure of the skin to UVRs elevates RS generation and damages DNA. Elevated levels of RS also act as secondary messengers in pro-inflammatory signaling pathways and upregulates inflammatory cytokines [interleukin (IL)-1, IL-6, IL-8 and tumor necrosis factor (TNF)-α] expression (Bashir et al., 2009b; Pillai et al., 2005; Robinson and Werth, 2015). Redox imbalances in epidermal and dermal layers of skin by chronic exposure to UVRs release the lipid mediators; cyclooxygenase-2 (COX-2) and prostaglandin E2 (PGE2) (Bosch et al., 2015). The release of pro-inflammatory cytokines [attracts and activates neutrophils, which migrates near the resident cells and stimulates generation of RS (Pillai et al., 2005)] and lipid mediators mediates the photocarcinogenesis, photoaging, and wrinkling of skin by activating different pathways (Bosch et al., 2015).

1.2.2.2. Hyperpigmentation

The color of skin is mainly maintained by melanin, which is produced by melanocytes present in the stratum basale of the epidermis (Lin and Fisher, 2007). Melanin is the main defensive pigment, whose production is increased by exposing to UVR to arrest skin damage (Agar and Young, 2005). Tyrosinase a copper-dependent enzyme plays an important role in melanin biosynthesis. Tyrosinase converts the L-tyrosine to 3, 4-dihydroxyphenylalanine (DOPA) and further DOPA to o-dopaquinone (precursor for melanin). These two steps are rate-limiting steps of melanin biosynthesis (Agar and Young, 2005; Song et al., 2009).

Epidermal melanocytes of skin are highly susceptible to RS (Denat et al., 2014). Chronic exposure of skin to UVRs elevates the RS production, which overwhelms the endogenous antioxidant defense system and triggers upregulation of tyrosinase,

tyrosinase-related protein (TRP)-1, and TRP-2 expression (Cho et al., 2009). Upregulation of tyrosinase triggers melanin biosynthesis. Excessive synthesis and accumulation of melanin lead to various skin diseases such as freckles, leukoplakia, post-inflammatory melanoderma, moles, melasma, and solar lentigo (Briganti et al., 2003; Cullen, 1998; Han et al., 2015; Urabe, 1998).

1.2.2.3. Sunburn

Chronic exposure of skin to UVRs (primarily UVB radiation with UVA) causes the sunburn, which is characterized by pain, erythema, and oedema (Nicolaou et al., 2011). Sunburn skin also shows epidermal thickening (histopathological changes), apoptosis of keratinocytes (sunburn cells) and infiltration of dermal neutrophils, monocytes, and lymphocytes. In sunburn skin, biochemical changes are also observed such as the production of nitric oxide, eicosanoids, and cytokines (Black et al., 1978; Hawk et al., 1988; Rhodes et al., 2001; Strickland et al., 1997; Teunissen et al., 2002; Warren, 1994).

1.2.2.4. Aging

Aging of skin is a complex process involving various genetic modifications, hormonal imbalance, and physical changes. Aging is characterized into two types; intrinsic and extrinsic aging. RS plays a crucial role in both intrinsic and extrinsic aging. Intrinsic aging is also known as true or chronological aging. RS produced by the normal metabolism are involved in the intrinsic aging process. It is related to different factors such as ethnicity, anatomical variations and hormonal changes (Ramos-e-Silva et al., 2013). Intrinsic aging generally results with age and the changes are observed in the areas that are not exposed to the sun (Gilchrest, 1989; Warren et al., 1991).

Extrinsic aging is the result of prolonged exposure of skin to UVRs, smoking, as well as other general lifestyle factors like lack of sleep and poor diet. Chronic exposure of skin to UVRs elevates the levels of RS in the body, which triggers the activation of nuclear factor-kappa B (NF-κB). Activated NF-κB stimulates the secretion of pro-inflammatory cytokines [IL-1α, IL-6, IL-8, and TNF-α]. The released proinflammatory cytokines activate the activator protein-1 (AP-1) and NF-κB in the epidermal and dermal region of the skin (Angel et al., 2001; Bashir et al., 2009a; Fisher et al., 2002; Kondo, 2000; Sárdy, 2009). Activated AP-1 upregulates the expression of Matrix metalloproteinases (MMPs) by the epidermal keratinocyte (MMP-2 and MMP-9) and dermal fibroblast cells (MMP-1 and MMP-3). MMP-1 initiates the degradation of type I

and III collagen, and fragmented collagen is further degraded by gelatinases (MMP-2 and MMP-9) (Angel et al., 2001). MMP-3 activates pro-MMP1 and also degrades type IV collagen (a basement membrane). Degradation of collagen and elastin fibers of the extracellular matrix (ECM) causes the loss of structural integrity of the skin (Sárdy, 2009).

1.2.2.5. Wrinkling

In humans, wrinkle formation is associated with a decrease in skin elasticity. Wrinkling of the skin is identified with dry and flaky rough skin, both coarse and fine wrinkles, poor elastic recoil and impaired wound healing (Brenneisen et al., 2002; Vayalil et al., 2004). Redox imbalance-induced in skin by chronic exposure to UVRs triggers the release of fibroblast elastase and neutrophil elastase, which degrades the elastin fibers of the dermis. Degradation of elastin fibers causes wrinkling and sagging of skin (Imokawa, 2009; Tsuji et al., 2001).

1.2.2.6. Skin Cancer

Skin cancer is one of the most common cancer at present days and its prominence increasing very rapidly. Approximately 70% of non-melanoma skin cancer (NMSC) is caused by prolonged exposure of skin to UVRs. Redox imbalance in cells by UVRs oxidizes the purine bases of DNA [8-oxo-deoxyguanine (8-oxodG)] and induce mutations (Dunaway et al., 2018). Whereas, UVB radiation-induced the formation of DNA photoproducts (CPD and 6-4PP) that results in DNA lesion and mutations (Ramasamy et al., 2017). DNA damage blocks the transcription and activates p53, which initiates the apoptotic cell death to remove mutated cells (Batista et al., 2009). However, UVRs induce mutation in p53 gene [Cytosine→Thymine (C→T) or CC→TT transitions] that leads to replication of mutated DNA and initiates to NMSC (Brash et al., 1991; Ziegler et al., 1994). Elevated levels of RS oxidize the lipids (lipid peroxidation) and proteins (leads to conformation changes by misfolding of the amino acids) of cells, which causes abnormal cell signaling and enhances the cell proliferation (Pattison et al., 2012).

Chronic exposure of skin to UVRs also induce epigenetic changes like histone modifications, DNA methylation, and microRNA (miRNA)-mediated gene regulation. These epigenetic changes lead to the initiation of skin cancer (Katiyar et al., 2012). Addition of methyl group to the 5^{th} carbon of cytosine in a 5'-Cytosine-phosphate-Guanosine-3' (CpG) dinucleotide controls gene expression. In humans, the methylated CpG dinucleotides form clusters in certain portions of DNA and they upregulate the promoter regions of half of the genes (Dunaway et al., 2018; Takai and Jones, 2003).

Several studies have reported that the distinct DNA methylation is seen in cancer cells than normal cells. For example, in cancer cells main tumor suppressor genes (CDKN2A and CDKN2D) are hypermethylated and silenced than normal cells (Baylin and Ohm, 2006). In addition to high levels of DNA methylation at promoter regions, loss of DNA hydroxymethylation mark and 5-hydroxymethylcytosine also serves as a biomarker for melanoma (Fu et al., 2017).

1.2.3. Antioxidants

1.2.3.1. Endogenous antioxidants

AOs are the chemical molecules, which could protect the cells from oxidative damage by scavenging/ neutralizing the elevated levels of RS. They travel in the body and eliminate the already formed RS, thereby reduced their deleterious effect on cellular damage (Sun, 1990). The skin consists of a large network of antioxidant molecules, which protect it from oxidative damage by scavenging/ reducing elevated levels of RS in response to pollutants and UVRs. The skin is enriched with enzymatic and non-enzymatic AOs. Both enzymatic and non-enzymatic AOs work together to maintain the redox balance of skin (Svobodová and Vostálová, 2010). The mechanism of AOs and their limitations are described below (**Table 1.2**).

1.2.3.1.1. Enzymatic antioxidants

1.2.3.1.1.1. Superoxide dismutase (SOD) (EC 1.15.1.1)

SOD is an enzymatic AO, which maintains the redox balance of skin. It converts the superoxide anions into molecular oxygen and hydrogen peroxide (Sasaki et al., 1997). Isozymes of SOD differs in their cofactors; manganese-SOD (MnSOD) and copper-zinc-SOD (CuZnSOD). MnSOD is a homotetramer (96 kDa) found in mitochondria, whereas, CuZnSOD is a homodimer (32 kDa) is present in the nucleus and localized in the cytosol. SOD activity is 2.3 fold higher in the epidermis than the dermis (Shindo et al., 1994a). Various studies have shown that UVRs affect SOD activity (Li et al., 2016; Liang et al., 2018; Vilela et al., 2016). UVB irradiation reduced CuZnSOD and MnSOD protein levels and their activities in the human keratinocytes, however, they showed recovery to the basal levels within 24 h of irradiation (Takahashi et al., 2000). Sasaki *et al*. reported that the MnSOD and CuZnSOD activity enhanced immediately after UVB irradiation and declined after 4 h of irradiation than base levels (Sasaki et al., 1997). However, their activity recovered within 24 h of UVB irradiation. The MnSOD and CuZnSOD protein levels differed in human keratinocytes by UVB irradiation. The CuZnSOD protein levels enhanced post irradiation with UVB radiations, however, their levels reaches to the base

levels after 24 h. While MnSOD protein levels were reduced in keratinocytes after UVB irradiation than control cells and gradually recovered within 24 h (Sasaki et al., 1997). Initially UVA and UVB irradiations also decreased MnSOD activity in human fibroblast cells, however, its activity and mRNA levels significantly enhanced within 5 days (Leccia et al., 2001). Another study showed that MnSOD activity was enhanced 3 folds higher in keratinocytes after irradiating with a low dose (50 mJ/cm^2) of UVB, however, irradiating with 100 mJ/cm^2 of UVB radiations decreased its activity and lead to apoptotic cells death (Wiswedel et al., 2007). UVB irradiations (0.24 J/cm^2) significantly declined SOD activity in BALB/C mice (Aricioglu et al., 2001). UVA (25 J/cm^2) or UVB (300 mJ/cm^2) radiations depleted the intracellular SOD levels in human skin fibroblast cells (Liang et al., 2018).

1.2.3.1.1.2. Catalase (CAT) (EC 1.11.1.6)

CAT is a heme-containing AO enzyme found in the mitochondria and peroxisomes. It catalyzes the conversion of hydrogen peroxide into water and molecular oxygen (Afaq and Mukhtar, 2001). CAT activity is 8 fold higher in the epidermis than the dermis and it has highest turnover rates than all other enzymes (a molecule of CAT could catalyze nearly 6 million of H_2O_2 into H_2O and O_2 per minute). Several studies have reported that the CAT activity is reduced in UVR irradiated skin (Martinez et al., 2018; Martinez et al., 2017a). The irreversible oxidation of the CAT by the RS generated by UVRs might have reduced its activity (Afaq and Mukhtar, 2001). Acute or chronic exposure of SKH-1 hairless mice to UVB radiations decreases CAT activity (Sharma et al., 2007). Irradiating hairless mice with increasing dosage of solar simulated light (2-25 J/cm^2) showed decreased in the CAT activity above 5 J/cm^2 (Shindo et al., 1994b). Human fibroblast cells irradiated with solar simulated radiation reduced CAT activity, however, their activity recovered within five days of exposure (Leccia et al., 2001). Stratum corneum of the human skin showed less CAT activity in summer as compared with winter (Hellemans et al., 2003). Dose-dependent UVA irradiation also decreased CAT activity of the stratum corneum within 24 h, however, CAT activity remained unchanged after UVB irradiation. The CAT activity recovered after 3 to 4 weeks of UVA irradiation (15 J/cm^2) (Hellemans et al., 2003).

1.2.3.1.1.3. Glutathione peroxidase (GPX) (EC 1.11.1.9)

GPX is a tetrameric protein containing selenocysteine at each active sites. It catalyzes the conversion of an organic peroxide or hydrogen peroxide into alcohol or water by utilizing glutathione (GSH) as a co-substrate (Brigelius-Flohe, 2006). GPX

activity was affected by the UVRs (Liang et al., 2018; Martinez et al., 2017b). Human skin fibroblast cells irradiated with UVA (25 J/cm^2) and UVB (300 mJ/cm^2) depletes intracellular GPX levels (Liang et al., 2018). UVB irradiation significantly reduced GPX activity in human keratinocytes and female Kunming mice than control groups (Xu et al., 2018). GPX activity was decreased in the human fibroblast cells after 4 h of irradiation with solar simulated light (5 or 20 mJ/cm^2 of UVB with 1 or 4 J/cm^2 of UVA). However, its activity has been recovered with 4-5 days after irradiation (Leccia et al., 2001). The SKH-1 female hairless mice irradiated with acute UVB radiation-induced minor reduction in the GPX activity, while prolonged UVB exposure resulted in significant depletion of its activity (Sharma et al., 2007). UVA+UVB irradiation (25 J/cm^2) immediately decreased GPX activity in the murine epidermis and dermis layers, however, its activity completely recovered after 3 h of irradiation and enhanced to 200-250%. In the epidermis, its activity attains 100% within 120 h. While GPX activity remained enhanced in the dermis (Shindo et al., 1994c). Human skin irradiated with a single 4 x minimal erythema dose (MED) also showed significant depletion of GPX activity after 24 h of exposure (Katiyar et al., 2001).

1.2.3.1.2. Non-enzymatic antioxidants

LMWMs protect the skin against oxidative damage by reducing the RS, which includes endogenous molecules [melanin and glutathione (GSH)] and exogenous molecules [vitamin C (Vit. C), vitamin E (Vit. E), polyphenols and carotenoids] (Svobodová and Vostálová, 2010). The lipophilic molecules are distributed in the cellular membrane (Vit. E) and hydrophilic molecules are localized in the cytoplasm (Vit. C and GSH). Stratum corneum of the epidermis is enriched with Vit. C, Vit. E and GSH, however, their distribution is not even. The distribution of non-enzymatic AOs are in gradient manner; on the outer layers, they are in low concentration and their concentration increases while moving into the deeper layers of the stratum corneum (Thiele et al., 1998; Weber et al., 1999). Non-enzymatic antioxidants enhance enzymatic AOs activity as well as protect the skin from oxidative damage by donating their electrons or by chelating transition metals (Kurutas, 2016; Svobodová and Vostálová, 2010). They are mutually interdependent; active LMWMs reduces oxidized molecules and restores their activity (Kohen and Gati, 2000). The role of non-enzymatic AOs in protecting the skin from oxidative damage and their limitations are described below.

1.2.3.1.2.1. Melanin

Melanin is the primary defensive pigment, which protects skin against UVR-induced DNA damage. The skin color also depends on the different types of melanin along with oxy/deoxy-hemoglobin and carotenoids (Stamatas et al., 2004). Melanin produced by the melanocytes is transported to the adjacent keratinocytes by dendrites (Brenner and Hearing, 2008). Melanocytes produce two types of melanin-based on the different melanogenic activity; sulfur-containing pheomelanin (lighter red/yellow) and eumelanin (darker brown/black) (Thody et al., 1991). The shielding effect of pheomelanin and eumelanin depends on the ability to absorb and scatter the UVR. Pheomelanin and melanin precursors 5, 6-dihydroxyindole (DHI) and 5-S-cysteinyldopa (SCN) absorbs UVRs and elevates the production of RS. Elevated levels of RS could in turn damage DNA. While eumelanin and melanin precursors (DHI and SCN) absorbs the UVR, scatters them and reduces elevated levels of RS (Steenvoorden and van Henegouwen, 1997). The shielding effect of eumelanin is superior to pheomelanin against UVR-induced oxidative damage (Brenner and Hearing, 2008). However, chronic exposure of skin to UVRs triggers the biosynthesis of melanin production, which causes various skin disorder including melanoma skin cancer (Han et al., 2015).

1.2.3.1.2.2. Glutathione (GSH)

GSH is a tripeptide (glycine, cysteine and glutamic acid) that is abundantly distributed in the nuclei, cytosol, and mitochondria of the cells (Svobodová and Vostálová, 2010; Tan et al., 2018). It plays an essential role in protecting skin from oxidative damage by reducing the elevated levels of RS. GSH reduces/scavenges the elevated levels of RS by donating the electrons of thiol groups of cysteine or by acting as a co-substrate of GPX and glutathione S-transferase (GST) (Farhat et al., 2018; Winterbourn, 2016).

GSH exists in two forms; reduced glutathione (GSH) (active form) and oxidized glutathione (glutathione disulfide; GSSG) (Kurutas, 2016). The oxidized glutathione accumulated in the cell and the ratio of GSH: GSSG is the potential indicator of the cellular redox state. Glutathione-disulfide reductase (GSR) catalysis the reduction of GSSG to GSH using NADPH as an electron donor and it maintains high levels of GSH (D'Orazio et al., 2013; Deponte, 2013). GSH is involved in Vit. C and Vit. E regeneration and also eliminate the products of lipid peroxidation (Masella et al., 2005). GSH also repairs damaged protein and DNA (Chatterjee, 2013). Both *in vitro* and *in vivo* studies reported that chronic exposure of cells and skin to UVRs declines GSH levels (Martinez

et al., 2018; Thiesen et al., 2017; Vilela et al., 2016). UVB radiation depletes the GSH levels by affecting the uptake of cystine by impairing the disulfide bonds between the light chain (xCT) and heavy chain (4F2hc) of Xc, a cystine transporter. Lipid peroxidation products produced by UVB irradiation also disturb the transport of cystine by interacting with Xc transporter (Zhu and Bowden, 2004). In mammals, UVA radiation-induced GSH depletion upregulated heme oxygenase gene expression (HO; response to oxidative stress) (Lautier et al., 1992). Depletion of GSH levels in skin elevates the generation of RS, which causes the skin damage.

1.2.3.1.2.3. Vitamin C (Vit. C)

Vit. C is a low molecular weight AO molecule, which is supplemented to the body through the diet. It is transported to the cells by the glucose transporter. Vit. C acts as an electron donor, which scavenges elevated levels of RS. It also acts as an important coenzyme in oxidative stress pathways (Zhong et al., 2017). It elevates GSH levels in the cells by protecting the thiol groups from oxidation. Vit. C also helps to reduce the oxidized form of α-tocopherol radicals (Kojo, 2004). It plays an important role in collagen production by activating the transcription of collagen synthesis as well as by stabilizing the procollagen mRNA (Telang, 2013; Traikovich, 1999). Vit. C could be oxidized to dehydroascorbic acid in the presence of metal ions, however, they reduced with semidehydroascorbate reductase by utilizing NADH (Chan, 1993; Kawashima et al., 2015). It protects the epidermal keratinocytes against UVB radiation-induced cell death and oncogenesis by reducing the elevated levels of RS (Savini et al., 1999; Stewart et al., 1996). Additionally, Vit. C also reduces UVB radiation-induced inflammation by downregulating inflammatory cytokine generation (Kang et al., 2007). Various studies have been reported that the oxidative stress induced in the skin by chronic exposure to UVRs or pollutants depletes Vit. C levels in the epidermal layer of skin (Pullar et al., 2017; Shindo et al., 1993). Vit. C levels also declined in the epidermal and dermal layer of photo-aged and aged skin (Rhie et al., 2001).

1.2.3.1.2.4. Vitamin E (Vit. E)

Vit. E is a lipophilic AO molecule supplemented to the human body through the diet. It naturally occurs in eight forms such as α, β, γ, and δ classes of tocopherol and tocotrienol. Among eight forms, α-tocopherol is present in a high amount and biologically active in the human body (Kurutas, 2016). α-tocopherol quickly reacts with peroxyl radical and forms a quite stable tocopheroxyl radical, which breaks the lipid peroxidation and protects polyunsaturated fatty acids. While breaking the lipid

peroxidation, Vit. E get oxidized by donating their hydrogen to the lipids. Oxidized α-tocopherol are regenerated at the aqueous interface by Vit. C. Oral supplementation or topical delivery of Vit. E raises its levels in the skin. However, its levels get depleted in UV irradiated, photo-aged or aged skin (Fernández-García, 2014; Rhie et al., 2001).

1.2.3.1.2.5. Carotenoids

Carotenoids are fat-soluble pigments occur in vegetables and fruits. Humans consuming fruits and vegetables are enriched with carotenoids; α, β-carotenes, and lycopene along with hydroxy carotenoids (xanthophylls; lutein and zeaxanthin) and α and β- cryptoxanthin (Oroian and Escriche, 2015). Carotenoids absorbed in the blood are transported to various tissues. The carotenoids were taken up by the cells using cholesterol transporters; a cluster of differentiation 36 (CD36) and scavenger receptor class B member 1 (SR-B1) (During et al., 2005; van Bennekum et al., 2005). The human epidermis is expressed with SR-B1 receptors, which helps to uptake carotenoids (Tsuruoka et al., 2002). The amount of carotenoids present in the different regions of skin varies and their levels are directly co-relates with the intake of fruits and vegetables (Fernández-García, 2014). The carotenoids possess various biological properties; antioxidant activity, pro-vitamin, harvest light and have photoprotection activity (Fernández-García, 2014; Oroian and Escriche, 2015). Carotenoids protect the skin against UV radiation-induced oxidative damage by scavenging the elevated levels of singlet oxygen ($^1O_2$). However, chronic exposure of skin to UVRs could inactive carotenoids, which leads to the degradation of dermal elastin and collagen (Amaro-Ortiz et al., 2014; Darvin et al., 2014; Lademann et al., 2011).

Endogenous AOs protect the skin against UVR and pollutants induced oxidative damage by scavenging the elevated levels of RS. However, chronic exposure of skin to UVR elevated the production of RS and depletes or inactivates the endogenous antioxidants that lead to various skin disorders. Researchers addressed these skin problems by topical delivering the exogenous antioxidants.

Table 1.2. *Mechanism of endogenous AOs in neutralizing the elevated levels of RS and their effects after UV irradiation.*

Antioxidants	Mode of action	Effect of UVRs on the enzyme activity	References
Superoxide dismutase	$O_2^- + O_2^- + 2H^+ \rightarrow H_2O_2 + O_2$		(Aricioglu et al., 2001; Liang et al., 2018; Sasaki et al., 1997; Vilela et al., 2016)
Catalase	$H_2O_2 \rightarrow 2H_2O + O_2$		(Afaq and Mukhtar, 2001; Hellemans et al., 2003; Martinez et al., 2018; Shindo et al., 1994b)
Glutathione peroxidase	$2GSH + H_2O_2 \rightarrow GSSG + 2H_2O$		(Brigelius-Flohe, 2006; Liang et al., 2018; Martinez et al., 2017b; Sharma et al., 2007)
Gluthathione reductase	$GSSG + NADPH + H^+ \rightarrow 2GSH + NADP^+$	Both enzymatic and non-enzymatic AOs are susceptible to depletion by prolonged exposure of skin to UV radiations	(D'Orazio et al., 2013)
Vitamin C	Reduces RS by donating their electrons and act as a coenzyme in oxidative stress pathways		(Pullar et al., 2017; Shindo et al., 1993; Zhong et al., 2017)
Vitamin E	Reduces RS by donating their electrons		(Fernández-García, 2014; Kurutas, 2016; Rhie et al., 2001)
Glutathione	GSH can restore vitamins C and E from		(Martinez et al., 2018; Svobodová and Vostálová,

	the oxidized to the reduced state		2010; Tan et al., 2018; Thiesen et al., 2017)
Carotenoids	Reduces singlet oxygen ($^1O_2$)		(Amaro-Ortiz et al., 2014; Darvin et al., 2014; Lademann et al., 2011).
Melanin	Absorbs the UVR, scatters them and reduces elevated levels of RS	Elevates the synthesis of melanin that causes various skin disorder including melanoma skin cancer	(Han et al., 2015; Steenvoorden and van Henegouwen, 1997)

1.2.3.2. Exogenous antioxidants

Exogenous AOs are not produced in the human body, they are supplemented by the fruits, vegetables, tea, chocolates, wine, and cocoa products. Several studies have reported that exogenous antioxidants reduces elevated levels of RS and protects skin from oxidative damage, photoaging, prevents cancer and minimize cardiovascular diseases and neurodegenerative disorders. Exogenous AOs are orally supplemented or topically delivered to protect skin from oxidative damage, photoaging, wrinkling, and skin cancer. However, topical delivery of exogenous AOs is an attractive strategy to protect the skin against pollutants and UVR-induced damage. Among them, few exogenous AOs are used as a potent AO in skin care cosmetics to protect the skin against UVR-induced damage (**Table 1.3**).

1.2.3.2.1. Vitamin C (Vit. C)

Vit. C is a hydrophilic AO obtained from different sources of fruits and vegetables. Topical delivery of Vit. C showed a protective effect against UVR-induced erythema, immunosuppression, and reduces sunburn cell formation (Lin et al., 2003; Nakamura et al., 1997). Clinical studies have reported that the topical delivery of Vit. C enhances collagen production in aged and young human skin (Farris, 2014; Telang, 2013). Clinical studies also have reported that topical delivery of Vit. C improved photodamaged skin by activating elastin fibers of the dermal layer and enhanced skin surface texture (Humbert et al., 2003; Traikovich, 1999). Vit. C reduced hyperpigmentation by inhibiting tyrosinase activity as well as maintains hydration of the

skin by protecting the epidermal barrier (Maia Campos et al., 2008; Matsuda et al., 2008). In comparison with sunscreen alone, Vit. C additions enhanced the photoprotective activity of sunscreen lotion (Chen et al., 2012; Darr et al., 1996).

In spite of protective effect against UVR-induced oxidative damage, photoaging and hyperpigmentation, Vit. C has a lot of drawbacks. For topical delivery (penetration through stratum corneum), it needs to be ionized because of that the formulation should make at pH 3.5, where, Vit. C lose its hydroxyl groups and become unstable (Chen et al., 2012). Therefore, many formulations used stable esterified substitutes; ascorbyl-6-palmitate and magnesium ascorbyl phosphate (Maia Campos et al., 2008; Nayama et al., 1999; Pinnell et al., 2001). In comparison with Vit. C, they are inferior in their protective effect. The lactone ring of Vit. C irreversibly opened in the formulations by oxidizing with UVR and air (Allemann and Baumann, 2008).

1.2.3.2.2. Vitamin E (Vit. E)

Vit. E (α-tocopherol) is a lipophilic antioxidant with strong biological activity (Chen et al., 2012). Topical delivery of Vit. E enhanced endogenous AO active and reduced immunosuppression, lipid peroxidation, photocarcinogenesis and photoaging in animals and humans (Bissett et al., 1990; Burke et al., 2000; Gensler and Magdaleno, 1991; Jurkiewicz et al., 1995; Lopez-Torres et al., 1998). Topical delivery of Vit. E reduced 55% of CPD formation in the epidermal p53 gene (Chen et al., 1997). In humans, topical delivery of 5% Vit. E prior to 24 h of UV irradiation inhibited macrophage metalloelastase (degrades elastin) (Chung et al., 2002). Topical delivery of Vit. C and E in combination showed stong photoprotection than individual delivery of Vit. C or Vit. E (Lin et al., 2003). However, the activity of topical delivered Vit. E depletes rapidly by dose-dependent UVB irradiation. Vit. E is also linked with various cutaneous side effects, including contact dermatitis (Hunter and Frumkin, 1991; Krol et al., 2000; Perrenoud et al., 1994).

1.2.3.2.3. Vitamin A (Vit. A)

Vit. A is a lipophilic antioxidant complemented to the human body in the form of carotenoids (mainly β-carotene; from plant sources) or retinoids (from animal sources). The epidermal region of skin is enriched with β-carotene and retinyl esters (esterification of retinol) (Antille et al., 2004). Retinoids are commonly found in skin care creams and sunscreen lotions. Topical delivered of retinoids have the ability to convert into any form of endogenous retinoids and enhances their epidermal concentration in mice and humans (Saurat et al., 1999; Sorg et al., 2005; Sorg and Saurat, 2014). Topical delivery of

retinoids (retinyl palmitate, retinol, retinoic acid, and retinaldehyde) inhibited UVB radiation-induced erythema, DNA damage and apoptosis in humans and mice skin (Antille et al., 2003; Sorg et al., 2005; Tran et al., 2001). Retinoids provide protection against UVR-induced photocarcinogenesis by upregulating the p53 expression and downregulating AP-1 and NF-κB transcription factors (Bayon et al., 2003; Darwiche et al., 2005; Fanjul et al., 1994; Mrass et al., 2004; Sorg and Saurat, 2014). Retinoids act as an anti-aging compound; they bind the retinoic acid receptors, nuclear receptors, and retinoid X and downregulates AP-1 and MMP-1 expression (Fisher et al., 1996). Topical delivery of 0.05% retinoic acid per day showed recovery of skin aging and reduces major side effects induced by UV irradiation. However, it causes retinoid dermatitis. Topical delivery of retinoids also enhances photocarcinogenesis in mice (Griffiths et al., 1995; Halliday et al., 2000; Leyden et al., 2004)

1.2.3.2.4. Polyphenols

Polyphenols are secondary metabolites of plants, which are stored in the leaves, fruits, nuts, flowers, bark, and seeds. They have more than one phenolic group per molecule. The polyphenols are divided into two types based on their based on number and type of phenolics; flavonoids (catechins, isoflavones, proanthocyanidins, and anthocyanins) and non-flavonoids (phenolic acids, benzoic acids, stilbene, and resveratrol) (Bosch et al., 2015). Polyphenols are known to possess antioxidant activity along with the immunomodulatory and anti-inflammatory activity. The AO properties of the polyphenols depend on the hydroxyl groups bound to the aromatic rings, which act as an electron or hydrogen donor to the free RS. In addition to AO activity, they also chelate the metal (Cu and Fe) and prevent RS formation from H_2O_2 by Fenton reaction (Bosch et al., 2015). Polyphenols obtained from green tea leaves, grape seeds and pomegranate are extensively investigated for their protective effect against UVR-induced in skin damage.

1.2.3.2.4.1. Green tea polyphenols (GTPs)

Green tea leaves are enriched with monomeric flavanols known as catechins; (−)-epigallocatechin, (−)-epigallocatechin-3-gallate (EGCG), (−)-epicatechin and (−)-epicatechin-3-gallate. Among them, EGCG has extensively studied catechins in the area of skin care protection (OyetakinWhite et al., 2012). Several *in vitro* and *in vivo* studies showed that the GTPs possess AO, anti-inflammatory and anti-cancer activity (Gensler et al., 1996; Katiyar et al., 2001; Katiyar et al., 1995; Wang et al., 1991). In human, topical applications of GTPs before UV irradiation reduced sunburn cells and protected

Langerhans cells from UVR damage (Elmets et al., 2001). Topical administration of EGCG prior to UVB irradiation reduced lipid peroxidation in guinea pig skin (Kim et al., 2001). Topical application of GTPs protected the human skin from UVB radiation-induced erythema and reduced CPD formation in both the epidermis and dermis (Katiyar et al., 2000). Topical administration of EGCG prior to UV irradiation (4 x MED) reduced the formation of nitric oxide and hydrogen peroxide and inhibited the infiltration of inflammatory leukocytes into the skin and lipid peroxidation (Katiyar et al., 2001).

GTPs have been used several cosmetic products to protect the skin against UVR-induced damage. However, little clinical data are available for the skin care products having GTPs, and their concentration is not standardized in several products. GTPs are sensitive to light-induced oxidation and also have poor penetrating ability through human skin (Fang et al., 2006; Fernández-García, 2014; Montenegro, 2014).

1.2.3.2.4.2. Grape seed polyphenols (GSPs)

Grape seeds are enriched with polyphenols such as catechin, epicatechin, and proanthocyanidins. The AO, anti-proliferative and anti-inflammatory activity of grape seed is due to the polyphenolic phytoalexin component resveratrol (3,5,4-trihydroxy-trans-stilbene). Topical delivery of resveratrol inhibited UVB radiation-induced edema and inflammation in SKH-1 mice by inhibition of inflammation mediator COX-2 and ornithine decarboxylase (ODC) and reduction of H_2O_2 (Afaq et al., 2003). Topical application of resveratrol improves the aging of human skin by enhancing the expression of silent information regulator 1 (SIRT1) (inhibit MMPs) and ECM proteins (collagen and elastin) (Lephart et al., 2014).

Resveratrol use in medical products are helpful, however, it is quickly metabolized and decline in biological activity (Lephart and Andrus, 2017). Therefore, topical delivery of resveratrol may be more suitable. Topical administration of resveratrol penetrates into the stratum corneum; the upper layer of stratum corneum showed 77% of resveratrol and deeper layers showed 5% (which is enough to show the protect the epidermis) (Alonso et al., 2017).

1.2.3.2.4.3. Pomegranate polyphenols (PPs)

Pomegranate fruit (*Punica granatum*) is enriched a wide range of polyphenols like flavonoids, ellagic acid, tannins and anthocyanidins along with Vit. C (Gil et al., 2000). PPs obtained from different parts of the fruit like seed, juice, and peel (Montenegro, 2014). Pomegranate extract protected normal human epidermal keratinocytes from UVA and UVB radiation-induced photodamage (Afaq et al., 2005;

Syed et al., 2006). Topical application of pomegranate peel extracts enhanced SOD, CAT, and peroxidase activity (Chidambara Murthy et al., 2002). Pomegranate seed oil contains different bioactive compounds like steroidal, 17-α-estradiol and estrogen estrone, which are a potent antioxidant and mildest and safest steroidal estrogen (Sharaf and Nigm, 1964). Pomegranate extract is used in many cosmetic creams, however, they lack clinical investigation.

1.2.3.2.5. Lycopene

Lycopene is carotenoid that imparts a red color to the vegetables and fruits (Story et al., 2010). It is known to possess antioxidant activity along with anti-cancer, anti-inflammatory and anti-mutagenic activity (Fazekas et al., 2003; Stahl and Sies, 1996). Topical delivery of lycopene significantly inhibited ODC activity in UVB irradiated mice and prevented inflammation and apoptosis by interfering with caspase-3 activity (Fazekas et al., 2003). However, the double bonds of the lycopene get oxidized by exposing to air and light (Montenegro, 2014; Sharma and Le Maguer, 1996). As well as penetration of lycopene into the deeper layers of the skin from the topical formulation is questionable due to its high lipophilicity (Montenegro, 2014).

1.2.3.2.6. Coenzyme Q10 (CoQ10)

CoQ10 is an AO in subcellular membranes, which prevents the UVA radiation-induced collagen degradation (Stojiljković et al., 2014). The concentration of CoQ10 is relatively low in the skin. Topical delivery of CoQ10 would protect skin against UVR induced skin damage by enhancing their concentrations in skin. Topical delivery of CoQ10 using ethanol showed 27% penetration in the dermis and 20% into the epidermis of the pig's skin (Burke, 2005). In humans, topical application of 0.3% CoQ10 cream for six months showed 27% reduction of the wrinkles. Another study showed that topical application of CoQ10 cream for 6 months reduced the size of corneocytes, which is equivalent to 20 years' rejuvenation (Burke, 2005; Stojiljković et al., 2014). Encapsulation of CoQ10 in nanostructure of lipid carrier and topically delivered them using skin care formulations has enhanced stability, activity, penetration through the stratum corneum and reduced skin irritation (Yue et al., 2010).

1.2.3.2.7. Idebenone

Idebenone is a synthetic analog of CoQ10. It showed better antioxidant activity than Vit. E, CoQ10, kinetin, Vti. C, and alpha lipoic acid (McDaniel et al., 2005b). In humans, topical delivery of idebenone reduced skin dryness/roughness and fine lines/wrinkles and enhanced the overall appearance of skin (McDaniel et al., 2005a).

However, anti-aging creams containing 0.5% idebenone caused contact dermatitis (Sasseville et al., 2007).

Table 1.3. *Skin care application of exogenous AOs and their limitations after UV irradiation.*

Antioxidants	Protective effect against skin damage	Limitations	References
Vitamin C	Oxidative damage, erythema, aging, immunosuppression, sunburn, photodamage, photoaging, hyperpigmentation, and prevents dehydration.	Vitamin C looses its activity at low pH. It gets oxidized with UVRs and air. Depletes by prolonged exposure to UVRs.	(Allemann and Baumann, 2008; Chen et al., 2012; Darr et al., 1996; Farris, 2014; Lin et al., 2003; Maia Campos et al., 2008; Matsuda et al., 2008; Nakamura et al., 1997; Telang, 2013)
Vitamin E	Oxidative damage, immunosuppression, lipid peroxidation, photocarcinogenesis and photoaging.	Vitamin E get depleted rapidly by dose-dependent UVB irradiation. It is also linked with various cutaneous side effects, including contact dermatitis.	(Bissett et al., 1990; Burke et al., 2000; Gensler and Magdaleno, 1991; Hunter and Frumkin, 1991; Jurkiewicz et al., 1995; Krol et al., 2000; Lopez-Torres et al., 1998; Perrenoud et al., 1994)
Vitamin A	Oxidative damage, erythema, DNA	Vitamin A cause's retinoid dermatitis.	(Antille et al., 2003; Bayon et

	damage, photocarcinogenesis, and anti-aging.	It enhances photocarcinogenesis. It gets depleted by chronic exposure to UVRs.	al., 2003; Darwiche et al., 2005; Fanjul et al., 1994; Fazekas et al., 2003; Fisher et al., 1996; Griffiths et al., 1995; Halliday et al., 2000; Leyden et al., 2004; Mrass et al., 2004; Sorg et al., 2005; Sorg and Saurat, 2014; Tran et al., 2001).
Green tea polyphenols	Oxidative damage, inflammation, cancer. Sunburn, immunosuppression, lipid peroxidation, erythema, and reduced CPD formation	They are sensitive to light-induced oxidation. They have poor human skin penetrating ability.	(Elmets et al., 2001; Fang et al., 2006; Fernández-García, 2014; Gensler et al., 1996; Katiyar et al., 2001; Katiyar et al., 1995; Katiyar et al., 2000; Kim et al., 2001; Montenegro, 2014; Wang et al., 1991)
Grape seed polyphenols	Oxidative damage, edema, inflammation reduction of H_2O_2, and aging	They lack clinical investigation	(Afaq et al., 2003; Lephart et al., 2014)

Pomegranate polyphenols	Oxidative damage, photodamage, and enhance endogenous antioxidant activity (SOD, CAT, and peroxidase)	They lack clinical investigation	(Afaq et al., 2005; Chidambara Murthy et al., 2002; Syed et al., 2006)
Lycopene	Oxidative damage, cancer, inflammatory, and mutagenesis, photodamage.	Lycopene gets oxidized by exposing to air and light. Penetration of lycopene into the deeper layers of the skin from the topical formulation is questionable due to its high lipophilicity	(Fazekas et al., 2003; Montenegro, 2014; Sharma and Le Maguer, 1996; Stahl and Sies, 1996)
Coenzyme Q10	Oxidative damage, photodamage, wrinkles, aging and skin irritation	It lacks complete clinical investigations	(Burke, 2005; Stojiljković et al., 2014; Yue et al., 2010)
Idebenone	Oxidative damage, skin dryness/roughness and reduces fine lines/wrinkles	It causes contact dermatitis	(McDaniel et al., 2005a, b; Sasseville et al., 2007)

1.2.3.3. Exploring silk sericin as a potent antioxidant in skin care applications

Silk is a natural protein polymer produced by wide varieties of arthropods; silkworms, spiders, scorpions, mites etc. The silkworms of Bombycidae and Saturniidae families produces two structural proteins; fibroin and sericin (Kundu et al., 2012). These proteins are synthesized by the specialized epithelial cells lining of the silk glands and store them in the lumen. During spinning the cocoons, silkworms secrete the liquid silk, which passes through the anterior gland and expelled out through the spinneret opening (Mondal, 2007). Fibroin is a core protein of cocoon (constitutes 70%), whereas, sericin (constitutes 20-30%) a glue protein envelops the fibroin and helps in the cocoon

formation (Rangi and Jajpura, 2015). Sericin also protects the pupa and fibroin from physical and biological assaulters.

Silkworms are categorized into mulberry and non-mulberry silk varieties based on the feeding habitat of the silk larvae. Silk larvae of the Bombycidae family feed on the leaves of mulberry plants (*Morus* species), whereas, larvae of the Saturniidae family feeds on the non-mulberry plants; Arjuna (*Terminalia arjuna*,), som (*Persea bombycina*), castor (*Ricinus communis*) etc. Unlike mulberry silkworms, non-mulberry silkworms are wider in distribution and wild. The silkworms are found in China, India, Japan, Thailand, Indonesia, and Namibia. India is the second largest producer of silk after China and contributes production of endemic silk varieties; Muga (*A. assamensis;* endemic to Assam, India), Eri (*P. ricini*), and Tasar (*A. mylitta*).

SS extracted from the cocoons is known to possess AO activity, inhibits lipid peroxidation, tumor and microbial growth, elastase, and tyrosinase activity (Chlapanidas et al., 2013; Jena et al., 2018; Kaewkorn et al., 2012; Kato et al., 1998; Sarovart et al., 2003). SS protects the skin against UVB radiation-induced oxidative damage (Dash et al., 2008; Zhaorigetu et al., 2003). SS also enhanced wound healing by enhancing cell attachment, proliferation, and collagen production (Ersel et al., 2016). It also acts as a moisturizer (Nagura et al., 2001). All these properties of the SS depending on its chemical composition (amino acids and associated secondary metabolites).

1.2.3.3.1. The chemical composition of silk sericin

SS is a glue protein secreted by the middle region of the silk glands consists of polypeptides with a different range of molecular weight (Kundu et al., 2008). The major polypeptide fractions of SS obtained from the cocoons different silk varieties are given in **Table 1.4**. SS polypeptides are composed of 18 amino acids among which serine (31.99%), aspartic acid (15.74%) and glycine (14.20%) are predominant along with other amino acids (Vaithanomsat and Kitpreechavanich, 2008). The molar percentage of amino acids vary by different extraction methods (**Table 1.5**) and also with silk varieties (**Table 1.6**). The amino acids composition of the SS plays a major role in contributing to its biomedical applications. Hydroxyl groups of serine and threonine and the electron donating groups of aromatic amino acids attributes to the AO activity of SS by donating their electrons to RS as well as chelating trace elements like copper and iron (Fan et al., 2009; Kato et al., 1998). However, the SS peptides generated during extraction from the cocoons using different physical and chemical methods affect the molar percentage of amino acids and the activity of SS (Butkhup et al., 2012). For example, the molecular

weight of the BMS ranges from 10 to 400 kDa based on the temperature, pH and processing time while extracting from the cocoons (Aramwit et al., 2012; Gimenes et al., 2014). BMS extracted using alkali-degradation showed a molecular weight range from 15-75 kDa, whereas, acid and heat-degraded peptides displayed 35-150 kDa (Aramwit et al., 2010a). Changes in the molar percentage of amino acids of SS and the effect-induced by the physical and chemical factors during extraction affects its activity; AO, anti-trypsin and anti-tyrosinase activity (Aramwit et al., 2010a; Kurioka et al., 2004).

Table 1.4. *The major polypeptides fractions of silk sericin extracted from the cocoons of different silk varieties.*

Silkworms	**Source**	**Molecular weight (kDa)**	**Reference**
B. mori	Cocoons	24, 150, 250 and 400	(Takasu et al., 2002; Tokutake, 1980)
A. mylitta	Cocoon	70, 200 and >200	(Dash et al., 2007)
A. assamensis	Cocoon	66	(Ahmad et al., 2004)
P. ricini	Cocoon	66	(Ahmad et al., 2004)
Cricula trifenestrata	Cocoon	400	(Yamada and Tsubouchi, 2001)

Table 1.5. *The amino acid composition of B. mori sericin extracted using various methods (molar percentage) (Aramwit et al., 2010b).*

Amino acid	SS extracted using different extraction methods			
	Urea	**Heat**	**Alkaline**	**Acid**
Serine	31.27	33.63	30.01	31.86
Aspartic acid	18.31	15.64	19.88	15.93
Glycine	11.23	15.03	11.01	10.49
Glutamic acid	5.27	4.61	5.93	5.75
Histidine	3.26	1.06	1.72	2.47
Arginine	5.41	2.87	4.92	4.92
Threonine	8.36	8.16	6.49	8.51
Alanine	4.33	4.10	4.21	3.72
Proline	1.46	0.54	1.24	0.78
Cysteine	0.39	0.54	0.23	0.53
Tyrosine	0.36	3.45	5.24	5.56
Valine	2.96	2.88	2.94	2.95
Methionine	0.12	3.39	0.15	0.06
Lysine	3.14	2.35	2.89	3.48
Isoleucine	0.96	0.56	0.75	0.87
Leucine	1.58	1.00	1.56	1.43
Phenylalanine	0.60	0.28	0.81	0.71

In addition to amino acids of SS, polyphenols, and flavonoids associated with it also contributed to the biological application. Polyphenols and flavonoids are the secondary metabolites of the plants stored in different parts; leaves, fruits, seeds etc. Leaves are the sole food of silk larvae, which feed on them continuously (Neog et al., 2011). Secondary metabolites present in the leaves are modified in the lumen of the silk larvae by glucosyltransferase, which could transfer glucose residue to the C-5 hydroxy position of quercetin (Butkhup et al., 2012). These secondary metabolites also play an important role in cocoon formation and they attribute to the AO properties along with other biochemical functions; anti-inflammatory and anti-tyrosinase activity (Neog et al., 2011; Park et al., 2008; Yokohira et al., 2008). SS extracted from the cocoons of mulberry

silk varieties are enriched with catechin, epicatechin, resveratrol, quercetin, kaempferol, procyanidin B1, Σ phenolics, naringenin, myricetin, procyanidin B2, rutin, and *trans*-luteolin, however, the percentage of these secondary metabolites varies based on the source (Butkhup et al., 2012). Whereas, SS extracted from the cocoons of Eri lacks naringenin, luteolin, kaempferol, and quercetin (Butkhup et al., 2012). Type of secondary metabolites associated with SS vary based on the feeding habitat of silk larvae and their total content associated with SS vary based on the extraction protocols, which pre-determined SS activity.

Table 1.6. *The amino acid composition of silk sericin extracted from the cocoons of different silk varieties (molar percentage).*

Amino acid	***B. mori* sericin** (Aramwit et al., 2010b)	***A. mylitta* sericin** (Dash et al., 2008)	***A. assamensis* sericin** (Devi et al., 2011)	***C. trifenestrata* sericin** (Yamada and Tsubouchi, 2001)
Serine	33.63	19.78	20.34	39.8
Aspartic acid	15.64	Not determined	5.25	Not determined
Glycine	15.03	16.11	17.94	20.8
Glutamic acid/ glutamine	4.61	5.70	8.52	1.5
Histidine	1.06	10.15	11.34	Not determined
Arginine	2.87	3.36	3.2	2.9
Threonine	8.16	13.22	10.46	13.1
Alanine	4.10	6.01	5.47	4.9
Proline	0.54	1.28	0.84	2.5
Cysteine	0.54	Not determined	Not determined	Not determined
Tyrosine	3.45	2.38	6.2	7.1
Valine	2.88	1.29	1.42	Not determined
Methionine	3.39	Not determined	Not determined	Not determined
Lysine	2.35	2.95	4.2	0.7
Isoleucine	0.56	1.56	1.92	0.8
Leucine	1.00	1.76	1.44	1.1
Phenylalanine	0.28	Not determined	1.12	Not determined

1.2.3.3.2. Cosmetics applications of silk sericin

The biological application like AO activity, inhibition of lipid peroxidation, tyrosinase, and elastase activity, protective effect against UVB radiation-induced oxidative damage and tumor promotion and collagen synthesis makes the SS as a valuable ingredient in food and cosmetic industries. BMS is used in various skin, hair, and nail care cosmetics (Padamwar and Pawar, 2004; Zhang, 2002). SS lotion and cream act as an anti-wrinkling and anti-aging agent by enhancing the elasticity of skin (Ogawa and Yamada, 1999; Yamada et al., 1998). SS gels enhanced hydroxyproline content in the stratum corneum and reduced skin impedance (Padamwar and Pawar, 2004). Gels prepared by blending SS with carbopol and pluronic prevented TEWL and restored NMF of the skin (Padamwar et al., 2005). The powder prepared with a mixture of SS (5-30%) and silk fibroin (70-95%) showed moisture absorbing activity and anti-static features (Kirikawa et al., 2000). Hydrolysate of SS controlled skin problems like dermatitis (Yasuda et al., 1998). Lotions containing 1% (W/W) SS and 4% (W/W) D-glucose acted as moisturizers and conditioners (Yamada et al., 2001b). Creams prepared with 0.001-30% w/w of SS showed increased cleansing effect with less skin irritation (Sakamoto and Yamakishi, 2000). SS hydrolysates coated with iron oxide, mica, talc, titania, and nylon have been used to formulate foundation cream and eyeliners (Yamada and Yuri, 1998). Using SS as an ingredient in sunscreen preparations improves the light screening effect of UV filters; cinnamic acid esters and triazines (Yoshioka et al., 2001). Low molecular weight (300-3000) SS hydrolysates are used as conditioners for skin and hair (Hata, 1987). Nail cosmetics containing SS (0.02–20%) prevented nail brittleness and impart nail gloss (Yamada et al., 2001a). Bath and hair preparations formulated with 0.02-2% SS and 0.01-1% olive oil, fatty acid or their salts showed a reduction of hair damage (Hoppe et al., 1984). Shampoos prepared with SS and pelargonic acid (pH<6) are used for cleaning and care of hairs (Engel and Hoppe, 1988).

MOTIVATION AND OBJECTIVES OF THE PRESENT INVESTIGATION

MOTIVATION AND OBJECTIVES OF THE PRESENT INVESTIGATION

Based on the available literature, as reported in chapter 1, it is quite useful to explore the properties of SS extracted from the different silk varieties, which could provide an opportunity to find a suitable extraction method to extract a potent AO activity possessing SS. The potent AO activity possessing SS could protect skin from oxidative damage, cancer, UVR-induced hyperpigmentation, photodamage, photoaging, and wrinkling. The present investigation and salient motivating factors originated from the following claims:

1. Though exogenous AOs, which are used in skin care cosmetics protects skin against pollutants and UVR-induced damage, however, most of the potential AOs get oxidized by exposure to air and UVRs. They also lack the ability to penetrate through the stratum corneum of the epidermis.
2. Some of the exogenous AOs also cause severe skin damage including contact dermatitis and also do not provide complete protection to skin. Therefore, a potent AO is required that could protect skin against pollutants and UVR-induced damage without getting oxidized by exposure to air and UVRs, while being unable to penetrate into deeper layers of the skin.
3. SS a globular protein polymer envelops the fibroin and helps in cocoon formation and is constantly exposed to air and UVRs. SS protects fibroin and pupa from environmental and biological assaults. SS is subjected to high temperature during its extraction from the cocoons, however, its activity remains intact.
4. SS extracted from the cocoons is known to possess AO activity and suppresses lipid peroxidation, tumor growth, elastase, and tyrosinase activity. SS extracted from the cocoons of BM and AM protected the SKH-1 female hairless mice and human keratinocytes against UVB radiation-induced oxidative damage.
5. Hydrolysate of BMS is used in skin care cosmetics to protect the skin from aging and wrinkling and prevention of TEWL, restoration of skin NMF, and controlling dermatitis. Presence of 30% serine (a major component of an NMF of human skin) makes the SS an excellent moisturizing agent and it is easily

absorbed by the stratum corneum of the skin. Plurality of biological applications have not been investigated using BMS extracted by specific methods.

6. AO activity along with other biological applications of SS can be attributed to its amino acid composition and associated secondary metabolites (flavonoids and polyphenols). The amino acid composition and associated secondary metabolites vary based on the source of SS, feeding habitat of the silk larvae and also on their extraction methods. The amino acids and secondary metabolites composition extracted from the cocoons pre-determines the SS activity. Therefore, exploring the properties of SS from different silk varieties (mulberry and non-mulberry silk varieties) using specific methods could be useful in identifying a potent antioxidant molecule that protects the skin from pollutants and UVR-induced damage.
7. Geographical pocket of the North-Eastern region of India is enriched with different silk varieties; *A. assamensis* (endemic to Assam, India), *P. ricini*, and *B. mori*. SS extracted from these varieties has not been much explored. Investigating the potential properties of SS for its AO activity and other biological properties could be useful to identify suitable/specific silk variety for prospective skin care applications. SS possessing potential antioxidant activity would be used as an ideal AO molecule in skin care formulations. **Fig.1.3** illustrates some of the properties of an ideal AO molecule.

Fig.1.3. *A schematic illustration of an ideal antioxidant molecule which would provide complete protection to the skin against UV radiation and pollutants induced oxidative damage, hyperpigmentation, skin cancer, wrinkling, and aging.*

The vast textile industry of India discards tons of SS as a by-product on a regular basis. Re-channeling such industrial waste into the cosmetic industry for value-added products is envisaged to generate good revenue and boost the sericulture industry. In order to identify potent AO activity possessing SS, we have framed the following essential objectives:

Objectives:

1. Optimization of silk sericin extraction, characterization, and evaluation of its antioxidant potential
2. Exploring the anticancer activity of mulberry and non-mulberry silk sericin
3. Analyzing the protective activity of silk sericin against UV radiation-induced oxidative damage
4. Exploring the inhibitory effects of silk sericin on elastase, hyaluronidase, collagenase, and UV radiation-induced skin aging

5. Exploring the inhibitory effect of silk sericin on tyrosinase and UV radiation-induced hyperpigmentation
6. Formulation and characterization of skin care preparation embedded with silk sericin.

Chapter 2

Optimization of Silk Sericin Extraction, Characterization, and Evaluation of Its Antioxidant Potential

This chapter illustrates the effect of different extraction methods on the molecular weight, secondary structural conformations and free radical scavenging activity of silk sericin along with its protective effect against H_2O_2 induced oxidative damage. Silk sericin extraction, biophysical characterization, biochemical assessment of antioxidant activity and protective effect against H_2O_2 induced oxidative damage are described in detail.

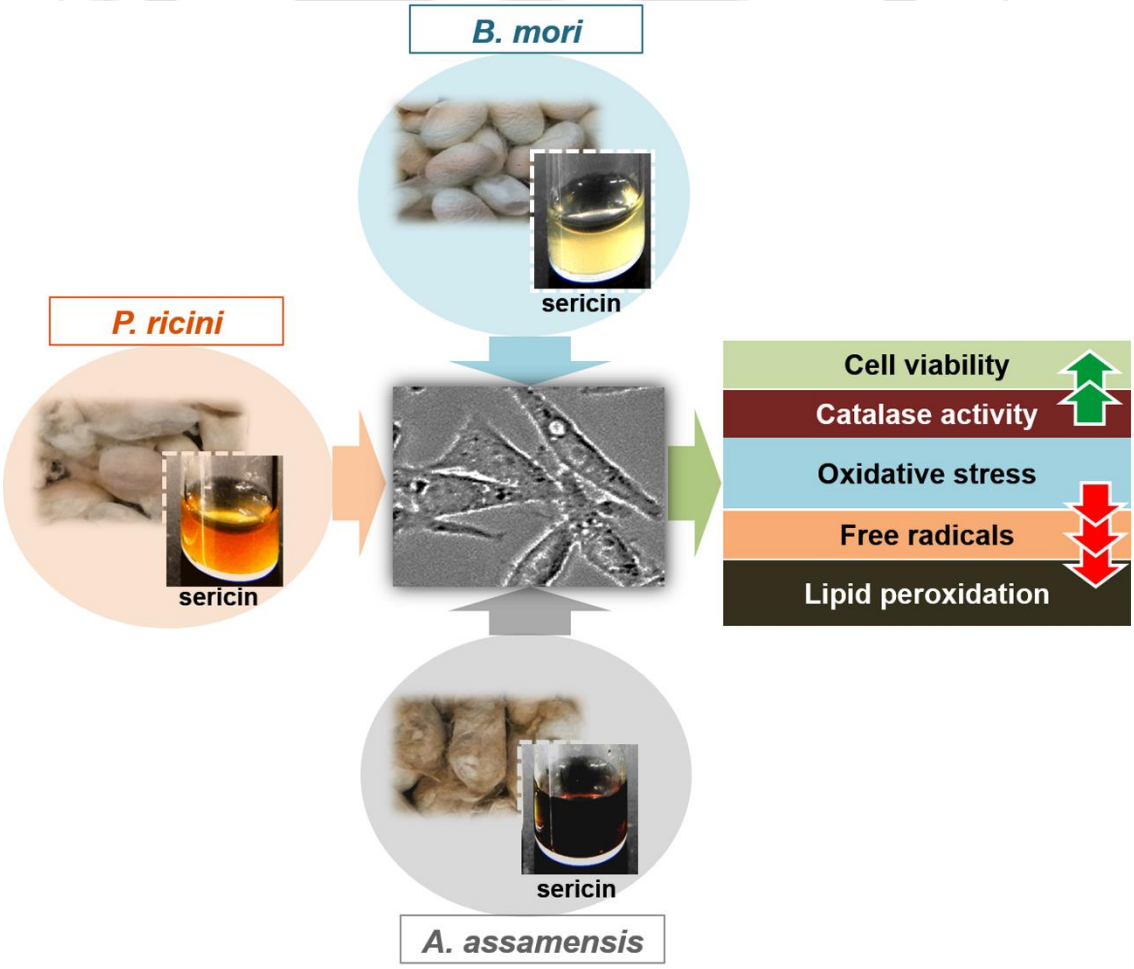

ABSTRACT

Sericin, a principal constituent of silk, is widely used in various biomedical applications. In addition, conferring protection against free radicals and oxidative damage add more value to its therapeutic potential. However, the antioxidant (AO) properties of silk sericin (SS) remains contingent on extraction procedures. In the present study, we have evaluated the effect of different extraction methods (conventional, autoclaving, urea, alkali and acid-degradation) on AO properties of sericin from three Indian silk varieties [*Antheraea assamensis* (AA), *Philosamia ricini* (PR), and *Bombyx mori* (BM)]. The physicochemical characterization studies revealed that the molecular weight of SS isolates of each method ranged from 10 to 220 kDa along with different protein structural biochemistry. SS extracts using urea-degradation (BM, PR, and AA), conventional method and alkali-degradation (BM) displayed a high percentage of β-sheets and random coils and turns. Acid-degraded SS (PR, followed by AA and BM) showed the highest total flavonoid content while conventional method (PR), autoclaving (AA) and alkali-degradation (BM) displayed lowest flavonoid levels. Interestingly, the SS extracted by autoclaving (for BM and AA), acid-degradation (for PR), conventional and alkali-degradation (for BM, AA, and PR) methods exhibited 50% reduction of 2, 2-diphenyl-1-picrylhydrazyl (DPPH) radical. Moreover, the efficacy of AO potential of SS extracted by different methods was found to be in the order of "alkali > autoclaving > conventional" methods of extraction in L929 cells. Correspondingly, the ALP activity of SS extracted by alkali method (for AA, BM, and PR) further confirmed the better AO properties amid others. Thus, the present study demonstrates that the extraction methods may affect AO activity of SS which might be important for potential cosmetic applications.

2.1. Introduction

Silk sericin (SS) is a glycoprotein, which is produced in the lumen of insects (silkworms) of Bombycidae and Saturniidae family (Dash et al., 2007). It comprises of 18 types of amino acids among which serine, histidine, glycine, threonine, tyrosine, aspartic acid, and glutamic acid are predominant (Aramwit et al., 2010c). Owing to diverse biological activities such as antioxidation (Takechi et al., 2014), anti-elastase (Chlapanidas et al., 2013), anticoagulation, suppression of lipid peroxidation and tyrosinase (Kato et al., 1998), biodegradability and proteinous nature, sericin is referred as a apposite material for biomedical applications and tissue engineering.

Earlier in an elegant study, Zhaorigetu and his group demonstrated that sericin has protective effects against UVB radiations. It reduces UVB radiation-induced oxidative damage and tumor promotion (Zhaorigetu et al., 2003). Further, in another report, the wound healing properties via enhancement in collagen synthesis has also been accounted with sericin (Ersel et al., 2016). Characteristically, it is apprehended that the properties of SS are attributed to the composition of its amino acids. Accordingly, it has been reported that the factors including hydroxyl groups of serine and threonine (Kato et al., 1998), the delocalizing electrons of aromatic acids (Fan et al., 2009) and the associated polyphenols (secondary metabolites) contribute to its distinct antioxidant (AO) properties. However, the associated amino acid composition, peptide length, molecular weight (10 to 400 kDa) and polyphenols content of SS may vary with their extraction methods (Butkhup et al., 2012). The dynamics of pH, temperature, chemicals and processing time will affect their molecular and functional properties (Aramwit et al., 2012; Gimenes et al., 2014). Previously, it has been shown that *Bombyx mori* sericin (BMS) extracted by acid and heat method showed a molecular weight ranging from 35-150 kDa whereas when alkali-degradation was used it ranged from 15-75 kDa (Aramwit et al., 2010a). Off note that the functional properties of SS could vary with their molecular weight (Aramwit et al., 2010a; Kurioka et al., 2004). The impact of alkali, acid, and urea-degradation extraction methods on thermal behavior and tyrosinase inhibition activity has also been underscored (Aramwit et al., 2010a). In fact, a marked difference in trypsin inhibitor activity was noticed when SS was extracted by either aqueous, alkali or acid solution (Kurioka et al., 2004). However, the effect of different extraction methods on secondary structure, solubility and AO potential of sericin is yet to be mapped.

The North-Eastern region of India is enriched with wild and domestic varieties of silk such as *Antheraea assamensis* (AA; endemic to Assam, India), *Philosamia ricini* (PR), and *B. mori* (BM). Previously, the AO potential of BM with respect to their extraction methods has been reported, however, the AO property of AA sericin (AAS) and PR sericin (PRS) has not been explored yet. Therefore, in this study, we have investigated the effect of different extraction methods on the SS extracted from these sources and evaluated its resultant AO property. We extracted SS from the cocoon of AA, PR, and BM by using autoclaving (high temperature under high pressure), the conventional method, urea, alkali, and acid-degradation methods. After extraction, the physicochemical characterization of isolated SS from each method was accomplished. Also to confirm the effect of extraction procedures on AO property of extracted SS, the biochemical assessment (FRAP, DPPH activity) followed by *in vitro* screening for protection from exogenous oxidants (hydrogen peroxide; H_2O_2) using L929 cells was performed. Our data clearly demonstrated that different extraction methods play an important role in preserving or augmenting AO potential of SS obtained from different varieties.

2.2. Materials and Methods

2.2.1. Materials

Sodium carbonate, urea, citric acid, dimethyl sulfoxide (DMSO) were sourced from SRL, India; Tris-HCl, sodium dodecyl sulfate (SDS), β-mercaptoethanol, glycerol, Coomassie brilliant blue G-250, sodium chloride, glycerol, trichloroacetic acid (TCA), α-tocopherol (Vit. E) were obtained from Himedia, India, and BenchMark™ protein ladder was supplied by Life Technologies, USA. Gallic acid, (+)-catechin, folin-ciocalteu reagent, sodium nitrite, aluminum chloride, ferric chloride, 2, 4, 6-Tris (2-pyridyl)-s-triazine (TPTZ), sodium acetate, iron (II) sulfate, 2,2-diphenyl-1-picrylhydrazyl (DPPH), thiazolyl blue tetrazolium bromide (MTT), dichloro-dihydro-fluorescein diacetate (DCFH-DA), nonidet P-40 (NP-40), sodium orthovanadate ($NaVO_3$), phenylmethylsulfonyl fluoride (PMSF), aprotinin, thiobarbituric acid (TBA), Trypan Blue, ascorbic acid (Vit. C), and LDH assay kit were sourced from Sigma, USA, sodium hydroxide, hydrochloric acid, hydrogen peroxide and acetic acid were obtained from Merck, India.

2.2.2. Extraction of silk sericin

2.2.2.1. Extraction of silk sericin by high temperature under high pressure (autoclaving)

SS was extracted from the cocoons using a modified protocol of Aramwit *et al*. (2010b). In brief, small pieces of cocoons were autoclaved in double distilled water (ddH_2O) at 120 °C, 15 lbs pressure for 20 min. The obtained protein solution was centrifuged followed by filtration to separate the silk fibroin along with other solid residues. The filtrate was frozen at -20 °C then lyophilized for 24 h and finally stored at -20 °C until further use.

2.2.2.2. Extraction of silk sericin by urea-degradation

SS from the cocoons was extracted using protocol reported by Tsubouchi *et al*. (2005) with few modifications. Briefly, 5 gm of freshly cut cocoon pieces were soaked in 8 M urea (100 mL) for 30 min followed by heating at 85 °C for 30 min. Post-treatment, SS solution was subjected to centrifugation and filtration to remove silk fibroin and other residues. The SS solution was then dialyzed (cellulose tube with MWCO of 12 kDa) for 48 h against ddH_2O with frequent changes. Dialyzed SS solution was freeze-dried and stored at -20 °C.

2.2.2.3. Extraction of silk sericin by acid and alkali-degradation

Acid and alkali-degraded SS was extracted from the cocoons using the modified protocol of Kurioka *et al*. (2004). Briefly, cocoons were cut into small pieces and soaked in 1.25% citric acid (for acid-degradation) or 0.5 M sodium carbonate (alkali-degradation) solution (5 gm/100 mL) and boiled for 30 min. Post boiling, silk fibers were removed followed by filtration and centrifugation. The obtained supernatant was dialyzed and pH of the final protein solution was measured to verify the removal of citric acid or sodium carbonate. Dialyzed protein solution was freeze-dried and preserved at – 20 °C.

2.2.2.4. Silk sericin extraction by a conventional method

SS from the cocoons was extracted using the protocol of kumar *et al*. (2016). In brief, small pieces of cocoons were boiled (5 gm/L) in 0.02 M sodium carbonate for 30 min. After removing fibroin, the protein solution was concentrated to 10 mL. Debris was removed by filtration and centrifugation. The obtained solution was dialyzed followed by freeze-drying and stored at -20 °C.

2.2.3. Biophysical characterization

2.2.3.1 SDS-PAGE

30 µL of aqueous SS solution (10 mg/mL) was mixed with 30 µL of sample buffer (1 M Tris-HCl (pH 6.8), 2% SDS, 12% β-mercaptoethanol, 20% glycerol) followed by heating at 95 °C for 5 min. SDS-PAGE was performed using a 10% resolving gel. Post running, the gel was washed with ddH_2O and stained with Coomassie brilliant blue G-250. BenchMark^{TM} protein ladder was used as a molecular weight standard.

2.2.3.2. Fourier transform infrared spectroscopy (FTIR)

IR spectra of SS extracted from the cocoons were recorded by FTIR spectrophotometer (Nicolet iS 10) equipped with a TE cooled DTGS detector. IR spectra in the transmittance mode were obtained in the spectral region of 1000-1800 cm^{-1}.

2.2.3.3. Circular dichroism (CD) spectroscopy

Secondary structural orientation of SS in an aqueous environment was determined using CD spectropolarimeter (Jasco, J-815), using quartz cuvette at 25 °C. CD spectra of SS were collected within the range of 240-190 nm, with 3 scans at 100 nm/min, response time constant was 0.25 s, bandwidth was 1 nm, and slit width was 500 µm. Obtained spectra were background corrected, and results expressed in terms of molar ellipticity (θ).

2.2.4. Estimation of total secondary metabolites

2.2.4.1. Determination of total phenolic content

Total phenolic content present in 1 mg of SS was determined by using folin-ciocalteu reagent as described by Butkhup *et. al*. (2012). In brief, 12.5 µL of SS (1 mg/mL) was first mixed thoroughly with 12.5 µL of ddH_2O followed by 12.5 µL of pre-diluted (10 times with ddH_2O) folin-ciocalteu reagent and then incubated for 6 min. Post incubation, 125 µL of 7% sodium carbonate and 100 µL of ddH_2O were added and the reaction mixture incubated for 90 min at room temperature. Absorbance was measured at 760 nm using multiplate reader (Tecan, infinite M200). Gallic acid was used as a standard to quantify the total phenolic content present in SS. The results were expressed as mg gallic acid equivalents (GAE)/10 gm.

2.2.4.2. Determination of total flavonoid content

Total flavonoid content present in 1 mg of SS was determined using a previously reported colorimetric assay (Butkhup et al., 2012). In brief, 25 µL of SS (1 mg/mL) was added to 125 µL of ddH_2O followed by the addition of 7.5 µL of 5% sodium nitrite and

incubated for 5 min. Post incubation, 15 µL of 10% aluminum chloride was added and incubated at room temperature for 5 min. 50 µL of 1 M sodium hydroxide was added to stop the reaction followed with an immediate dilution using 27.5 µL ddH_2O. The absorbance of reaction mixture was taken at 510 nm using multiplate reader (Tecan, infinite M200). Total flavonoid content present in SS was quantified from the (+)-catechin standard curve. Obtained results were exhibited as mg (+)-catechin equivalents (CE)/10 gm.

2.2.5. Biochemical assays to determine antioxidant properties

2.2.5.1. Ferric ion reducing antioxidant power (FRAP) assay

The ability of SS to convert Fe^{3+} to Fe^{2+} was studied with the protocol of Butkhup *et al.* (2012). FRAP reagent was prepared from 1:1:10 (v/v/v) ratio of 20 mM ferric chloride, 10 mM TPTZ in 40 mM HCl and 300 mM acetate buffer (pH 3.6). FRAP reagent was warmed at 37 °C. 30 µL of SS (1 mg/mL) was added separately to 270 µL of the FRAP reagent followed by incubation at room temperature for 30 min. Post incubation, absorbance was taken at 595 nm by using a multiplate reader (Tecan, infinite M200). Conversion of Fe^{3+} to Fe^{2+} was quantified using the standard curve of iron (II) sulfate. The results were expressed as Fe (II) mg/10 gm.

2.2.5.2. 2, 2-diphenyl-1-picrylhydrazyl (DPPH) scavenging activity of silk sericin

DPPH scavenging activity of SS was evaluated based on the method proposed by Akowuah *et al*. (2005). In brief, 100 µL of different concentration of SS or vitamin C (Vit. C) (as a positive control) was added to 100 µL of 0.2 mM DPPH (dissolved in methanol) and incubated in the dark for 1 h. Post incubation, the absorbance was taken at 520 nm using multiplate reader. The DPPH scavenging ability of SS was calculated using the following equation:

$$\text{Scavenging activity} = \frac{\text{Absorbance of sample at 520 nm}}{\text{Absorbance of control at 520 nm}} \times 100 \qquad (2.1)$$

2.2.6. *In vitro* antioxidant potential

2.2.6.1. Cell culture

Mouse fibroblast (L929) cells were procured from the National Centre for Cell Science (NCCS), Pune, India. L929 cells were maintained in Dulbecco's modified Eagle's medium (DMEM) with low glucose (Gibco, USA), supplemented with 10% fetal bovine serum (FBS) (Gibco, USA), 100 units/mL antibiotic and antimycotic solution (Himedia, India) and 10 mM non-essential amino acid (Sigma, USA).

2.2.6.2. Cytocompatibility assay

Cytocompatibility of SS was assessed using MTT assay. L929 cells were plated at a density of 1×10^4 cells per well in 96-well plate and incubated for 12 h at 37 °C in 5% CO_2. Post incubation, media was replaced with fresh media containing different concentration (10, 50, 100, 200, 400 μg/mL) of SS and incubated for 24 h. 10:1 ratio of phosphate buffer saline (PBS) and MTT solution (5 mg/mL in PBS at pH 7.4) was added to each well after 24 h of treatment with SS. Post incubation, MTT solution was removed and formazan crystals were solubilized in DMSO. The absorbance was taken by multiplate reader at 570 nm.

2.2.6.3. Sensitivity of L929 cells to H_2O_2

H_2O_2 induced cell death was analyzed by using MTT assay. 1×10^4 cells per well were plated in 96-well plate and incubated for 12 h. Post incubation, spent media was replaced with fresh medium containing H_2O_2 of different molarity (10, 50 and 100 μM) and incubated for 24 h. Post incubation, cells were treated with MTT solution. After 4 h of incubation, MTT solution was removed and formazan crystals were solubilized in DMSO. Absorbance was recorded by multiplate reader at 570 nm.

2.2.6.4. Protective action of silk sericin against H_2O_2 induced cell death

Protective action of SS against H_2O_2 induced cell death was evaluated by MTT assay. L929 cells were plated at a density of 0.5×10^4 cells per well in 96-well plate and incubated for 12 h at 37 °C. Post incubation, cells were pretreated with different concentration (10, 50 and 100 μg/mL) of SS for 24 h. After pre-treatment, cells were treated with 100 μM H_2O_2 and incubated for 24 h. Post incubation, cell were treated with MTT and incubated for a further 4 h. After completion of incubation, MTT was removed and the insoluble formazan crystals were solubilized in DMSO. Absorbance was measured by multiplate reader at 570 nm.

The MTT assay was further used to evaluate the ability of the SS treated cells to recover from the induction of H_2O_2 mediated oxidative stress. The medium containing H_2O_2 was replaced with fresh medium and incubated for 72 h. Post 72 h, MTT was added to each well and incubated for 4 h. After 4 h, MTT was removed and the formazan crystals were solubilized in DMSO. The absorbance was recorded by microplate reader at 570 nm.

2.2.6.5. Trypan Blue exclusion assay

Protection of cells against H_2O_2 induced oxidative damage by SS was assessed using Trypan Blue exclusion studies. In brief, 2×10^4 cells per well were plated in 24 well plate and incubated for 12 h. Post incubation, cells were treated with different concentration of SS (10, 50 and 100 µg/mL). After 24 h, cells were treated with 100 µM H_2O_2. Post-treatment, cells were trypsinized and complete media was added to neutralize the trypsin activity followed by centrifugation at 1000 rpm for 5 min. After centrifugation, the supernatant was discarded followed by re-suspension in 1 mL PBS. 20 µL of sample was mixed with 20 µL of Trypan Blue (0.4% Trypan Blue stock) and cells were counted using hemocytometer. The percentage of viable cells was calculated using following formula:

$$\text{Viable cells (\%)} = \frac{\text{Total no.of viable cells per mL of aliquot}}{\text{Total no.of cells per mL of aliquot}} \times 100 \qquad (2.2)$$

2.2.6.6. Lactate dehydrogenase (LDH) assay

Protective action of SS cells from oxidative stress was further determined by LDH activity using LDH assay kit. Briefly, 0.5×10^4 cells per well were plated in 96 well and incubated for 12 h. Post incubation, cells were pretreated with SS for 24 h. After 24 h, cells were treated with 100 µM H_2O_2. Post-treatment, 50 µL of media was collected and treated with substrate as described by the manufacturer's protocol. The reaction mixture was incubated at 37 °C for 2-3 min and initial absorbance was taken at 450 nm using multiplate reader (Tecan, infinite M200). The reaction mixture was incubated at 37 °C and absorbance were recorded every 5 min until the value of the most active sample was greater than the value of the highest standard. A standard curve of NADH (2.5, 5, 7.5, 10 and 12.5 nmol/well) was prepared. The amount of NADH generated by the kinase assay between the initial time point ($T_{initial}$) and final time point (T_{final}) was calculated from the standard curve. The LDH activity of a sample was determined by the following equation:

$$\text{LDH activity} = \frac{B \times \text{Sample dilution factor}}{(\text{Reaction time}) \times V} \times 100 \qquad (2.3)$$

Where B= Amount (nmol) of NADH generated between $T_{initial}$ and T_{final}

Reaction time= T_{final} - $T_{initial}$ (minutes)

V= Sample volume (mL) added to well

2.2.6.7. Determination of intracellular antioxidant activity of silk sericin

Intracellular antioxidant properties of SS were assessed using the protocol described by Rakkestad *et al*. (2010) with some modifications. Briefly, 1×10^4 cells per well were plated in 96-well plate and incubation for 24 h. Post incubation spent media was removed and fresh media was added which contained different concentrations (10, 50 and 100 µg/mL) of SS and 10 µM of DCFH-DA; this mixture was incubated for 1 h. Post incubation, media was removed and the cells were washed with PBS. Medium containing 200 μL of 4 mM H_2O_2 was added and incubated for an hour. Control cells were treated with DCFH-DA plus H_2O_2 and blank wells were treated with only DCFH-DA and further incubated for 60 min. Post incubation, fluorescence was measured in multiplate reader with λ_{ex} 488 nm and λ_{em} 530 nm.

2.2.6.8. Catalase (CAT) assay

10 and 100 µg/mL of SS that exhibited better cell protection (on day 1 and 3) were selected and evaluated for their CAT activity by Amplex red catalase assay kit (Life science). Briefly, 1×10^6 L929 cells per sample were lysed with 200 µL cell lysis buffer (2 mM Tris-HCl, pH 8.0, 1% NP-40, 13.7 mM NaCl, 10% glycerol, 1 mM $NaVO_3$, 1 mM PMSF and 2 µg/mL Aprotinin) for 20 min on ice. Lysates were centrifuged at 14000 rpm for 15 min at 4 °C. The supernatant of each sample was pretreated with SS and incubated for 30 min at 37 °C. 25 µL of sample was taken to analyze the catalase activity, using the Amplex red catalase assay kit (according to the manufacturer's protocol). Vit. C and arbutin (10 and 100 µg/mL) were used as positive controls.

2.2.6.9. Anti-lipid peroxidation activity of silk sericin

Anti-lipid peroxidation (ALP) activity of SS was determined using previously reported protocol (Konwarh et al., 2011), after modification. Briefly, 1×10^6 L929 cells per sample were used for ALP assay. Post trypsinization, L929 cells were spun down by centrifugation (1000 rpm, 10 min). The cell pellets were washed with ice-cold PBS (pH 7.4) and centrifuged (1000 rpm, 10 min). Cell lysates (1×10^6 cells per 0.4 mL ice-cold PBS) were prepared by sonication (SONICS, VC-505, 20 kHz, and acoustic power density 500 W/cm^2, USA) for 20 s (with 5 s/5 s ON/OFF pulse cycle) over ice. 0.4 mL of cell lysate was pretreated with 100 µL of different concentrations of SS (10 and 100 µg/mL). The reaction mixture was incubated at 37 °C for 30 min. Post incubation, reaction mixtures were treated with 4 mM H_2O_2 and incubated for 30 min. To stop the reaction, 1 mL of 10% TCA-0.67% TBA in acetic acid (50%) was added and heated for

1 h at 95 °C. Post heating, the reaction mixture was cooled to room temperature and centrifuged (10,000 rpm, 10 min). 200 µL of supernatant was taken in 96 well plates and absorbance was recorded at 535 nm. Similar experiments were conducted to determine the absorbance in peroxidation (with H_2O_2) induced cells and control. Vit. E and Vit. C were used as the positive controls in this study (Ferreira et al., 2009). Percentage of ALP was estimated using the following formula:

$$\%\text{ALP} = \frac{\text{Abs of } H_2O_2 \text{ induced peroxidation} - \text{Abs of sample}}{\text{Abs of } H_2O_2 \text{ induced peroxidation} - \text{Abs of control}} \times 100 \qquad (2.4)$$

Where Abs represents absorbance at 535 nm.

2.7. Statistical analysis

All experiments were carried out three times in triplicates. Results were expressed as mean ± SD for n=3. Statistical analysis was performed using one-way analysis of variance (ANOVA) with Holm-Sidak method. Statistical difference between groups in the range of $p \leq 0.005$ was considered statistically significant and values in the range of $p \leq 0.001$ as highly significant.

2.3. Results

2.3.1. SDS-PAGE

Fig.2.1 shows the 10% SDS-PAGE gels exhibiting the molecular weight (10 kDa to 220 kDa) distribution of BMS, AAS, and PRS after extracting from the cocoons using urea-degradation, autoclaving, conventional, acid and alkali-degradation methods. BMS extracted using urea-degradation exhibited clear band pattern with a molecular weight ranging from 10 to 120 kDa and PRS showed smear with a clear band at 75 kDa. Whereas, AAS extracted using urea-degradation exhibited smear. Acid-degraded BMS and PRS showed smear, however, AAS displayed clear band at 75 kDa. BMS, AAS and PRS extracted by autoclaving exhibited only smear without any clear bands. BMS, AAS, and PRS extracted using alkali-degradation displayed smear along with a clear band at 75 kDa. SS extracted from the BM and AA cocoons using conventional method displayed smear, whereas the PRS showed clear bands at 75 kDa along with smear. Extraction of SS using different methods thus resulted in variation in their molecular weight distribution.

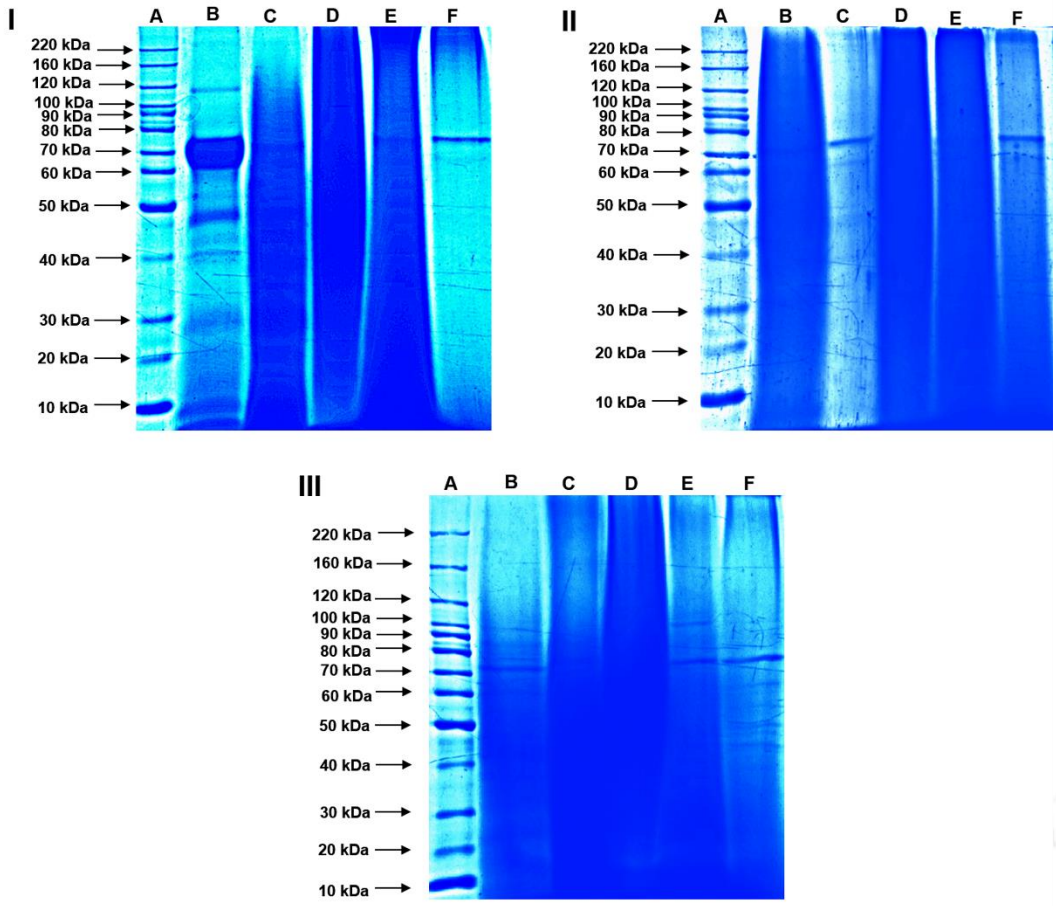

Fig.2.1. *Molecular weight distribution of silk sericin extracted from cocoons using different extraction methods analyzed by SDS-PAGE. 10% SDS page gel showing bands of (A) protein ladder and silk sericin extracted from (I) BM, (II) AA, and (III) PR using (B) urea-degradation, (C) acid-degradation, (D) autoclaved, (E) conventional method, and (F) alkali-degradation.*

2.3.2. Fourier transform infrared (FTIR) spectroscopy

The conformational changes in the secondary structure of SS extracted by various methods were investigated by FTIR (**Fig.2.2**) spectroscopy. SS exhibits characteristic protein bands, namely the amide I (corresponding to C=O stretching) in the range of 1610-1695 cm^{-1}, amide II (corresponding to N-H bending) in the range 1508-1570 cm^{-1} and amide III (C-N stretching vibration) in the region of 1243 cm^{-1} (Mandal et al., 2011). BMS, PRS, and AAS extracted using urea and acid-degradation displayed characteristic amide I peaks in the region of 1624 and 1650 cm^{-1} which represent the presence of β-sheets and random coils in SS. SS extracted using autoclaving from the cocoons of BM and PR exhibited characteristic amide I peak in the 1624 and 1650 cm^{-1}, however, AAS showed a peak at only 1650 cm^{-1}. BMS and PRS showed the presence of β-sheets and

random coils, whereas β-sheets were absent in AAS. SS extracted using conventional and alkali-degradation methods showed characteristic amide I peak in the region of 1652 cm^{-1}, which indicated the presence of α-helical structure (Kumar et al., 2016).

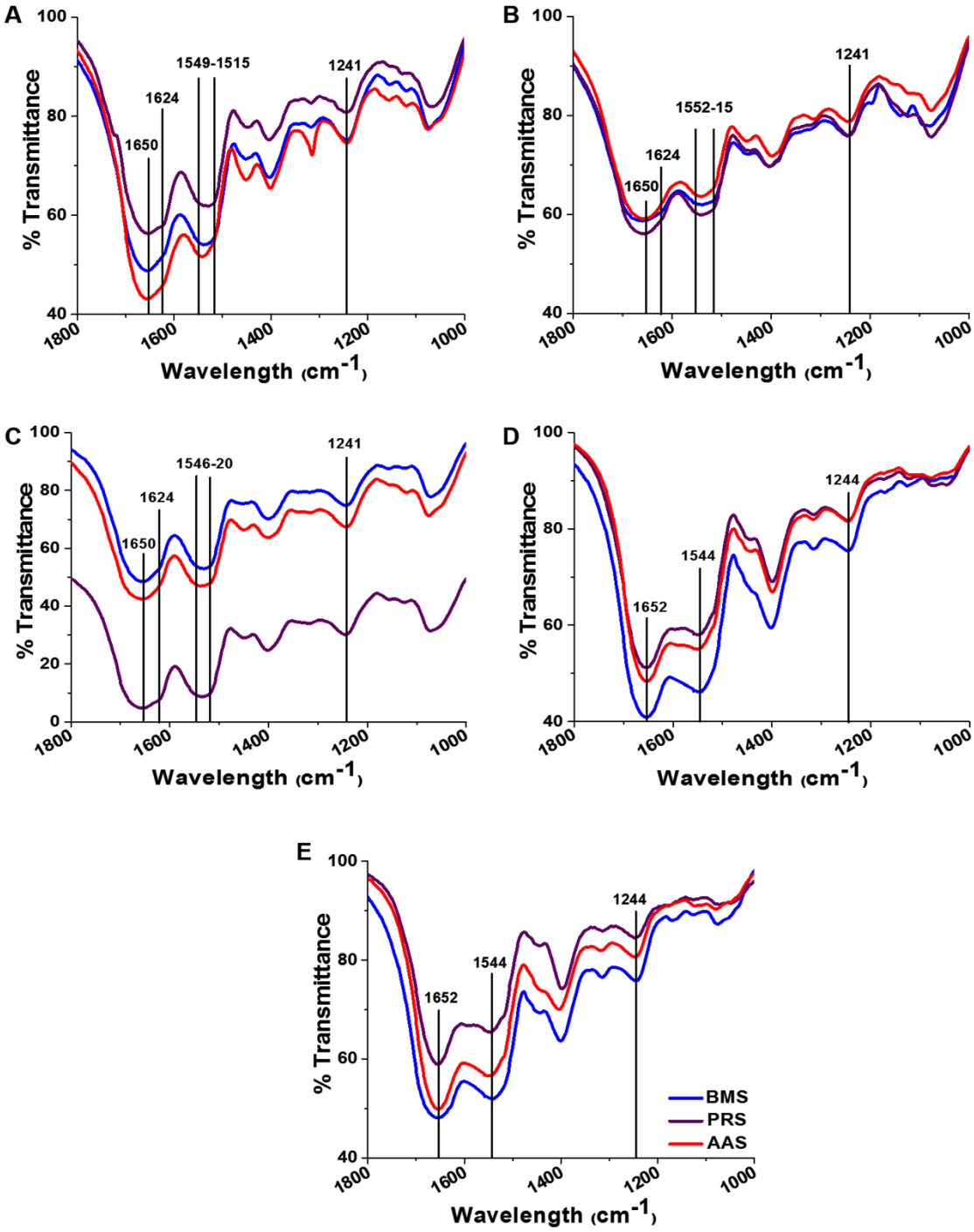

Fig.2.2. *FTIR spectra of silk sericin extracted from the cocoons of BM, PR, and AA using (A) urea-degradation, (B) autoclaving, (C) acid-degradation, (D) conventional method and (E) alkali-degradation.*

2.3.3. Circular dichroism (CD) spectroscopy

Secondary structural orientation of SS in aqueous medium was investigated by far-UV CD spectroscopy. The CD spectral pattern of PRS, BMS, and AAS extracted by various methods are depicted in **Fig.2.3**. Percentage of distribution of α–helix, β-sheet, random coil and turns in SS are given in **Table 2.1**. The % of α–helix, β-sheet, random coil and turns in SS varied depending on the extraction method. SS extracted from the BM, PR and AA cocoons using urea-degradation displayed high percentage (%) of β-sheets and random coils that represented the native conformation. PRS extracted using autoclaving, acid-degradation, conventional method and alkali-degradation exhibited different % of α–helix, β-sheet, random coil, and turns. SS extracted from the cocoons of BM by conventional methods and alkali-degradation displayed presence of α–helix, random coil and turns. Whereas, α–helical structures were absent in BMS extracted by autoclaving. AAS extracted by all methods with the exception of urea-degradation displayed an absence of β-sheet in their secondary structure.

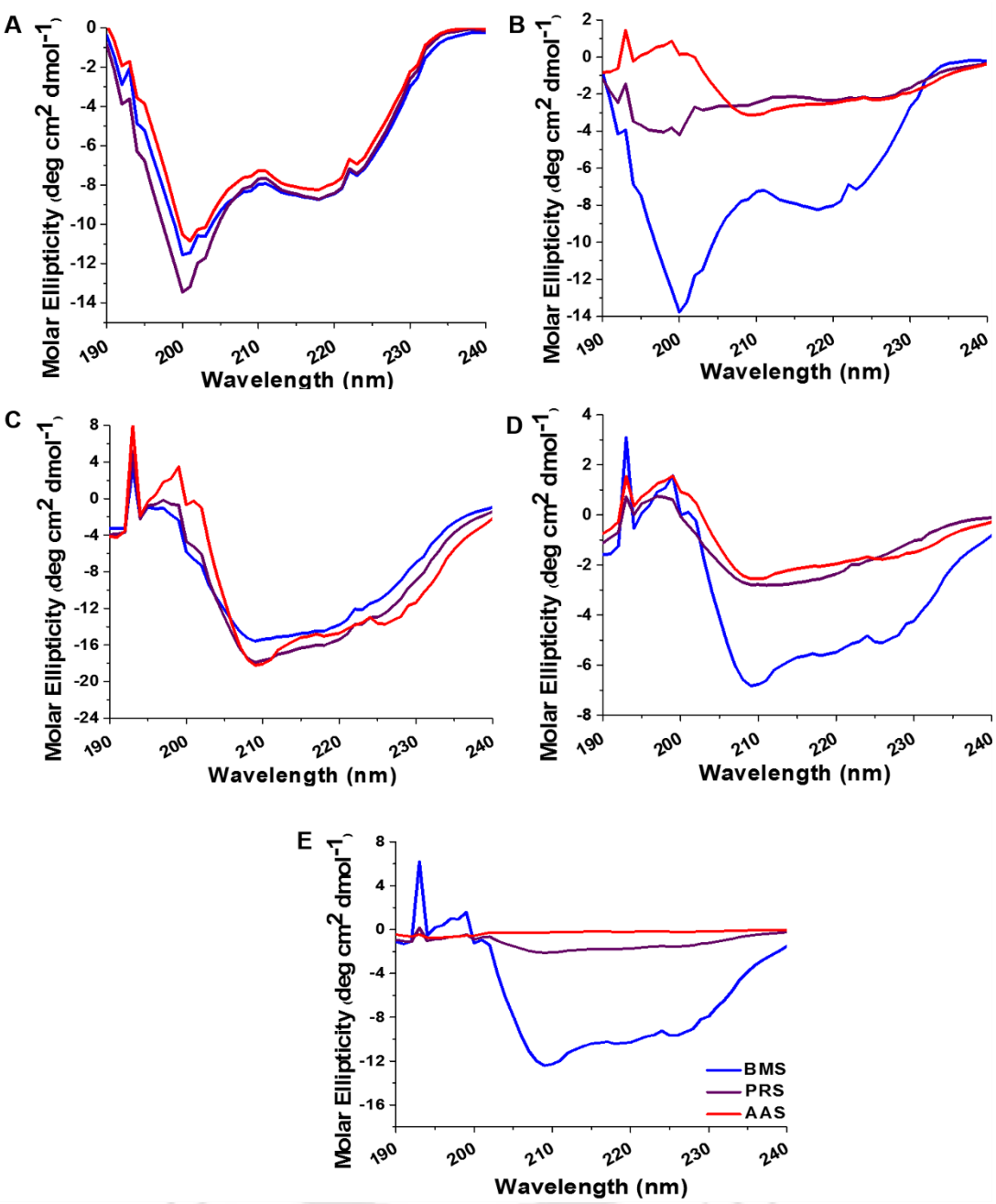

Fig.2.3. *Secondary structural distribution by CD-spectroscopy. Far UV spectra of silk sericin extracted from the cocoons of BM, PR, and AA using (A) urea-degradation, (B) autoclaving, (C) acid-degradation, (D) conventional methods, and (E) alkali-degradation.*

Table 2.1. *Distribution of % of α–helix, β-sheet, random coil and turns based on their extraction methods.*

Extraction method	Silk variety	% Secondary structure			
		Helix	Beta	Turns	Random coils
Urea-degradation	*B. mori*	2.8	54.5	4.0	38.7
	P. ricini	0.0	58.9	1.6	39.5
	A. assamensis	0.0	62.6	0.0	36.7
Autoclaved	*B. mori*	0.0	56.2	2.5	41.3
	P. ricini	2.0	12.1	24.8	51.0
	A. assamensis	29.0	0.0	35.5	35.5
Acid-degradation	*B. mori*	14.9	34.8	17.0	33.3
	P. ricini	18.5	25.7	21.8	34.0
	A. assamensis	28.4	0.0	34.9	36.7
Conventional	*B. mori*	28.8	0.0	35.1	36.1
	P. ricini	15.1	40.8	16.4	27.8
	A. assamensis	32.0	0.0	37.1	30.8
Alkali-degradation	*B. mori*	28.5	0.0	33.8	37.8
	P. ricini	21.0	10.1	29.8	38.9
	A. assamensis	10.9	0.0	34.9	54.2

2.3.4. Total phenolic content

Phenolic content varied with the extraction procedure. Total phenolic content present along with SS has been determined by using folin-ciocalteu reagent (**Table 2.2**). SS extracted from the cocoons of PR, BM and AA by urea-degradation showed less

phenolic content. Whereas, increased phenolic content was obtained for BM and AA by autoclaving method in comparison with alkali-degradation, conventional, acid and urea-degradation, respectively. Whereas, SS extracted from the cocoons of PR by alkali-degradation exhibited higher phenolic content. The free radical scavenging and antioxidant attribute of the polyphenols endow SS with biological relevance.

Table 2.2. *Total phenolic content of mulberry and non-mulberry silk sericin extracted through different methods.*

Silk varieties	**Extraction methods**	**Total phenol content (mg GAE/10 gm)**
P. ricini	Conventional	377.26 ± 13.70
	Autoclaving	353.69 ± 15.36
	Urea-degradation	247.38 ± 15.25
	Alkali-degradation	424.40 ± 12.78
	Acid-degradation	276.90 ± 9.62
B. mori	Conventional	253.40 ± 9.10
	Autoclaving	319.40 ± 5.70
	Urea-degradation	200.23 ± 13.50
	Alkali-degradation	257.73 ± 12.00
	Acid-degradation	256.07 ± 12.37
A. assamensis	Conventional	427.38 ± 31.90
	Autoclaving	497.50 ± 21.65
	Urea-degradation	285.35 ± 10.29
	Alkali-degradation	488.92 ± 26.10
	Acid-degradation	401.30 ± 10.68

2.3.5. Total flavonoid content

Total flavonoid content in the SS (extracted from the cocoons of PR, BM, and AA) are given in **Table 2.3**. In comparison to other treatments acid-degraded SS showed the highest total flavonoid content in PR, followed by AA and BM, respectively. Lowest flavonoid yields resulted when PR was extracted by a conventional method; followed by AA by autoclaving and finally BM by alkali-degradation. Among all extraction methods, PRS showed highest total flavonoid content when acid-degradation was used and it showed lowest flavonoid content when conventional methods were used.

Table 2.3. *Total flavonoid content of PRS, BMS, and AAS extracted by different methods.*

Silk varieties	Extraction methods	Total flavonoid content (mg CE/10 gm)
P. ricini	Conventional	63.89 ± 33.29
	Autoclaving	750.04 ± 33.29
	Urea-degradation	439.44 ± 29.92
	Alkali-degradation	369.89 ± 11.35
	Acid-degradation	2513.55 ± 49.83
B. mori	Conventional	328.79 ± 47.81
	Autoclaving	381.00 ± 47.45
	Urea-degradation	539.93 ± 46.80
	Alkali-degradation	210.01 ± 30.09
	Acid-degradation	708.80 ± 54.49
A. assamensis	Conventional	228.81 ± 30.95
	Autoclaving	228.01 ± 29.55
	Urea-degradation	541.12 ± 54.52
	Alkali-degradation	432.11 ± 57.02

Acid-degradation	745.33 ± 66.51

2.3.6. Ferric reducing ability of plasma (FRAP) assay

FRAP is a simple and reproducible assay to evaluate the antioxidant properties of dietary polyphenols (Al-Duais et al., 2009; Antolovich et al., 2002). Conversion of Fe^{3+} to Fe^{2+} by PRS, BMS, and AAS extracted by various methods are given in **Table 2.4**. Fe^{3+} to Fe^{2+} reduction ability of SS was dependent on the extraction methods. Maximum Fe^{3+} to Fe^{2+} reduction ability was shown by AAS extracted using a conventional method and minimum reduction was shown by the BMS extracted by acid-degradation. In general, AAS showed maximum Fe^{3+} to Fe^{2+} reducing ability followed by PRS and BMS.

Table 2.4. *Ferric to ferrous conversion ability of mulberry and non-mulberry silk sericin extracted by different methods.*

Silk varieties	**Extraction methods**	**Ferric to ferrous conversion (Fe^{2+} mg/10 gm)**
P. ricini	Conventional	323.91 ± 16.60
	Autoclaving	222.06 ± 9.30
	Urea-degradation	217.77 ± 8.75
	Alkali-degradation	130.19 ± 4.80
	Acid-degradation	57.60 ± 4.11
B. mori	Conventional	101.17 ± 3.50
	Autoclaving	214.67 ± 5.46
	Urea-degradation	116.70 ± 9.15
	Alkali-degradation	90.36 ± 4.24
	Acid-degradation	19.41 ± 0.98
A. assamensis	Conventional	430.39 ± 4.88

Autoclaving	298.15 ± 10.11
Urea-degradation	251.34 ± 14.27
Alkali-degradation	190.85 ± 7.08
Acid-degradation	129.45 ± 1.60

2.3.7. DPPH scavenging activity of silk sericin

Based on the extraction methods the DPPH scavenging activities varied with the concentration of SS. % of DPPH reduction after treating with different concentration of SS and Vit. C are depicted in **Fig.2.4**. SS extracted from the cocoons of BM and AA by alkali-degradation, conventional and autoclaving methods exhibited DPPH 50% reduction. PRS extracted by conventional, alkali and acid-degradation and conventional methods also resulted in 50% DPPH reduction.

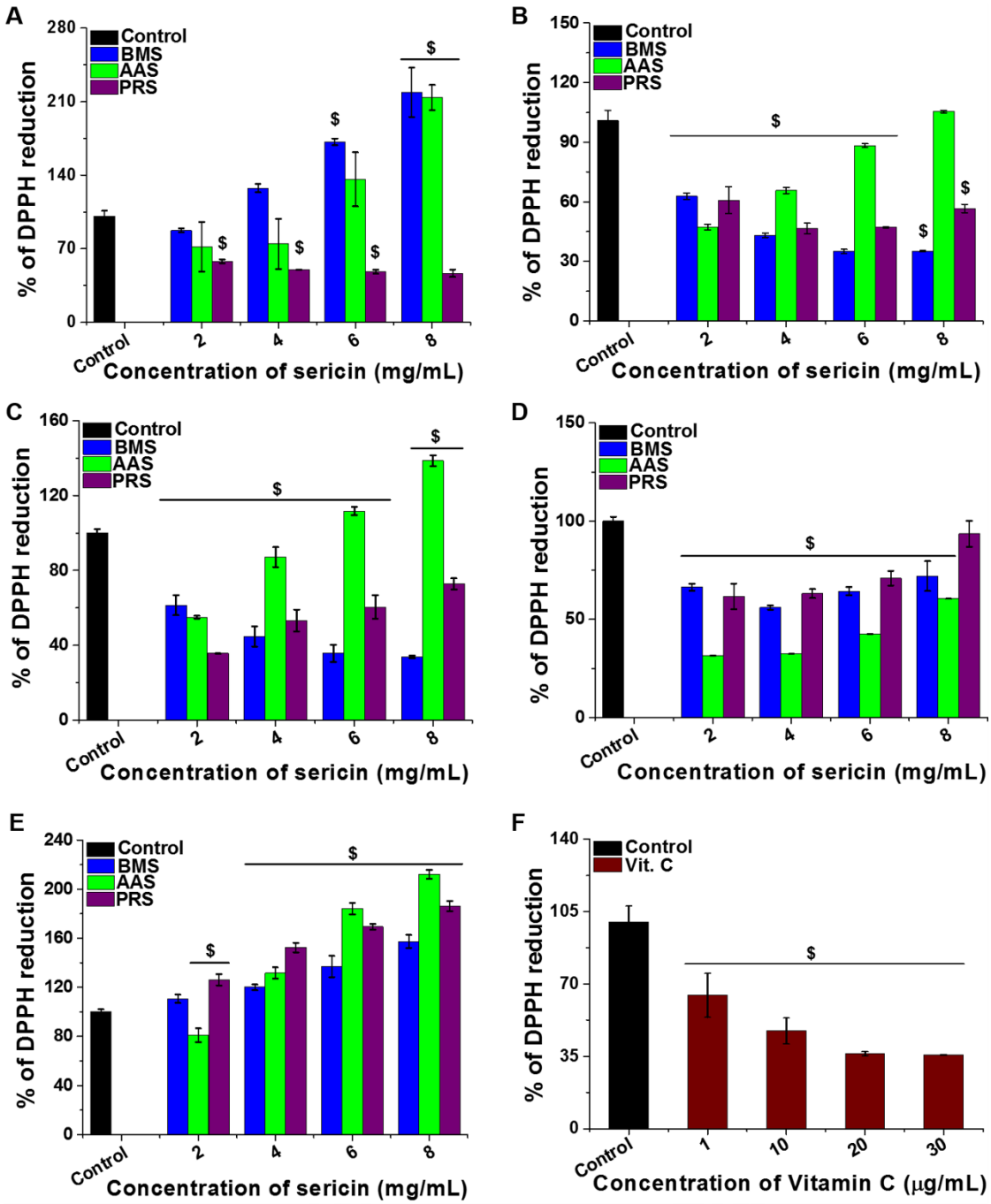

Fig.2.4. *DPPH scavenging activity of silk sericin, where silk sericin extracted using* ***(****A) acid-degradation, (B) alkali-degradation, (C) conventional method, (D) autoclaving, (E) urea-degradation, and (F) positive control (Vit. C). ($p≤0.001 in comparison to control).*

2.3.8. Cytocompatibility studies

Cytocompatibility of BMS, AAS and PRS showing DPPH reduction was evaluated by MTT assay. SS showed significant cell proliferation ($p≤0.001$) up to a concentration of 400 µg/mL (**Fig.2.5**). In comparison with control, L929 cells treated with 400 µg/mL of BMS extracted by conventional and autoclaving methods showed

significantly low ($p \leq 0.001$) viability. Cytocompatibility of the positive controls was also evaluated. Vit. C and arbutin showed significant cell enhancement. However, cells treated with a high concentration (400 µg/mL) of arbutin showed significantly low ($p \leq 0.001$) viability.

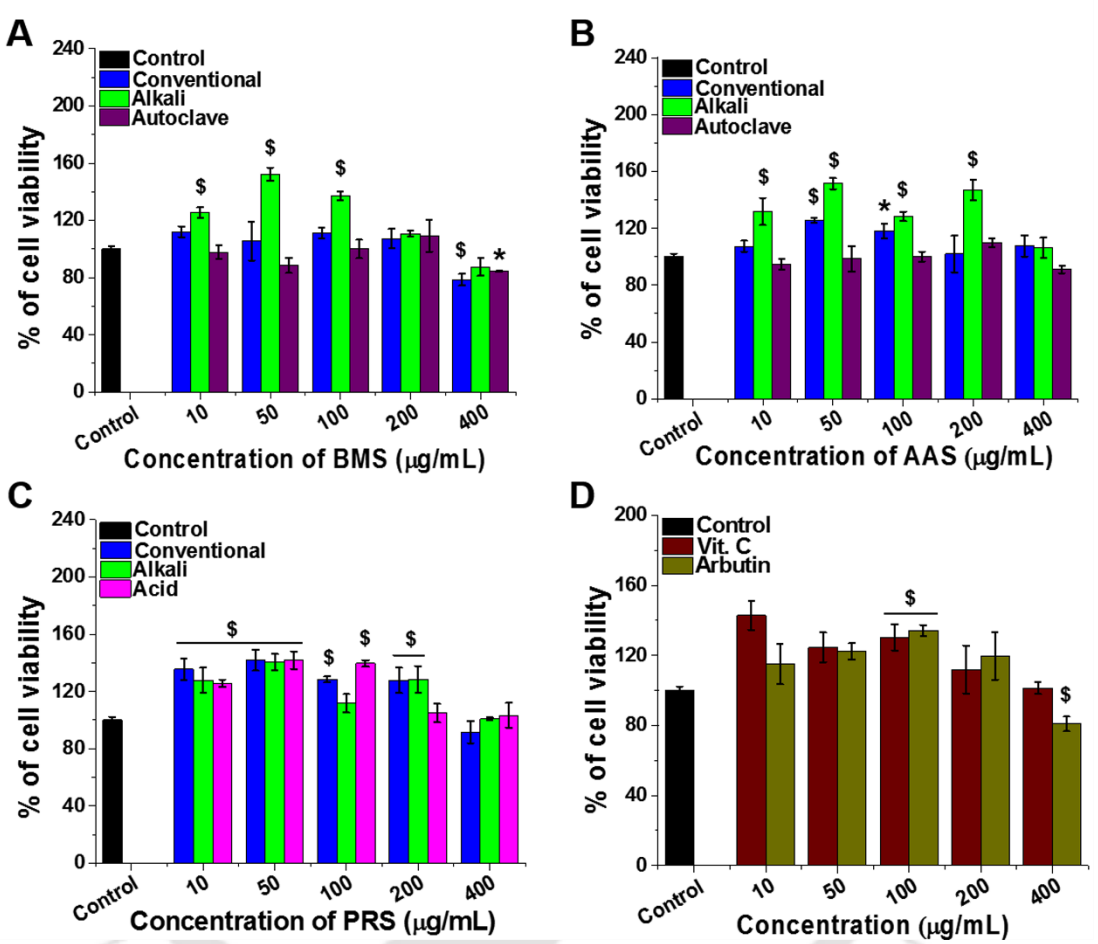

Fig.2.5. *Effect of silk sericin on the viability of L929 cells after 24 h of treatment was assessed using MTT assay. Where (A) BMS, (B) AAS, (C) PRS and (D) positive control (Vit. C and arbutin) treated cells. ($p≤0.001, *p≤0.01 in comparison to control).*

2.3.9. Sensitivity of L929 cells to H_2O_2

H_2O_2 treated cells showed concentration-dependent cell death. In comparison with control, significantly low viability was observed by the H_2O_2 treated cells ($p \leq 0.001$). Cell treated with 100 µM H_2O_2 displayed 50% cell death.

2.3.10. Prevention of H_2O_2 mediated cell death by silk sericin

Protection of L929 cells from the oxidative stress-induced cell death using SS was evaluated using MTT assay (**Fig.2.6** and **Fig.A2.1.**). SS pretreated L929 cells were subjected to oxidative stress by using H_2O_2 (non-radical ROS). Overall, significant ($p \leq 0.01$) difference was observed in the viability of H_2O_2-treated and SS pretreated cells in comparison with control; SS pretreated cells when compared with H_2O_2-treated cells. Cells pretreated with SS showed better cell viability (post 24 h of H_2O_2 treatment) and recovery (after 72 h of H_2O_2 treatment) than untreated cells. After 24 h of H_2O_2 treatment, 10 µg/mL of SS showed better protection when compared with 100 µg/mL of SS. However, post 72 h of H_2O_2 treatment, cells pretreated with 100 µg/mL of SS showed enhanced viability in comparison with 10 µg/mL of SS. SS extracted by alkali methods from the cocoons for all three varieties of silkworms exhibited better results, along with SS extracted from the cocoons of AA by autoclaving method. AAS extracted by autoclaving method showed better cell protection and cell recovery. AAS (extracted by conventional methods), PRS (extracted by citric acid method) and BMS (extracted by autoclaving and conventional) pretreated cells did not show significant recovery. Positive controls (Vit. C and arbutin) exhibited cell protection against H_2O_2 but failed to show significant cell revival.

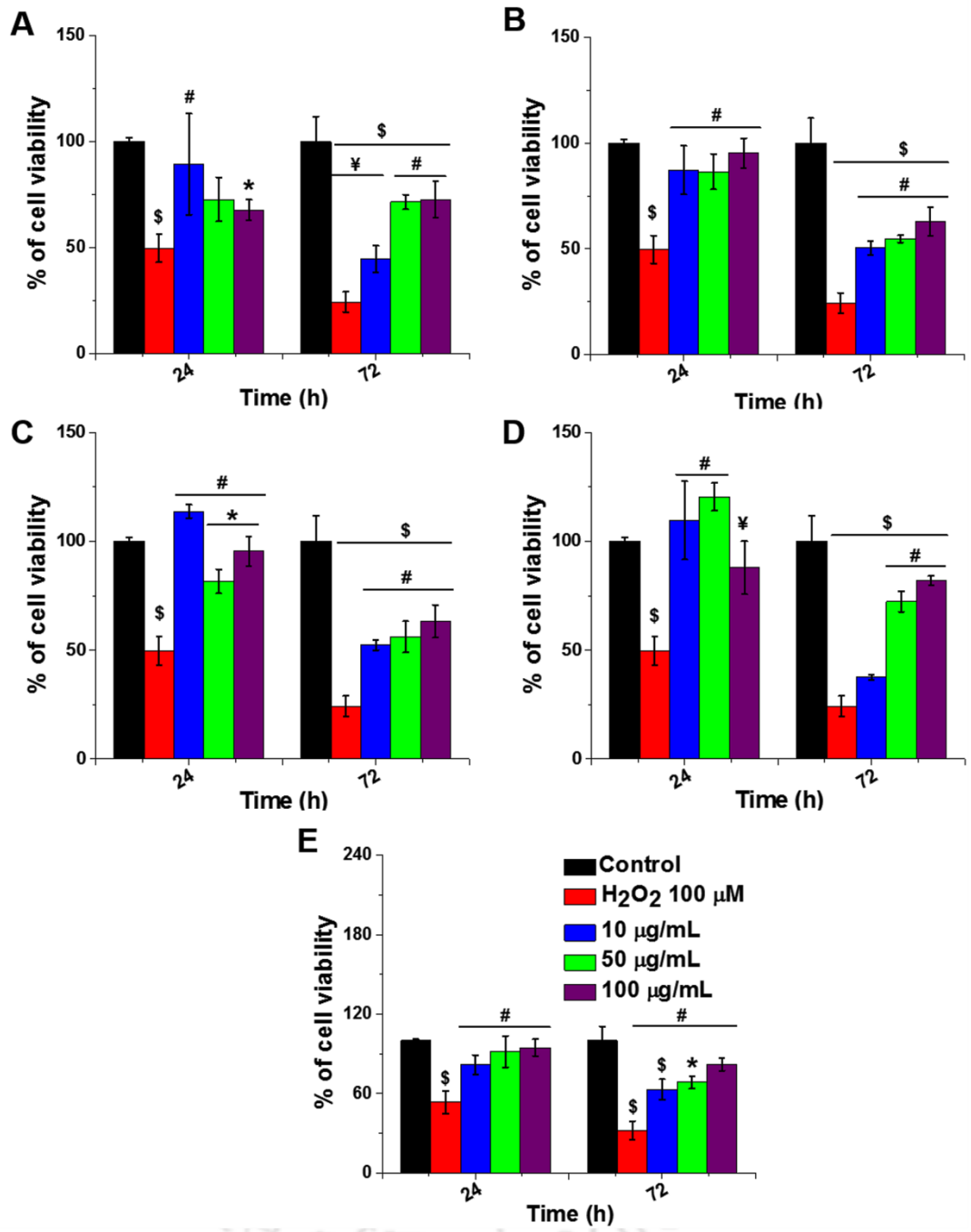

Fig.2.6. *Protective effect of silk sericin against H_2O_2 induced oxidative damage and promotion of cellular viability on L929 cells by MTT assay. Cells were pretreated with SS extracts, where (A) alkali-degraded BMS, (B) conventionally extracted PRS, (C) alkali-degraded PRS, (D) alkali-degraded AAS, and (E) autoclaved AAS. ($p≤0.001 and *p≤0.01 in comparison with control; #p≤0.001 and ¥p≤0.01 in comparison with SS untreated cells)*

2.3.11. Trypan Blue exclusion assay

In MTT assay, BMS, AAS, and PRS displayed cell protection and recovery post 24 h and 72 h of H_2O_2 treatment. These SS variants were further selected and investigated for their cell protective activity using Trypan Blue exclusion assay. **Fig.2.7** displays the viability of SS pretreated and untreated L929 cells after treatment with H_2O_2. Similar to MTT assay, SS pretreated cells exhibited significantly higher viability in trypan exclusion assay when compared to SS untreated cells post H_2O_2 treatment ($p \leq 0.01$).

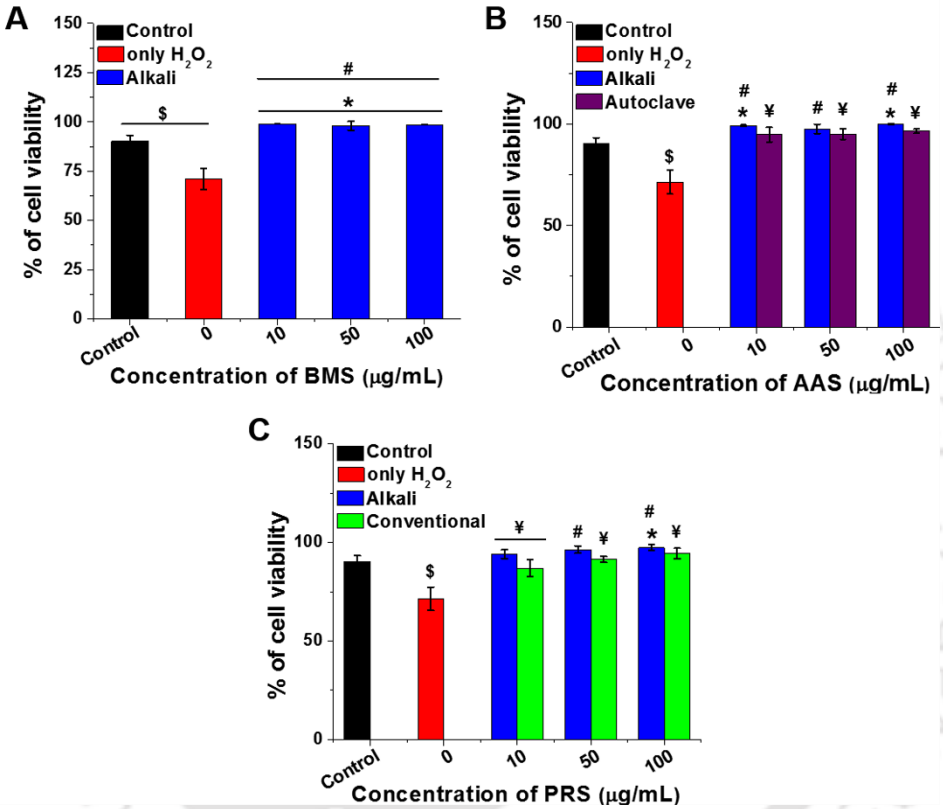

Fig.2.7. *Protective effect of silk sericin against H_2O_2 induced oxidative damage and promotion of cellular viability on L929 cells by Trypan Blue exclusion assay. Prior to H_2O_2 exposure cells were treated with different extracts of sericin, where (A) BMS, (B) AAS and (C) PRS. ($p≤0.001 and *p≤0.01 compared to control; #p≤0.001 and ¥p≤0.01 compared to silk sericin untreated cells)*

2.3.12. Lactate dehydrogenase (LDH) assay

H_2O_2 induced cytotoxicity was assessed by evaluating the membrane integrity using the LDH assay. LDH activity of BMS, AAS, and PRS pretreated and untreated cells after H_2O_2 treatment is depicted in **Fig.2.8**. In comparison with control, no significant difference in LDH activity was exhibited by SS pretreated cells.

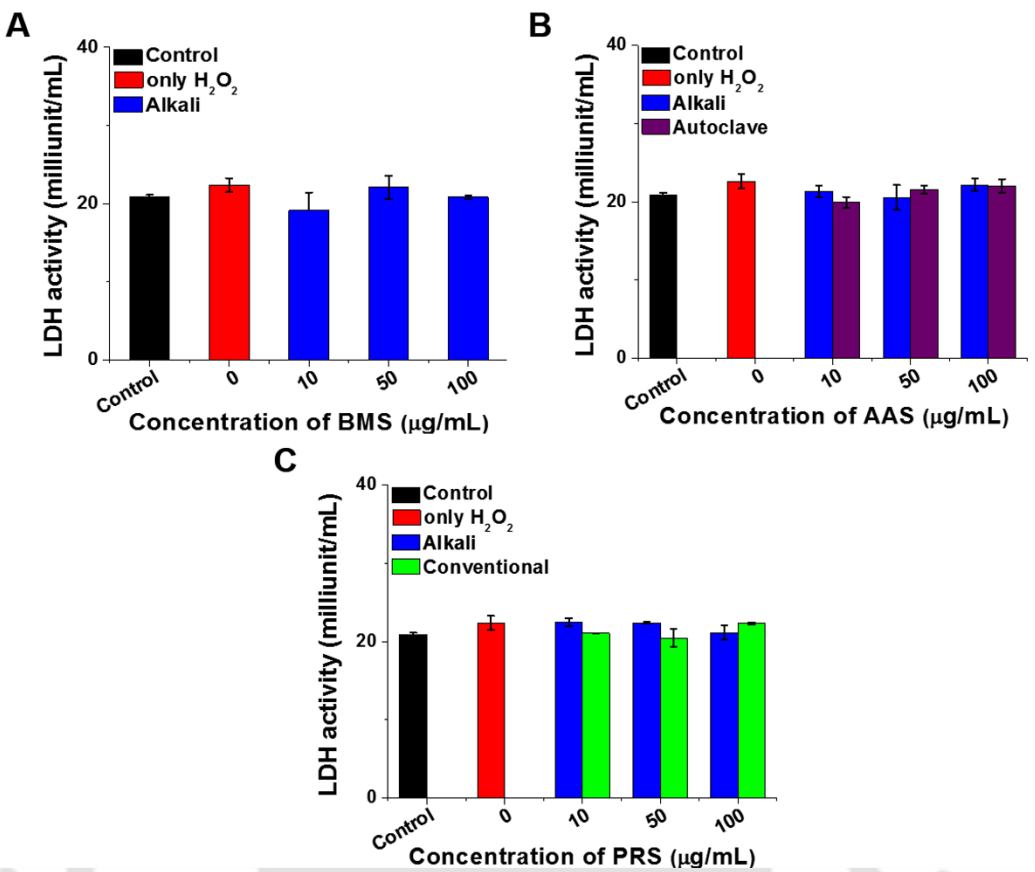

Fig.2.8. *Protective effect of silk sericin against H_2O_2 induced oxidative damage and promotion of cellular viability on L929 cells by LDH assay. Prior to H_2O_2 exposure cells were treated with different extracts of sericin, where (A) BMS, (B) AAS, and (C) PRS.*

2.3.13. Determination of intracellular antioxidant activity of silk sericin

Intracellular ROS scavenging ability of SS was determined using DCFH-DA. As shown in **Fig.2.9**, SS extracted from the cocoons of BM, AA and PR scavenged intracellular ROS, which was produced after H_2O_2 treatment. In comparison with the ROS levels in H_2O_2 treated L929 cells, significantly low ($p \leq 0.001$) ROS levels were exhibited by SS and positive control (Vit. C and arbutin) pretreated L929 cells. 10 µg/mL of AAS and PRS extracted by the alkali method showed maximum ROS scavenging ability. 10 µg/mL of AAS extracted by autoclaving also showed equivalent ROS scavenging ability. This result confirmed the ability of SS to prevent ROS generation mediated by H_2O_2.

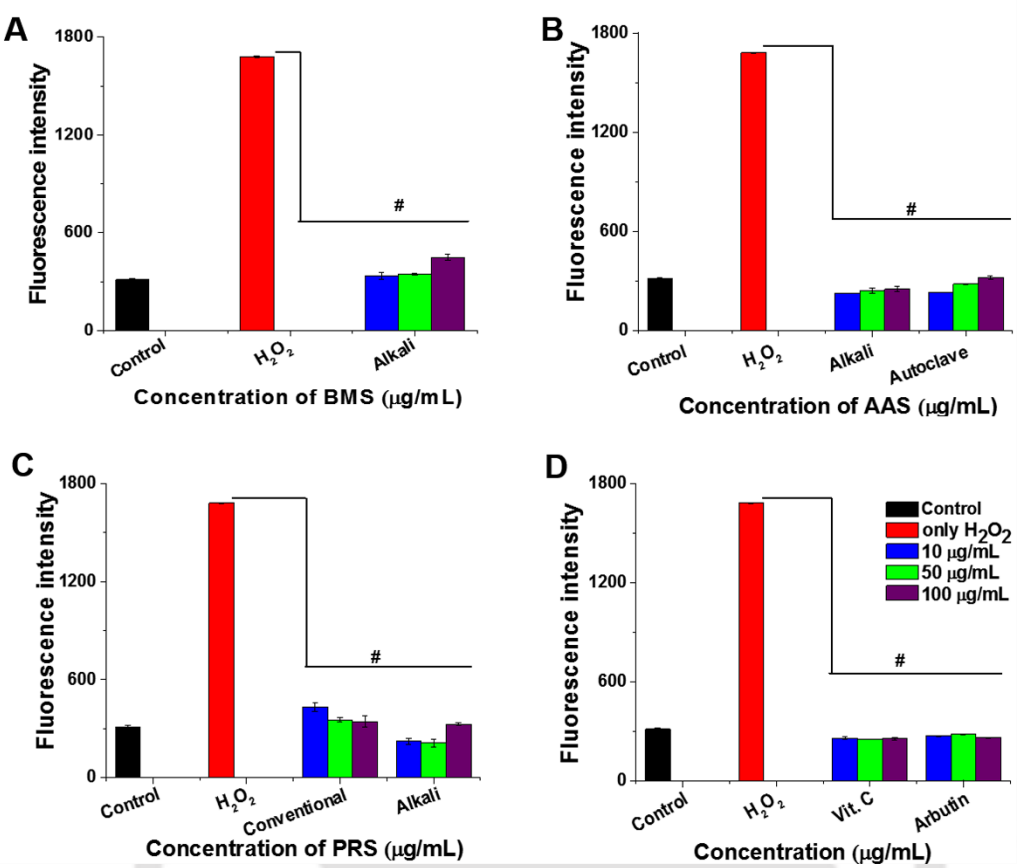

Fig.2.9. *Effect of silk sericin on H_2O_2 induced intracellular ROS levels of L929 cells was assessed using DCFH-DA. Cells were pretreated with sericin extracts, where (A) BMS, (B) AAS, (C) PRS, and (D) positive control (Vit. C and arbutin). (#p≤0.001 in comparison with only SS untreated cells)*

2.3.14. Catalase (CAT) assay

The catalase activity in presence of SS is depicted in **Fig.2.10**. SS treated cell lysate showed significantly (p≤0.01) enhanced catalase activity when compared with SS untreated cell lysate. 10 µg/mL of BMS and AAS extracted by conventional and autoclaving methods showed maximum H_2O_2 scavenging ability in comparison to the high concentration of 100 µg/mL. Whereas, BMS and AAS extracted by alkali-degradation enhanced H_2O_2 scavenging ability with increasing SS concentration. PRS and positive control (Vit. C and arbutin) also showed better H_2O_2 scavenging ability at both concentrations.

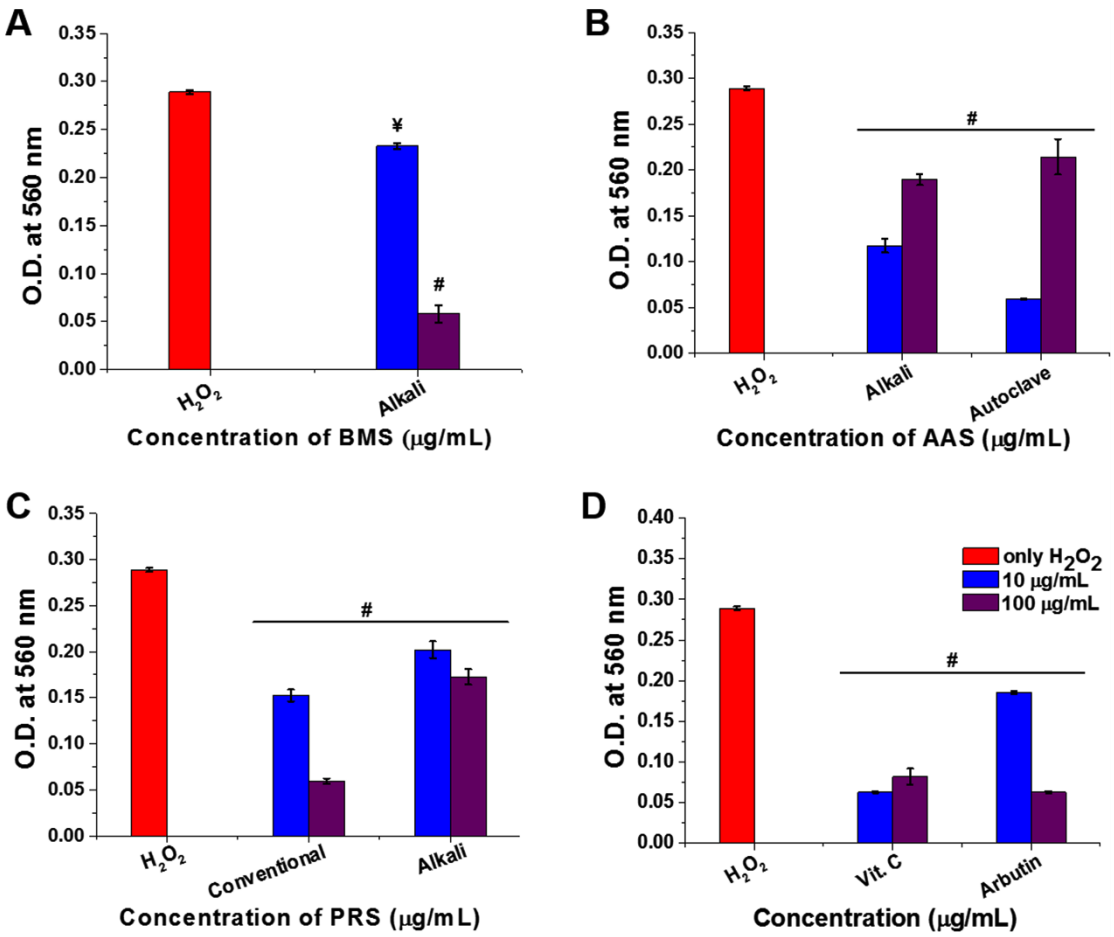

Fig.2.10. *Effect of silk sericin on H_2O_2 induced catalase activity was assessed using Amplex red catalase assay kit. Cells were pretreated with sericin extracts, where (A) BMS, (B) AAS, (C) PRS, and (D) positive control (Vit. C and arbutin). (#p≤0.001 and ¥p≤0.01 in comparison to silk sericin untreated cells)*

2.3.15. Anti-lipid peroxidation activity of silk sericin

Anti-lipid peroxidation (ALP) activity of SS was measured by TBA assay for malondialdehyde (MDA) production. The percentage of ALP activity of SS extracted from the cocoons of BM, AA and PR are illustrated in **Fig.2.11**. SS extracted from the cocoons of AA, BM and PR showed ALP (75-90%) activity depending on the concentration of SS. Vit. C exhibited 65% of ALP activity, whereas Vit. E displayed 85-90% activity.

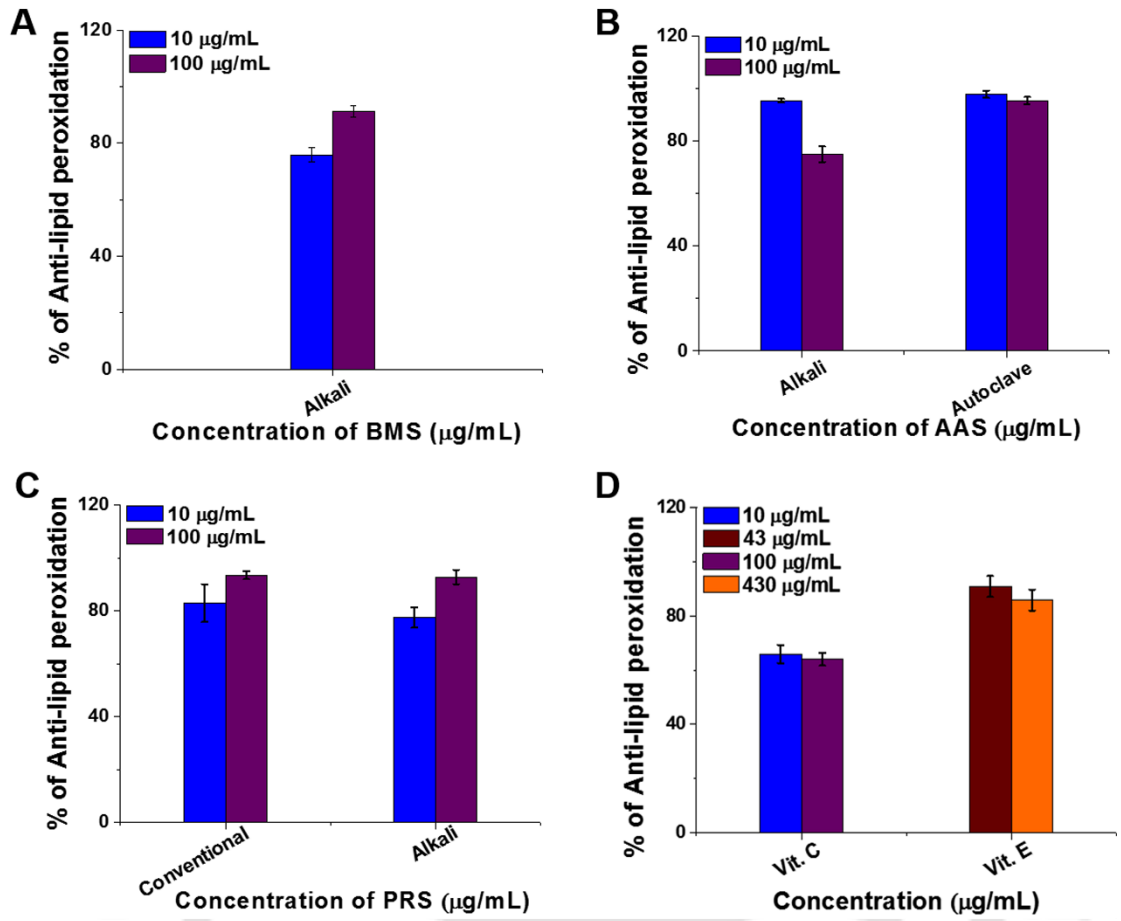

Fig.2.11. *Anti-lipid peroxidation potential of silk sericin was assessed using TBA assay. Cell homogenates treated with sericin extracts prior to H_2O_2 treatment, where (A) BMS, (B) AAS, (C) PRS, and (D) positive control (Vit. C and Vit. E).*

2.4. Discussion

ROS are highly unstable free radicals, which are produced by aerobic organisms during cellular metabolism (Weydert and Cullen, 2010). Low levels of ROS enhances cell survival (proliferation), whereas elevated ROS, oxidizes the intracellular biomolecules which subsequently leads to cytotoxicity (Aprioku, 2013; Cao et al., 2009; Lee et al., 2002). Thus, an equilibrium between oxidative stress and antioxidant defense (redox balance) is essential for maintaining healthy biological systems. Basically, antioxidants (AOs) are natural or synthetic molecules that at a very low concentration quenches free radicals present in the body. They can be categorized as endogenous or exogenous on the basis of their synthesis in the body. Under normal physiological conditions, the members of endogenous AO defense system e.g., glutathione (GSH), superoxide dismutase (SOD), catalase (CAT), glutathione peroxidase (GPx) plays

considerable role against ROS elements like superoxide anions, hydroxyl, alkoxyl, and peroxyl radicals and maintains body's homeostasis (Poljsak et al., 2013). Off note, this context of endogenous defense is incomplete without the support of exogenous reducing compounds (e.g. vitamins, polyphenols, copper, zinc etc.). These exogenous AOs not only support the endogenous defense system but also play a significant role in many antioxidant mechanisms in living organisms. Therefore, exogenous antioxidants are in incessant demand as they are capable to maintain redox homeostasis.

SS, a natural macromolecular protein produced by the silkworms (Bombycidae and Saturniidae family) is known to possess many biological functions including AO activity. However, their AO efficacy may vary depending upon their molecular weight and amino acid composition (Suzuki et al., 2004). It has been apprehended that the quality of the sericin isolate is influenced not only by the chemicals used in the extraction process but also by physical conditions employed during the process of extraction. Therefore, in the present study, the effect of extraction methods on AO properties of SS isolates of three varieties of North-East Indian Silk was investigated.

The physical and chemical changes during extraction process not only randomly cleaves the peptide bonds but also effects the covalent and non-covalent interaction between silk fibroin and SS, resulting in the peptides of divergent lengths and of wide molecular weights (10 to 400 kDa) (Kato et al., 1998; Takasu et al., 2002). During extraction from cocoons, the high temperature under high pressure (autoclaving) might lead to dissolution. Additionally, change in pH of protein microenvironment (using acid or base along with heat energy) alters the ionization of amino acid which consecutively results in the different length of SS containing various percentage of α-helix, β-sheets, random coils and β-turns (da Silvaa et al., 2014). Moreover, the amount of percentage of β-sheets and random coils reflect the crystalline or amorphous nature of SS respectively (Dash et al., 2007; Teramoto et al., 2006). In the present study, the observed discrete clear bands and smear pattern in electrophoresis analysis (with each extraction procedure) demonstrated the breakage of SS into different length peptides which are of wide-ranging molecular weights (10-220 kDa) (**Fig.2.1**). Autoclaving method (BMS and PRS) exhibited high molecular weight SS with a large percentage of β-sheets indicates its crystalline nature whereas predominant percentage of random coils, α-helix, β-turns displayed its amorphous pattern. The SS extracted from PRS using autoclaving, acid-degradation, conventional method and alkali-degradation exhibited varied percentage of

α–helix, β-sheet, random coil, and turns. On the other hand, SS extracted from the cocoons of BM by a conventional method and alkali-degradation displayed presence of α–helix, random coil and turns. Notably, α–helical structures were absent in BMS extracted by autoclaving. AAS extracted by all methods except urea-degradation displayed an absence of β-sheet in their secondary structure (**Fig.2.2** and **2.3**).

Secondary metabolites ingested by silkworm from the leaves are associated with composition of silk protein solution (Butkhup et al., 2012) and play an important role in cocoon formation (Neog et al., 2011). In addition to SS, secondary metabolites also contribute to the AO properties (Kurioka and Yamazaki, 2002). Accordingly, the total amount of secondary metabolite present in SS after extraction was estimated. Interestingly, in the methods (autoclaving, conventional, alkali and acid-degradation) where high thermal energy was used, higher yield of polyphenols was observed. On the contrary, low yield of polyphenolic content was obtained for methods like urea-degradation where low thermal energy was employed (**Table 2.2.**). These observations further confirm the notion that high energy consumption tends to break the covalent and non-covalent bonds between silk fibroin and allow SS to attain high phenolic content. Total amount of polyphenolic and flavonoid content is also known to vary based on the extraction methods (Butkhup et al., 2012). Flavonoids bind with silk proteins by glycosidic bonds, thus the breakage of glycosidic bonds replicates high yield of flavonoids (Kurioka and Yamazaki, 2002; Tamura et al., 2002). Citric acid might contribute to the breakage of glycosidic bonds between silk proteins and flavonoids by donating protons (H^+), hence high flavonoid content yield. Conversely, a base like sodium carbonate was unable to break the glycosidic bonds leading to low yield of flavonoids. The use of autoclaving with its natural high thermal energy, applied high temperature under high pressure might have cleaved the glycosidic bonds and therefore released higher amount of flavonoids from the cocoons of AA (**Table 2.3**).

Further in order to evaluate the effect of extraction methods on AO properties of SS isolates of BM, AA and PR, FRAP analysis, DPPH scavenging ability and cytocompatibility with L929 cells were performed. SS contains 76% hydrophilic amino acids. Kato *et al*. (1998) hypothesized that hydroxyl groups of serine and threonine contributes to AO property of SS by chelating the elements like copper and iron. Fan *et al.* (2009) reported that the aromatic amino acids (by donating their delocalizing electrons) and hydroxyl groups of serine and threonine contributes to AO property of SS.

A study conducted by Sangwong *et al.* (2016) exhibited that SS treated with DTT (dithiothreitol) and β-mercaptoethanol lower the AO activity in comparison to untreated SS. They also reported that SS lacking polyphenols (coloring compounds extracted by ethanol) exhibited AO activity. Thus, the presence of free reducing groups on SS and secondary metabolites play an important role in reducing the oxidant molecule. Our results displayed highest Fe^{3+} to Fe^{2+} conversion in the AAS and PRS extracted by conventional methods, which suggested the presence of high percentage of free reducing groups. Conversely, acid-degraded BMS, PRS, and AAS exhibited minimum Fe^{3+} to Fe^{2+} due to the less availability of reducing groups (**Table 2.4**). Further, in DPPH scavenging assay, we found SS extracted by urea-degradation, autoclaving and acid-degradation showed the precipitation of SS in methanol which might be due to the presence of high percentage of β-sheets (Siritienthong et al., 2012). Precipitation of SS reduces the availability of reducing groups of SS and associated secondary metabolites to DPPH. Small fragments of SS with predominant α-helices and random coils were produced using conventional method and alkali-degradation, which gets rapidly solubilized in methanol and reduces DPPH (**Fig.2.4)**. Therefore, the extractions that qualified the DPPH scavenging analysis were further selected and tested for the cytocompatibility assessment using MTT assay (**Fig.2.5**). High cell viability was recorded at lower doses of SS however at higher doses, a slight decrement in the cell viability was observed. This is in line with previous reports where lower concentrations of SS enhanced cell attachment and proliferation (Nagai et al., 2009) and at higher concentrations suppressed cell growth due to its pro-oxidant activity (Terada et al., 2002).

Hydrogen peroxide (H_2O_2) is a stable ROS, which reacts with various intracellular targets, including proteins, lipids, and DNA that would lead to cell death (Bienert et al., 2006). Here we used H_2O_2 induced oxidant model to investigate the AO properties of SS. Interestingly, the pretreatment of SS conferred significant protection in few groups against H_2O_2 induced oxidative stress. Off note, SS extracted by alkali-degradation from the cocoons for all three varieties of silkworms exhibited better results, along with SS extracted from the cocoons of AA using an autoclaving method by scavenging intracellular ROS (**Fig.2.6** and **2.9**). However, cells pretreated with BMS (extracted using the conventional method and autoclaving), PRS (extracted using acid-degradation) and AAS (extracted by conventional method) were unable to show recovery even after 72 h of H_2O_2 treatment. This might be attributed to their inability to scavenge

the elevated ROS levels. Elevated levels of ROS might alter the mitochondrial activity (Zorov et al., 2014). Therefore, in addition to MTT assay, Trypan Blue exclusion assay was performed to evaluate the viability of SS pretreated and untreated cells (**Fig.2.7**). SS pretreated cells displayed enhanced viability in comparison with SS untreated cells which might be due to ROS scavenging ability of SS. Cell protective activity of SS confirmed by MTT assay further correlates with Trypan Blue exclusion studies. This study exhibits that the SS protected cells from oxidative stress-induced cell death. The protective activity of SS was also evaluated by LDH assay (**Fig.2.8**). Disruption of cellular membrane integrity by oxidants release LDH into media from the cytoplasm. Cells treated with 100 µM H_2O_2 causes cell death without disrupting the membrane integrity (Xiang et al., 2016), due to which no significant difference was observed between SS pretreated and untreated cells after H_2O_2 treatment.

Oxidative stress generated by H_2O_2 is neutralized by converting it to water and oxygen by catalase (Sharma et al., 2012). However, at high concentrations, H_2O_2 depletes the activity of catalase (Park, 2013). Here in this study, the enhanced activity of catalase was noted in the groups where pre-treatment of SS enhanced the viability upon H_2O_2 treatment (**Fig.2.10**). This indicated that pretreatment of SS might enhance the catalase activity and reduce the oxidative stress generated by exogenous H_2O_2 treatment. The overproduction of ROS is known to cause lipid peroxidation, which is responsible for pathological disorders. ROS reacts with the polyunsaturated fatty acids of membrane lipids, which leads to the formation of lipid peroxides such as MDA (Debnath et al., 2013). Antioxidants could restore cell functions by reducing the ROS (Poljsak et al., 2013). Here, we also noted that SS showed anti-lipid peroxidation activity by scavenging the ROS generated after treatment with H_2O_2 (**Fig.2.11**).

2.5. Significant Findings

The salient findings of this chapter are as follows:

1. The physical and chemical methods used to extract SS from the cocoons of BM, AA and PR cleaved the polypeptides at different positions, which generated peptides with wide variation in length, molecular weight (10-220 kDa), and secondary structural conformations.

2. In addition to the peptide length of SS, the total content of secondary metabolites (polyphenols and flavonoids) also varied during the extraction of SS from the cocoons.
3. Low molecular weight SS peptides with predominant random coils and α-helix in their secondary structure orientation reduce DPPH radical levels.
4. Additionally, L929 cells were clearly protected from H_2O_2 induced oxidative damage by scavenging the elevated levels of intracellular ROS especially by the SS extracted using autoclaving (for AA), alkali-degradation (for AA, BM, and PR) and conventional (for PR) methods.
5. SS pretreatment enhanced CAT activity and prevented lipid peroxidation of L929 cells.
6. SS extraction using autoclaving (for AA), conventional (for PR) and alkali-degradation (for AA, BM, and PR) generated desirable peptide length of SS that possessed potential AO properties.

In the constant search for a potential AOs that could protect skin from pollutants and UVR-induced damage, the present study provides an opportunity to select an extraction method, which helps to extract SS possessing AO activity. This chapter provided an avenue for extracting the different length SS peptides from the cocoons of mulberry and non-mulberry silk varieties that could protect and recover cells from oxidative damage. SS extracted from the cocoons of BM, AA, and PR using alkali-degradation protected and helped the cells to recover from H_2O_2 induced oxidative damage. In specific, it would be interesting to evaluate the anti-tumor and protective effects of alkali-degraded BMS, AAS, and PRS against UVR-induced skin damage. In harmony with this rationale, the next chapter describes the anti-tumor activity of alkali-degraded silk sericin.

Chapter 3

Exploring the Anticancer Activity of Mulberry and Non-mulberry Silk Sericin

This chapter explores the anti-tumor activity of silk sericin extracted from the cocoons of mulberry and non-mulberry silk varieties using alkali-degradation. The effect of silk sericin on the redox status, endogenous antioxidant activity, cell cycle, mitochondrial membrane potential, cellular senescence, gene, and protein expression of human cancer cells are described in detail.

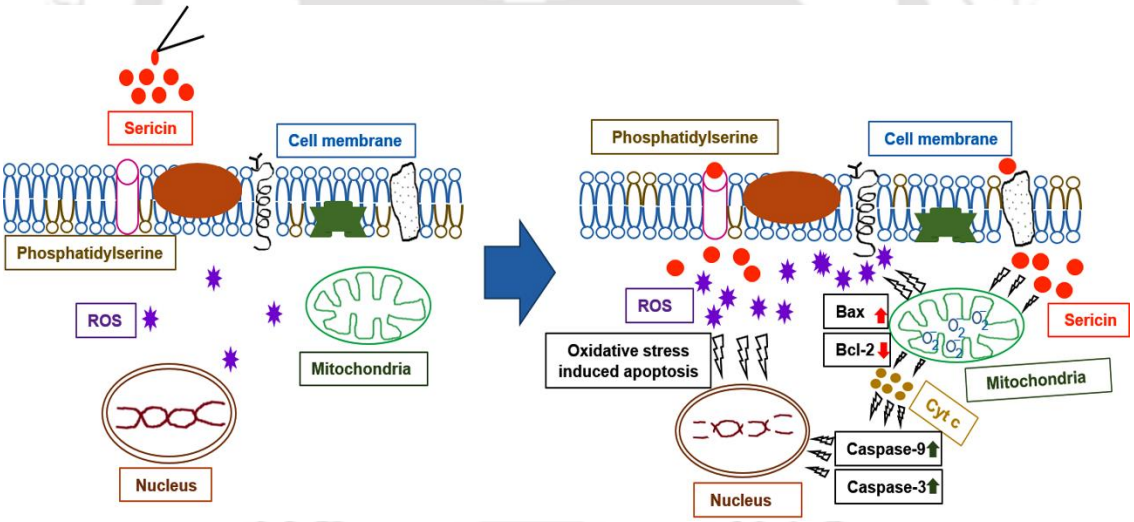

ABSTRACT

Pro-oxidative stress induced by dietary polyphenols elevates reactive oxygen species (ROS) production in cancer cells, which subsequently leads to oxidative stress-mediated apoptosis. Sericin, a principal component of silk is associated with a mixture of polyphenols and flavonoids, possesses various biomedical attributes including anticancer activity. In the present study, we have evaluated the pro-oxidative effect of *Bombyx mori* sericin (BMS), *Antheraea assamensis* sericin (AAS), and *Philosamia ricini* sericin (PRS) against different cancer cells. Cytotoxicity of SS evaluated using A431, SAS, and MCF-7 cells showed ≥50% reduction in their viability at 4 mg/mL. Intracellular ROS levels, cell cycle arrest, and apoptosis assessed using flow cytometry corroborated that SS treatment elevated the intracellular ROS levels, caused cell cycle arrest at the sub-G1 phase and resulted in apoptotic cell death. SS treated A431 and SAS cells showed upregulation of p53 and dysregulation of Bax and Bcl-2 gene expression. Whereas, AAS treated MCF-7 cells showed upregulation of Bax and downregulation of Bcl-2 gene expression. AAS treated MCF-7 and SAS cells showed downregulation of Bcl-2 protein expression in comparison to their control cells. Thus, the present study demonstrates that the pro-oxidative effect induced by SS suppresses the cancer growth indicating its potential anticancer activity.

3.1. Introduction

Reactive oxygen species (ROS) are produced in mitochondria as a by-product of aerobic metabolism. They act as secondary messengers in various biological processes and cell signaling pathways (Glasauer and Chandel, 2014). Regulation of ROS levels plays an important role in maintaining the health and longevity of the organism (McCord and Fridovich, 1988). Alteration in the redox balance by endogenous or exogenous factors lead to elevation or depletion of ROS compared to basal levels. Depletion of ROS levels disrupts cell signaling and biological process that affects cellular homeostasis (Cairns et al., 2011). Elevated ROS levels induce oxidative stress that damages cellular bio-macromolecules and leads to carcinogenesis (Trachootham et al., 2009), diabetes, atherosclerosis (Paravicini and Touyz, 2006), aging (Haigis and Yankner, 2010), and neurodegeneration (Shukla et al., 2011).

Cancer cells bypass senescence and uncontrollably proliferate by hijacking the mechanism of normal cells (Hanahan and Weinberg, 2011). Hyper-metabolism of cancer cells elevates their intracellular ROS levels which play a key role in cancer progression, spreading and regulating signaling pathways; like angiogenesis and metastasis (Weinberg and Chandel, 2009; Weinberg et al., 2010). However, the elevation of ROS levels beyond a critical threshold induces oxidative stress that causes cell cycle arrest and apoptotic cell death. In order to maintain the redox balance, cancer cells elevate the production of endogenous antioxidants and scavenge the elevated levels of ROS (Gorrini et al., 2013). Therefore, elevation of ROS levels in cancer cells than their basal levels induces apoptotic/ necrotic cell death.

In recent years, the pro-oxidant strategy also known as oxidant therapy is gaining much interest in cancer treatment (León-González et al., 2015). Dietary agents (polyphenols, flavonoids, resveratrol, and curcumin) and drug molecules (paclitaxel, doxorubicin, and cisplatin) that elevates the ROS levels could efficiently kill cancer cells (Fang et al., 2009; Lee et al., 2013). Any compound which can disrupt redox balance could affect both normal and cancer cells. Thus, a potential pro-oxidant compound must ideally elevate oxidative stress that could kill cancer cells and affect normal cells marginally (León-González et al., 2015). Conventional drug molecules are non-specific and induce oxidative stress that kills both normal and cancer cells. Dietary polyphenols, flavonoids, vitamin E, and vitamin C act as antioxidants and scavenge the elevated levels of intracellular ROS (León-González et al., 2015; Padayatty et al., 2003; Traber and Atkinson, 2007). However, at higher concentrations, they also act as pro-oxidants,

elevates ROS levels in the cells and leads to oxidative stress-mediated apoptotic/necrotic cell death (León-González et al., 2015; Pearson et al., 2006). The concentration of dietary polyphenols and flavonoids used should strategically trigger a marginal or minimal side effect on normal cells while proving fatal for cancer cells.

SS is a natural protein polymer produced by the silkworms (Dash et al., 2007). It possesses various biological activities such as anti-oxidation, suppression of elastase and tyrosinase activity (Chlapanidas et al., 2013; Kumar and Mandal, 2017). SS reduces ROS, protect the cells from H_2O_2 and UVB radiation-induced oxidative damage, and prevents cancer progression (Kumar and Mandal, 2017; Zhaorigetu et al., 2003). Kaewkorn et al. reported that SS extracted from the cocoons of *Bombyx mori* suppressed the proliferation of colon cancer and induced apoptotic cell death (Kaewkorn et al., 2012). The effect of SS on the redox balance of cancer cells not yet explored. The biological properties of SS are attributed to its amino acid compositions and associated secondary metabolites (polyphenols and flavonoids) (Kumar and Mandal, 2017). Mulberry silk varieties are enriched with quercetin, catechin, epicatechin, *trans*-resveratrol, rutin, procyanidin B1, kaempferol, procyanidin B2, myricetin, luteolin, naringenin, and Σ phenolics, however, their content varies based on their source (Butkhup et al., 2012). Whereas, Eri silk lacks quercetin, luteolin, naringenin, and kaempferol (Butkhup et al., 2012). It has been reported that polyphenols and flavonoids of fruits and vegetables (mixture of quercetin, kaempferol, myricetin, catechin, epicatechin, rutin, isorhamnetin, malvidin-3-glucoside, caffeic acid, chrysin, galangin, apigenin, fisetin, luteolin, morin, and several anthocyanidins) significantly suppressed the growth of human breast carcinoma (MCF-7) by arresting the cell cycle at G1 phase (Kubatka et al., 2016). They also induced apoptosis in MCF-7 cells and caused DNA fragmentation (Kubatka et al., 2016). A mixture of polyphenols and flavonoids associated with SS vary based on their source as well as extraction methods. Therefore, exploring the pro-oxidant activity of SS against cancer cells would be beneficial in understanding the impact of SS and associated secondary metabolites (polyphenols and flavonoids) on controlling the cancer growth.

In the present study, we aimed to explore the effect of SS extracted from the cocoons of BM, AA, and PRS on the redox balance of cancer cells. Further, we tried to understand the influence of redox imbalance on the endogenous antioxidant activity, mitochondrial membrane potential and their role in suppressing the cancer growth. To elucidate these reservations we have investigated the anticancer activity of BMS, AAS,

and PRS using human breast carcinoma (MCF-7), oral carcinoma (SAS) and squamous carcinoma (A431) cells. Human cancer (A431, SAS, and MCF-7) cells were treated with SS and thereafter, assessed for anticancer activity in the context of cytotoxicity, ROS levels, cell cycle arrest, and mitochondrial membrane potential. The effect of SS on the expression of p53, cytochrome *c* (cyt *c*), Bax and Bcl-2 genes and apoptotic/anti-apoptotic proteins in cancer cells have been studied.

3.2. Materials and Methods

3.2.1. Materials

Dimethyl sulfoxide (DMSO) and sodium carbonate were sourced from SRL, India; Antibiotic-antimycotic solution, Tris-base, and sodium chloride were obtained from Himedia, India. MTT) Bradford's reagent, epidermal growth factor (EGF), cholera toxin, insulin, RNase A, superoxide dismutase (SOD) detection kit, nonidet P-40 (NP-40), sodium orthovanadate, sodium deoxycholate, SDS, PMSF, aprotinin, dichloro-dihydro-fluorescein diacetate (DCFH-DA), dithiothreitol (DTT), Triton X-100, and hydrocortisone were obtained from Sigma-Aldrich, USA. Propidium iodide (PI), Annexin V-FITC/PI assay kit, JC-1 assay kit, Amplex red catalase assay kit, and horse serum were supplied by Invitrogen, USA. DMEM, DMEM/F12, and FBS were procured from Gibco, USA.

3.2.2. Extraction of silk sericin using alkali-degradation

SS was extracted from the cocoons of AA, BM, and PR using our previously established protocol (Kumar and Mandal, 2017). In brief, cocoons were chopped and boiled in 0.5 M Na_2CO_3 for 30 min. Post boiling, silk fibers were removed; the protein solution was centrifuged and filtered to remove the residual solid particles. Further, the filtrate was dialyzed against MilliQ H_2O for 48 h. Dialyzed protein solution was freeze-dried and stored at -20 °C.

3.2.3. *In vitro* cell culture studies

3.2.3.1. Cell culture

Human squamous carcinoma (A431), breast adenocarcinoma (MCF-7) and keratinocyte (HaCaT) cell lines were sourced from the NCCS, Pune, India. Human tongue carcinoma (SAS), HaCaT, MCF-7, and A431 cells were cultured in high glucose DMEM, supplemented with 10% FBS and 1X antibiotic-antimycotic solution. Whereas, non-tumorigenic epithelial (MCF-10) cells were cultured in DMEM/F12 media

supplemented with 5% horse serum, 0.5 mg/mL hydrocortisone, 20 ng/mL EGF, 10 µg/mL insulin and 100 ng/mL cholera toxin.

3.2.3.2. Cytotoxicity study of silk sericin

Cytotoxicity of SS was assessed using the MTT assay. Briefly, 1×10^4 cells per well were seeded in 48 well plates, cultured for 24 h at 37 °C and treated with different (500, 1000, 2000 and 4000 µg/mL) concentration of SS. After 24, 48 and 72 h of treatment, cells were incubated with 200 µL of MTT (1: 9 ratio of MTT and phosphate buffer saline) solution for 4 h. Formazan crystals formed by mitochondrial dehydrogenase were dissolved in DMSO and absorbance was measured at 570 nm by using a multiplate reader (Tecan, Infinite 200).

3.2.3.3. Lactate dehydrogenase (LDH) assay

The effect of SS on the cellular membrane integrity of cancer cells was assessed using the LDH assay. In brief, cancer cells (2×10^4) were cultured in 48 well plates for 24 h and treated with 4 mg/mL of SS for 24 h. Post-treatment, 50 µL of spent media was collected and analyzed for LDH activity according to the manufacturer's protocol.

3.2.3.4. Determination of intracellular reactive oxygen species (ROS) level

The change in the intracellular ROS levels of SS treated cancer cells were assessed using DCFH-DA (Kumar et al., 2017). In brief, a density of 3×10^5 cells per well was seeded in 6 well plates, incubated for 24 h and treated with 4 mg/mL of SS. After 24 h, cells were incubated with 10 µM DCFH-DA for 1 h at 37 °C. Fluorescence generated by the hydrolysis of DCFH-DA to DCF due to cellular esterases and intracellular ROS was measured using flow cytometer (FACS Calibur, BD). For each sample, 50,000 events were collected and the results were analyzed using FCS Express 6.

2.3.5. Determination of endogenous antioxidant activity

3.2.3.5.1. Superoxide dismutase (SOD) activity

SOD activity in SS treated cancer cells was assessed using the SOD assay kit. Briefly, 3×10^5 cells per well were seeded in 6 well plates, cultured for 24 h and treated with 4 mg/mL of SS. Cells were scraped and lysed in 50 µL of cell lysis buffer (20 mM HEPES-KOH (pH-7.4), 2 mM EDTA, 250 mM NaCl, 1% Triton X-100, 1 mM DTT, 1 µg/mL of pepstatin A and 2 µg/mL of aprotinin) for 30 min on ice. Cell lysates were centrifuged and the aliquots of the supernatants were analyzed for SOD activity according to the manufacturer's protocol. The assay kit utilized water-soluble

tetrazolium (WST-1) salt, which converted to water-soluble formazan upon reduction of superoxide anion (O_2^-). Conversion of WST-1 to formazan was recorded at 450 nm using the multiplate reader.

3.2.3.5.2. Catalase (CAT) activity

The effect of SS on the CAT activity was assessed using the Amplex red catalase assay kit. Cancer cells (3×10^5 cells) were seeded in 6 well plate and cultured for 24 h followed by SS (4 mg/mL) treatment. After 24 h of treatment, cells were scraped and lysed in 50 µL of cell lysis buffer for 30 min followed by centrifugation. Aliquots of the supernatant were used to analyze catalase activity according to the manufacturer's protocol.

3.2.3.6. Cell cycle analysis

Cancer cells (3×10^5 cells per well) were cultured in 6 well plates for 24 h and treated with 4 mg/mL of SS. After 24 h of treatment, cells were harvested and assessed for cell cycle arrest by PI using our previously established protocol (Kumar et al., 2016). For each sample, 50,000 events were collected and the results were analyzed using FCS Express 6.

3.2.3.7. Mitochondrial membrane potential (ψm) analysis

Change in inner mitochondrial membrane potential of the cancer cells after SS treatment was analyzed by flow cytometer using the JC-1 assay kit. In brief, cancer cells were seeded in 6 well plates at a density of 3×10^5 cells per well and cultured for 24 h. Cells were treated with 4 mg/mL of SS for 24 h, harvested, labeled with JC-1 dye and analyzed using flow cytometer. For each sample, 50,000 events were collected and the results were analyzed using FCS Express 6.

3.2.3.8. Annexin V/PI assay

Apoptotic cell death was determined using the Annexin V-FITC/ PI assay kit. Cancer cells were seeded in 6 well plates at a density of 3×10^5 cells per well and cultured for 24 h. Cells were treated with SS (4 mg/mL) for 24 h, harvested and labeled with FITC conjugated Annexin V and PI, and analyzed using flow cytometer. For each sample, 50,000 events were collected and the results were analyzed using FCS Express 6.

3.2.3.9. Gene expression studies

A density of 5×10^5 cancer cells was cultured in 60 mm Petri dishes for 24 h at 37 °C and treated with 4 mg/mL of SS. After 24 h of treatment, RNA was extracted from the cancer cells using TRIzol reagent. The concentration and purity of the RNA were

measured using NanoDrop (Eppendorf, Germany) spectrophotometer. 1 µg of RNA was reverse transcribed to cDNA using High-capacity cDNA Reverse Transcription kit (Applied Biosystems, Thermo Fisher Scientific, USA) in a thermal cycler (Takara, Japan). The expression level of p53, Bcl-2, Bax, cyt *c*, β-actin, caspase-3, caspase-8, and 9 genes were quantified using Power SYBR Green PCR master mix (Applied Biosystems, Life Technologies) in a real-time polymerase chain reaction (RT-PCR) machine (Applied Biosystems 7500) with the sequences shown in **Table 3.1**.

Table 3.1. *Description of primer sequences*

Gene	Primer	Sequence	Accession number
p53	Forward	5′-GCCCAACAACACCAGCTCCT-3′	NM_001126118.1
	Reverse	5′-CCTGGGCATCCTTGAGTTCC-3′	
Bcl-2	Forward	5′-TTGTGGCCTTCTTTGAGTTCGGTG-3′	NM_000657.2
	Reverse	5′-GGTGCCGGTTCAGGTACTCAGTCA-3′	
Bax	Forward	5′-CCTGTGCACCAAGGTGCCGGAACT-3′	NM_001291431.1
	Reverse	5′- CCACCCTGGTCTTGGATCCAGCCC-3′	
Caspase-8	Forward	5′-CTGCTGGGGATGGCCACTGTG-3′	NM_001080125.1
	Reverse	5′-TCGCCTCGAGGACATCGCTCTC-3′	
Caspase-9	Forward	5′-AGTTCCCGGGTGCTGTCTAT-3′	NM_032996.3
	Reverse	5′-GCCATGGTCTTTCTGCTCAC-3′	
Caspase-3	Forward	5′-ACATGGCGTGTCATAAAATACC-3′	NM_001354779.1
	Reverse	5′-CACAAAGCGACTGGATGAAC-3′	
Cyt *c*	Forward	5′-ATGGTCTCTTTGGGCGGAAG-3′	NM_018947.5
	Reverse	5′-GGCAGTGGCCAATTATTACTCA-3′	
β-actin	Forward	5′-CCCTGGCACCCAGCAC -3′	

Reverse	5′-GCCGATCCACACGG AGTAC-3′	NM_001101.4

3.2.3.10. Western blotting

Cancer cells (3×10^5) were cultured in 6 well plates for 24 h and treated with 4 mg/mL of SS. Post-treatment, cells were washed with PBS, trypsinized and lysed in 50 µL of RIPA buffer [10 mM Tris (pH 8), 0.1% NP-40, 150 mM NaCl, 0.5% sodium deoxycholate, 1 mM sodium orthovanadate, 0.1% SDS, 1 mM PMSF and 4 µg/mL of aprotinin] (Liang et al., 2001). The cell lysates were centrifuged and the total protein concentration in the supernatants was determined using the Bradford assay (Sigma, USA). An equal amount of protein (30 µg) was separated using SDS-PAGE (12% separation gel and 5% stacking gel) and transferred to Immobilon-P PVDF membrane (Merck Millipore, USA) using a western blot apparatus. The blot was blocked with Tris-buffered saline-Tween (TBST) blocking buffer containing 5% skim milk for 1 h followed by incubation in specific primary antibodies; anti-Bcl-2 (mouse monoclonal, Invitrogen, USA) (1:500), anti-Bax (mouse monoclonal, Invitrogen, USA), and anti-GAPDH (mouse monoclonal, Abcam, UK) (1:1000). The blot was washed with TBST wash buffer and incubated for 1 h in goat anti-mouse IgG, 1:5000 antibodies conjugated to horseradish peroxidase (Abcam, USA). Using ECL kit (Biorad, USA), the protein expression levels were found using an image analyzer (Biorad, USA).

3.2.4. Statistical analysis

All quantitative experiments were carried out in triplicate and data were analyzed to attain mean ± standard deviation. ANOVA was examined with the Holm-Sidak method using Sigma-plot software.

3.3. Results

3.3.1. Cytotoxicity study of silk sericin

Metabolically active viable cells convert water-soluble thiazolyl blue tetrazolium bromide to water-insoluble formazan in the presence of mitochondrial dehydrogenases. The viability of A431, MCF-7, SAS, HaCaT and MCF-10 cells after SS treatment was assessed by measuring their mitochondrial activity using the MTT assay. The viability of cancer (A431, SAS, and MCF-7 cells) and normal (HaCaT and MCF-10 cells) cells after SS treatment for 24, 48 and 72 h are depicted in **Fig.3.1**. The viability of both cancer

and normal cells remained unaffected after treating with SS up to 1 mg/mL; however, with increasing SS concentration the viability of cells was decreased. In comparison with control cells, A431 and SAS cells treated with 4 mg/mL of BMS, PRS, and AAS showed <50% cell viability. Whereas, MCF-7 cells treated with AAS (4 mg/mL) exhibited >50% growth inhibition. HaCaT and MCF-10 cell lines treated with 4 mg/mL of SS showed ~70% viable cells. This indicated that SS is more toxic to cancer cells than normal cell lines. 4 mg/mL of AAS (A431, MCF-7, and SAS), BMS (A431 and SAS cells), and PRS (A431 and SAS cells) were selected for further evaluation of their anticancer activity against specific cancer cells based on their IC_{50} value.

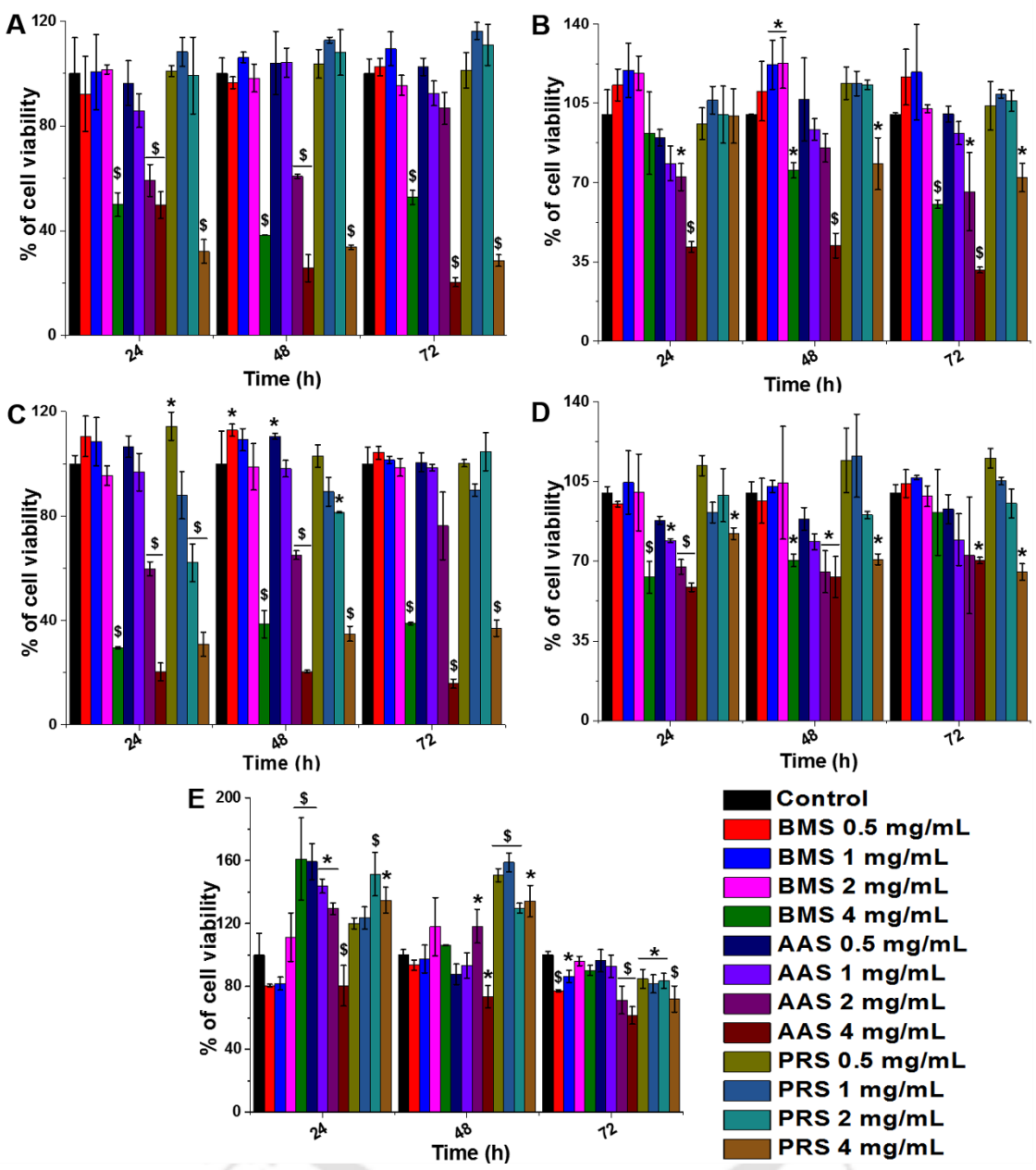

Fig.3.1. *The effect of silk sericin on the viability of (A) A431, (B) MCF-7, (C) SAS, (D) HaCaT, and (E) MCF-10 cells was assessed using MTT assay. ($p≤0.001 and *p≤0.01 in comparison with control).*

3.3.2. Lactate dehydrogenase (LDH) assay

Pro-oxidant compounds might also induce cytotoxicity by disrupting cellular membrane integrity. The release of cytoplasmic LDH into surrounding media is an early marker for cellular membrane disruption. The effect of SS on the membrane integrity of cancer cells was assessed using the LDH assay kit. **Fig.3.2** illustrates the LDH activity of SS treated cancer cells. In comparison with control cells, AAS and PRS treated cancer

cells showed significantly low LDH activity ($p \leq 0.01$), however, LDH activity of BMS treated cancer cells remain unchanged.

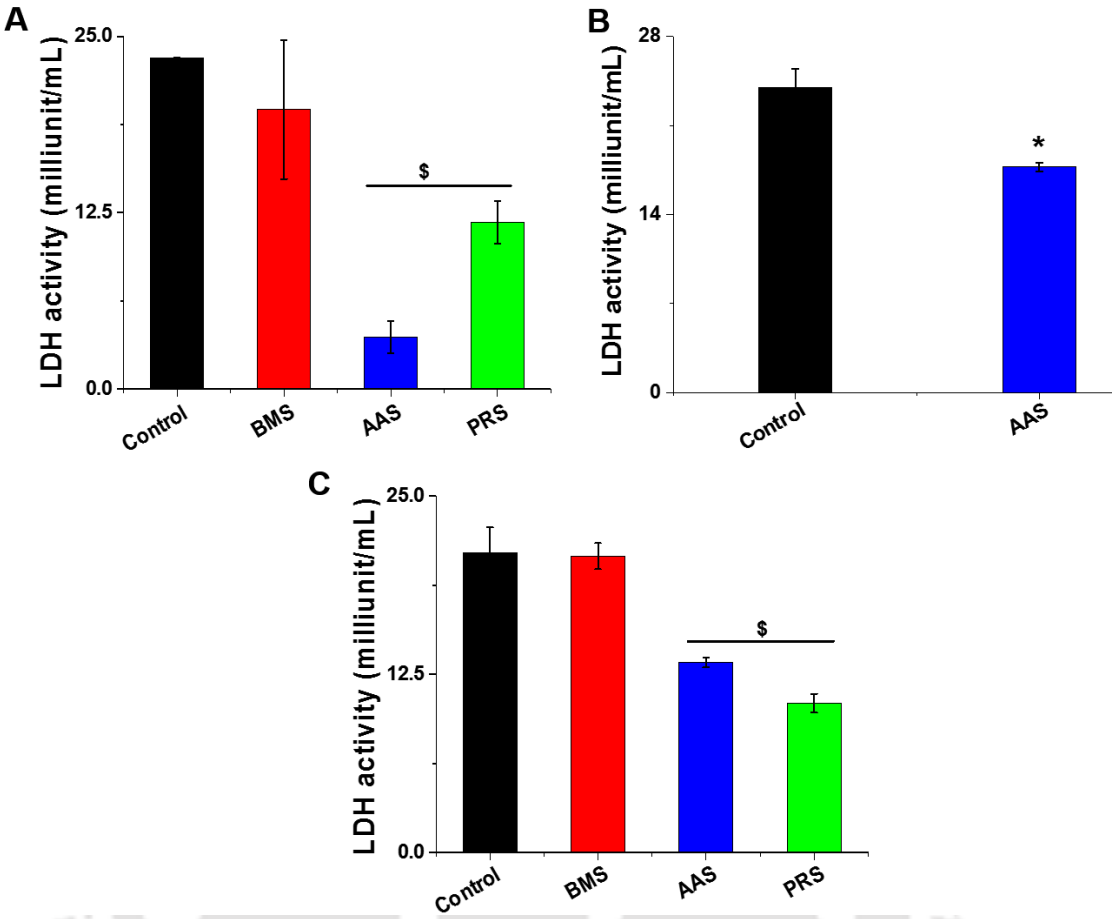

Fig.3.2. *The effect of silk sericin on the cellular membrane integrity of (A) A431, (B) MCF-7, and (C) SAS cells were assessed by determining their LDH activity. ($p≤0.001 and *p≤0.01 in comparison with control).*

3.3.3. Determination of intracellular reactive oxygen species (ROS) level

Pro-oxidant compounds induce oxidative stress in cancer cells by elevating their intracellular ROS levels. The change in the intracellular ROS levels was determined using DCFH-DA. The intracellular ROS levels of cancer cells are illustrated in **Fig.3.3**. SS treatment significantly enhanced ROS levels of cancer cells in comparison with their perspective control cells.

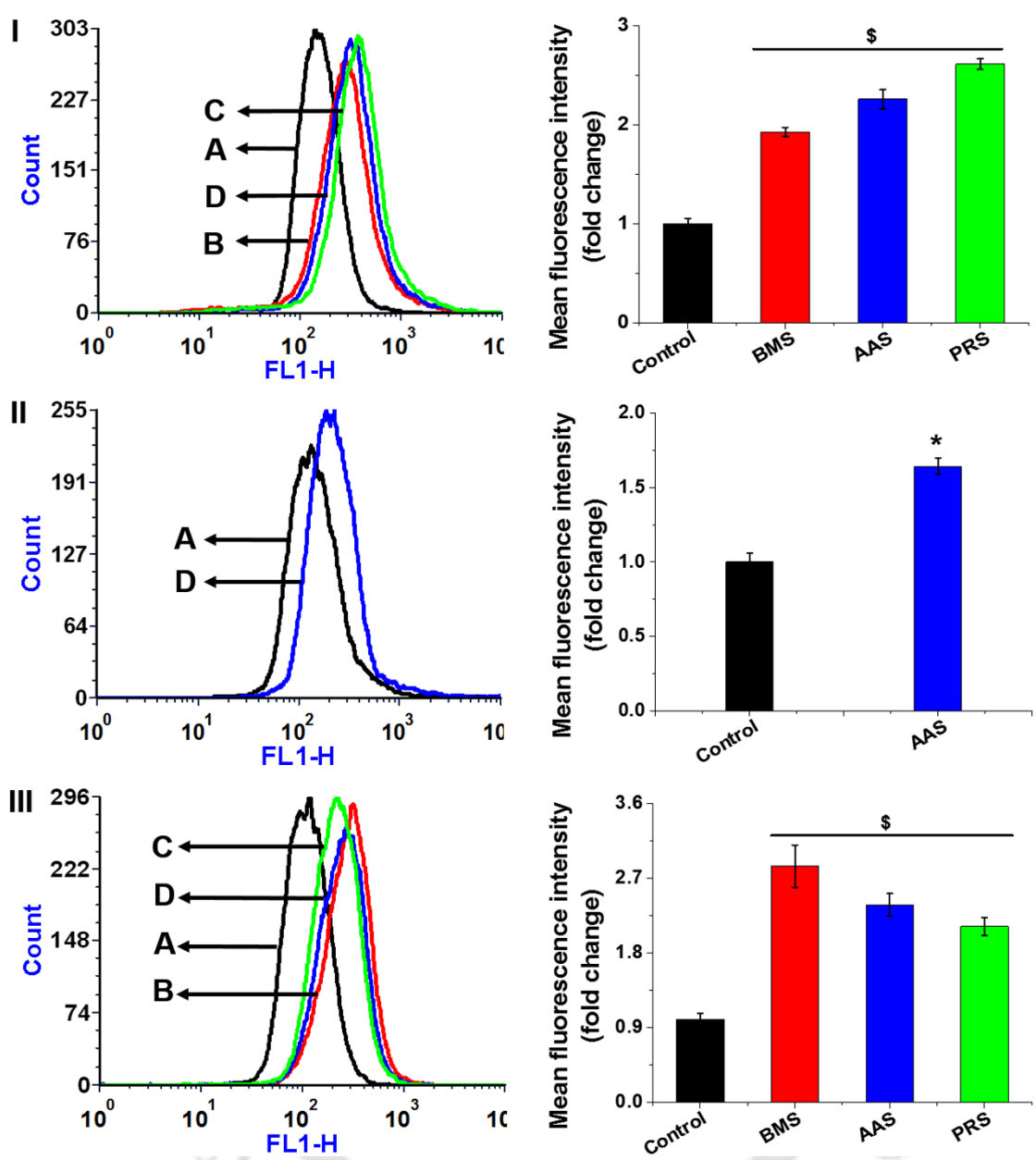

Fig.3.3. *The effect of silk sericin on the intracellular ROS levels of (I) A431, (II) MCF-7, and (III) SAS cells was assessed using DCFH-DA; where (A) control, (B) BMS, (C) PRS, and (D) AAS treated cells. ($p≤0.001 and *p≤0.01 in comparison with control)*

3.3.4. Superoxide dismutase (SOD) activity

SOD, an endogenous antioxidant enzyme converts highly unstable superoxide (O_2^-) to stable hydrogen peroxide and molecular oxygen (Gough and Cotter, 2011). Loss of SOD activity, in turn, enhances ROS production in the cells resulting in oxidative damage. SOD activity was assessed by the inhibition of formazan formation from WST-1 using the superoxide anion produced by xanthine oxidase utilizing xanthine and molecular oxygen. **Fig.3.4** depicts endogenous SOD activity of SS treated cancer cells.

In comparison with control cells, SOD activity was significantly reduced in AAS treated cancer cells ($p \leq 0.01$). Whereas, SOD activity of A431 cells was increased by BMS and PRS treatment.

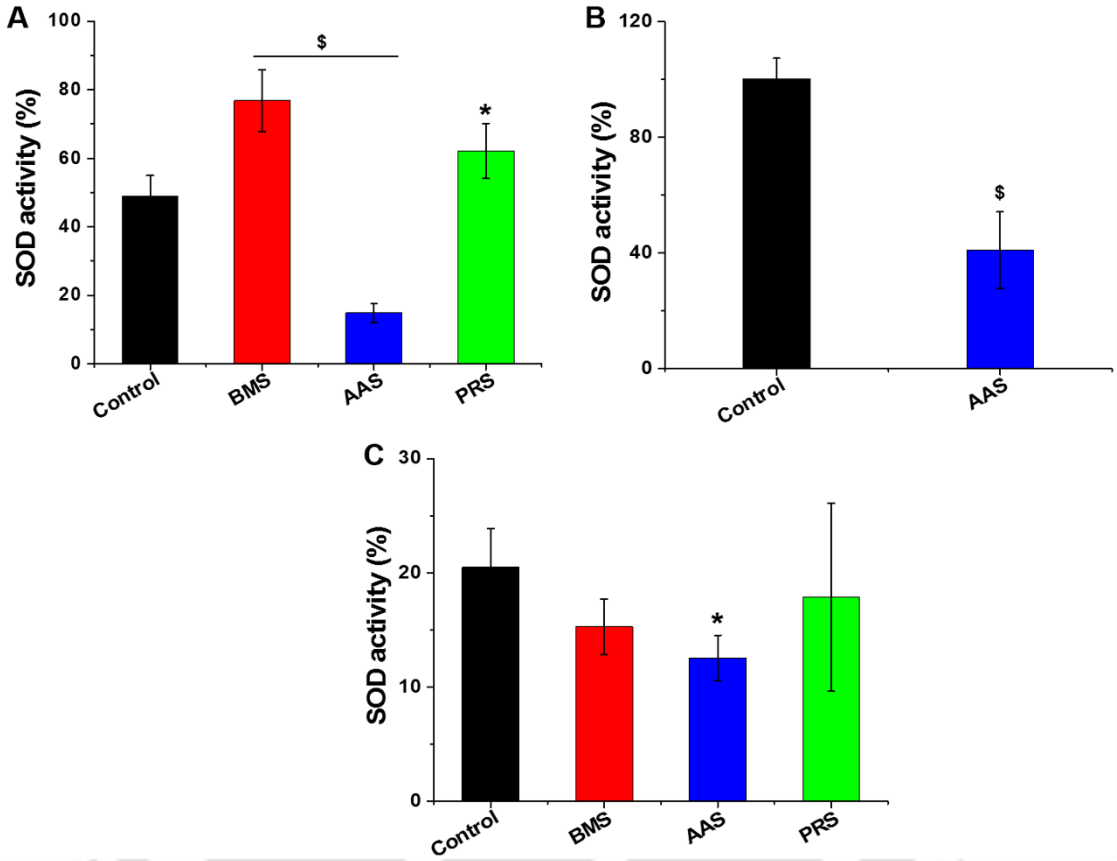

Fig.3.4. *The effect of silk sericin on the activity of endogenous SOD activity of (A) A431, (B) MCF-7, and (C) SAS cells were assessed by the percentage inhibition of the formazan formation from WST-1 using the superoxide anion produced by xanthine oxidase. ($p≤0.001 and *p≤0.01 in comparison with control).*

3.3.5. Catalase (CAT) activity

CAT is a cytoplasmic antioxidant enzyme that converts hydrogen peroxide to water and molecular oxygen (Gough and Cotter, 2011). CAT activity was evaluated using Amplex red, which reacts with hydrogen peroxide in 1:1 ratio and emits fluorescence. **Fig.3.5** illustrates the absorbance of remaining hydrogen peroxide present after breakdown to water and molecular oxygen by the endogenous CAT of cancer cells. In comparison with control, the CAT activity of SS treated cancer cells remained unaffected.

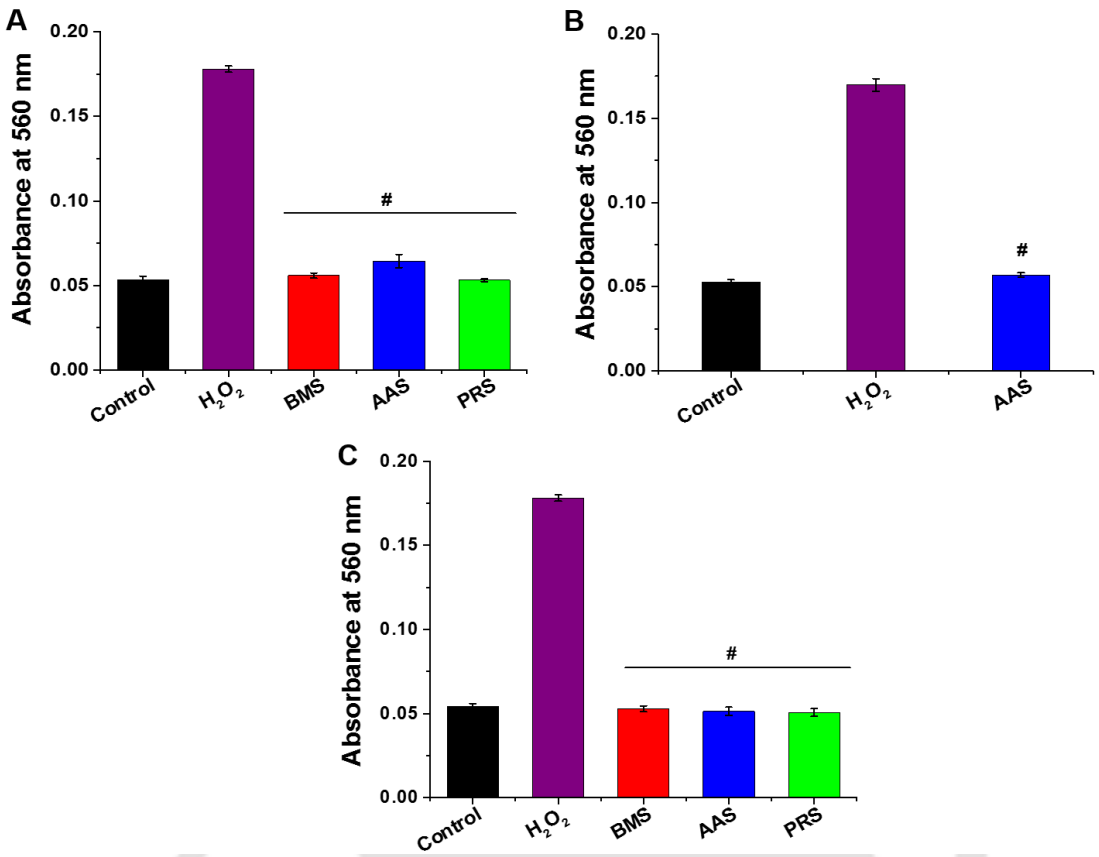

Fig.3.5. *The effect of silk sericin on the endogenous CAT activity of (A) A431, (B) MCF-7, and (C) SAS cells were assessed using the Amplex red assay kit. (#p≤0.001 in comparison with only hydrogen peroxide).*

3.3.6. Cell cycle analysis

Most of the anticancer/pro-oxidant compounds induce cell cycle arrest and cause apoptotic cell death. The effect of SS on the cell cycle of cancer cells was analyzed by flow cytometry using PI. **Fig.3.6** depicts the percentage of the gated population of cancer cells present in different phases of the cell cycle. Gated cell population represented in sub-G1 and G1 phase correspond to cell death by apoptosis/ necrosis and cell cycle arrest, respectively. In comparison with A431 control cells, AAS and PRS treated cells showed a significantly high percentage of gated cell population at the sub-G1 phase and reduced gated population at G1 phase ($p \leq 0.01$). As compared with MCF-7 control cells, AAS treatment increased the percentage of gated cell population at sub-G1 phase ($p \leq 0.001$), without changing the population at G1 phase. Whereas, the gated population of SS treated MCF-7 and A431 cells remained unchanged at S and G2 phases. SS treated SAS showed a high percentage of the gated population at the sub-G1 phase and reduced gated population at G1 and G2 phases than control cells ($p \leq 0.01$).

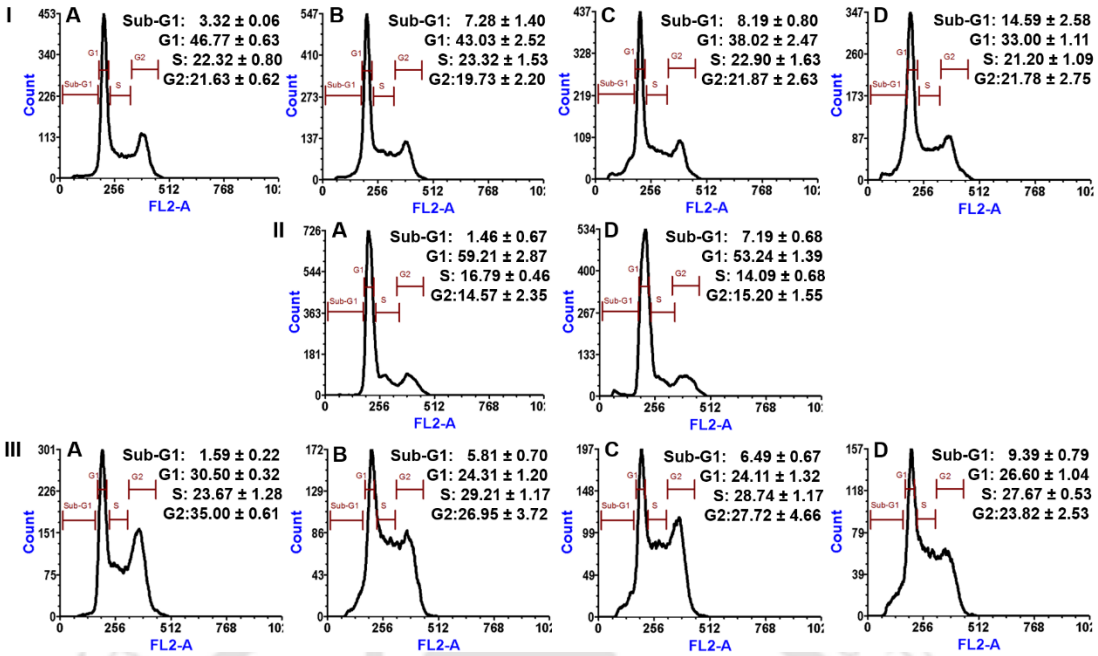

Fig.3.6. *The effect of silk sericin on the cell cycle analysis of (I) A431, (II) MCF-7, and (III) SAS cells was assessed by flow cytometer using PI: Where (A) control, (B) BMS, (C) PRS and (D) AAS treated cancer cells. Data are expressed as mean ± S.D (n=3).*

3.3.7. Mitochondrial membrane potential (ψm) analysis

Depletion of inner mitochondrial membrane potential is an early marker during apoptotic cell death (Garg and Chang, 2004). Changes in inner mitochondrial membrane potential were monitored by flow cytometer using JC-1 cationic fluorescent dye. **Fig.3.7** depicts the change in the inner mitochondrial membrane potential of SS treated cancer cells. The degree of mitochondrial membrane potential change varied with the source of SS. In comparison with control, the mitochondrial membrane potential of SS treated A431 and SAS cells remain unchanged, however, AAS treated MCF-7 cells showed 35.2 fold depletion of inner mitochondrial membrane potential.

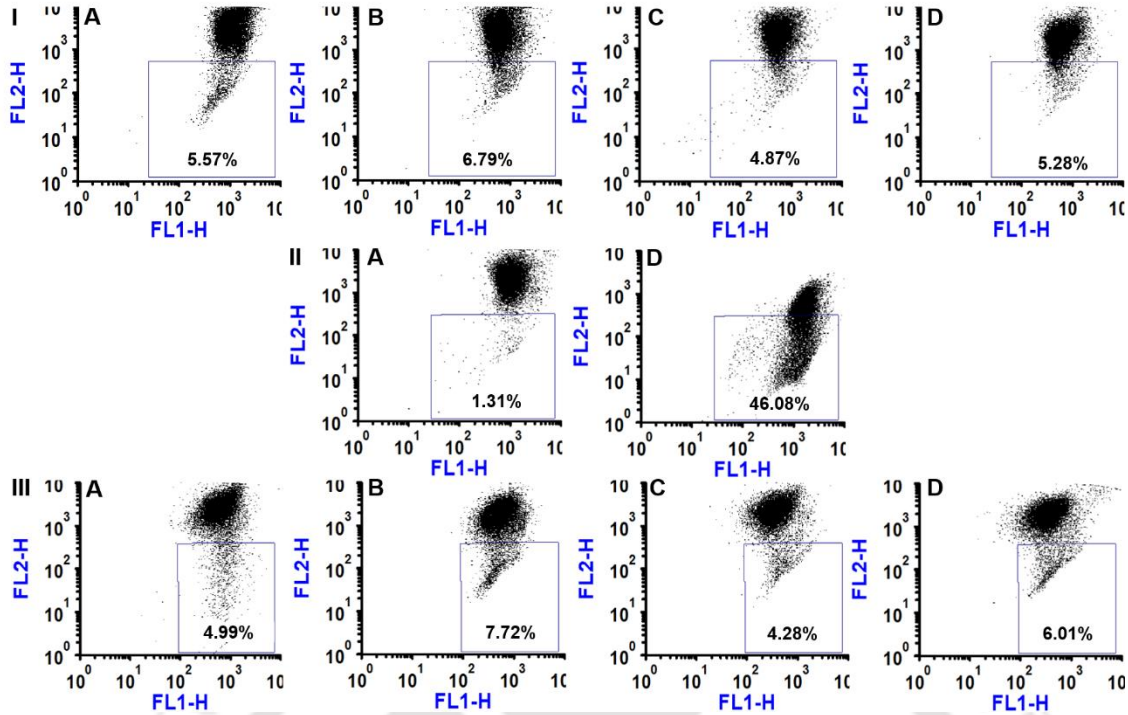

Fig.3.7. *The change in the inner mitochondrial membrane potential of silk sericin treated (I) A431, (II) MCF-7, and (III) SAS cells was assessed using the JC-1 assay kit. Where (A) control, (B) BMS, (C) PRS, and (D) AAS treated cancer cells.*

3.3.8. Annexin V/PI assay

Apoptotic cell death caused by SS treatment was assessed by flow cytometer using Annexin V/PI staining kit. **Fig.3.8** depicts the quadrat plots, which represents the percentage of cell population present at early (positive for Annexin V only), late (positive for both Annexin V and PI) apoptosis and dead (positive for PI only) phase. SS treatment induced the apoptotic death in cancer cells. BMS, PRS, and AAS treated A431 cells enhanced percentages of cell population at early (6.3, 3, and 3.6 folds, respectively) and late (3.7, 3.1, and 4.47 folds, respectively) apoptotic phase. AAS treated MCF-7 cells showed 9.6 and 9.2 fold enhanced cell population at early and late apoptotic phase, respectively. When compared to SAS control cells, BMS, PRS, and AAS treated cells showed enhanced cell population at early (3.9, 1.5 and 2.9 fold, respectively) and late (24.3, 5.6, 13.33 fold, respectively) apoptotic phase.

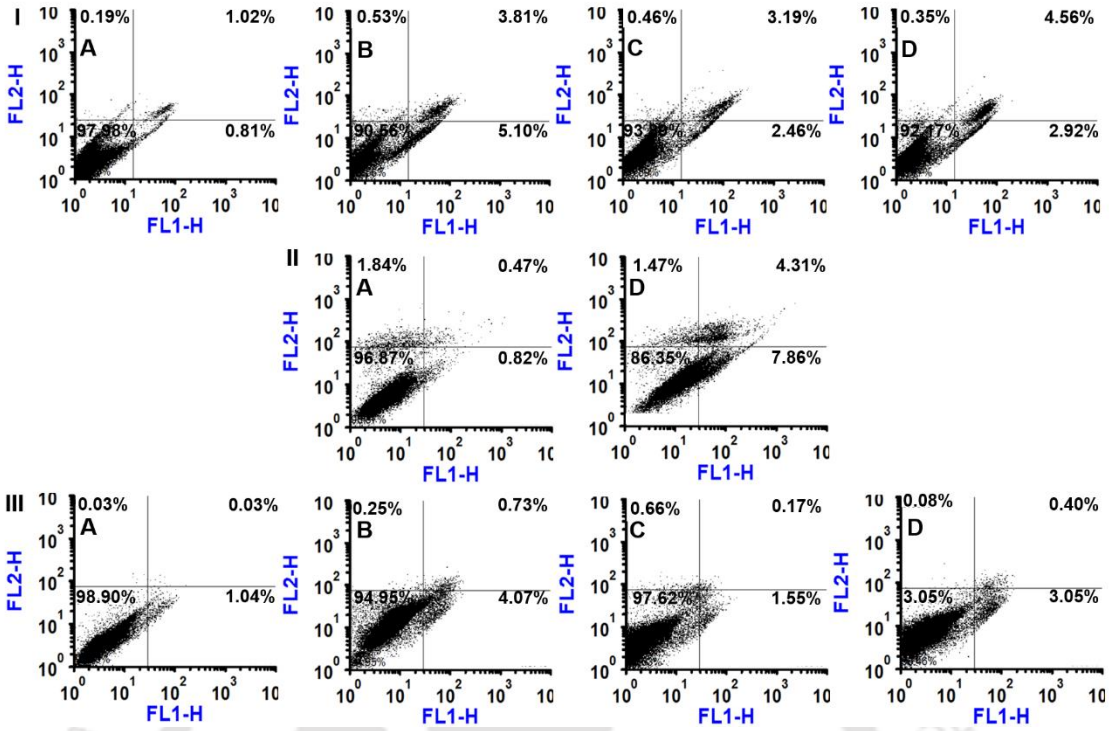

Fig.3.8. *Apoptotic death induced by oxidative stress-mediated with silk sericin treatment in (I) A431, (II) MCF-7, and (III) SAS cells was assessed using Annexin V/PI. Where (A) control, (B) BMS, (C) PRS, and (D) AAS treated cells.*

3.3.9. Gene expression studies

Pro-oxidants/ anticancer compounds induce redox imbalance, which leads to the upregulation of tumor suppressor, pro-apoptotic, and caspase gene expression along with downregulation of anti-apoptotic genes and results in apoptotic death. The effect of SS on the expression of a tumor suppressor (p53), cyt *c*, caspase-3, caspase-8, caspase-9, Bax and Bcl-2 genes was evaluated using quantitative RT-PCR. **Fig.3.9** depicts the expression of p53, cyt *c*, caspase-3, caspase-8, caspase-9, Bax, and Bcl-2 genes in SS treated cancer cells. In comparison with control cells, SS treated A431 and SAS cells showed ~1.5 and 2 fold high expression of p53 gene, respectively, whereas, in MCF-7 cells p53 gene expression remain unaffected. A431 cells treated with BMS and PRS showed upregulation of cyt *c*, caspase-3, caspase-8, and caspase-9 gene expression than control. While AAS treated A431 cells showed 9.8 fold upregulation of caspase-9 expression, however, cyt *c*, caspase-3, and caspase-8 gene expression remained unchanged. When compared to control cells, SS treated A431 cells exhibited dysregulation of Bax/Bcl-2 genes. AAS treated MCF-7 cells showed upregulation of cyt *c* (2 fold), caspase-9 (1.3 fold) and Bax (4.2 fold) expression, whereas, downregulation

of Bcl-2 and caspase-8 expression. SAS cells showed upregulation of cyt *c*, caspase-3 (for BMS, AAS, and PRS treated cells), caspase-9 (for AAS and PRS treated cells), caspase-8, and Bcl-2 (for BMS and PRS treated cells) expression after SS treatment than control cells. In SS treated SAS cells, Bax expression remained unchanged.

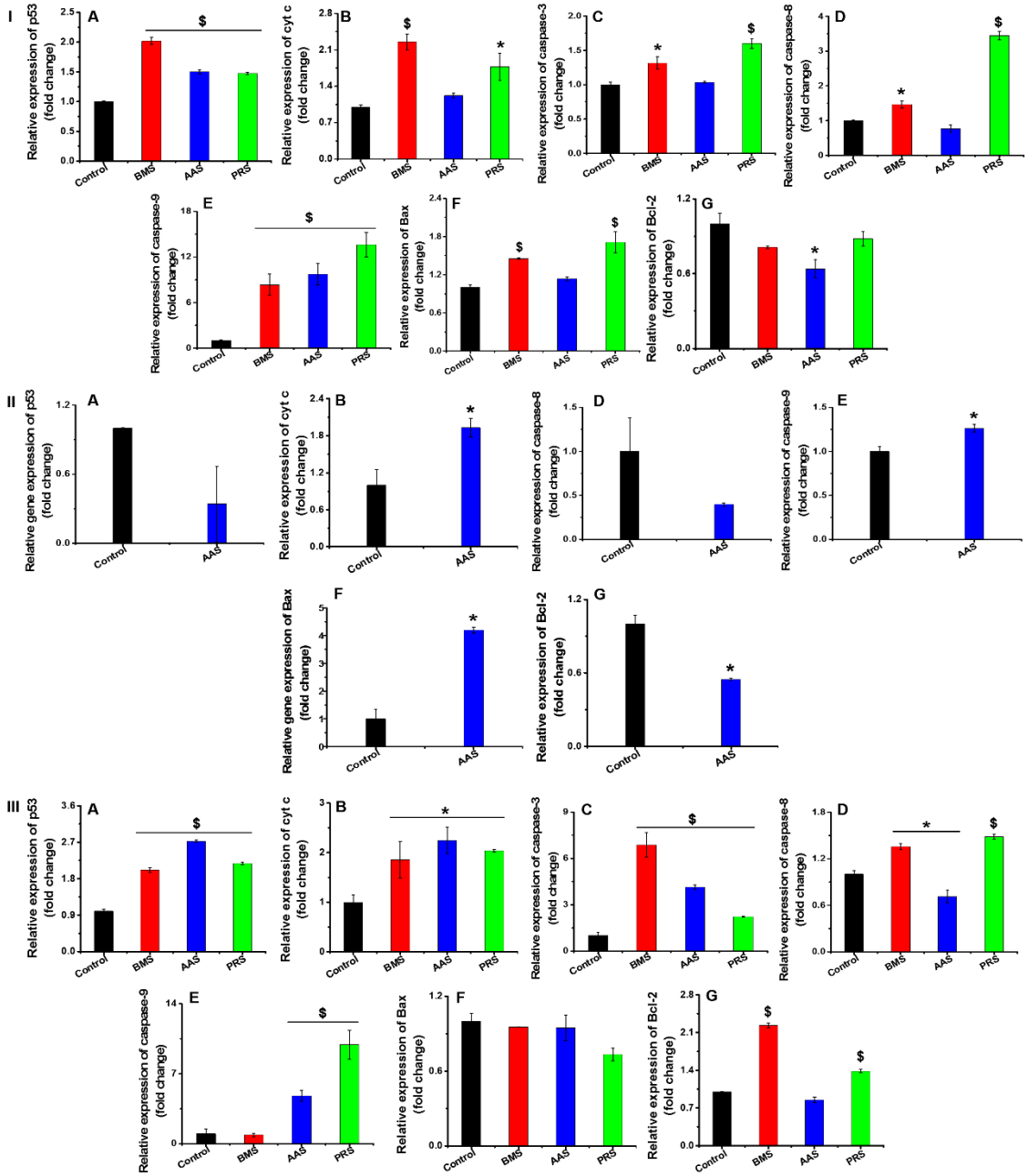

Fig.3.9. *The effect of silk sericin on the relative expression of (A) p53, (B)* cyt *c, (C) caspase-3, (D) caspase-8, (E) caspase-9, (F) Bax, and (G) Bcl-2 genes in (I) A431, (II) MCF-7, and (III) SAS cells was assessed using RT-PCR. ($p≤0.001 and *p≤0.01 in comparison with control)*

3.3.10. Western blotting

Bax and Bcl-2 protein expression play an important role in regulating apoptotic cell death. Redox imbalance induced by pro-oxidants/ anticancer compounds upregulate Bax and downregulates Bcl-2 protein expression that leads to apoptotic death. The effect of redox imbalance induced by the various source of SS on the expression of Bax and Bcl-2 proteins was assessed using western blotting. Bax and Bcl-2 expression in A431, SAS, and MCF-7 cells post-treatment with SS are depicted in **Fig.3.10**. The Bax expression was upregulated in AAS treated A431 cells when compared to control cells, however, its expression was unchanged in BMS and PRS treated cells. Similar Bcl-2 expression was observed in SS treated A431 cells and its counterparts. In comparison with their control cells, AAS treatment significantly downregulated Bcl-2 expression in MCF-7 and SAS cells, while BMS and PRS treatment did not change its expression. The Bax expression in SS treated MCF-7 and SAS remained similar with control cells.

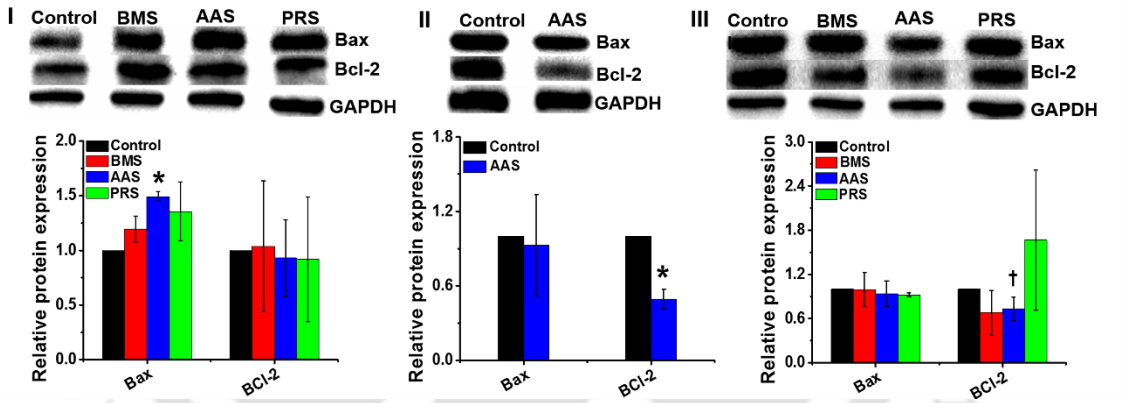

Fig.3.10. *The effect of silk sericin on the expression of Bax and Bcl-2 protein in (I) A431, (II) MCF-7, and (III) SAS cells was determined by western blotting. (*p≤0.01, and* †p≤0.05 *in comparison with control)*

3.4. Discussion

ROS play a key role in cancer initiation, progression, and metastasis (Weinberg and Chandel, 2009; Weinberg et al., 2010). Endogenous antioxidants protect the cancer cells from ROS induced oxidative damage by maintaining them at basal levels (Gorrini et al., 2013). However, insufficient endogenous antioxidant mechanism elevates intracellular ROS levels that lead to oxidative stress-mediated apoptosis in cancer cells (Palanivel et al., 2014). Accumulation of intracellular ROS in cancer cells due to chemotherapeutics (doxorubicin, cisplatin etc.) and pro-oxidants (polyphenols,

flavonoids, curcumin, and resveratrol) is one of the major strategies for inducing apoptosis (Fang et al., 2009; Lee et al., 2013).

Dietary polyphenols and flavonoids protect the cells from oxidative stress-induced damage by reducing the ROS and modulating the activity/ expression of endogenous antioxidants enzymes (Pietta, 2000; Tadić et al., 2008). Further, they reduce the risk of occurrence of various diseases like cancer, neurodegeneration, metabolic and cardiovascular diseases (Cotelle, 2001; Dai and Mumper, 2010; León-González et al., 2015; Mink et al., 2007). In certain conditions like high polyphenol concentrations and the presence of redox active transition metals cations, they can act as pro-oxidants and induce oxidative stress (Park and M Pezzuto, 2012). The pro-oxidant properties of polyphenols depend on the formation of labile aroxil radical or redox complex with transition metal ion. The labile aroxil radicals react with molecular O_2 and results in the formation of superoxide anions (O_2^-) (Hodnick et al., 1988). O_2^- induce redox imbalance in cancer cells that leads to oxidative stress mediated apoptotic cell death.

SS, a glycoprotein known to possess antioxidant activity along with other biological properties (Chlapanidas et al., 2013; Kumar and Mandal, 2017). The antioxidant properties of SS are attributed to the amino acids (hydroxyl group of serine and threonine; delocalizing electron of aromatic amino acids) and secondary metabolites (polyphenols and flavonoids) associated with it (Kumar and Mandal, 2017). Their composition varies with the source of sericin as well as with extraction methods (Kumar and Mandal, 2017). The amino acids of SS and associated secondary metabolites, which contribute to antioxidant activity, may act as pro-oxidants, elevate intracellular ROS production and lead to oxidative stress-mediated apoptotic death in cancer cells. Therefore, in the present study, the pro-oxidant activity of SS isolated from the BM, AA, and PR was investigated using A431, MCF-7, and SAS cells.

The properties of SS alters with respect to the extraction methods (Kumar and Mandal, 2017). In our previous study, alkali-degraded BMS, AAS and PRS showed antioxidant activity and protected the L929 cells against H_2O_2 induced oxidative stress (Kumar and Mandal, 2017). Alkali-degraded BMS, AAS, and PRS were selected in the current study to evaluate the anticancer activity by inducing oxidative stress. Cytotoxicity of SS evaluated by MTT and LDH assay revealed that 4 mg/mL of SS inhibited >50% cancer cells proliferation **(Fig.3.1)** without disrupting their cellular membrane integrity **(Fig.3.2** and **Fig.A3.1)**; whereas, ~30% decrease in cell viability was observed in SS treated normal cells. Cancer cells exhibit higher endogenous ROS levels than normal

cells and disruption of their ROS levels induces cell death (Zhu et al., 2014). At low concentrations, SS acts as an antioxidant and maintain intracellular ROS levels (Terada et al., 2002). Whereas, at high concentration, the mixture of polyphenols and flavonoids associated with SS might have interacted with O_2 and induced the formation of O_2^- anion that elevated ROS levels and leads to the death of the cancer cells (Hodnick et al., 1988; Park and M Pezzuto, 2012). Intracellular ROS levels determined using DCFH-DA also showed that SS (4 mg/mL) treatment enhanced ROS production in both cancer cells **(Fig.3.3)** and normal cells **(Fig.A3.2)**.

Endogenous antioxidants protect the cells from oxidative damage by scavenging the elevated ROS levels (Birben et al., 2012). O_2^- is a primary ROS produced by the aerobic organisms (Brand, 2010). SOD present in mitochondria and cytoplasm convert O_2^- to H_2O_2 and O_2 in the presence of metal ion co-factors such as Zn, Cu, and Mn (Gough and Cotter, 2011). H_2O_2 is converted to H_2O and O_2 by the catalytic activity of CAT (Gough and Cotter, 2011). AAS treated cancer cells showed a significant reduction of SOD activity, whereas, significantly high SOD activity was seen in BMS and PRS treated A431 cells (**Fig.3.4**). Co-factors of the SOD play an important role in the stability of enzyme and its activity (Al-Naama et al., 2015; Chan et al., 1999), however, depletion of co-factors decreases the SODs activity (Al-Naama et al., 2015). Hydroxyl groups of serine and threonine of SS chelate the trace elements such as copper and iron (Kato et al., 1998). Serine and threonine of AAS might have chelated the copper ion of SOD and reduced its activity. Whereas in BMS and PRS treated A431 cells, SOD activity was upregulated to reduce the elevated levels of ROS. Amino acid and secondary metabolites present in BMS, PRS, and AAS were unable to disturb the co-factor of CAT due to which there was no loss in its activity (**Fig.3.5**).

Oxidative stress induced by redox imbalance activates the tumor suppressor genes and inhibits the cyclin-dependent kinases (CDK) that result in cell cycle arrest at Go/G1 or G2/M phases (Habold et al., 2008). Redox imbalance induced by SS in cancer cells might have activated tumor suppressor genes and inhibited the CDK that resulted in cell cycle arrest at G1 phases followed by cell death (sub-G1 phase). These changes resulted in an increased and decreased percentage of gated cell population at the sub-G1 phase and G1 phase, respectively (**Fig.3.6**). Whereas, redox imbalance induced by SS in HaCaT cells resulted in cell cycle arrest at G1 phases, however, they did not enter into death phase (sub-G1) (**Fig.A3.3**). Redox imbalance also destabilizes the inner mitochondrial potential of cells and initiates apoptosis by releasing the cytochrome c (cyt

c) into the cytoplasm (Li et al., 1999). AAS treated A431, SAS, and MCF-7 cells showed redox imbalance and low SOD's activity. These changes caused the depletion of inner mitochondrial membrane potential in MCF-7, whereas, the inner mitochondrial membrane potential was retained in A431 and SAS cells (**Fig.3.7**). Elevation of ROS levels, cell cycle arrest and change in inner mitochondrial membrane potential (MCF-7 cells) occurred by the redox imbalance after treating with SS triggered the apoptosis in cancer (A431, SAS, and MCF-7) cells (**Fig.3.8**).

The p53 gene is an important regulator of apoptosis (Wolff et al., 2008). p53 proteins translocate to mitochondria, where it interacts with the Bax and causes depletion of mitochondrial membrane potential that release cyt *c*, activates caspase and results in apoptotic cell death (Chipuk et al., 2004). p53 also induces apoptosis by downregulating the expression of the Bcl-2 protein (Hemann and Lowe, 2006). Redox imbalance induced in cancer cells activates the p53 gene and protein expression that leads to apoptosis (Habold et al., 2008). Redox imbalance induced in cancer cells by SS treatment upregulated the expression of the p53 gene in A431 and SAS (**Fig.3.9 I** and **IIIA**), whereas in AAS treated MCF-7, its expression remained unchanged (**Fig.3.9 IIA**). Polyphenols extracted from strawberry induced apoptosis in MCF-7 cells by activating p73 (tumor suppressor gene, structurally similar to p53 protein) gene without upregulating p53 (Somasagara et al., 2012). Redox imbalance induced in MCF-7 due to AAS treatment might have upregulated p73 gene expression and initiate apoptotic pathway. In BMS and PRS treated A431 cells, p53 gene upregulated the expression of cyt *c*, Bax, caspase-3, caspase-8 and caspase-9 gene (**Fig.3.9 IB, C, D, E,** and **F**). However, the p53 gene activated by AAS treatment induced the upregulation of caspase-9 and downregulation of Bcl-2 without altering the expression of cyt *c*, Bax, caspase-3, and 9 genes (**Fig.3.9 I**). Activated p53 gene induces the upregulation of cyt *c* and caspase-3, caspase-8 and caspase-9 gene expression in SAS (**Fig.3.9 IIIB, C, D,** and **E**). While BMS and PRS treated SAS cells tried to overcome the oxidative stress-mediated cell death through upregulated Bcl-2 gene expression (**Fig.3.9 IIIG**). MCF-7 cells are negative to caspase-3 activity (Liang et al., 2001), we have studied the effect of AAS induced oxidative on the expression of caspase-3, caspase-8, caspase-9 along with cyt *c*, Bax, and Bcl-2 expression. AAS mediated oxidative stress induced the upregulation of cyt *c*, Bax, and caspase-9, downregulation of Bcl-2 and caspase-3 expression was undetermined (**Fig.3.9 II**).

In addition to tumor suppressor gene activation, elevated levels of ROS also activates the cJun-terminal kinases (JNKs), which catalyzes the downregulation of Bcl-2 and Bcl-XL (Cadenas, 2004; Habold et al., 2008). p53 protein activation leads to the downregulation of Bcl-2 expression and upregulates the Bax expression that causes the cell senescence (Adams and Cory, 1998). AAS treatment upregulated Bax expression in A431 cells and downregulated Bcl-2 expression in MCF-7 and SAS cells (**Fig.3.10**). Redox imbalance induced in cancer cells by AAS treatment might have activated the JNK pathway along with p53 protein expression that upregulated Bax protein expression in A431 cells and downregulated the Bcl-2 expression in MCF-7 and SAS cancer cells. Upregulation of Bax or downregulation of Bcl-2 expression inhibits the dimerization of Bax/Bcl-2 and leads to the death of cancer cells (Adams and Cory, 1998). Amino acids of SS and mixture of polyphenols and flavonoids associated with it induced oxidative stress in cancer cells and leads to cell cycle arrest, depleted mitochondrial membrane potential (MCF-7), upregulated the tumor suppressor gene and downregulated the anti-apoptotic gene expression, which in turn inhibited the proliferation of cancer cells.

3.5. Significant Findings

The significant findings of this chapter are as follows:

1. At 4mg/mL, SS acted as pro-oxidant and induced redox imbalance by elevating intracellular ROS levels.
2. Redox imbalance in cancer cells caused 50% cell death by triggering cell cycle arrest at the sub-G1 phase and mitochondrial membrane potential depletion (MCF-7 cells).
3. AAS treatment caused the reduction of endogenous SOD activity in cancer cells.
4. SS treatment upregulated p53 and dysregulated Bax and Bcl-2 gene expression in A431 and SAS cells. Whereas, AAS treatment upregulated Bax and downregulated Bcl-2 gene expression in MCF-7 cells.
5. AAS treatment downregulated Bcl-2 protein expression in MCF-7 and SAS cells.
6. SS suppressed the cancer growth with marginal effect on normal cells.

The present chapter displays that AO activity possessing SS could act as pro-oxidant at higher concentration (4 mg/mL) and causes fatal damage to cancer cells with minimal effect on normal cells. This chapter provided a platform that SS could protect

the skin by suppressing the cancer growth while marginally effecting normal cells. UV radiations are one of the major environmental factors, which cause skin damage. Chronic exposure of skin to UV radiation-induced oxidative damage of the skin. Therefore, in the next chapter, it would be interesting to assess the protective effect of alkali-degraded BMS, AAS, and PRS against UV radiation-induced oxidative damage.

Chapter 4

Analyzing the Protective Activity of Silk Sericin against UV Radiation-Induced Oxidative Damage

This chapter describes the protective effect of silk sericin against UV radiation-induced skin damage. Silk sericin pretreated human keratinocytes and SKH-1 mice are irradiated with UV radiations and assessed for protective effect of silk sericin in details.

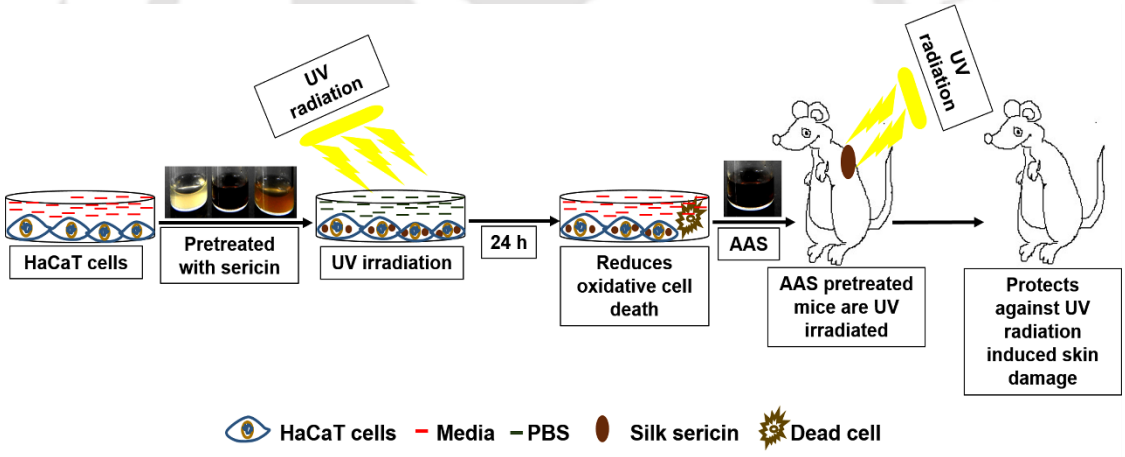

ABSTRACT

Topical delivery of potential antioxidants protects the skin against ultraviolet (UV) radiation-induced oxidative damage through maintaining redox balance. Sericin, one of the major components of silk, possesses antioxidant property along with skin-protective activity against UVB radiation-induced damage. However, the protective activity of silk sericin (SS) extracted from different sources has not been explored against UVA and UVB radiation-induced oxidative damage. In the present study, we have systematically investigated the protective activity of sericin against UVA and UVB radiation-induced skin damage. MTT and neutral red assays showed that *Philosamia ricini* sericin (PRS) and *Antheraea assamensis* sericin (AAS) (10 µg/mL) treatment prior to UVA (12 J/cm^2) and UVB (120 mJ/cm^2) irradiations enhanced the viability of human keratinocytes. Examination of cell cycle arrest and apoptotic/necrotic cell death using flow cytometry showed that sericin treatment before UVA and UVB irradiation protected the cells from apoptotic cell death by arresting the cell cycle at G1 phase. Sericin pretreatment downregulated the interleukin (IL)-6 and IL-8, upregulated p53 and decrease the dysregulation of Bcl-2/Bax gene expression. AAS treatment prior to UVB irradiation significantly reduced skin inflammation, DNA fragmentation, and lipid peroxidation in the female SKH-1 hairless mouse skin. Altogether, our results substantiate the use of AAS in effectively ameliorating UVA and UVB radiation-induced skin damage, which holds prospects as a potent antioxidant supplement in preparation of skin care products.

4.1. Introduction

The skin confers physical protection against microbes, pollutants, ultraviolet (UV) radiations, and thermal or mechanical factors (Costin and Hearing, 2007). However, chronic exposure of skin to UV radiations (UVRs) elevates reactive oxygen species (ROS) generation that induces redox imbalance and results in inflammation, immunosuppression, photoaging, erythema, edema, and skin cancer (Gil and Kim, 2000; Rittié and Fisher, 2002). Thus, the protection of skin from UVRs is crucial to overcoming UV radiation (UVR)-induced oxidative damages (Nichols and Katiyar, 2010; Yin et al., 2013).

In the electromagnetic spectrum, UVRs fall in the range of 200-400 nm and are categorized into three different regions; 400-320 nm is ultraviolet A (UVA), 320−280 nm is ultraviolet B (UVB), and 280−200 nm is ultraviolet C (UVC) Among the total UV radiations reaching earth, 90-98% is UVA, 1-10% is UVB, whereas, UVC radiations are absorbed by the ozone layer (Hou et al., 2015). UVA radiations penetrate deeper into the skin and elevate ROS production. Elevated levels of ROS eventually oxidize the cellular lipids, proteins, DNA; further eliciting apoptotic cell death (Kulms and Schwarz, 2000; Pillai et al., 2005). UVB radiations are a minor component of the total UV radiations that reach earth, however, it is more capable of inducing skin damage than UVA radiations (Dai et al., 2011). UVB radiations induce DNA damage by the formation of photoproducts. UVB radiations also elevate the ROS levels in skin cells (keratinocytes), which induce oxidative damage and further lead to tumor initiation (Lee et al., 2012). The thwart of the ROS is counterbalanced by the endogenous antioxidant defensive system, which includes both enzymatic and non-enzymatic antioxidants (Godic et al., 2014). The members of the endogenous antioxidant defense system play a considerable role against ROS and maintain body's redox balance. However, extreme production of ROS overwhelm the endogenous antioxidant activity and induces redox imbalance in the skin that results in oxidative damage and pathological conditions by altering gene expression, biochemical and signal transduction pathways (Afaq et al., 2003). Therefore, topical delivery of exogenous antioxidants might effectively counteract the ROS-induced oxidative damage.

Lepidoptera insects belonging to the Bombycidae and Saturniidae families produce two structural proteins; fibroin and sericin (Dash et al., 2007). Silk sericin (SS) is a glycoprotein, which plays an important role in cocoon formation and protects the pupa and fibroin against UVR-induced oxidative damage (Kaur et al., 2013). SS

extracted from the cocoon is known to possess various biological properties such as antioxidant, anti-lipid peroxidation, antimicrobial and antitumor activity along with suppression of tyrosinase and elastase activity (Chlapanidas et al., 2013; Kumar and Mandal, 2017, 2019; Sarovart et al., 2003). The biomedical applications of SS are endorsed to the metal chelating and electron donating groups of amino acids and associated secondary metabolites (Kumar and Mandal, 2017). Zharigetu *et al.* (2003) reported that the topical application of *Bombyx mori* sericin (BMS) protected female SKH-1 hairless mouse from UVB radiation-induced sunburn and tumor initiation. Likewise, Dash *et al.* (2008) reported that SS extracted from *Antheraea mylitta* cocoons protected human keratinocytes against UVB radiation-induced apoptotic death. Though evidence of UV protective activity of SS is documented, however, the protective effect of SS extracted from different sources of silk against UVA and UVB radiation-induced skin damage is yet to be explored holistically. Therefore, evaluating the protective effect of SS extracted from the cocoons of different silk varieties (both mulberry and non-mulberry) would be beneficial in identifying potential antioxidant molecules, which could protect skin from UV radiation-induced oxidative damage and skin carcinogenesis.

Here, we aimed to investigate the protective effect of *A. assamensis* sericin (AAS), BMS, and *Philosamia ricini* sericin (PRS) against UVA and UVB radiation-induced oxidative damage of skin. To elucidate the protective effect of SS against UVA and UVB radiation-induced skin damage, we pretreated human keratinocytes (HaCaT) with SS followed by UVA and UVB irradiation. The UVA and UVB irradiated cells were used to evaluate the protective effect of SS in the context of cell viability, intracellular ROS levels, anti-lipid peroxidation, cell cycle arrest, mitochondrial membrane potential, apoptotic/necrotic cell death, and expression of inflammatory cytokines [interleukin (IL)-6 and IL-8], p53, caspase-3, apoptotic (Bax) and anti-apoptotic (Bcl-2) genes. AAS, which showed the protective effect against UVA and UVB radiation-induced oxidative damage, were selected to evaluate the protective effect against UVB radiation-induced skin damage in the female SKH-1 hairless mice.

4.2. Materials and Methods

4.2.1. Materials

Ascorbic acid (vitamin C), Neutral red, thiazolyl blue tetrazolium bromide, RNase, Bradford's reagent and dichloro-dihydro-fluorescein diacetate (DCFH-DA) were acquired from Sigma, USA. Annexin V-Alexa 488/PI kit, PI, and JC-1 assay kit were

sourced from Invitrogen, USA. Sodium carbonate and dimethyl sulfoxide (DMSO) were obtained from SRL, India; Antibiotic-antimycotic and trypsin-EDTA were procured from HiMedia, India. High glucose Dulbecco's Modified Eagle Medium (DMEM) and fetal bovine serum (FBS) and were sourced from Gibco, life technology, USA.

4.2.2. Extraction of silk sericin using alkali-degradation

Sericin was isolated from the BM, AA, and PR cocoons using our established protocol (Kumar and Mandal, 2017). In brief, cocoon pieces were boiled for 30 min in 0.5 M Na_2CO_3 followed by dialysis with double distilled H_2O for 48 h, lyophilized and preserved at -20 °C.

4.2.3. *In vitro* studies

4.2.3.1. Cell culture

Human keratinocytes (HaCaT) cells were sourced from National Centre for Cell Science, Pune, India. HaCaT cells were cultured and maintained in high glucose DMEM complemented with 1X antibiotic-antimycotic solution and 10% FBS.

4.2.3.2. Cytocompatibility study of silk sericin

HaCaT cells were cultured in 96 well plates for overnight and treated with 10 and 100 µg/mL of SS for 24 h. Cells were incubated with MTT solution for 4 h followed by the dissolution of formazan crystals in DMSO. Optical density was recorded using multiplate reader (Tecan Infinite M200 PRO, Switzerland) at 570 nm.

4.2.3.3. Ultraviolet irradiation system

Prior to UV irradiation, cells were rinsed and covered with phosphate buffer saline (PBS) and irradiated with UVA and UVB radiation using UVP crosslinker, CL-1000L, UK consisting of 5×8 W lamps with a maximum emission peak at 365 nm and 302 nm, respectively. Overheating of the PBS during UV irradiation was prevented by keeping the tissue culture plate on ice.

4.2.3.4. MTT assay

The impact of UV radiations on the viability of HaCaT cells and protective activity of SS against UV radiation-induced cell death was assessed by MTT assay. HaCaT cells were seeded in 48 well plates and cultured until they reach 80% confluence and separately irradiated with a different dosage of UVA (0.5, 1, 3, 6, 12, 24, and 36 J/cm^2) and UVB (10, 30, 60, 120, 240, 480, and 960 mJ/cm^2) radiations. After 24 h of UV irradiation, MTT assay was executed.

In order to assess the shielding effect of SS against UVA and UVB radiation-induced cytotoxicity, we pretreated cells with 10 and 100 µg/mL of SS or Vit. C for 1 h

and irradiated with UVA (12 J/cm^2) and UVB (120 mJ/cm^2) radiations. After 24 h of UV irradiation, MTT assay was performed.

4.2.3.5. Neutral red assay

The viability of the UV irradiated cells was also evaluated by neutral red assay according to the protocol of Svobodova *et al.* (2007). In brief, HaCaT cells cultured in 48 well plates were treated with 10 and 100 µg/mL of SS or Vit. C for 1 h and irradiated with UVA (12 J/cm^2) and UVB (120 mJ/cm^2) radiations. After 24 h of irradiation, cells were incubated with 0.03% (w/v) neutral red for 2 h and washed with washing solution (0.25% w/v $CaCl_2$ and 0.125% v/v formaldehyde). Neutral red retained in the cells were dissolved in dissolving solution (50% v/v methanol and 1% v/v acetic acid) and absorbance was measured at 540 nm using a multiplate reader.

4.2.3.6. Measurement of intracellular reactive oxygen species generation

ROS scavenging ability of SS was assessed using our previously established protocol (Kumar and Mandal, 2017). In brief, HaCaT cells were cultured in 96 well plates for 24 h and treated with SS or Vit. C for 1 h. Post-treatment, cells were irradiated with UVA (12 J/cm^2) and UVB (120 mJ/cm^2) radiations and incubated with media containing 10 µM of DCFH-DA for 30 min at 37 °C. Post incubation, cells were washed and covered with PBS. The fluorescence intensity was recorded using the multiplate reader at an excitation 488 nm and emission 525 nm.

4.2.3.7. Cell cycle analysis

HaCaT cells were cultured in 6 well plates and allowed to reach 80% confluency followed by SS or Vit. C treatment for 1 h. Cells were irradiated UVA and UVB radiations followed by 24 h of incubation and the cells were trypsinized and labeled with PI using our previously established protocol (Kumar et al., 2017). The changes in the percentage of cell population at different phases of cell cycle was recorded using flow cytometer (BD, Accuri^{TM} C6 Plus).

4.2.3.8. Mitochondrial membrane potential (ψm) analysis

HaCaT cells were seeded in 6 well plates and allowed to reach 80% confluence, pretreated with SS or Vit. C for 1 h and irradiated with UVA and UVB radiations. After 30 min of irradiation, cells were trypsinized and labeled with a JC-1 dye according to the manufacturer's protocol. The change in the mitochondrial membrane potential recorded using flow cytometer.

4.2.3.9. Annexin V/PI assay

HaCaT cells were seeded in 6 well plates and at 80% confluence, they were pretreated with SS or Vit. C for 1 h and irradiated with UVA and UVB radiations. Post 24 h of irradiation, cells were harvested and re-suspended in 100 µL of binding buffer, labeled with AnnexinV/PI according to the manufacturer's protocol. The samples were analyzed using flow cytometer.

4.2.3.10. Gene expression study

HaCaT cells were seeded in 60 mm Petri dishes and cultured until they reached 80% confluence followed by SS or Vit. C treatment for 1 h and irradiated with UVA and UVB radiation. After 24 h of incubation, RNA was extracted from the cells and reverse transcribed to cDNA as described previously (Kumar and Mandal, 2019). The expression level of IL-8, IL-6, p53, caspase-3, Bax, and Bcl-2 were quantified and normalized with GAPDH genes expression using Power SYBR Green PCR master mix (Applied Biosystems, Life Technologies) using RT-PCR by Applied Biosystems Quantstudio 5 with the sequences shown in **Table 4.1**.

Table 4.1. *Illustration of primer sequences*

Gene	Primer	Sequence	Accession number
IL-6	Forward	5′- CTCAATATTAGATCTCAACCCCCA -3′	NM_000600.4
	Reverse	5′- GAGAAGGCAACTGGACCGAA -3′	
IL-8	Forward	5′- CCACCGGAGCACTCCATAAG -3′	NM_001354840.1
	Reverse	5′-GATGGTTCCTTCCGGTGGTT-3′	
p53	Forward	5′-GCCCAACAACACCAGCTCCT-3′	NM_001126118.1
	Reverse	5′-CCTGGGCATCCTTGAGTTCC-3′	
Bcl-2	Forward	5′-TTGTGGCCTTCTTTGAGTTCGGTG-3′	NM_000657.2
	Reverse	5′-GGTGCCGGTT CAGGTACTCAGTCA-3′	
Bax	Forward	5′-CCTGTGCACCAAGGTGCCGGAACT-3′	

	Reverse	5′- CCACCCTGGTCTTGGATCCAGCCC-3′	NM_001291431.1
Caspase-3	Forward	5′-ACATGGCGTGTCATAAAATACC-3′	NM_001354779.1
	Reverse	5′-CACAAAGCGACTGGATGAAC-3′	
GAPDH	Forward	5′- GACCTGACCTGCCGTCTA -3′	NM_001289745.2
	Reverse	5′- GTTGCTGTAGCCAAATTCGTT-3′	

4.2.4. *In vivo* studies

4.2.4.1. Animal care and treatment protocol

5-6 week old female SKH-1 hairless mice (22 ± 2 gm) were procured from Charles River Laboratories (Wilmington, MA, USA). The mice were adapted in the animal house (22 ± 2 °C temperature, 50-60% relative humidity, and 12 h dark or light cycle) of CSIR-Indian Institute of Toxicological Research (IITR), Lucknow. The mice were kept in a plastic cage having corncob bedding with free access to H_2O and fed with commercial pellet diet (Altromin International, supplied by ATNT Laboratories Mumbai, India) an *ad libitum* under standard laboratory conditions. After acclimation period (1 week), mice were separated into 6 groups having 3 mice in each group, where group 1: control, group 2: UVB (180 mJ/cm^2) irradiated [UVB dosage were selected based on previous studies (Kumar et al., 2012; Zhaorigetu et al., 2003)], group 3: AAS (5 mg/100 µl glycerol) + UVB, group 4: NAC (10 µmol/100 µL glycerol) + UVB, group 5: AAS (5 mg/100 µL glycerol), group 6: NAC (10 µmol/100 µL glycerol). AAS and NAC were applied topically before 30 min of UVB irradiation per day for seven days. The mice were irradiated with UVB radiation in a custom designed chamber consisting with four 100 W TL01 fluorescent lamps (Phillips, Amsterdam, Netherlands) emitting predominantly UVB radiation (9.87% UVA; 82.4% UVB) with a maximum emission peak at ~313 nm (Alam et al., 2018). The specific UVB dose was calculated using the following equation:

$$\mathrm{J}/cm^2 = \frac{\mathrm{mW/cm^2}}{1000} \times (\mathrm{sec}) \qquad (4.1)$$

The dorsal skin of mice was irradiated with UVB radiations for 252 sec to deliver 180 mJ/cm^2 of energy. All the tests that involved animals were approved by the CSIR-IITR animal ethical committee (IITR/IAEC/38/14-13/16-59/17).

4.2.4.2. Measurement of skin bifold thickness and wet/dry weight ratio

The protective activity of AAS against UVB radiation-induced skin edema was assessed by measuring the bifold skin thickness and wet/dry weight ratio of skin (Alam et al., 2018). First, the thickness of the skin was measured prior to treatment using an electronic digital caliper (Marathon, Inc., Belleville, ON, Canada). Subsequently, to observe the bifold skin thickness, the skin thickness was measured prior to the termination of the experiment after seven days. Post seven days, 1 cm diameter of skin was excised from all the mice, fat was removed and weighed. The skin was dried for 24 h at 50 °C and weighed to calculate the wet/dry weight ratio.

4.2.4.3. Measurement of epidermal thickness and sunburn cells

Epidermal thickness and sunburn cells were assessed from the histopathological sections of skin prepared using the established protocol (Alam et al., 2018). In brief, skin samples were fixed with paraformaldehyde and dehydrated in graded ethanol, xylene and finally embedded in paraplast (Oxford Labware, St. Louis, MO, USA). Samples were cut into 5 µm thick sections, deparaffinized, and stained with H&E and mounted with DPX mount. The stained sections were examined under a light microscope (Leica, Buffalo Grove, IL, USA) to evaluate the histopathological alterations and sunburn cells. The epidermal thickness was measured using ImageJ 1.8.0_112 (NIH, Wayne Rasband, USA). Sunburn cells were counted from the H&E stained images.

4.2.4.4. Determination of anti-lipid peroxidation of silk sericin

ALP activity of AAS was assessed using the protocol of Wright *et al.* (1981). The microsomal fractions of skin were prepared using the protocol of Katiyar *et al.* (2001). Briefly, the skin irradiated with UV radiations was washed with PBS and homogenized in phosphate buffer containing potassium chloride (1.19%, w/v) using a Polytron homogenizer and centrifuged at 18000 *g* for 15 min at 4 °C. 100 µl of epidermal microsomal fractions were incubated with 1 mM ferric ion and 5 mM ADP (prepared in 0.1 M Ca^{2+} free phosphate buffer containing 0.1 mM $MgCl_2$, pH 7.4) for 1 h at 37 °C. The reaction was stopped by the addition of 0.6 mL of 10% (w/v) TCA and 1.2 mL of 0.5% (w/v) TBA followed heating at 90 °C for 20 min and cooled to room temperature. Further, the reaction mixture was centrifuged and aliquots of the supernatant were used

to measure the fluorescence intensity using a multiplate reader at an excitation 530 nm and emission 550 nm wavelength to evaluate the MDA levels.

4.2.4.5. Determination intracellular glutathione activity

The effect of UVB radiations on the endogenous GSH activity was assessed using a glutathione assay kit (Cayman, Ann, Arbor MI). In brief, skin tissues were rinsed with PBS and homogenized in cold 50 mM 4-Morpholine ethane sulfonic acid (MES) buffer containing 1 mM EDTA, pH 7.4 followed by centrifugation at 10000 g at 4 °C for 15 min. Aliquots of supernatant were used for analysis of GSH levels as per the manufacturer's protocol. The absorbance was recorded at 405-414 nm using a Spectra Max M5 (Molecular Devices, Sunnyvale, CA, USA).

4.2.4.6. Alkaline comet assay

DNA damage of UV irradiated epidermal cells was evaluated by alkaline comet assay using the protocol of Singh *et al.* (1988). ~2 cm^2 pieces of skin were excised from all the groups of sacrificed mice followed by the separation of epidermis from the dermis and preparation of single cell suspension as reported earlier (Das et al., 2005). Slides were prepared and recorded with an image analyzer (Kinetic Imaging, Liverpool, UK) that attached to a fluorescence microscope (Leica, Wetzlar, Germany). The images were recorded at 400X magnification and used to analyze the olive tail moment (OTM) and % tail DNA using Komet 5.0 software.

4.2.5. Statistical analysis

Experiments were done thrice and analyzed results were represented as mean ± standard deviation. A significant difference between groups was assessed by the Holm-Sidak method via Sigma-plot software.

4.3. Results

4.3.1. Protective effect of silk sericin against UV radiation-induced cell death

Prior to exploring the protective effect of SS against UVA and UVB radiation-induced HaCaT cells damage, the cytocompatibility of SS, as well as the cytotoxicity of UV radiations, was assessed using 3-(4,5-dimethylthiazol-2-yl)-2,5 diphenyl tetrazolium bromide (MTT) assay. In comparison to control, the viability of SS treated HaCaT cells was unaffected. HaCaT cells irradiated with UVA and UVB underwent radiation-induced dose-dependent cell death (**Fig.A4.1**). Explicitly, 12 J/cm^2 of UVA decreased the viability by 40-50% and 120 mJ/cm^2 of UVB reduced the viability of cells by 30-40%. Hence, the aforementioned UV dosages were selected to evaluate the protective

effect of SS against UVA and UVB radiation-induced oxidative damage by MTT and Neutral red assay.

Our previous study showed that mouse fibroblast cells treated with 10 and 100 µg/mL of SS prior to H_2O_2 treatment protected them from oxidative damage and enhanced their viability (Kumar and Mandal, 2017). Hereby, we have selected these two concentrations of SS to evaluate their protective effect against UVA and UVB radiation-induced damage in HaCaT cells using MTT and Neutral red assay. MTT assay (viability assessed based on the mitochondrial activity) displayed that pre-treatment of HaCaT cells with 100 µg/mL of BMS, 10 and 100 µg/mL of AAS, PRS, and vitamin C (Vit. C) before UVA irradiation had significantly enhanced their viability than the untreated cells (**Fig.4.1 IA**). Similarly, BMS (100 µg/mL), AAS and PRS (10 and 100 µg/mL) pretreated cells showed significantly higher viability post UVB irradiation as compared to the cells without pre-treatment (**Fig.4.1 IB**). The viability assessed using Neutral red assay (viability assessment based on the presence of intact lysosomes within cells) showed that pretreatment with either of AAS or PRS (10 µg/mL each) shielded HaCaT cells against UVA and UVB radiation-induced cell death and significantly enhanced their viability in contrast to their untreated counterparts(**Fig.4.1 II**).

MTT and Neutral red assays showed that HaCaT cells pretreated with 10 µg/mL of AAS and PRS significantly protected them against UVA and UVB radiation-induced cell death. Henceforth, 10 µg/mL of AAS, PRS, and Vit. C (positive control) were selected to further evaluate their protective by assessing the intracellular ROS generation, cell cycle arrest, mitochondrial membrane depolarization, apoptosis, and gene expression.

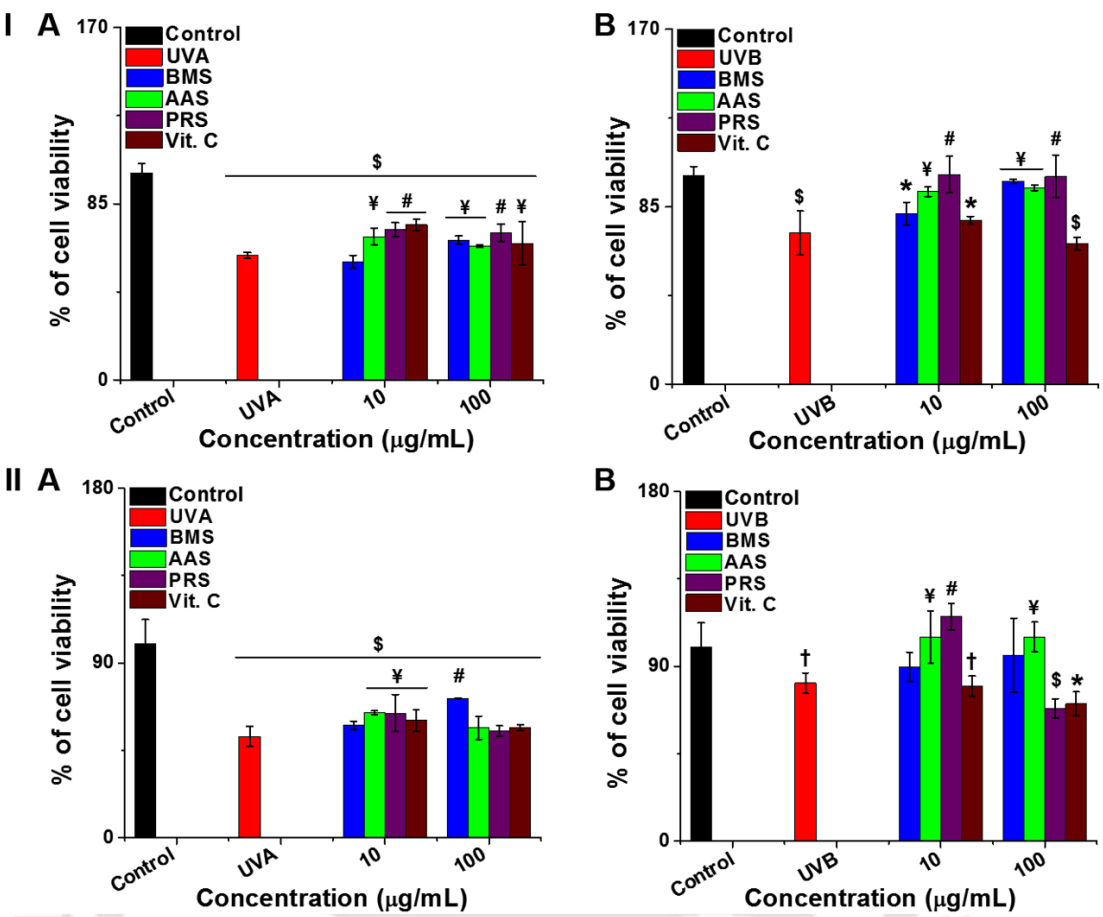

Fig.4.1. *Viability of silk sericin pretreated HaCaT cells was assessed using (I) MTT and (II) Neutral red assay after irradiating with (A) UVA and (B) UVB radiations. ($p≤0.001, *p≤0.01, and †p≤0.05 in comparison with control cells; #p≤0.001 and ¥p≤0.01 in comparison with only UV irradiated cells)*

4.3.2. Measurement of intracellular reactive oxygen species generation

ROS levels of UV irradiated HaCaT cells were determined using dichloro-dihydro-fluorescein diacetate (DCFH-DA). **Fig.2 A** and **B** depict the ROS levels of HaCaT cells post UVA and UVB irradiation, respectively. UVA and UVB irradiation significantly enhanced the intracellular ROS generation in HaCaT cells in contrast to non-irradiated control. However, SS or Vit. C pretreatment significantly reduced ROS generation in HaCaT cells than SS untreated cells.

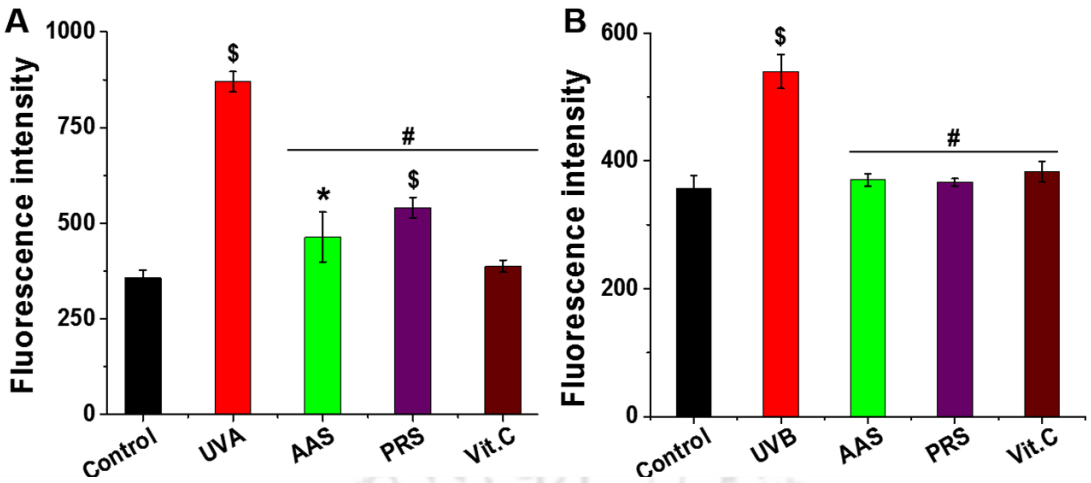

Fig.4.2. *Effect of (A) UVA and (B) UVB radiations on the generation of intracellular ROS in silk sericin pretreated cells was determined using DCFH-DA. ($p≤0.001 and *p≤0.01 in contrast with control cells; #p≤0.001 in contrast with the only UV irradiated cells)*

4.3.3. Cell cycle analysis

The effect of UVA and UVB radiation on cell cycle was analyzed using propidium iodide (PI). The DNA content of gate cell population at G1 (N) and G2 (2N) phases are uniform in size, whereas, DNA content is fragmented in sub-G1 phase (cell death by apoptosis) (Pozarowski and Darzynkiewicz, 2004). **Fig.4.3** illustrates the percentage of cell population at different phases of the cell cycle after irradiating with UVA and UVB radiations. The gated cell population of UVA-irradiated cells (both SS pretreated or untreated cells) present at different phases of the cell cycle was similar to control cells. In comparison with control, UVB irradiation enhanced cell population by 2.49 and 1.1 folds at sub-G1 and G1 phases of cell cycle, respectively. Whereas, a 0.28 fold decrease was observed in the cell population at the G2 phase of the cell cycle. HaCaT cells treated with SS before UVB irradiation significantly reduced cell population at the sub-G1 phase and enhanced at the G1 phases of the cell cycle. Whereas, Vit. C pretreated cells showed a 3.4 fold increase in the cell population at a sub-G1 phase in contrast to control.

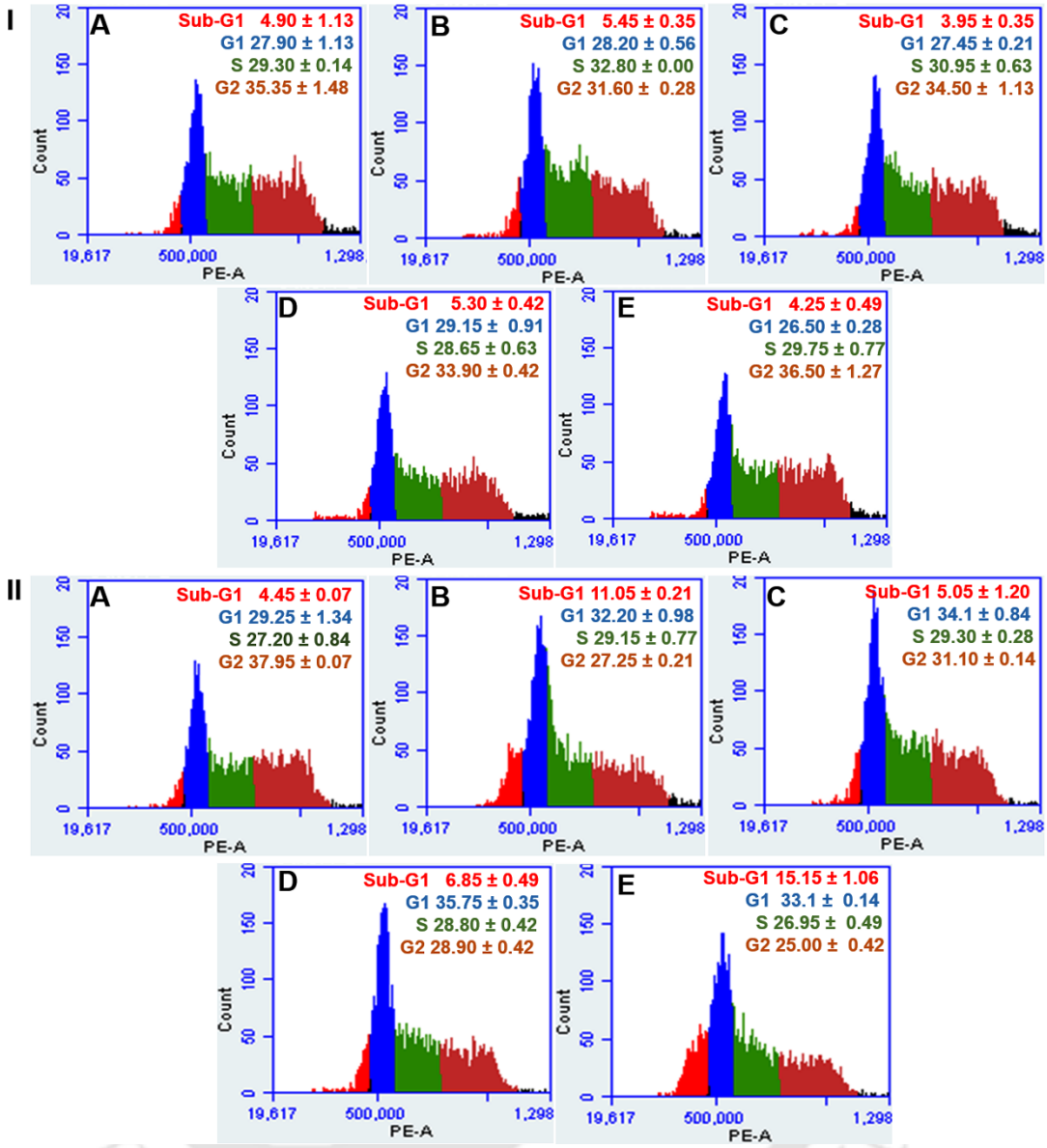

Fig.4.3. *Cell cycle analysis of silk sericin pretreated HaCaT cells after irradiating with (I) UVA and (II) UVB radiations were assessed using PI. Where (A) control, (B) only UV irradiated cells, (C) AAS, (D) PRS and (E) Vit. C pretreated cells. Data are expressed as mean ± S.D (n=3)*

4.3.4. Mitochondrial membrane potential (ψ) analysis

UV radiation-induced redox imbalance causes the mitochondrial membrane depolarizations and initiates the apoptotic cell death (Assefa et al., 2005). The effect of SS pre-treatment on the UV radiation-induced mitochondrial membrane depolarization was assessed using JC-1 dye. UVA and UVB irradiation induced the depolarization of the mitochondrial membrane of HaCaT cells. While, AAS (both UVA and UVB irradiated cells), PRS (UVA-irradiated cells), and Vit. C (UVA-irradiated cells)

treatment prior to UV irradiation reduced the depolarization of mitochondrial membrane of HaCaT cells (**Fig.4.4**).

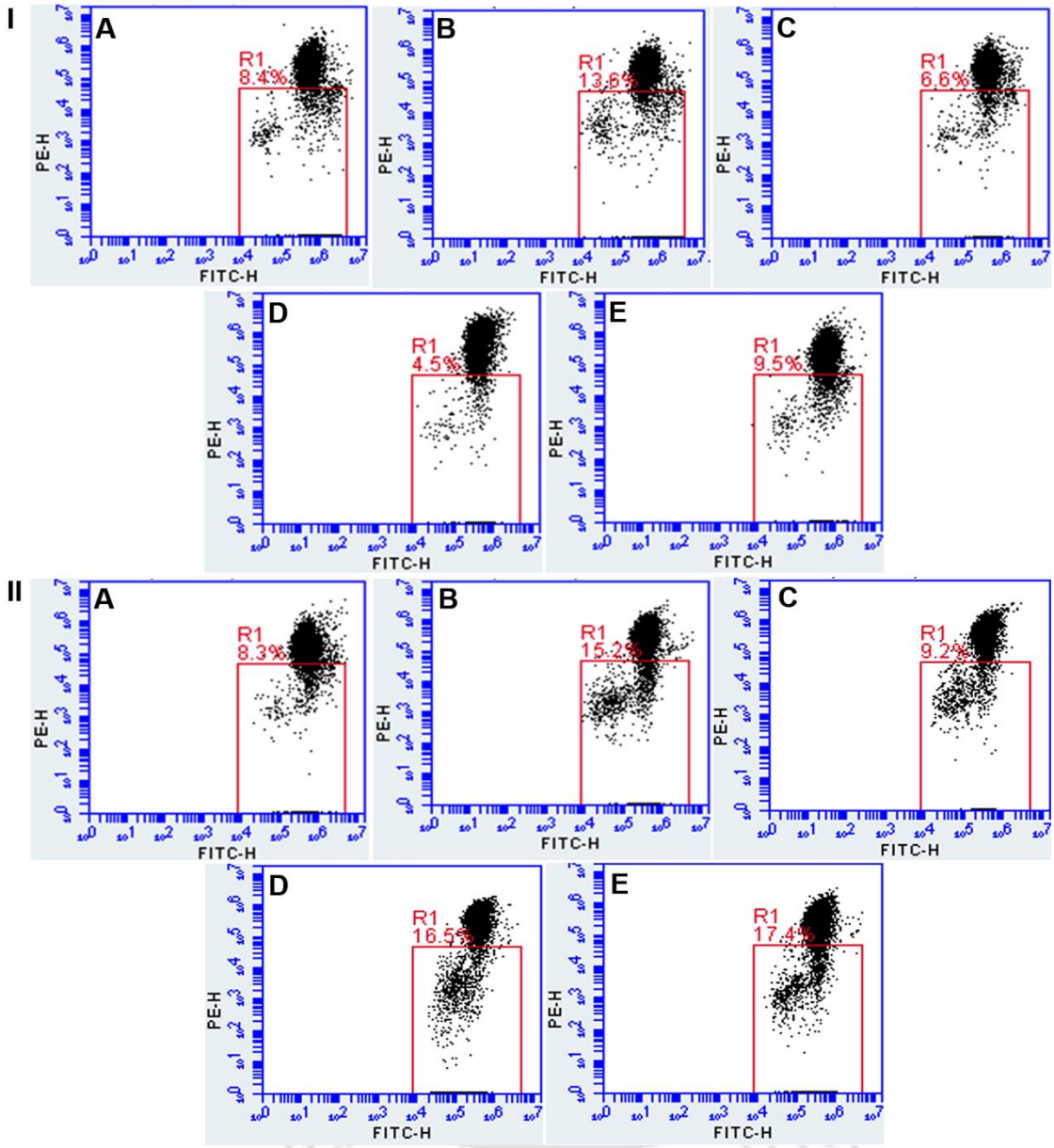

Fig.4.4. *Depolarization of mitochondrial membrane of silk sericin pretreated HaCaT cells after irradiating with (I) UVA and (II) UVB radiations were evaluated using the JC-1 assay kit. Where (A) control, (B) only UV irradiated cells, (C) AAS, (D) PRS and (E) Vit. C pretreated cells.*

4.3.5. Annexin V/PI assay

The protective effect of SS against UV radiation-induced apoptotic cell death was assessed using Annexin V/PI assay kit. As shown in **Fig.4.5 I**, AAS and PRS pretreated cells exhibited lesser early apoptotic death (15.1% and 17.8%, respectively) after

irradiating with UVA in comparison with SS untreated cells (23.7%). AAS pretreatment protected HaCaT cells from UVB induced apoptotic cell death, while PRS pretreated cells exhibited low apoptotic cell death (16.9%) than SS untreated (22.6%) (**Fig.4.5 II**).

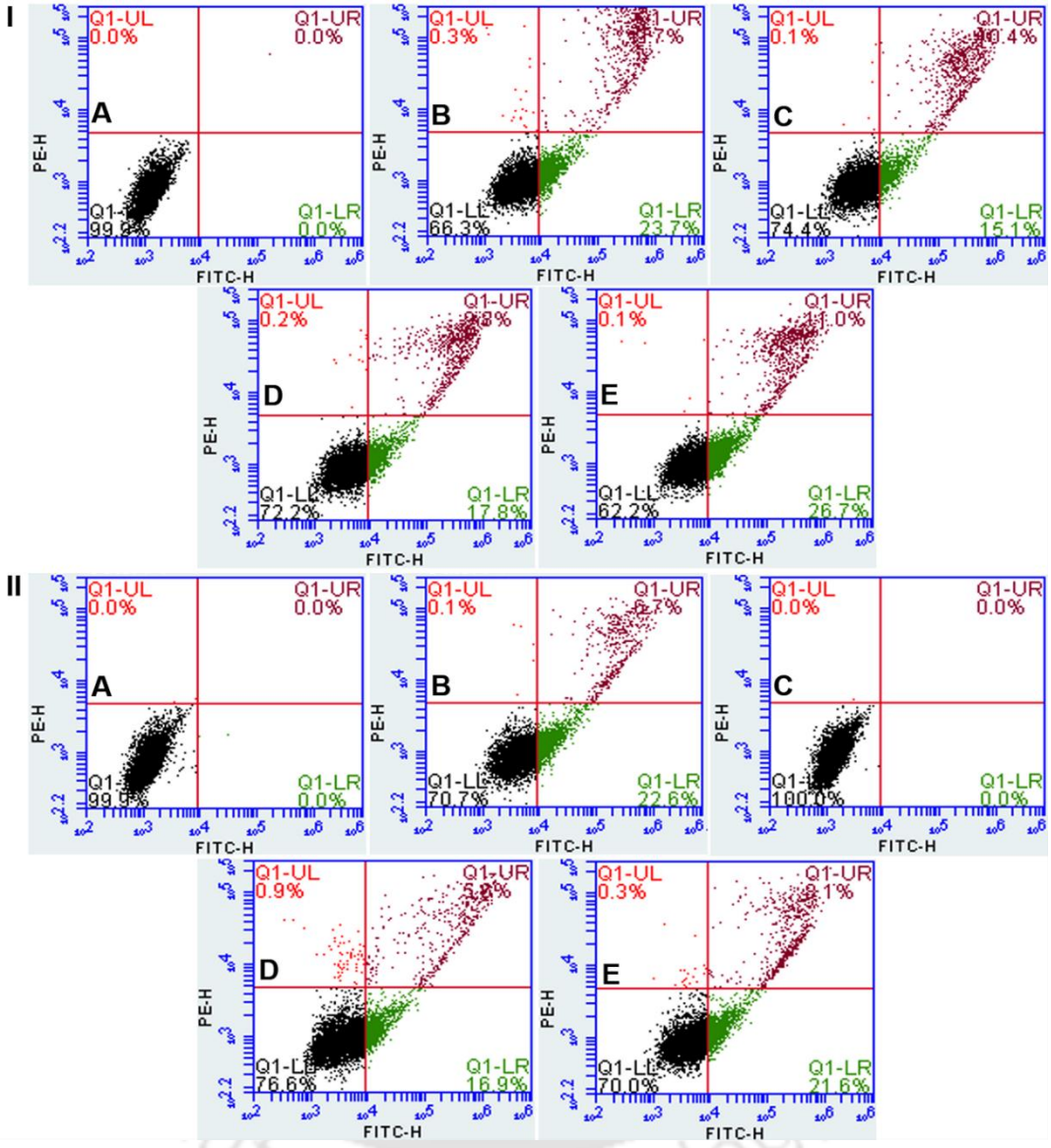

Fig.4.5. *Protective effect of silk sericin against (I) UVA and (II) UVB radiation-induced apoptotic death in HaCaT cells was assessed using Annexin V/PI assay kit. Where (A) control, (B) only UV irradiated cells, (C) AAS, (D) PRS and (E) Vit. C pretreated cells.*

4.3.6. Gene expression study

The expression of inflammatory cytokines, p53, caspase-3 apoptotic (Bax) and anti-apoptotic (Bcl-2) genes in SS pretreated or untreated cells post UV irradiation was assessed using real-time polymerase chain reaction (RT-PCR) (**Fig.4.6**). UVA and UVB irradiation significantly upregulated the expression of IL-6 and IL-8 gene in HaCaT cells.

Where SS pretreatment significantly downregulated IL-6 and IL-8 gene expression after UVA (except IL-6 expression in PRS pretreated cells) and UVB irradiation. SS pretreatment prior to UV irradiation upregulated the p53 gene expression in HaCaT cells than those of SS untreated cells. UV irradiation induced the upregulation of caspase-3 and dysregulation of Bax and Bcl-2 gene expression in SS pretreated and untreated HaCaT cells.

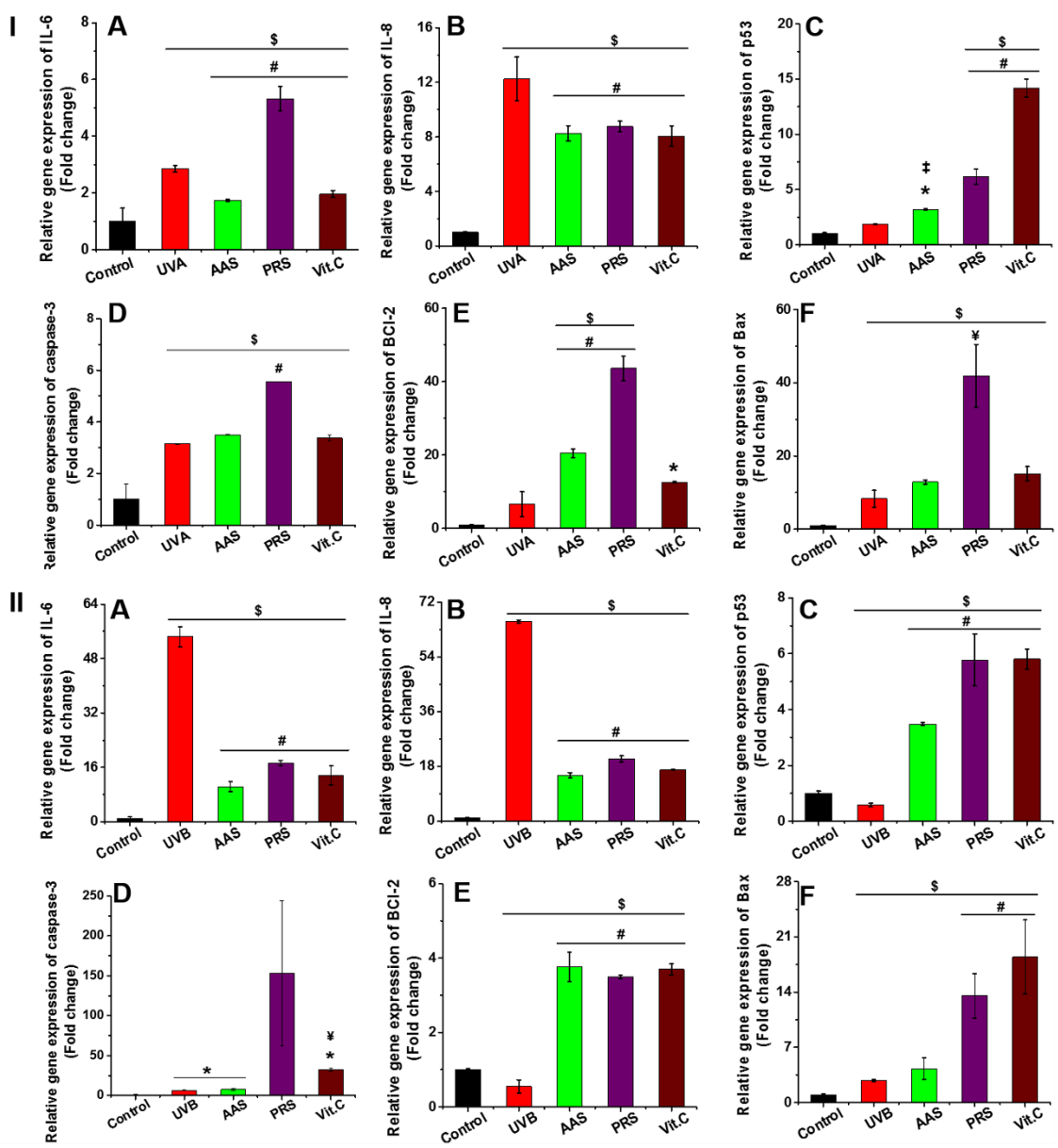

Fig.4.6. *The relative expression of (A) IL-6, (B) IL-8, (C) p53, (D) caspase-3, (E) Bcl-2, and (F) Bax genes in silk sericin pretreated HaCaT after irradiated with (I) UVA and (II) UVB radiations were assessed using RT-PCR. ($p≤0.001 and *p≤0.01 in comparison with control cells; #p≤0.001, ¥p≤0.01, and ‡p≤0.05 in comparison with the only UV irradiated cells.*

4.3.7. Measurement of skin bifold thickness and wet/dry weight ratio

SS extracted from the cocoons of *A. assamensis* exhibited better protective activity against UVA and UVB radiation-induced human keratinocytes death than PRS and BMS, respectively. AAS was selected to evaluate the protective activity against UVB radiation-induced mice skin damage. We have evaluated the effect of AAS against UVB radiation-induced skin edema by studying the bifold skin thickness and the wet/dry weight ratio of skin. Irradiating female SKH-1 hairless mice with UVB radiations resulted in a significant enhancement of bifold skin thickness (16.77 ± 0.22 fold) than the skin of control mice (**Fig.4.7 A**). However, topical delivery of AAS or N-acetylcysteine (NAC) showed 9.85 ± 0.27 and 8.27 ± 0.32 fold enhancement in bifold skin thickness, respectively. AAS or NAC pretreatment significantly reduced skin punch wet/dry weight ratio than the only UVB irradiated mice skin (**Fig.4.7 B)**.

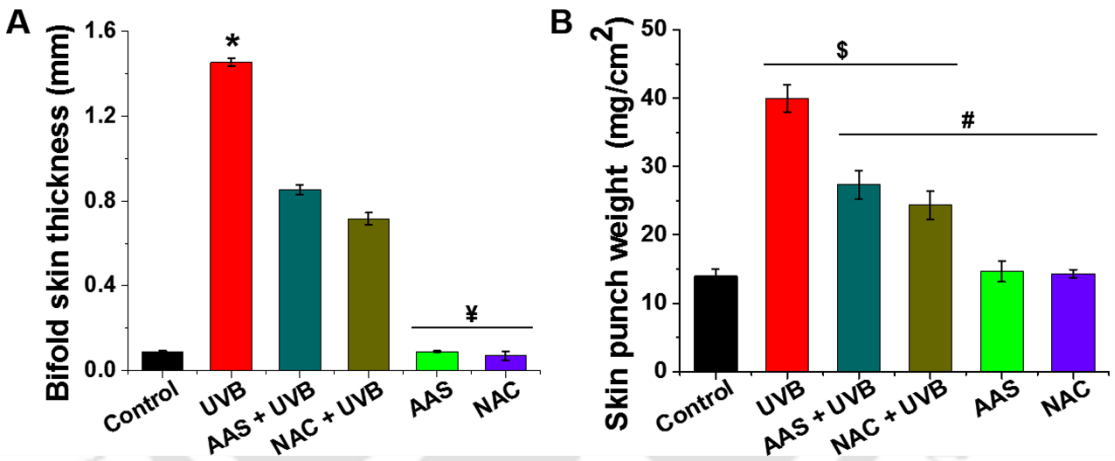

Fig.4.7. *Protective activity of silk sericin against UVB radiation-induced edema was evaluated by assessing the (A) bifold skin thickness and (B) wet/dry weight ratio of mice skin. ($p≤0.001 and *p≤0.01 in contrast with control mice skin; #p≤0.001 and ¥p≤0.01 in contrast with the only UVB irradiated mice skin)*

4.3.8. Measurement of epidermal thickness and sunburn cells

Prolonged exposure of skin to UV radiation-induced physiology changes (epidermal thickness) in the skin and also causes apoptotic death of keratinocytes (sunburn cells) (D'Orazio et al., 2013). Alterations in epidermal thickness and sunburn cells were assessed using Haemotoxylin and Eosin (H & E) staining. UVB irradiation-induced epidermal thickness and enhanced sunburn cells than control. Topical delivery of AAS or NAC before UVB irradiation significantly reduced the epidermal thickness and sunburn cells (**Fig.4.8**).

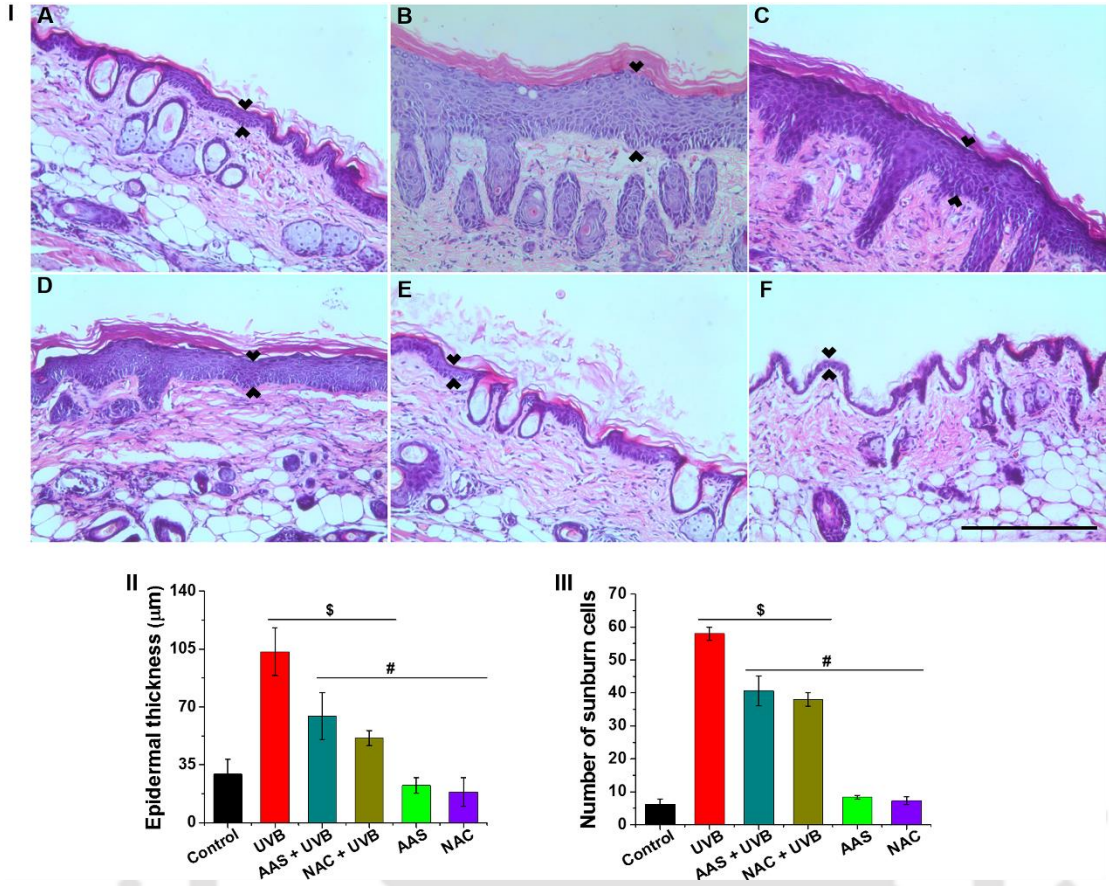

Fig.4.8. *Protective activity of AAS against UVB radiation-induced (I and II) epidermal thickness and (III) sunburn cells was assessed using H & E staining. Where (A) control mice, (B) only UVB irradiated mice (C) mice treated with AAS before UVB irradiation, (D) mice treated with NAC before UVB irradiation, (E) only AAS treated mice and (F) only NAC treated mice. ($p≤0.001 in contrast with control mice skin; #p≤0.001 in contrast with the only UVB irradiated mice skin). Scale 200 µm*

4.3.9. Determination of anti-lipid peroxidation of silk sericin

Cellular membrane lipids are susceptible to UV radiation-induced oxidative damage (Katiyar et al., 2001). ROS elevated by UV irradiation induce the peroxidation of membrane lipids that results in the collapse of the cell membrane and organelles (Katiyar et al., 2001). The effect of AAS against UVB radiation-induced lipid peroxidation was assessed by measuring the malondialdehyde (MDA) levels. Topical delivery of AAS prior to UVB irradiation significantly reduced MDA levels (12.3 nmol/µg) in female SKH-1 mice than only UVB irradiated mice (17.8 nmol/µg) (**Fig.4.9 I**).

4.3.10. Determination intracellular glutathione activity

UV radiation induces the depletion of endogenous glutathione (GSH), which leads to the accumulation of ROS in cells and causes oxidative damage (Heck et al., 2003). The effect of UVB radiation on the expression of GSH was assessed using a glutathione assay kit. UVB irradiation-induced depletion of endogenous GSH levels in comparison with control mice, however, AAS or NAC pretreatment prevented the depletion of GSH levels (**Fig.4.9 II**).

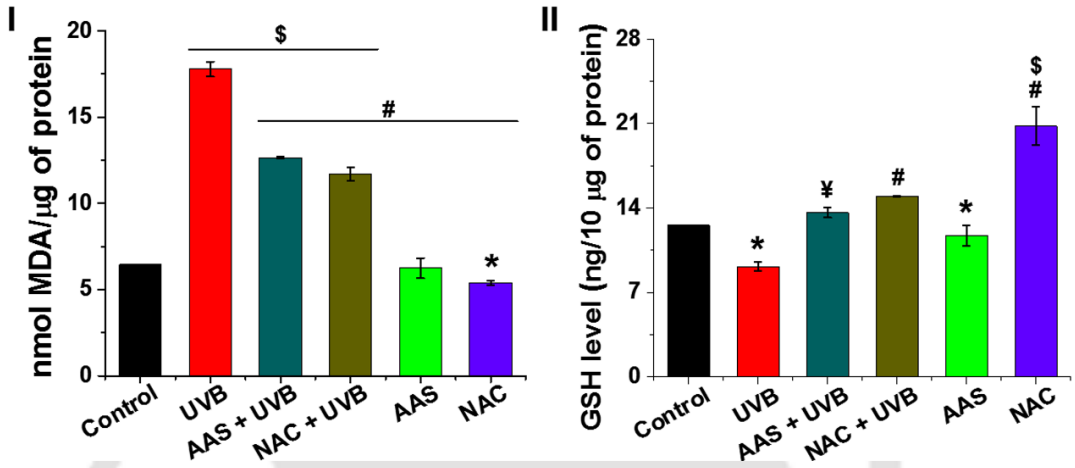

Fig.4.9. *(I) Antilipid peroxidation of AAS was assessed by measuring the amount of MDA formed in the skin after irradiating with UVB radiations. (II) The defensive effect of AAS against UVB radiation-induced oxidative damage of endogenous antioxidant activity was assessed by measuring GSH levels. ($p≤0.001 and *p≤0.01 in contrast with control mice skin; #p≤0.001 and ¥p≤0.01 in contrast with the only UVB irradiated mice skin)*

4.3.11. Alkaline comet assay

Oxidative stress induced by UVB irradiation causes DNA damage by interfering with the genomic stability. The effect of topical delivery of AAS against UVB radiation-induced DNA fragmentation was assessed using the alkaline comet assay. In comparison with control mice, UVB irradiation significantly increased tail DNA (7.2 fold) and OTM (24.8 fold) in mice. Topical delivery of AAS before UVB irradiation significantly reduced tail DNA (4.8 fold) and OTM (12.4 fold) than the only UVB irradiated mice (**Fig.4.10**).

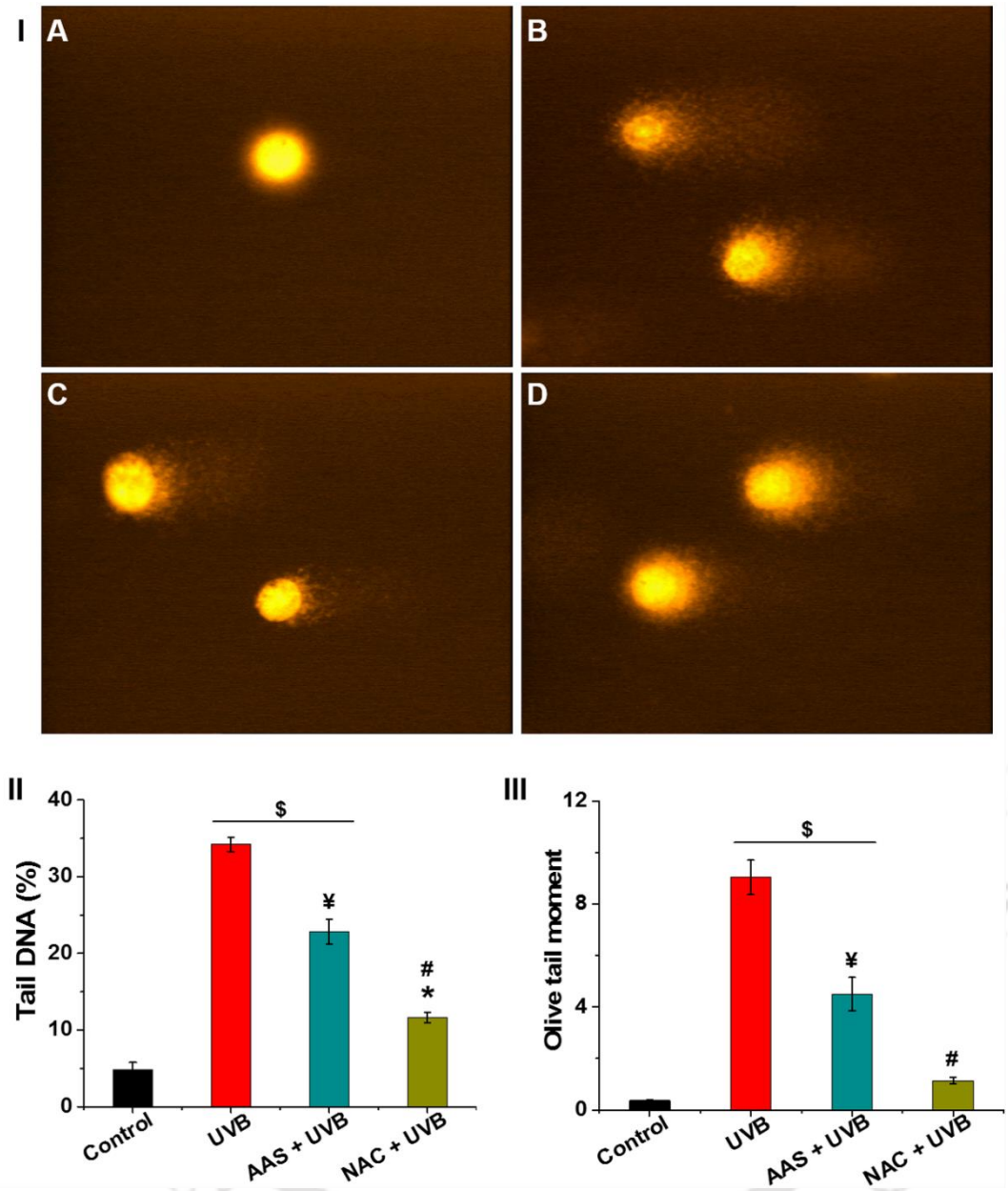

Fig.4.10. *Shielding effect of AAS against UVB radiation-induced DNA fragmentation was assessed using the comet assay. (I) Representative image of comet assay at 400X magnification and graphical illustration of (II) % of tail DNA and (III) olive tail moment. Where (A) control mice, (B) only UVB irradiated mice (C) mice treated with AAS before UVB irradiation, and (D) mice treated with NAC before UVB irradiation ($p≤0.001 and *p≤0.01 in contrast with control mice skin; #p≤0.001 and ¥p≤0.01 in contrast with the only UVB irradiated mice skin)*

4.4. Discussion

Endogenous antioxidants protect the skin from oxidative damage induced by pollutants, chemicals, and UV radiations by scavenging the elevated levels of ROS (Godic et al., 2014). However, chronic exposure of skin to UV radiations depletes the endogenous antioxidant activity and elevates the production of ROS. Elevated ROS oxidizes cellular biomacromolecules, which results in inflammations, skin cancer (melanoma and non-melanoma), aging and wrinkling (Gil and Kim, 2000; Kulms et al., 2002; Rittié and Fisher, 2002). Topical delivery/ supplementation of potential exogenous antioxidants might be an effective strategy to thwart the deleterious effect of ROS produced by UV radiations (Nichols and Katiyar, 2010; Yin et al., 2013). Protecting the skin against UV radiations using exogenous antioxidants is often known as photo-chemoprevention (Afaq et al., 2003). Several studies have shown the photo-chemopreventive activity of dietary agents (polyphenols, flavonoids, vitamins etc) against UV radiation-induced oxidative damage including hyperpigmentation, skin cancer, aging, and wrinkling (Kagan et al., 1992; Nichols and Katiyar, 2010; Oresajo et al., 2008; Yin et al., 2013).

Silk sericin (SS) is known to own free radicals scavenging activity along with other biomedical applications including photoprotective effect against UVB radiation-induced skin damage (Dash et al., 2008; Zhaorigetu et al., 2003). SS also absorbs UVA radiation and protect pupa and fibroin against UV radiation-induced oxidative damage (Kaur et al., 2013). The biological properties of SS depend on the amino acid composition and associated polyphenols and flavonoids (Kumar and Mandal, 2017). Hydroxyl groups of serine (32.16%) and threonine (8.04%), electron donating groups of aromatic amino acids [tyrosinase (3.14%), histidine (1.46%) etc] attributes to the antioxidant activity of SS by chelating trace elements like iron and copper and donating their electrons to free radicals (Fan et al., 2009; Kato et al., 1998). However, the molar percentage of these amino acids varies based on the source of SS as well as the peptide length generated during their extraction from the cocoons. These changes determine the properties (antioxidant activity, suppression of tyrosinase and trypsin) of SS (Aramwit et al., 2010a; Aramwit et al., 2010b; Kumar and Mandal, 2017; Kurioka et al., 2004). Despite low quantity, AAS showed high UV blocking capacity than BMS (Kaur et al., 2013). In addition to these amino acids, SS is associated with polyphenols and flavonoids, which contributes to its antioxidant, anti-tyrosinase and anti-inflammatory activities (Park et al., 2008; Yokohira et al., 2008). SS extracted from mulberry silk varieties is enriched

with kaempferol, procyanidin B1, myricetin, Σ phenolics, naringenin, procyanidin B2, *trans*-resveratrol, epicatechin, luteolin, catechin, quercetin, and rutin, however, the percentage of these secondary metabolites varies based on the source (Butkhup et al., 2012). Whereas, SS extracted from the cocoons of Eri lacks kaempferol, luteolin, naringenin, and quercetin (Butkhup et al., 2012). Total polyphenol and flavonoid content associated with SS vary based on the extraction methods that pre-determines its activity (Kumar and Mandal, 2017). Therefore, exploring the protective effect of SS extracted from a different source against UVA and UVB radiation could help to identify a potent silk variety. Hence, in the present study, we have explored the protective effects of SS extracted from the cocoons of *B. mori* (BM), *A. assamensis* (AA), and *P. ricini* (PR) against UVA and UVB radiation-induced skin damage.

ROS produced by chronic exposure to UVA and UVB radiations oxidize the cellular biomacromolecules that lead to senescence of epidermal keratinocytes (D'Orazio et al., 2013). Irradiation with increasing dosage of UV radiations elevated the oxidative damage resulting in significant loss of viability of HaCaT cells, as observed in **Fig.A4.1**. AAS and PRS (10 µg/mL) treatment prior to UVA (12 J/cm^2) and UVB (120 mJ/cm^2) irradiation significantly reduced the ROS (**Fig.4.2**) and enhanced the viability of keratinocytes (**Fig.4.1**) as compared to SS untreated UV irradiated cells. Electron donating groups of amino acids of SS and associated secondary metabolites (polyphenols and flavonoids) contribute their electrons and reduced the elevated levels of ROS, which might be a plausible reason for the observed decline in UV radiation-induced oxidative damage and enhanced cell viability (Kumar and Mandal, 2017).

Keratinocytes injured by UV radiations activate damage response pathway by activating p53 gene, which alters the cell physiology, induces cell cycle arrest and activates DNA repair (D'Orazio et al., 2013). In highly damaged keratinocytes, p53 activation induces apoptotic death. Cell cycle analysis showed that UVA irradiation did not cause cell cycle arrest, whereas, UVB-induced cell cycle arrest at G1 phases was followed by cell death at the sub-G1 phase (**Fig.4.3**). Redox imbalance induced by UVA radiation probably failed to activate damage response pathway due to that there was no significant change at different phases of cell cycle analysis. Keratinocytes irradiated with UVB radiations might have activated p53 that resulted in cell death at sub-G1 phase. Whereas, AAS and PRS treatment prior to UVB irradiation scavenged the elevated levels of ROS by donating their electron and reduce redox imbalance in cells. Maintaining the redox balance of cells cell death prevented the apoptotic cell death at the sub-G1 phase

and arrested at G1 phase to repair the damaged DNA by p53 activation (**Fig.4.3 II**). Redox imbalance induced by UV irradiation leads to the mitochondrial membrane depolarization and releases cytochrome *c* (cyt *c*) into the cytoplasm that initiates the apoptosis (Assefa et al., 2005). SS treatment prior to UV irradiation reduced the elevated levels of ROS that prevented the mitochondrial membrane depolarization (**Fig.4.4**) and reduced apoptotic cell death (**Fig.4.5**).

Chronic exposure of skin to UV radiation-induced the secretion of pro-inflammatory cytokines by the keratinocytes that results in an inflammatory response (Nishimura et al., 1999). UV irradiations also activate the oncogenes and downregulate the expression of tumor suppressor genes, which could lead to skin carcinogenesis (Kim and He, 2014). The effects of SS pretreatment on the expression of IL-6, IL-8, p53, caspase-3, Bcl-2, and Bax were assessed using gene expression studies. SS treatment before UVA and UVB irradiation downregulated the expression of IL-6 and IL-8; however, PRS treated cells showed upregulation of IL-6 post irradiating with UVA (**Fig.4.6**). Polyphenols and flavonoids are known to possess anti-inflammatory activity (Park et al., 2008; Yokohira et al., 2008). SS and associated secondary metabolites uptaken by the cells scavenged the elevated levels of ROS produced due to UVA and UVB irradiation and maintained the redox balance, which might have resulted in downregulation of inflammatory cytokines. Downregulation of p53 gene enhances the proliferation of injured keratinocytes and results in skin carcinogenesis. Whereas, upregulation of p53 gene induces the activation of cyclin-dependent kinase (CDK) inhibitor and results in cell cycle arrest, repairs UV radiation-damaged DNA and protects cells from apoptotic cell death (McKay et al., 2001). Cells treated with SS prior to UVA and UVB irradiation showed upregulated expression of p53 to repair DNA damage (**Fig.4.6**). Bax and Bcl-2 gene expression play an essential role in the viability of cells. Oxidative stress induced in HaCaT cells by UVA irradiation dysregulated the Bax/Bcl-2 expression, whereas, DNA damage induced by UVB irradiation downregulated the Bcl-2 expression and upregulated the expression of Bax. Reducing the UVA and UVB radiation-induced oxidative stress by AAS pretreatment might have upregulated the Bcl-2 expression, however, PRS was unable to prevent the dysregulation of Bax/Bcl-2 expression. Protection from depolarization of mitochondrial membrane and upregulation of Bcl-2 counteract the caspase-3 activity, which prevents cell death (Dispersyn et al., 1999; Grünenfelder et al., 2001). SS peptides produced during extraction from the *A. assamensis* cocoons and their associated secondary metabolites showed better protection

against UVA and UVB radiation-induced oxidative damage by maintaining the redox balance of cells than PRS and BMS, respectively. Therefore, AAS was selected to evaluate the protective effect against UVB induced skin damage using the SKH-1 hairless mice.

UVB radiations are more potent carcinogen than UVA radiations. UVB radiations induce redox imbalance in human and murine epidermal keratinocytes that lead to secretion of pro-inflammatory cytokines that result in the invasion of inflammatory cells in the epidermal region of skin (Nishimura et al., 1999). The inflammatory responses result in cutaneous edema (accumulation of fluids in the skin), erythema (red of skin) and enhance epidermal cell proliferation (intraepithelial neoplasia) (Alam et al., 2018; Zhaorigetu et al., 2003). Redox imbalance induced by UVB radiations also causes oxidation of biomacromolecules, which subsequently leads to the collapse of cellular membrane integrity, depletes the activity of endogenous antioxidants and DNA fragmentation (apoptosis of epidermal cells) (Agarwal et al., 1993; Haywood et al., 2008; Podda et al., 1998). Topical or oral delivery of exogenous antioxidants maintain the redox balance of epidermal cells and downregulates the secretion of pro-inflammatory cytokines that result in the reduction of erythema, edema and epidermal thickening (Alam et al., 2018; Nichols and Katiyar, 2010; Yin et al., 2013). Exogenous antioxidant supplementation also suppresses the oxidation of biomacromolecules that protects cellular membrane from oxidative damage, enhances the activity of endogenous antioxidants and prevents DNA fragmentation (apoptotic cell death) (Afaq et al., 2003; Alam et al., 2018; Nichols and Katiyar, 2010; Yin et al., 2013). Protective effects of AAS against UVB induced oxidative damage was evaluated using female SKH-1 hairless mice. Topical delivery of AAS prior to UVB irradiation significantly reduced edema, erythema, and epidermal thickening by downregulating the expression of inflammatory cytokines (**Fig.4.7, Fig.4.8,** and **Fig.A4.2)**. Electron donating groups of AAS and associated secondary metabolites donate their electron to reduce the ROS produced after UVB irradiation and maintained the redox balance of epidermal keratinocytes, which reduced the oxidation of lipids (**Fig.4.9 I**), edema (**Fig.4.7**), erythema (**Fig.A4.2**), depletion of intracellular GSH activity (**Fig.4.9 II**), epidermal thickening (**Fig.4.8 II**), and DNA fragmentation (**Fig.4.10**) that results in a reduction of sunburn cells (apoptotic cells) (**Fig.4.8 III**).

4.5. Significant Findings

The salient findings of this chapter are as follows:

1. AAS and PRS (10 µg/mL) treatment prior to UVA and UVB irradiation enhanced the viability of HaCaT by minimizing the redox imbalance of the cells.
2. HaCaT cells treated with SS prior to UVRs reduced population of cells in sub-G1 phase, mitochondrial membrane depolarization state and those undergoing apoptotic cell death by upregulating p53 and Bcl-2 gene expression.
3. AAS exhibited a better protective effect against UVA and UVB radiation-induced HaCaT cell death and thus was selected to evaluate its protective effect against UVB radiation-induced skin damage.
4. Topical delivery of AAS also protected the SKH-1 hairless mice against UVB radiation-induced skin damage by scavenging elevated levels of ROS and preventing the oxidation of endogenous antioxidants.
5. *In vitro* and *in vivo* studies endorse the protective activity of AAS against UVR-induced oxidative damage by maintaining redox balance and upregulating endogenous AOs.

This chapter provided a platform to understand the protective role of SS against UVA and UVB radiation-induced skin damage. Redox imbalance induced in epidermal and dermal layers of the skin by UVA and UVB radiations also triggers the upregulation of MMPs, which degrades collagen and elastin fibers and leads to premature aging and wrinkling. Hence, in the next chapter, we have investigated the shielding effect of alkali-degraded BMS, AAS, and PRS against UVR-induced aging and wrinkling.

.

Chapter 5

Exploring the Inhibitory Effects of Silk Sericin on Elastase, Hyaluronidase, Collagenase, and UV Radiation-Induced Skin Aging

This chapter illustrates the protective effect of silk sericin against UV radiation-induced photoaging and wrinkling. Anti-aging and anti-wrinkling activity of alkali-degraded silk sericin has been investigated using biochemical assays and in vitro studies.

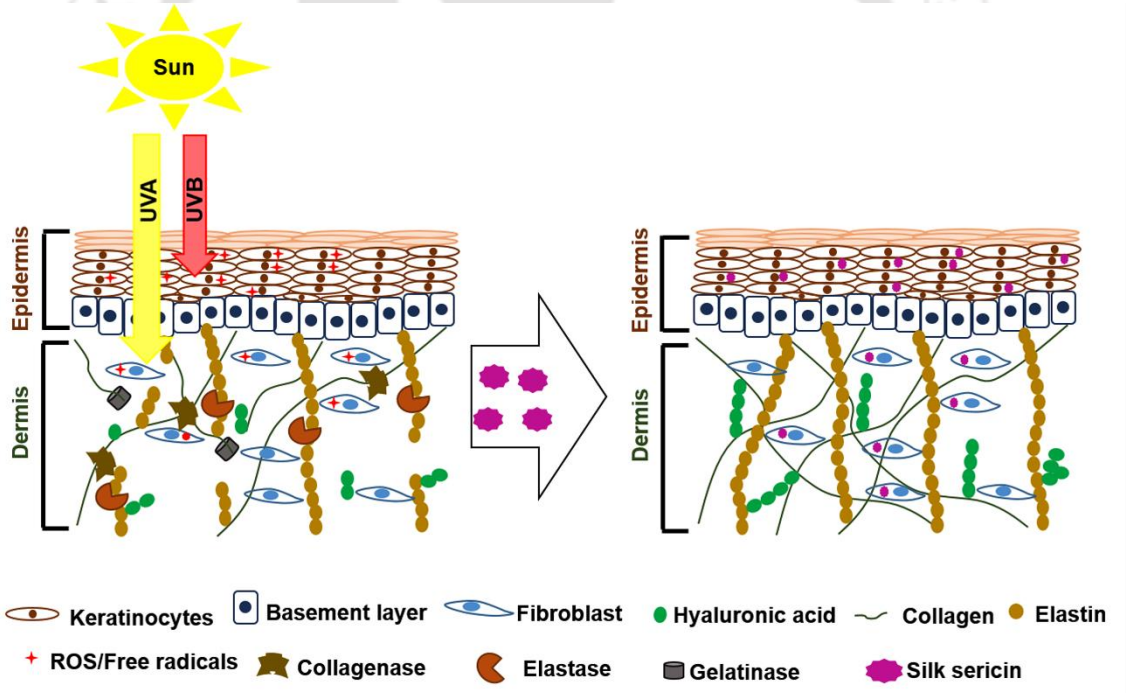

ABSTRACT

Topical delivery of potent antioxidants maintains the redox balance of the skin, which leads to the downregulation of matrix metalloproteinases (MMPs) expression and prevent UV radiation-induced photoaging. In this study, we aimed to investigate the inhibitory role of sericin isolated from the cocoons of different silk varieties against UV radiation-induced MMPs expression. Incubation of elastase and hyaluronidase with *Antheraea assamensis* sericin (AAS) inhibited their 50% activity. Assessment of total collagen content using Sirius red assay showed that the AAS (10 µg/mL) and *Philosamia ricini* sericin (PRS) (100 µg/mL) post-treatment significantly enhanced total collagen content in UVA1 and UVB irradiated HDF cells. Gene expression studies showed that AAS and PRS post-treatment downregulated the expression of interleukin (IL)-6, and MMP-1 and upregulated procollagen genes in UV irradiated HDF cells. Gelatin zymography study displayed that AAS post-treatment downregulated the release of MMP-2 and MMP-9 by HaCaT cells. Overall results validate that the AAS efficiently shields UV radiation-induced collagen and elastin degradation by downregulation MMPs expression, substantiating its further use as a potent antioxidant complement in the skin care formulations.

5.1. Introduction

Aging of the human skin is marked by the degradation of collagen, loss of structural integrity and physiological functions by intrinsic and extrinsic factors (Hashem et al., 2008; Jung et al., 2014). Chronic exposure of skin to environmental factors influences both intrinsic and extrinsic aging processes (Egbert et al., 2014). Intrinsic or chronological aging is a natural process of physiological changes, which affects all the body organs, whereas extrinsic aging is triggered by the prolonged exposure of skin to environmental factors such as pollutants, ultraviolet (UV) radiations and smoking (nicotine) (Hashem et al., 2008; Krutmann et al., 2017). UV radiations are one of the major causes of extrinsic aging, which also lead to skin dryness, decreases skin elasticity and induce wrinkle formation by affecting the human dermal fibroblast and keratinocytes (Fisher et al., 2002; Yaar and Gilchrest, 2007; Krutmann et al., 2017).

Solar UV radiations of the electromagnetic spectrum and are classified into UVA (400-320 nm), UVB (320-280 nm), and UVC (280-200 nm) based on their wavelength (Liu et al., 1994). Among total UV radiations, UVA (90-98%) and UVB (1-10%) radiations reach earth atmosphere (Hou et al., 2015). UVA radiations pierce into the dermal layer of skin and induce redox imbalance in dermal fibroblast cells by elevating the reactive oxygen species (ROS) production (Tyrrell, 1996). While UVB radiations majorly cause the DNA damage of epidermal keratinocytes by forming photoproducts and also damages bio-macromolecules by elevating ROS production (Lee et al., 2012). Oxidative stress induced by UV radiations stimulate the activation of nuclear factor (NF)-κB, which stimulates the transcription of pro-inflammatory cytokines such as interleukins (IL)-1α, IL-6, IL-8, and tumor necrosis factor (TNF)-α in epidermal and dermal cells (Angel et al., 2001; Bashir et al., 2009a). The pro-inflammatory cytokines act through the cell surface receptors and trigger the activation of activator protein (AP)-1 and NF-κB (Fisher et al., 2002). Activated AP-1 causes the upregulation of matrix metalloproteinases (MMPs) expression in dermal fibroblast (MMP-1 and MMP-3) and epidermal keratinocytes (MMP-2 and MMP-9) (Angel et al., 2001). Upregulated MMP-1 (collagenase) causes fragmentation of collagen, whereas, MMP-2 and MMP-9 (gelatinases) degrade the fragmented collagen (gelatin), which results in skin aging (Angel et al., 2001; Kondo, 2000). Redox imbalance also stimulates the production of fibroblast elastase and neutrophil elastase, which degrades the elastin fibers of the skin and results in wrinkling or sagging (Imokawa, 2009; Tsuji et al., 2001). Endogenous antioxidants (enzymatic and non-enzymatic antioxidants) counteract ROS and reduce

oxidative stress in the dermal and epidermal region of the skin, which prevents the inflammation, immunosuppression, loss of skin elasticity, skin dryness, aging, and cancer (Godic et al., 2014). However, ROS generated by UV irradiation overwhelms the endogenous antioxidants activity and leads to redox imbalance in the skin, which inevitably leads to skin wrinkling and aging (Afaq et al., 2003; Langton et al., 2010). Therefore, supplementation of exogenous antioxidants such as phytonutrients, dietary polyphenols, green tea polyphenols, and tea polyphenols is sought after as it increases the activity of endogenous antioxidants and thwarts the UV radiation-induced inflammation, immunosuppression, skin cancer, and aging (Bae et al., 2008; Chiang et al., 2011; Katiyar, 2003; Wood et al., 2017).

Silk sericin (SS), a hydrophilic protein polymer composed of 18 amino acids among which glutamic acid (5%), threonine (6%), glycine (14.20%), aspartic acid (15.74%), and serine (31.99%) are predominant (Vaithanomsat and Kitpreechavanich, 2008; Züge et al., 2017). It is produced by the insects belonging to Bombycidae and *Saturniidae* families, which constitutes 20-30% dry weight of cocoons and shields the pupa from UV radiation-induced damage (Dash et al., 2007; Kaur et al., 2013). SS is known to own different biological properties such as antioxidation, inhibits tumor progression, lipid peroxidation, elastase, and tyrosinase activity (Chlapanidas et al., 2013; Kumar and Mandal, 2017, 2019). Constitution of 30% serine (a major component of a natural moisturizing factor of human skin) makes the SS an excellent moisturizing agent (Nagura et al., 2001). SS extracted from *Bombyx mori* (BM), *Antheraea mylitta* and *A. assamensis* (AA) silk varieties protected skin against UV radiation-induced oxidative damage (Dash et al., 2008; Kumar et al., 2018; Zhaorigetu et al., 2003). It was also reported that BMS enhanced wound healing by increasing cell attachment, proliferation and collagen production (Ersel et al., 2016). All these applications of SS depend on the amino acid composition and associated secondary metabolites (polyphenols and flavonoids).). SS isolated from the cocoons of mulberry silk varieties is known to have different polyphenols and flavonoids like quercetin, catechin, epicatechin, resveratrol, Σphenolics, procyanidin B1, procyanidin B2, kaempferol, luteolin, myricetin, trans-311, rutin, and naringenin.(Butkhup et al., 2012) However, their percentage varies depending on the mulberry silk varieties. While SS obtained from the cocoons of Eri lacks few varieties of secondary metabolites; quercetin, luteolin, kaempferol, and naringenin.(Butkhup et al., 2012) The amino acid conformation of SS and associated secondary metabolites vary based on the source of protein and their

molecular weight range varies with extraction methods, which influences their properties (Butkhup et al., 2012; Kumar and Mandal, 2017). Hence, exploring the properties of SS extracted from a different source would be helpful in identifying the potential silk variety..

Here, we aimed to determine the inhibitory activity of SS against UVA and UVB radiation-induced MMPs expression. SS extracted from the cocoons of *Philosamia ricini* (PR), BM and AA using alkali-degradation was assessed for their anti-collagenase, anti-elastase, and anti-hyaluronidase using biochemical assays. The shielding effect of SS against UV radiation-induced photoaging was evaluated using human dermal fibroblast (HDF) and keratinocytes (HaCaT). UV irradiated HDF cells were treated with SS and assessed for their total collagen content using Sirius red assay. SS (PRS and AAS), which enhanced the total collagen content in UV irradiated cells were selected to evaluate their effect on intracellular ROS levels, and the expression of IL-6, TNF-α, MMP-1, procollagen; collagen1alpha1 (Col1α1) and collagen1alpha2 (Col1α2) genes in HDF cells. Similarly, SS (PRS and AAS) treated HaCaT cells were used to determine the effect of sericin on the expression MMP-2, and MMP-9 proteins and intracellular ROS reducing ability.

5.2. Materials and methods

5.2.1. Materials

Sodium carbonate, urea, and dimethyl sulfoxide (DMSO) were procured from SRL, India. Ascorbic acid (Vitamin C), Bradford's reagent, 2, 7-dichlorofluorescein diacetate (DCFH-DA), pepsin, thiazolyl blue tetrazolium bromide, Direct red, formaldehyde, elastase from porcine pancreas, epigallocatechin gallate (EGCG) analytical standard, N-succinyl-$(Ala)_3$-p-nitroanilide, hyaluronic acid sodium salt, collagenase from *Clostridium histolyticum*, hyaluronidase from bovine and N-[3-(2-furyl) acryloyl]-Leu-Gly-Pro-Ala (FALGPA) were obtained from Sigma, USA. Antibiotic-antimycotic solution, potassium carbonate, Tris (hydroxymethyl) aminomethane, trypsin-EDTA, sodium chloride, and bovine serum albumin (BSA) were sourced from HiMedia, India. Fetal bovine serum (FBS) and Dulbecco's Modified Eagle Medium (DMEM) were procured from Gibco, ThermoFisher Scientific, USA. Glacial acetic acid, hydrochloride, sodium hydroxide were sourced from Merck, India. Tissue culture flasks and plates were procured from Nunc, ThermoFisher Scientific, USA.

5.2.2. Isolation of silk sericin

SS was isolated from the cocoons of *A. assamensis*, *B. mori*, and *P. ricini* using our previously established protocol (Kumar and Mandal, 2017). Briefly, small cocoon pieces were washed with tap water and boiled in 0.5 M Na_2CO_3 for 30 min. SS was separated from the solid residues by centrifugation and filtration. The filtrate was dialyzed with double distilled H_2O for 48 h and freeze-dried.

5.2.3. Biochemical assays

5.2.3.1. Determination of the anti-collagenase activity

The anti-collagenase activity of SS was determined with the modified protocol of Thring *et al.* (2009). In brief, 1 U/mL of collagenase and 2 mM FALGPA was prepared using 50 mM Tricine buffer with 400 mM NaCl and 10 mM $CaCl_2$. 15 µL of collagenase was incubated with 40 µL of different (0.5, 1, 2, 4, 6, 8, and 10 mg/mL) concentrations of SS, BSA, and EGCG (100, 200, 400, 600, and 800 µg/mL) for 20 min at room temperature. Post incubation, 60 µL of the substrate was added to the reaction mixture, the final reaction volume was made up to 150 µL using a Tricine buffer and incubated for 30 min at 37 °C. Post incubation, absorbance was measured at 335 nm by a multiplate reader (Tecan Infinite M200 PRO, Switzerland). The % of collagenase activity was calculated using the following equation:

$$\text{Collagenase activity (\%)} = (100) - \left(\frac{\text{Abs}_s - \text{Abs}_b}{\text{Abs}_{FALGPA}}\right) \times 100 \qquad (5.1)$$

Where Abs_s is the absorbance of the test sample, Abs_b is absorbance of blank (without substrate), and Abs_{FALGPA} is absorbance of the substrate without collagenase.

5.2.3.2. Determination of the anti-elastase activity

The anti-elastase activity of SS was determined by the modified protocol of Chlapanidas *et al.* (2013). Briefly, 125 µL of enzyme (1.2 U/mL of elastase was prepared in 20 mM phosphate buffer pH 6.8) was incubated with 40 µL of different concentrations (0.5, 1, 2, 4, 6, 8 and 10 mg/mL) of SS, BSA, and EGCG (50, 100, 200, 400 and 800 µg/mL) for 20 min at room temperature. Post incubation, 20 µL of substrate (0.6 mM of N-Succinyl-$(Ala)_3$-p-nitroanilide was prepared with 2 mM Tris pH 8) was added and incubated for 20 min and optical density was recorded at 410 nm via multiplate reader. The % of elastase activity was determined using the following equation:

$$\text{Elastase activity (\%)} = \frac{OD_s - OD_b}{OD_c - OD_b} \times 100 \qquad (5.2)$$

Where OD_c is the optical density of control, OD_s is the optical density of test samples and OD_b is the optical density of the blank.

5.2.3.3. Determination of the anti-hyaluronidase activity

The anti-hyaluronidase activity of SS was determined with the modified protocol of Nema *et al.* (2011). In brief, 100 µL [15 U/mL of enzyme was prepared in 20 mM sodium phosphate buffer (pH 7) added with 0.01% BSA and 77 mM sodium chloride] of hyaluronidase was incubated with 40 µL of different concentrations (0.5, 1, 2, 4, 6, 8, and 10 mg/mL) of SS, BSA, and oleanolic acid (OA) (50, 100, 200, 400, and 800 µg/mL) for 20 min at 37 °C. 100 µL of hyaluronic acid (HA) (0.03% in 300 mM sodium phosphate buffer, pH 5.35) was added to the reaction mixture and incubated for 45 min at 37 °C. Undigested HA was precipitated with 1 mL of acid albumin solution (0.1% BSA in sodium acetate 24 mM and acetic acid 79 mM, pH 3.75) and absorbance was measured at 600 nm after 10 min of incubation. The % of hyaluronidase activity was calculated using the following equation:

$$\text{Hyaluronidase activity } (\%) = (100) - \left(\frac{\text{Abs}_s - \text{Abs}_b}{\text{Abs}_{HA}}\right) \times 100 \quad (5.3)$$

Where Abs_s is the absorbance of the test sample, Abs_b is absorbance of blank (without HA), and Abs_{HA} is absorbance of HA without hyaluronidase.

5.2.4. Moisturizing properties of silk sericin

Moisture absorption properties of SS was evaluated with the modified protocol of Li *et al.* (2011). In brief, SS was dried in a hot air oven for 4 h at 60 °C and placed in a humidified chamber maintained with 43% relative humidity (RH) using saturated potassium carbonate at 25 °C for different time points (3, 6, 12 and 24 h). Urea was used as positive controls to evaluate the moisturizing properties of SS. Moisture absorption rate of SS was assessed by the following equation:

$$R_a\ (\%) = \frac{W_t - W_0}{W_0} \times 100 \quad (5.4)$$

Where R_a is the moisture absorption rate of the sample, W_0 is the dry weight of samples and W_t is the weight of samples post moisture absorption at the specific time point.

SS was incubated in a humidified chamber (RH was maintained with water) for 24 h at 25 °C and transferred to another humidified chamber containing potassium carbonate to dehydrate at 25 °C for 12 h. Moisture retention rate was calculated using the following equation:

$$R_r\ (\%) = \frac{W_w - W_t}{W_w - W_0} \times 100 \quad (5.5)$$

Where R_r is moisture retention rate, W_0 is the dry weight of samples, W_w is the weight attained by the sample in the water chamber, and W_t weight attained post dehydration in potassium carbonate.

5.2.5. *In vitro* studies for determining the anti-aging activity of silk sericin

5.2.5.1. Maintenance of the cell lines

Human dermal fibroblast (HDF) and keratinocyte (HaCaT) cells were obtained from HiMedia and National Centre for Cell Sciences (NCCS), India, respectively. HDF and HaCaT cells were grown and maintained in DMEM high glucose added with 10% FBS and 1× antibiotic-antimycotic solution

5.2.5.2. Cytocompatibility.

Cytocompatibility of SS was evaluated using the MTT assay. HDF and HaCaT cells (1×10^4 cells/well) were seeded in 96 well plates, incubated for 12 h, and treated with 10 and 100 µg/mL of SS or vitamin C (Vit. C) for 24 h and MTT assay was executed.(Kumar and Mandal, 2019)

5.2.5.3. UV radiation system

Before UV irradiation, cells were washed and covered with a thin layer of PBS. Cells were irradiated with UVA and UVB radiation by UVP crosslinker (CL-1000L, UK) with a maximum emission peak at 365 nm and 302 nm, respectively. Post irradiating, cells were incubated with serum-free medium with or without SS for specific time points to evaluate cell viability, total collagen content, relative gene expression, MMP-2, and MMP-9 activity. Control cells were treated with the same experimental conditions without exposing to UV radiation.

5.2.5.4. Cell viability assay

The viability of HDF cells after UVA and UVB irradiations was evaluated using the MTT assay. In brief, HDF cells were plated in 96 well plates and allowed to attain 80% confluence and irradiated with 2, 4, 6, 8, 10 and 12 J/cm^2 of UVA and 10, 30, 60 and 120 mJ/cm^2 of UVB radiation. After 24 h, the MTT assay was done (Kumar et al., 2018).

The influence of SS treatment on the viability of UVA (8 J/cm^2) and UVB (60 mJ/cm^2) irradiated cells was assessed using the MTT assay. In brief, HDF cells were irradiated UVA and UVB radiations followed by treatment with 10 and 100 µg/mL of

BMS, AAS, PRS, and Vit. C for 24 h and MTT assay was performed (Kumar et al., 2018).

5.2.5.5. Estimation of total collagen production by Sirius red assay

Total collagen content produced by HDF cells after UV irradiation was assessed using Sirius red assay. HDF cells cultured in 60 mm petri dish and until they attain 80% confluence. Cells were irradiated with UVA (8 J/cm^2) and UVB (60 mJ/cm^2) radiation followed by SS treatment for 48 h. Cells were washed with cold PBS and digested using pepsin digestion buffer (0.1 M acetic acid, 0.5 M NaCl and 1mg/mL of pepsin) for 48 h. After digestion, 200 µL of sample was collected and transferred to 96 well plates and dried at 37 ºC for 24 h. Samples were treated with 100 µL of Direct red (1 mg /mL) for 1 h and fixed with fixing solution (5 mL of 35% formaldehyde, 1 mL of glacial acetic acid, and 15 mL of picric acid). After 10-20 min of fixing, the cells were washed with 0.01 N HCl and dried at room temperature. Samples were dissolved in 100 µL of 0.1 N NaOH and absorbance was measured at 550 nm with a multiplate reader.

5.2.5.6. Gene expression study

The influence of UV radiation on the relative expression of IL-6, TNF-α, Col 1α1, Col 1α2, and MMP-1 genes was assessed using real-time polymerase chain reaction (RT-PCR). HDF cells cultured in 60 mm dishes allowed to attain 80% confluence and irradiated UVA (8 J/cm^2) and UVB (60 mJ/cm^2) radiation. UV irradiated cells were treated with SS for 24 h. RNA was isolated from the cells and reverse transcribed to cDNA as described.(Kumar and Mandal, 2019) GAPDH was used as an endogenous control and the primer sequences shown in **Table 5.1**.

Table 5.1. *Depicts the primer sequences*

Gene	Primer	Sequence	Accession number
IL-6	Forward	5′-CTCAATATTAGATCTCAACCCCCA-3′	NM_000600.4
	Reverse	5′-GAGAAGGCAACTGGACCGAA-3′	
TNF-α	Forward	5′-TCTTCTCGAACCCCGAGTGA-3′	NM_000594.3
	Reverse	5′- CCTCTGATGGCACCACCAG-3′	
Col1α1	Forward	5′- TGGAGCAAGAGGCGAGAG-3′	NM_000088.3
	Reverse	5′-CACCAGCATCACCCTTAGC-3′	
Col1α2	Forward	5′- TCAAGGTTTCCAAGGACCTG-3′	NM_000089.3
	Reverse	5′- GTGTCCCCTAATGCCTTTGA-3′	
MMP-1	Forward	5′- ATGCACAGCTTTCCTCCACTG-3′	NM_002421.3
	Reverse	5′- ACTGGGCCACTATTTCTCCG -3′	
GAPDH	Forward	5′- GACCTGACCTGCCGTCTA -3′	NM_001289745.2
	Reverse	5′- GTTGCTGTAGCCAAATTCGTT-3′	

5.2.5.7. Determination of *in vitro* anti-elastase activity

HDF cells were cultured in 6 well plates till they attain 80% confluency followed by UVA (8 J/cm^2) and UVB (60 mJ/cm^2) irradiations and incubated with SS for 48 h. After 48 h, spent media was collected and preserved to analyze the elastase activity. Cells were trypsinized, lysed with cell lysis buffer for 30 min on ice, centrifuged and the supernatant was collected (Kumar and Mandal, 2017). The concentration of the protein was measured by the Bradford assay. 30 µg of cell lysate or 40 µL of spent samples were incubated with 150 µL of the substrate [0.6 mM of N-Succinyl-$(Ala)_3$-p-nitroanilide was prepared with 100 mM Tris pH 8] for 30 min. The optical density of the reaction mixture was recorded at 410 nm with a multiplate reader. The % of elastase activity was calculated using the following equation:

$$\text{Elastase activity (\%)} = \frac{OD_s - OD_b}{OD_c - OD_b} \times 100 \qquad (5.6)$$

Where OD_c is the optical density of control, OD_s is the optical density of test samples and OD_b is the optical density of the blank.

5.2.5.8. Determination of intracellular reactive oxygen species level

Intracellular ROS levels in UV irradiated HDF and HaCaT cells were determined by our established protocol (Kumar et al., 2018). In brief, UV irradiated cells incubated fresh serum-free media containing SS or Vit. C and 10 µM of DCFH-DA for 30 min. After 30 min, fluorescence intensity was measured at λ_{ex} 488 nm and λ_{em} 525 nm with a multiplate reader.

5.2.5.9. Gelatin zymography

The effect of SS on the expression of gelatinase (MMP-2 and MMP-9) was determined by gelatin zymography by the adopted protocol from Abcam. HaCaT cells were cultured in 6 well plates till they attain 80% confluence and irradiated with UV radiations and incubated with SS for 48 h. The spent media was collected and preserved to analyze gelatinase expression. Cells were harvested, lysed with cell lysis buffer for 30 min and centrifuged.(Kumar and Mandal, 2017). The supernatant was used to measure the protein concentration via Bradford assay. An equal concentration of protein was used to assess gelatinase activity using 7.5% acrylamide gel with 0.1% of gelatin.

5.2.6. Statistical analysis

All experiments were done in triplicates and results were represented as mean ± SD. Statistical difference between the groups was determined with the Holm-Sidak method through Sigma-plot software.

5.3. Results

5.3.1. Determination of the anti-collagenase activity

Collagenase degrades the collagen of the extracellular matrix (ECM), which results in the loss of structural integrity of the skin (Kondo, 2000). Inhibition of collagenase activity would prevent collagen degradation. The anti-collagenase activity of SS was assessed by measuring the degradation of FALGPA after incubation with collagenase from *Clostridium histolyticum*. In comparison with control (incubation of collagenase with FALGPA), collagenase activity did not change after incubation with SS or BSA, while its activity inhibited by EGCG (**Fig.5.1**).

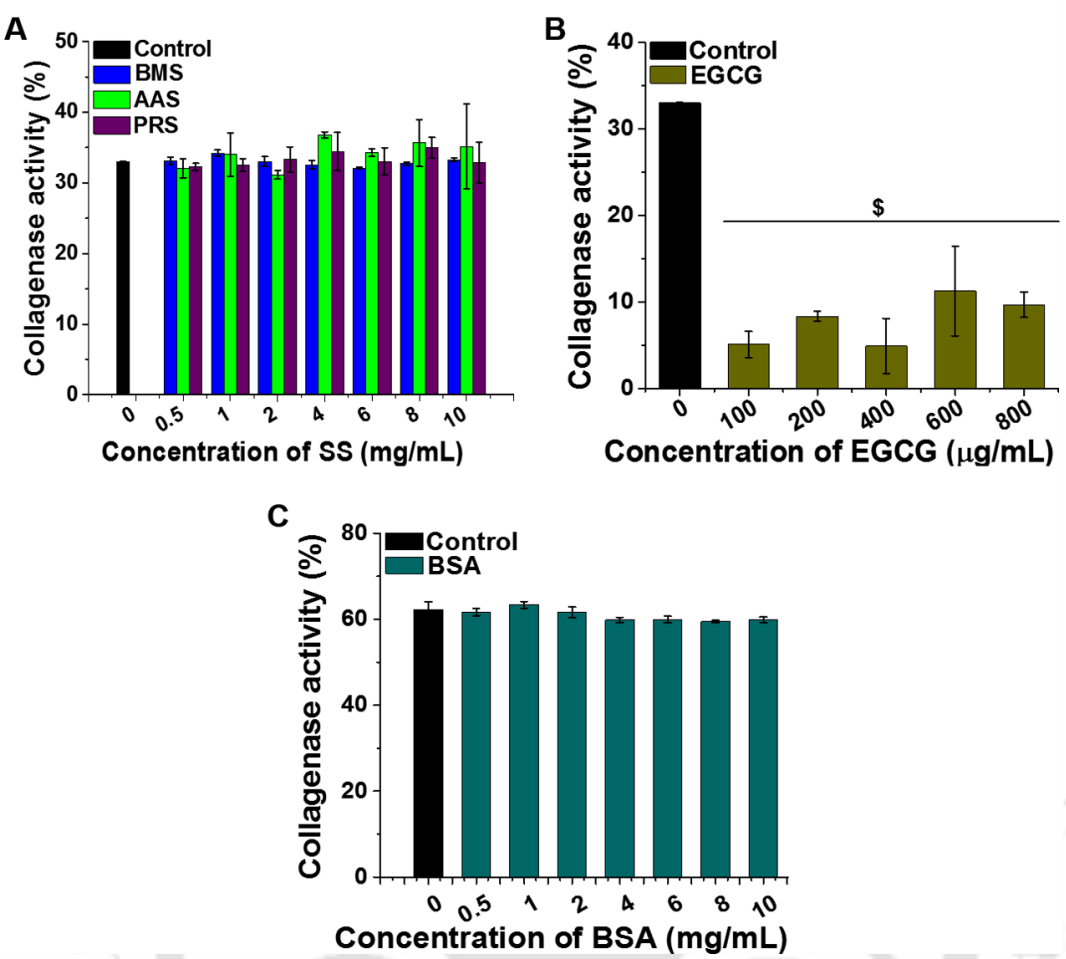

Fig.5.1. *The anti-collagenase activity of (A) silk sericin, (B) epigallocatechin gallate and (C) bovine serum albumin was assessed by measuring the degradation of FALGPA with collagenase from Clostridium histolyticum. ($p≤0.001 in comparison with control)*

5.3.2. Determination of the anti-elastase activity

Elastase degrades the elastic fibers of ECM and leads to wrinkling of the skin (Tsuji et al., 2001). Inhibition of elastase activity would prevent the wrinkling of the skin. The anti-elastase activity of SS was assessed by measuring the release of p-nitroanilide after digesting with porcine pancreas elastase. In comparison with control (incubation of elastase with N-Succinyl-$(Ala)_3$-p-nitroanilide), the elastase activity was significantly inhibited after incubating with higher concentrations of SS (**Fig.5.2**). While elastase activity remains unaffected after treatment with 10 mg/mL of PRS. AAS exhibited 50% inhibition of elastase activity at 10 mg/mL. Elastase activity remained unchanged with control after incubating with BSA or EGCG.

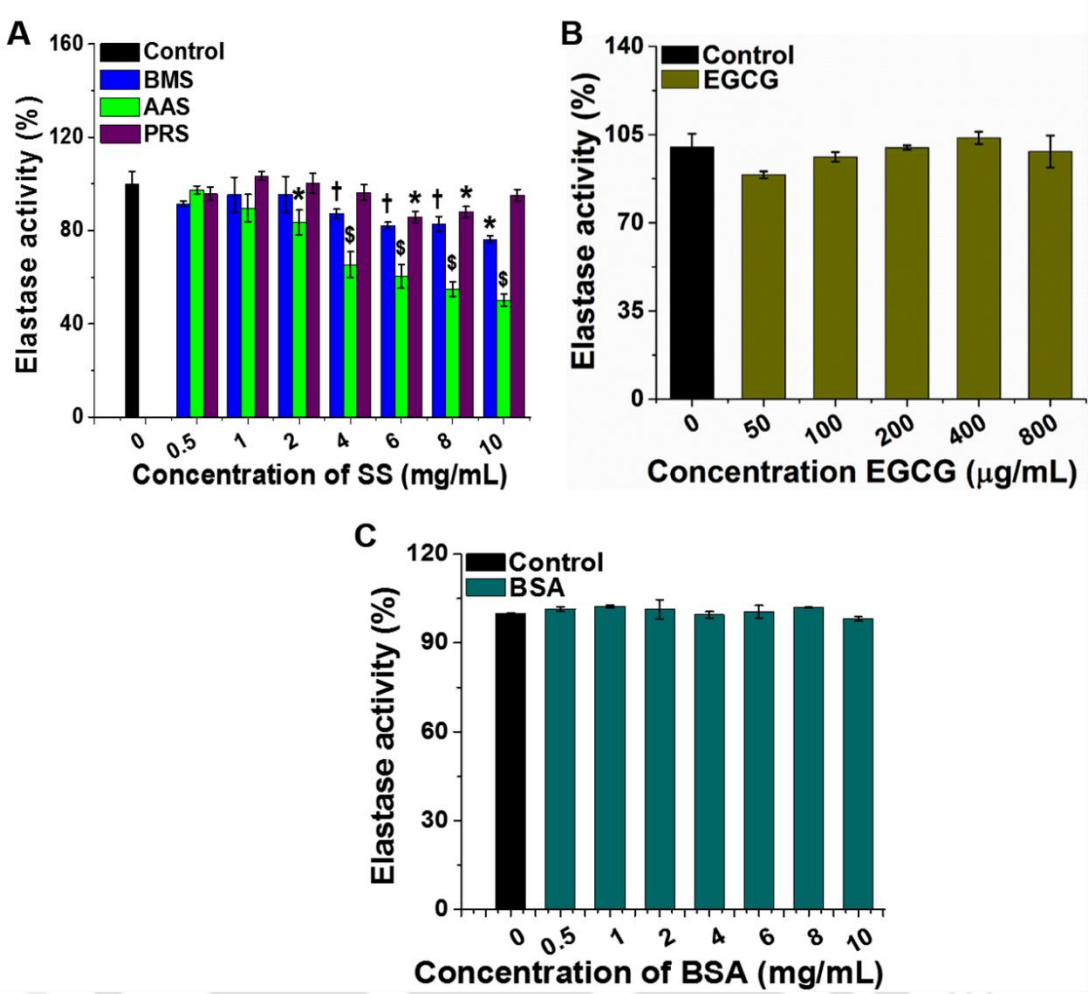

Fig.5.2. *The anti-elastase activity of (A) silk sericin, (B) epigallocatechin gallate, and (C) bovine serum albumin was assessed by measuring the release of p-nitroanilide from the N-Succinyl-$(Ala)_3$-p-nitroanilide after digesting with porcine pancreas elastase ($p≤0.001, *p≤0.01 and †p≤0.05 in comparison with control)*

5.3.3. Determination of the anti-hyaluronidase activity

The anti-hyaluronidase activity of SS was assessed by measuring the % of hyaluronic acid precipitation in acid albumin solution after digesting with hyaluronidase. **Fig.5.3A and B** depict the % of HA precipitate formed in acid albumin after treating hyaluronidase with SS and OA, respectively. Incubation of hyaluronidase with BMS, AAS, and OA significantly reduced the degradation of HA than control (incubation of hyaluronidase with HA). Whereas, hyaluronidase activity remain unaffected after incubation with PRS. AAS showed 50% inhibition of hyaluronidase activity at 6 mg/mL. Incubation of hyaluronidase with BSA completely prevented HA degradation and enhanced its precipitation.

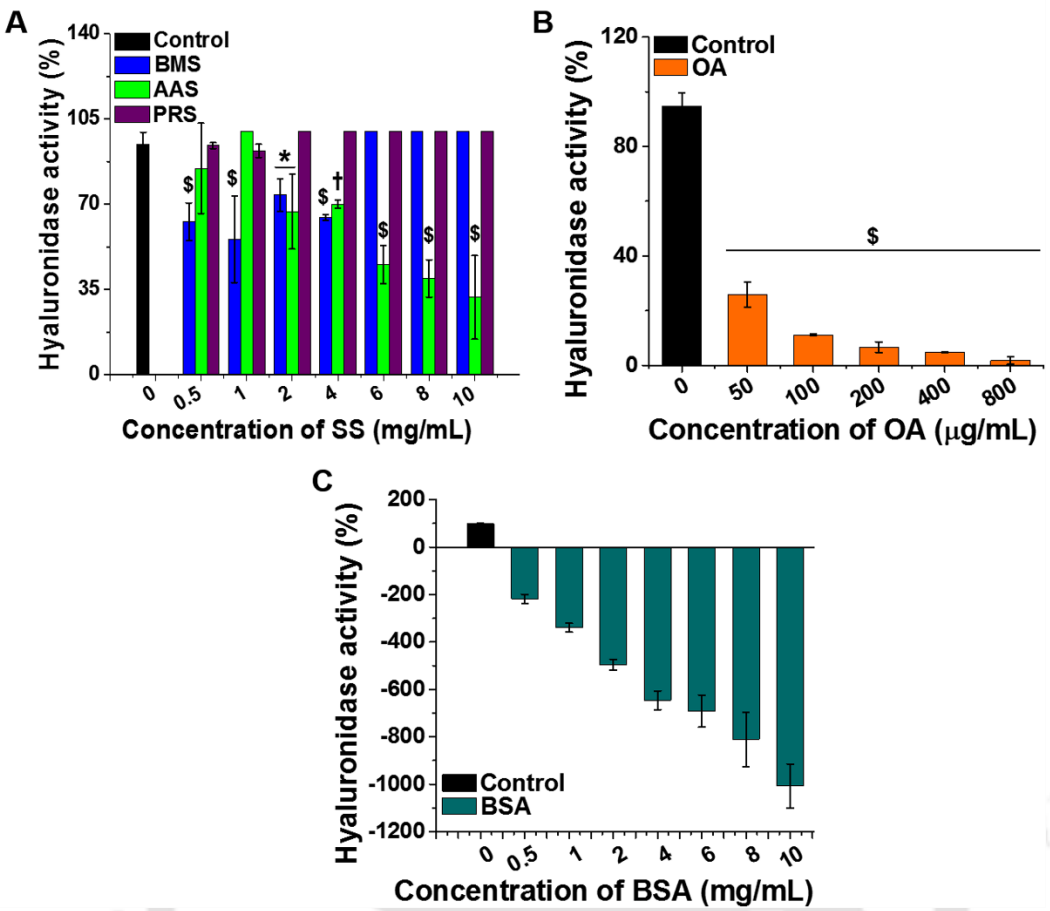

Fig.5.3. *The anti-hyaluronidase activity of (A) silk sericin, (B) oleanolic acid and (C) bovine serum albumin was determined by measuring the precipitate formed by hyaluronic acid in acid albumin after digesting with hyaluronidase ($p≤0.001, *p≤0.01 and †p≤0.05 in comparison with control)*

5.3.4. Moisturizing properties of sericin

SS is a hydrophilic protein that constitutes 30% of serine, which is a major amino acid of a natural moisturizing factor of human skin. The moisture absorption and retention activity of SS were assessed using K_2CO_3. In the dehydrating chamber, SS and urea showed less than 0.15% of moisture absorption (**Fig.5.4A**). For evaluating the moisture retention activity of SS, we placed the SS in a humidified chamber for 24 h and further changed to dehydrating chamber for 12 h. In the dehydrating chamber, SS showed 60-65% moisture retention, whereas, urea exhibited 99% moisture retention (**Fig.5.4B**).

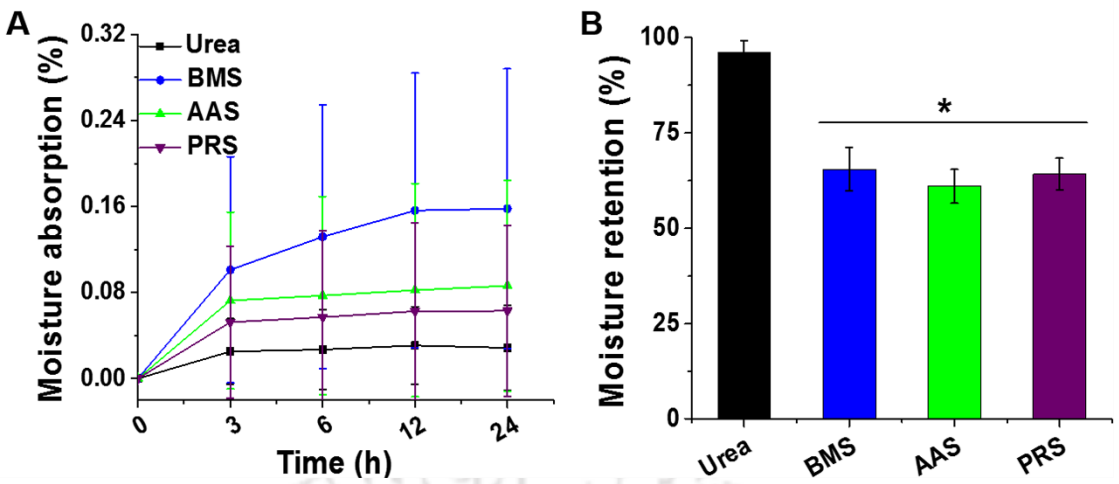

Fig.5.4. *(A) Moisture absorption by silk sericin and urea was assessed in the dehydrating chamber (43% relative humidity maintained using saturated K_2CO_3). (B) Moisture retained by silk sericin and urea in the dehydrated chamber. (*p≤0.01 in comparison with urea)*

5.3.5. Cytocompatibility study

Mitochondrial dehydrogenase of viable cells converts the MTT to formazan. The effect of SS or Vit. C on the viability of HDF and HaCaT cells was determined by evaluating the mitochondrial dehydrogenase activity using the MTT assay. The viability of BMS, AAS, PRS, and Vit. C treated HDF and HaCaT cells were similar to control cells (**Fig.5.5**).

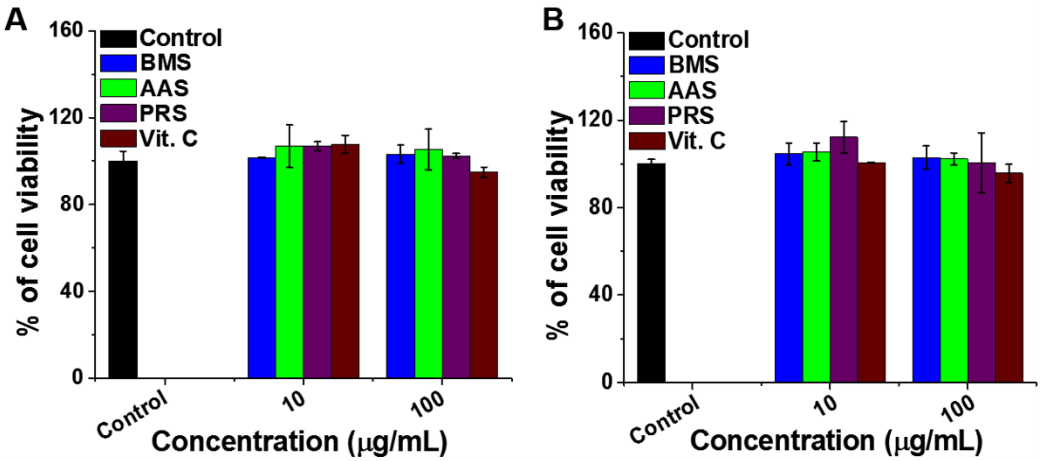

Fig.5.5. *The impact of silk sericin or vitamin C on the viability of (A) HDF and (B) HaCaT cells was determined by the MTT assay.*

5.3.6. Cell viability assay

The cytotoxicity of UVA and UVB radiations against HDF cells was assessed using the MTT assay. The viability of HDF cells after irradiating with different dosage of UVA and UVB radiations is depicted in **Fig.5.6 IA and B**, respectively. In comparison with control cells (unirradiated cells), the viability of HDF cells remained unaffected after irradiating with UVA radiation up to 8 J/cm^2. Whereas, cells irradiated with 10 and 12 J/cm^2 of UVA radiations showed significantly low viability. HDF cells irradiated with 120 mJ/cm^2 of UVB radiations displayed low viability than control cells.

8 J/cm^2 (UVA) and 60 mJ/cm^2 (UVB) dosage were selected to evaluate the shielding activity of SS against UVA and UVB radiation-induced skin aging. The effect of SS post-treatment on the viability of UVA and UVB irradiated HDF cells was evaluated using the MTT assay. **Fig.5.6 IIA and B** depict the viability of UVA (8 J/cm^2) and UVB (60 mJ/cm^2) irradiated HDF cells after treating with SS. AAS and PRS (100 µg/mL) post-treatment significantly reduced the viability of UVA-irradiated cells ($p \leq 0.01$) than control cells; while the viability of UVB irradiated cells did not change after treating with SS.

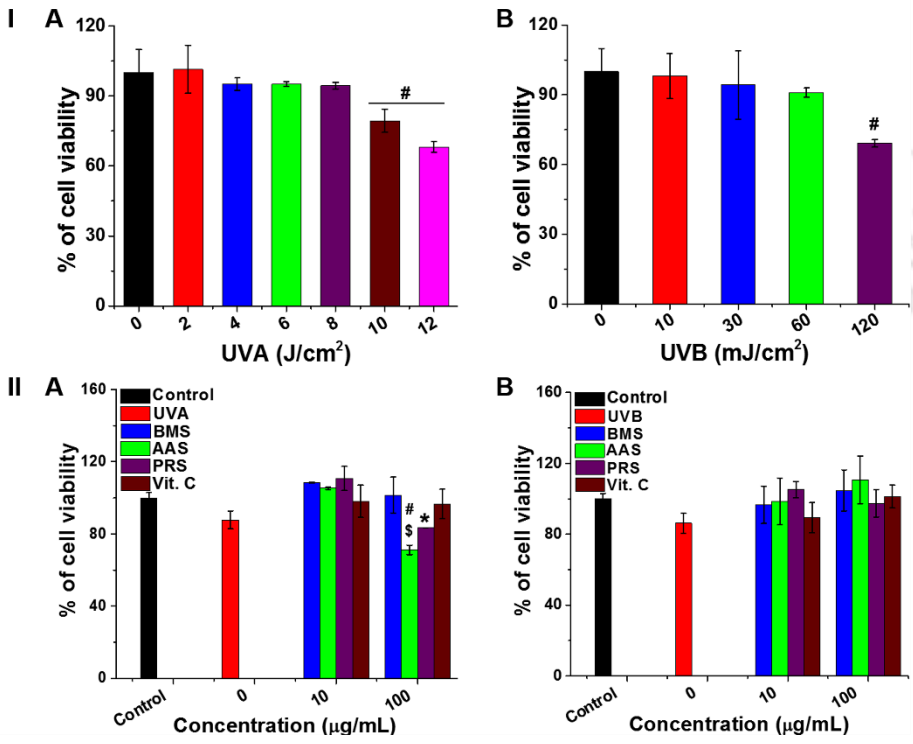

Fig.5.6. *The viability of (I) UV irradiated and (II) silk sericin or vitamin c post-treated HDF cells was assessed using the MTT assay. Where HDF cells were irradiated with (A) UVA and (B) UVB radiations. ($p≤0.001 and *p≤0.01 in comparison with control cells; #p≤0.001 in comparison with silk sericin untreated cells)*

5.3.7. Estimation of total collagen production by Sirius red assay

Oxidative stress induced by UV radiations upregulate the expression of MMP-1 (collagenase) in HDF cells along with MMP-3, which results in the degradation of collagen and lead to loss of structural integrity of the skin (Kondo, 2000). Inhibitory effect of SS against UV radiation-induced collagen degradation was assessed by analysis the total collagen content using Sirius red assay. **Fig.5.7A and B** depict the total collagen content produced by UVA and UVB irradiated HDF cells after SS treatment, respectively. In comparison with the control cells, UVA and UVB irradiation significantly reduced the collagen production in HDF cells. Whereas, AAS (10 µg/mL), PRS (100 µg/mL), and Vit C (10 µg/mL) post-treatment significantly enhanced the collagen content in both UVA and UVB irradiated cells than SS untreated cells. However, BMS (100 µg/mL) post-treatment significantly enhanced total collagen content in UVA-irradiated cells.

We have selected silk varieties [PRS (100 µg/mL) and AAS (10 µg/mL)] which enhanced collagen content in UVA and UVB irradiated cells along with Vit. C (10 µg/mL) to evaluate their role in relative gene expression, levels of ROS, MMP-2 and 9 expressions.

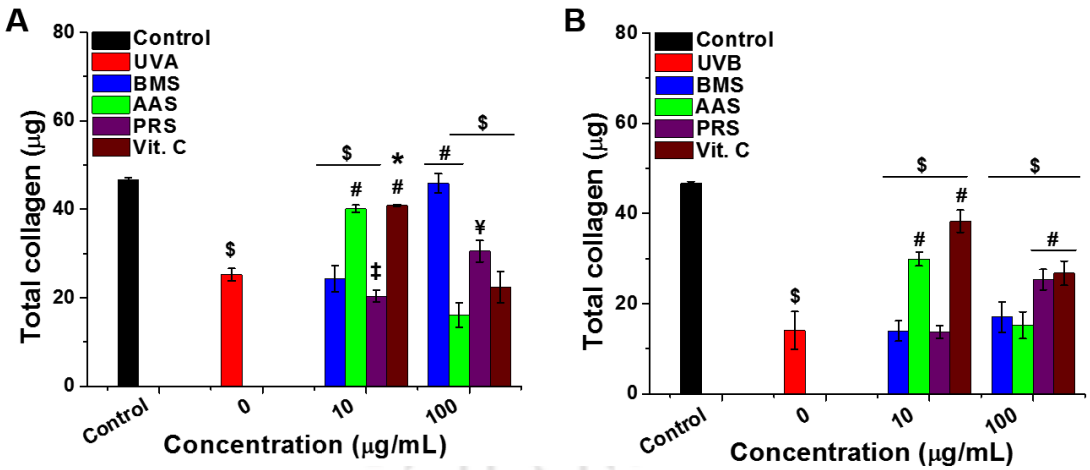

Fig.5.7. *The total collagen content present in (A) UVA and (B) UVB irradiated HDF cells was assessed after treating with silk sericin or vitamin c for 48 h using Sirius red assay. ($p≤0.001 and *p≤0.01 compared to control cells; #p≤0.001, ¥p≤0.01, and ‡p≤0.05 compared to silk sericin untreated cells)*

5.3.8. Gene expression studies

The impact of AAS (10 µg/mL) or PRS (100 µg/mL) post-treatment on the relative expression of IL-6, TNF-α, MMP-1, Col1α1, and Col1α2 genes in UV irradiated and control HDF cells was assessed using RT-PCR (**Fig.5.8).** SS post-treatment significantly downregulated the expression of IL-6 in UVA and UVB irradiated cells than only UV irradiated cells. While Vit. C post-treatment upregulated the expression of IL-6 in UVA-irradiated cells. TNF-α expression was upregulated after UVA and UVB irradiation in HDF cells, however, AAS (UVA and UVB irradiated cells), PRS, and Vit. C (UVB irradiated cells) post-treatment downregulated its expression. HDF cells irradiated with UVA and UVB radiations showed the downregulation of Col1α1 and upregulation of Col1α2 gene expression than control cells. While SS post-treatment upregulated Col1α1 and Col1α2 gene expression than SS untreated cells. SS or Vit. C post-treatment downregulated the MMP-1 expression in UVA1 and UVB irradiated cells than only UV irradiated cells.

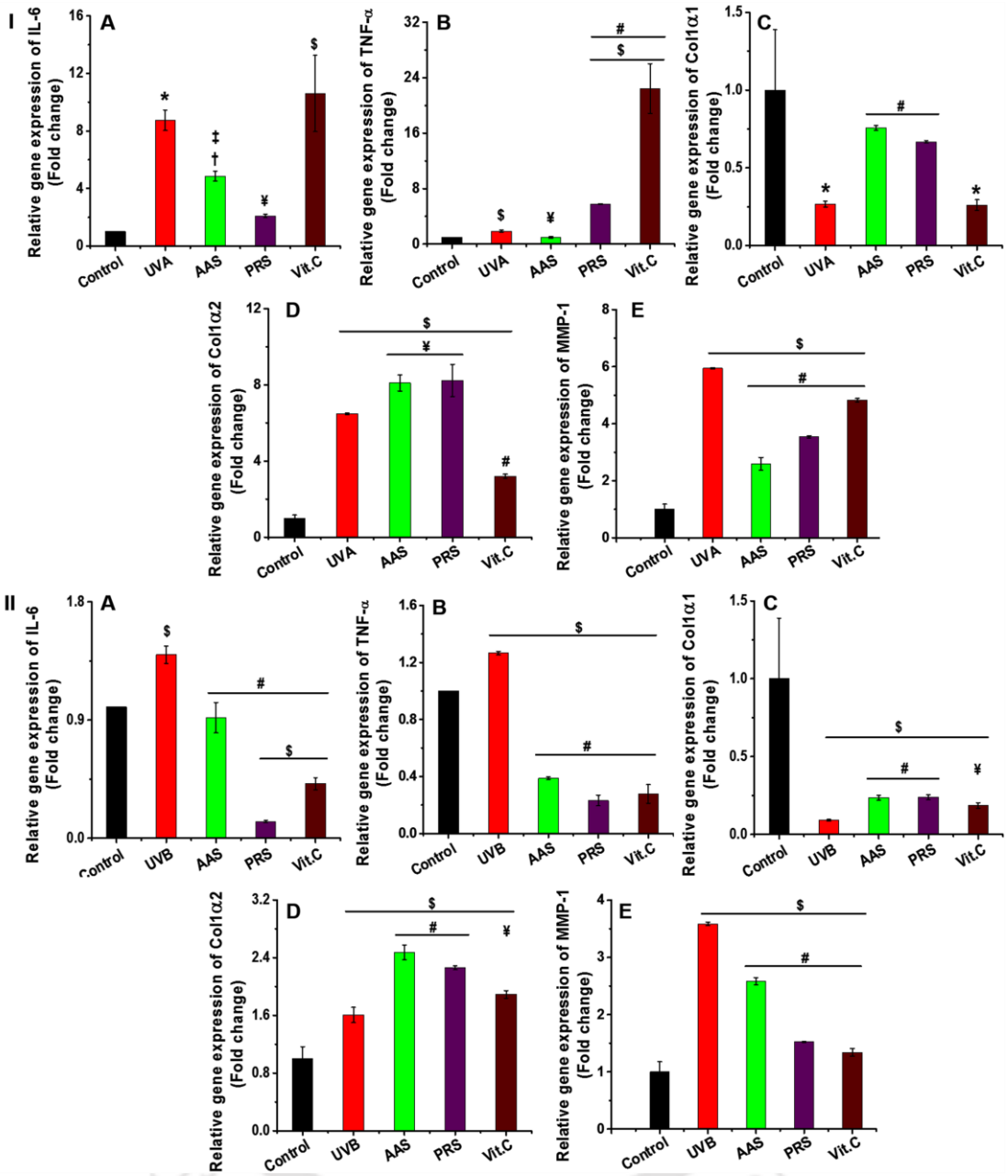

Fig.5.8. *The impact of silk sericin or vitamin c post-treatment on the expression of (A) IL-6, (B) TNF-α, (C) Col1α1, (D) Col1α2, and (E) MMP-1 gene in (I) UVA and (II) UVB irradiated cells using RT-PCR. ($p≤0.001, *p≤0.01, and †p≤0.05 compared to control cells; #p≤0.001, ¥p≤0.01, and ‡p≤0.05 compared to silk sericin untreated cells)*

5.3.9. Determination of *in vitro* anti-elastase activity of silk sericin

UV radiations upregulate the expression of fibroblast elastase (MMPs expressing elastase activity), which plays a critical role in the degradation of elastic fibers and results in skin wrinkling (Tsuji et al., 2001). The effect of SS post-treatment on the expression of elastase by UV irradiated HDF cells was assessed using the release of p-nitroanilide

from the N-Succinyl-$(Ala)_3$-p-nitroanilide after incubation with cell lysate or spent media. In comparison with control cells, UVA or UVB irradiation significantly increased the expression of fibroblast elastase and released into the media. AAS or PRS post-treatment significantly downregulated the UVA or UVB radiation-induced fibroblast elastase expression in spent media than SS untreated cells, however, Vit C post-treated cells showed enhanced elastase activity (**Fig.5.9**).

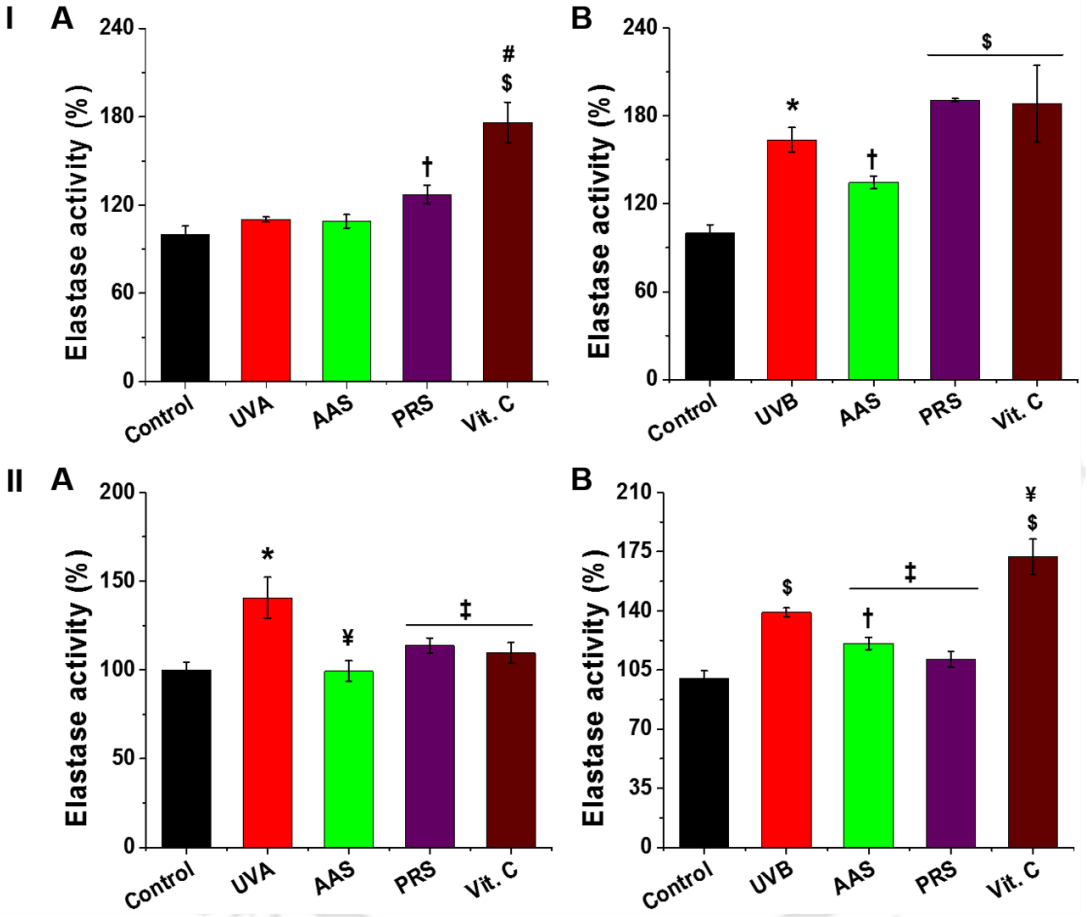

Fig.5.9. *The inhibitory activity of silk sericin or vitamin C against (A) UVA and (B) UVB induced elastase expression was assessed by analyzing the release of p-nitroanilide from the N-Succinyl-$(Ala)_3$-p-nitroanilide after incubating with (I) cell lysate and (II) spent media. ($p≤0.001, *p≤0.01, and †p≤0.05 compared to control cells; #p≤0.001, ¥p≤0.01, and ‡p≤0.05 compared to silk sericin untreated cells)*

5.3.10. Determination of intracellular reactive oxygen species level

Elevated levels of ROS induces oxidative stress that damages biomacromolecules and also results in mutations. UV radiations are one of the major factors that elevate the ROS generation in both human keratinocytes and dermal fibroblast cells that leads to

secretion of MMPs, which causes the degradation of collagen and gelatin (Kondo, 2000). ROS scavenging ability of SS was evaluated by DCFH-DA AAS (10 µg/mL) or PRS (100 µg/mL) or Vit. C (10 µg/mL) post-treatment significantly reduced the intracellular ROS levels of UVA and UVB irradiated HDF and HaCaT cells in comparison to SS untreated cells (only UV irradiated cells) (**Fig. 5.10**).

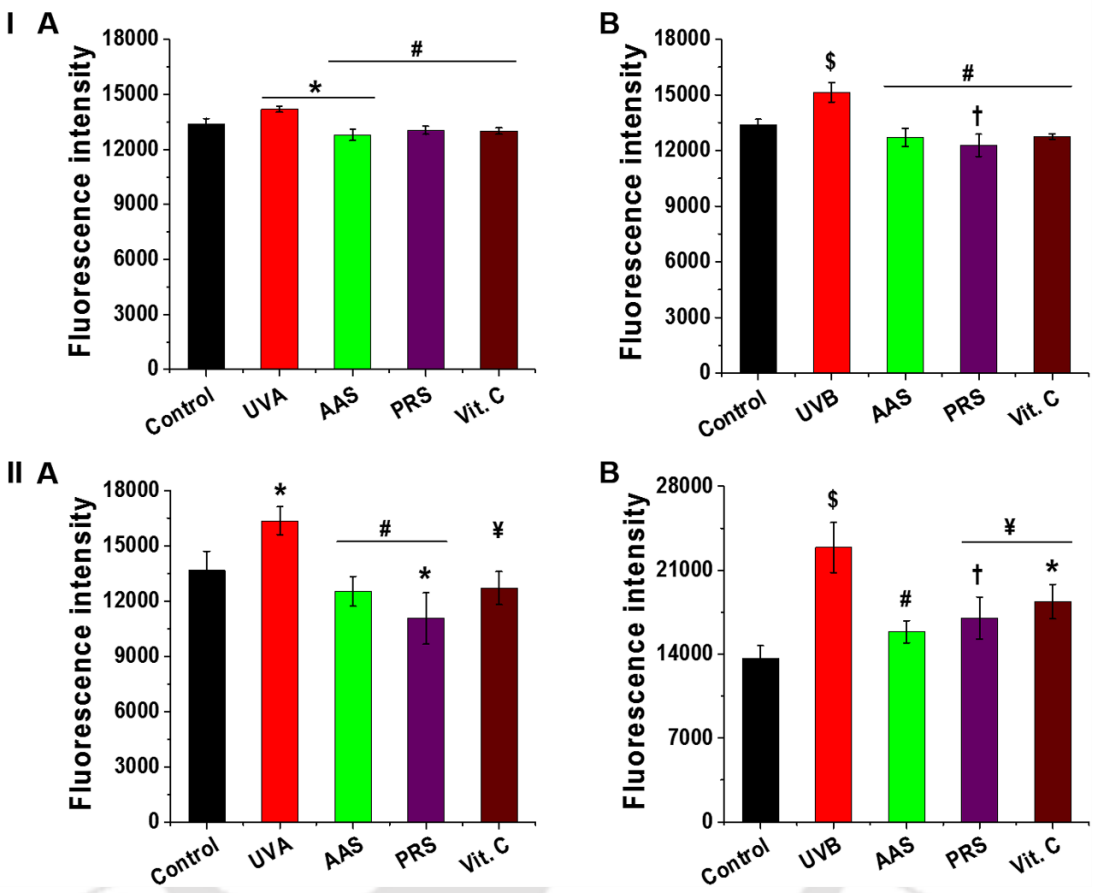

Fig.5.10. *The effect of silk sericin post-treatment on the intracellular ROS levels of (I) HDF and (II) HaCaT cells was evaluated using DCFH-DA. Where (A) UVA and (B) UVB irradiated cells. ($p≤0.001, *p≤0.01, and †p≤0.05 compared to control cells; #p≤0.001 and ¥p≤0.01 to compared to silk sericin untreated cells)*

5.3.11. Gelatin zymography

UV radiations induce secretion of gelatinase (MMP-2 and MMP-9) by human keratinocytes, which degrades partially degraded collagen and enhances skin aging (Kondo, 2000). The effect of SS post-treatment on the production of gelatinase by UV irradiated HaCaT was assessed using gelatin zymography. MMP-2 and MMP-9 released into surrounding media and present in the UVA and UVB irradiated HaCaT cells are depicted in **Fig.5.11**. UVA and UVB irradiated cells induce the upregulation of MMP-2

and MMP-9 expression and released them into surrounding media when compared to control cells. However, AAS (10 µg/mL) or PRS (100 µg/mL) or Vit. C (10 µg/mL) post-treatment downregulated the expression of gelatinase in HaCaT. MMP-2 released by UVA-irradiated HaCaT cells after treating with PRS and Vit C remain unaffected in comparison to SS untreated cells.

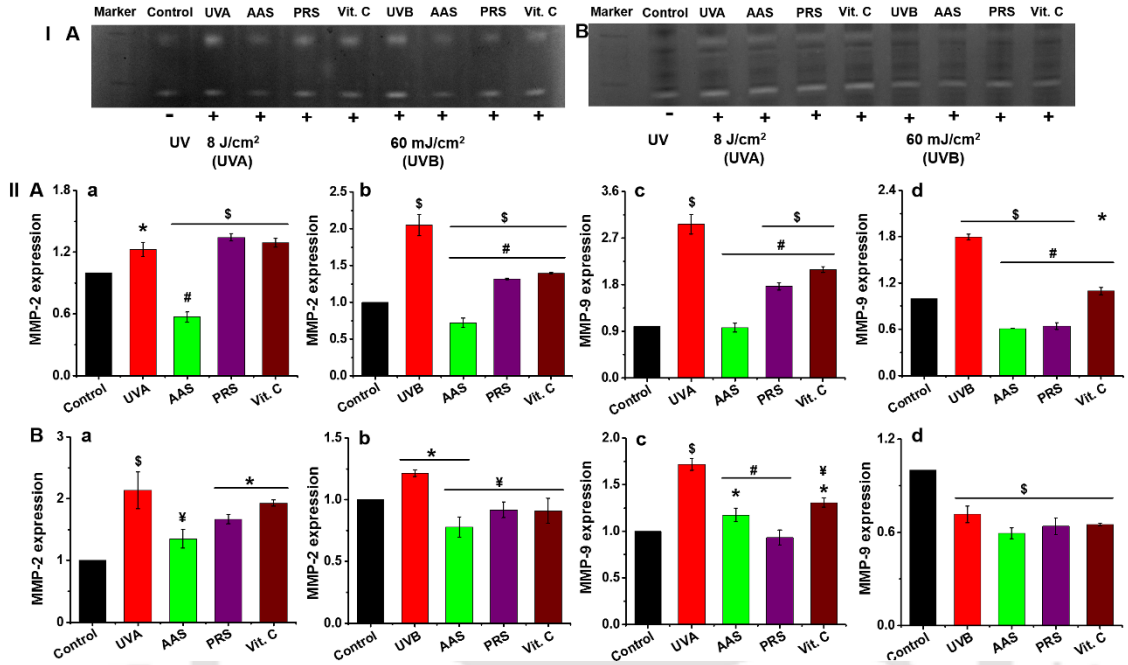

Fig.5.11. *The effect of silk sericin or vitamin C post-treatment on the expression of MMP-2 (a and b) and MMP-9 (c and d) protein by UVA and UVB irradiated HaCaT cells was assessed using gelatin zymography. Where (I) pictorial representation of gelatin zymographic gel and (II) graphical representation of MMP-2 and MMP-9 protein expression; MMP-2 and MMP-9 expressed in (A) spent media and (B) cell lysate. ($p≤0.001 and *p≤0.01 compared to control cells; #p≤0.001 and ¥p≤0.01 compared to silk sericin untreated cells*

5.4. Discussion

Silk sericin (SS), a structural protein polymer produced by the insects of Bombycidae and Saturniidae families is known to possess antioxidant activity along with other biological attributes (Kumar and Mandal, 2017; Zhaorigetu et al., 2003). The properties of SS depends on their amino acid conformation and associated secondary metabolites, however, they vary based on the source and isolation methods (Kumar and Mandal, 2017). Hence, exploring the inhibitory activity of SS extracted different silk varieties against UVA and UVB radiation-induced aging could be useful to identify

potential silk varieties. Therefore, in the present study, we have focused on the SS extracted from the three silk varieties; PR, BM, and AA.

Collagenase, elastase, and hyaluronidase are the enzymes, which plays a critical role in modulating the structural integrity, elasticity, and smoothness of the skin by degrading the collagen, elastin, and hyaluronic acid, respectively (Afaq et al., 2003; Csoka et al., 2001; Kondo, 2000; Tsuji et al., 2001). SS obtained from the cocoons of PR, AA, and BM using alkali-degradation were assessed for their anti-collagenase, anti-elastase, and anti-hyaluronidase activity. Collagen is an important structural protein polymer of the dermal layer of skin produced by fibroblast cells, which maintain structural integrity (Hashem et al., 2008). MMP-1 (collagenase) degrades the collagen of the dermal layer of skin, which results in the loss of skin structural integrity, aging, and wrinkling (Hashem et al., 2008). Inhibition of collagenase prevents the loss of skin structural integrity. Anti-collagenase activity of SS assessed using collagenase from *Clostridium histolyticum* exhibited that the collagenase activity remained unchanged after incubating with SS, whereas, epigallocatechin gallate (EGCG) inhibited its activity (**Fig.5.1)**. It was reported that the galloyl radicals of tea catechins (epicatechin gallate and EGCG) inhibit the collagenase activity by inducing aggregation (Makimura et al., 1993). However, catechins associated with SS might not able to precipitate the collagenase from *Clostridium histolyticum*.

Elastin fibers of the dermal layer of skin maintain the elasticity of the skin. Elastase degrades the elastin fibers of the skin and results in its wrinkling or sagging (Imokawa, 2009; Tsuji et al., 2001). Inhibition of elastase activity would prevent the wrinkling or sagging of skin. Elastase inhibitor activity of SS assessed using porcine elastase showed that BMS, AAS, and PRS inhibited its activity, however, AAS displayed the greater extent of elastase inhibition than PRS and BMS (**Fig.5.2**). Polyphenols inhibit the elastase activity by forming the complex structures with elastase (Brás et al., 2010; Silva et al., 2017). Polyphenols and flavonoids associated with AAS might have efficiently formed stable complexes with elastase than BMS and PRS, respectively. Metal chelating agents also inhibit the endopeptidase and aminopeptidase (Homsy et al., 1988). Metal chelating (hydroxyl groups of serine and threonine chelates the metal ions; copper and iron) amino acids of SS might have also inhibited elastase activity (Kato et al., 1998).

Hyaluronic acid (HA) (a glycosaminoglycan) is an important component of ECM, which is responsible for water retention in the skin and also acts as a lubricant in joints

(Papakonstantinou et al., 2012). Aging leads to the degradation of HA results in dehydration and roughness of skin along with a decrease in elasticity (Papakonstantinou et al., 2012). Hyaluronidase is an enzyme, which degrades the hyaluronic acid (Csoka et al., 2001). Collagen degradation induced by UV radiations also downregulates the synthesis of HA by inhibiting the hyaluronic acid synthases (Dai et al., 2007). Inhibition of hyaluronidase activity controls the degradation of HA, which enhances structural integrity, hydration, and smoothness of the skin. Polyphenols and flavonoids inhibit the activity of hyaluronidase (Bralley et al., 2008). Hyaluronidase activity was significantly inhibited by incubation with AAS and BMS (**Fig.5.3A)**, whereas, incubation of hyaluronidase with PRS did not inhibit its activity. Inhibition of hyaluronidase activity was correlated with the total polyphenols and flavonoids associated with AAS and BMS (Bralley et al., 2008). At low pH 4 and under low ionic condition BSA able to compete with hyaluronidase and forms electrostatic and non-catalytic complexes with HA that prevents its degradation (Lenormand et al., 2009). Non-catalytic complexes formed between BSA and HA might have precipitated in the acid albumin solution. Therefore, with an increase in the BSA concentration, the precipitate also increased and there was no precipitation observed in the blank solution (**Fig.5.3C**). Serine is a major amino acid of a natural moisturizing factor, which helps in the water retention of skin (Aramwit and Sangcakul, 2007). Constitution of 30% serine in the amino acid sequence of SS might have led to the moisture absorption and retained 65% of moisture after placing them in the dehydrating chamber (**Fig.5.4B**).

Human dermal fibroblasts are frequently exposed to UV radiation that caused the redox imbalance in it that leads to the activation of MMP-1 and MMP-3 as well as dysregulation of collagen production (Angel et al., 2001; Kondo, 2000). We tried to focus the protective effect of SS post UV irradiation in order to understand its recovery effect in the damaged skin. UVA and UVB irradiated HDF cells post-treated with AAS (10 µg/mL) or PRS (100 µg/mL) showed significant enhancement in the total collagen content than only UV irradiated cells. BMS (100 µg/mL) post-treatment significantly enhanced total collagen content in UVA-irradiated cells, whereas, total collagen content of BMS post-treated UVB irradiated HDF was similar with collagen content SS untreated cells. BMS post-treatment might not able to protect against UVB radiation-induced collagen degradation. We further selected SS varieties that enhanced collagen production in both UVA and UVB irradiated HDF cells and studied their protective effect against UV irradiation.

Chronic exposure of skin to UV radiations elevates the intracellular ROS levels, which reacts with proteins and lipids and produces protein hydroperoxide, lipid hydroperoxide, and damage cellular membranes (Halliwell, 2007; Reguera et al., 2015). They also damage other structures containing proteins and lipids as well as DNA (Reguera et al., 2015). Elevated levels of ROS triggers the upregulation of NF-κB, which induce the secretion of pro-inflammatory cytokines. The pro-inflammatory cytokines act through the receptors and activate AP-1 and NF-κB, which results in the upregulation of collagenase and gelatinase expression. Upregulated collagenase and gelatinase degrades collagen bundles into small oligopeptides and causes loss of structural integrity of the skin (Angel et al., 2001; Kondo, 2000). SS, a potential antioxidant absorbs UV radiations, scavenge the elevated levels of ROS and protects the fibroin and pupa against UV radiation-induced oxidative damage (Kaur et al., 2013). SS pretreatment absorbed the UV radiations and scavenged the elevated levels of ROS that protected the skin of SKH-1 hairless mice against UV radiation-induced oxidative damage by preventing the oxidation of glutathione (a tripeptide, antioxidant) and lipids and DNA damage (Kumar et al., 2018). SS post-treatment reduced the oxidative stress-induced by UVA or UVB radiations by reducing the elevated levels of ROS (**Fig.5.10 I**). Reduction of ROS by AAS or PRS post-treatment downregulated the expression of IL-6 (**Fig.5.8 I and IIA**) and TNF-α (except PRS post-treated UVA-irradiated HDF cells) genes (**Fig.5.8 I and IIB**). ROS generated during UV irradiation reacts with proteins and lipids and forms protein hydroperoxides and lipid hydroperoxides (Halliwell, 2007; Reguera et al., 2015). PRS or Vit. C post-treatment might not able to scavenge the initially formed ROS and their effect on the protein, lipids and signaling pathway due to that there was upregulation of TNF-α expression in UVA-irradiated HDF cells. Whereas, AAS post-treatment might have reduced the initially formed ROS species and break oxidative chain initiated in the biomacromolecules. Downregulation of pro-inflammatory cytokines might have caused low MMP-1 gene expression in UVA (**Fig.5.8 IE**) or UVB (**Fig.5.8 IIE**) irradiated cells. Downregulation of MMP-1 by AAS (10 µg/mL) or PRS (100 µg/mL) post-treatment might have prevented the degradation of collagen produced by HDF cells (**Fig.5.7**).

Col1α1 and Col1α2 are the precursors of the type-1 collagen, which is a primary structural protein of skin ECM (Hashem et al., 2008). Alteration in the synthesis of procollagen changes the collagen homeostasis. UV irradiation downregulates the expression of procollagen as well as alters the collagen homeostasis (Quan et al., 2010). AAS or PRS post-treatment significantly enhanced the expression of Col1α1 in UVA

and UVB irradiated HDF cells (**Fig.5.8 I and IIC**). Reduction of the elevated levels of ROS by AAS or PRS post-treatment might have reduced the oxidative stress in HDF cells, which lead to the upregulation of Col1α1 expression in comparison to SS untreated cells. AP-1 binding sites mediate the upregulation of Col1α2 gene by TGF-β and TNF-α (Chung et al., 1996). TNF-α upregulated by UV irradiation might have enhanced the expression of Col1α2 gene (**Fig.5.8 I and IID**).

Oxidative stress induced by UV radiations upregulates the pro-inflammatory cytokines in epidermal keratinocytes, which triggers the activation of AP-1 and NF-κB and induces the secretion of gelatinase (Pittayapruek et al., 2016). Gelatinases released by epidermal keratinocytes to degrade the partially degraded collagen and enhances skin aging. AAS or PRS post-treatment reduced elevated levels of ROS in UVA and UVB irradiated HaCaT cells (**Fig.5.10 II**). Reduction of ROS by AAS or PRS post-treatment might have downregulated the expression of pro-inflammatory cytokines in HaCaT cells, which reduced the release of MMP-2 (except PRS post-treated UVA-irradiated HaCaT cells) and MMP-9 (**Fig.5.11 I and II**). PRS post-treatment might not able neutralize primary ROS produced during UVA irradiation due to that there was no significant difference was observed in the release of MMP-2 protein in PRS post-treated and only UVA1 irradiated cells.

Prolonged exposure of skin to UV radiation-induced the upregulation of dermal fibroblast elastase (MMPs possessing elastase activity) and neutrophil elastase, which degrades elastic fiber and results in wrinkling of the skin (Tsuji et al., 2001). Supplementation of exogenous antioxidants maintains the redox balance that regulates the expression of dermal fibroblast elastase and neutrophil elastase (Silva et al., 2017). Incubation of UV irradiated HDF cells with AAS and PRS downregulate the expression of fibroblast elastase (**Fig.5.9**). Maintenance of redox balance by scavenging the elevated levels of ROS (**Fig.5.10 I**) as well as metal chelating (hydroxyl groups of serine and threonine chelates the metal ions; copper and iron) nature of SS might have downregulated the release of fibroblast elastase (Metallo elastase) (Kato et al., 1998).

5.5. Significant Findings

The salient findings of this chapter are as follows:

1. AAS significantly inhibited the elastase and hyaluronidase activity.

2. AAS or PRS post-treatment enhanced the collagen production in UV irradiated HDF cells by reducing the elevated levels of ROS, downregulating MMP-1 and upregulating pro-collagen gene expression.
3. AAS or PRS post-treatment downregulated the production and release of elastase activity possessing MMPs by HDF cells.
4. AAS post-treatment downregulated MMP-2 and MMP-9 protein expression and release into the surrounding environment in UV irradiated HaCaT cells.

This chapter provided a platform to understand the effect of SS on the activity of collagenase, elastase, and hyaluronidase along with UVR-induced collagen and elastin degradation by upregulating MMPs expression. In this chapter, AAS inhibited the elastase and hyaluronidase activity. PRS or AAS post-treatment reduced collagen and elastin degradation by downregulating expression of MMPs in UVR-irradiated cells. Redox imbalance induced in melanocytes by UVRs triggers the upregulation of tyrosinase activity that leads to the biosynthesis and accumulation of melanin in the skin. Therefore, in the next chapter, we have explored the anti-tyrosinase activity of SS and its protective effect against UVR-induced hyperpigmentation.

Chapter 6

Exploring the Inhibitory Effect of Silk Sericin on Tyrosinase and UV Radiation-Induced Hyperpigmentation

This chapter illustrates the shielding effect of silk sericin against UV radiation-induced hyperpigmentation. Anti-tyrosinase activity of SS and its protective effect against UV radiation-induced melanogenesis are investigated in detail.

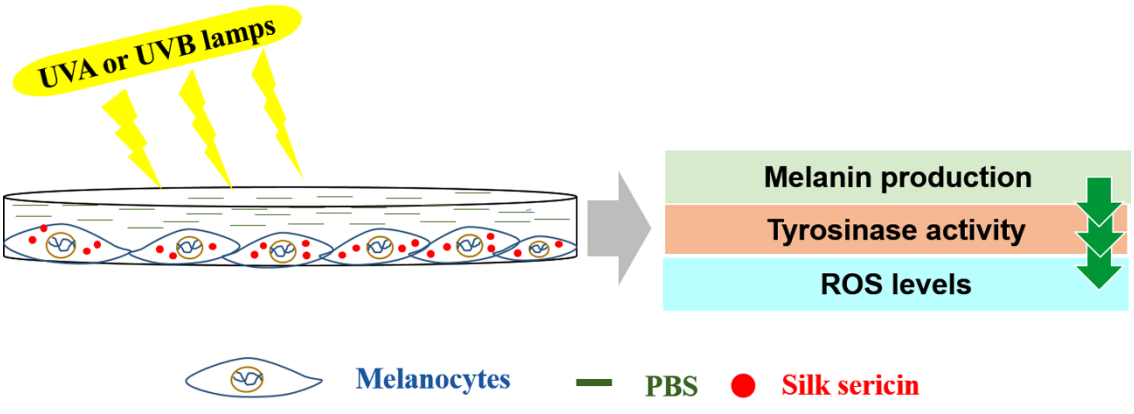

ABSTRACT

Ultraviolet (UV) radiation-induced redox imbalance in melanocytes triggers activation of tyrosinase that results in hyperpigmentation and its related skin disorders. Supplementation of biological reductants or anti-tyrosinase compounds inhibits such hyperpigmentation. Silk sericin (SS), a globular protein is known to possess antioxidant and anti-tyrosinase activity along with other biological attributes. However, its protective effect against UV radiation-induced hyperpigmentation is yet to be explored. In the current study, we have scientifically explored the protective effect of SS against UVA and UVB radiation-induced hyperpigmentation. Anti-tyrosinase activity of SS assessed using mushroom tyrosinase showed that *Philosamia ricini* sericin (PRS) and *Antheraea assamensis* sericin (AAS) inhibited 50% of its activity. Protective effect of SS against UVA and UVB radiation-induced hyperpigmentation was assessed by measuring the cellular melanin, intracellular tyrosinase activity and reactive oxygen species (ROS) levels in mouse melanoma. SS pretreatment significantly reduced cellular melanin and ROS production in UV irradiated melanocytes than SS untreated cells. AAS treatment prior to UVA and UVB irradiation significantly inhibited tyrosinase activity. Altogether, our results validate that AAS efficiently inhibited UVA and UVB radiation-induced hyperpigmentation and it could be used as a potent antioxidant molecule in skin care cosmeceutics.

6.1. Introduction

Melanin is a pigment of skin produced by the melanocytes present in the stratum basale of the epidermis (Lin and Fisher, 2007). It is a defensive pigment, whose production is upregulated to shield the skin against ultraviolet (UV) radiation-induced DNA damage (Mohania et al., 2017). Excessive synthesis and accumulation of melanin lead to various skin diseases such as freckles, leukoplakia, post-inflammatory melanoderma, melasma, solar lentigo, and moles (Briganti et al., 2003; Cullen, 1998; Han et al., 2015; Urabe, 1998). In melanin synthesis, L-tyrosinase a copper-dependent enzyme plays a vital role by catalyzing the hydroxylation of L-tyrosine to 3, 4-dihydroxyphenylalanine (L-DOPA) and further oxidize L-DOPA to o-dopaquinone (precursor of melanin) (Parvez et al., 2006). These two steps are rate-limiting steps of melanin synthesis pathway (Parvez et al., 2006).

Total solar UV radiations reaching the earth's surface, induce skin damage by elevating the production of reactive oxygen species (ROS) and forming DNA photoproducts (Lee et al., 2012; Liu et al., 1994; Tyrrell, 1996). These changes lead to immunosuppression, inflammation, skin cancer (melanoma or non-melanoma), and photoaging (Gil and Kim, 2000; Rittié and Fisher, 2002). On the other hand, melanin is a defensive pigment, which absorbs, distributes and reduces the penetration of UV radiations and prevents DNA damage (Gloster and Neal, 2006; Venza et al., 2015). Redox imbalance induced by UV radiation overwhelms intracellular antioxidants and promotes melanogenesis by upregulating the expression of tyrosinase, tyrosinase-related protein-1 (TRP-1), and TRP-2 (Alam et al., 2017; Cho et al., 2009). Hence, maintaining the ROS at basal levels prevent melanin biosynthesis. Thus, scientists have developed biological reductants (ROS scavengers) and tyrosinase inhibitors such as arbutin, sulfite, and kojic acid to reduce hyperpigmentation induced skin damage (Alam et al., 2017; Garcia-Gavin et al., 2010; Jones et al., 2002). However, whitening agents based on tyrosinase inhibitory activity causes severe side effects including poor water solubility and cellular toxicity (Alam et al., 2017; Garcia-Gavin et al., 2010; Jones et al., 2002). Therefore, assessing the anti-melanogenesis activity of natural materials could develop safe and effective depigmenting agents in cosmetic research.

Silk sericin (SS) is a water-soluble globular protein produced by the Lepidoptera insects belonging to Bombycidae and Saturniidae families (Dash et al., 2007). SS constitutes about 20-30% dry weight of cocoon, which plays a vital role in cocoon formation and also protects the fibroin and pupa from UV radiation-induced damage

(Kaur et al., 2013). SS extracted from the cocoons is recognized to own antioxidant activity along with other properties like suppression of bacterial and tumor growth, lipid peroxidation, elastase activity and protecting the skin against UVA and UVB radiation-induced oxidative damage (Chlapanidas et al., 2013; Dash et al., 2008; Kaur et al., 2014; Kumar et al., 2018; Kumar and Mandal, 2017, 2019). SS extracted from different strains of *Bombyx mori* cocoons have been reported to suppress mushroom tyrosinase activity (Aramwit et al., 2010a; Chlapanidas et al., 2013). These properties of SS vary based on their source and extraction methods. Hence, there is a need to assess the anti-tyrosinase activity of underexploited SS extracted from the different silk varieties (especially the non-mulberry SS) as well as to evaluate their protective effect against UVA and UVB radiation-induced hyperpigmentation.

Here, we have systematically explored the anti-melanogenesis activity of PRS, AAS, and BMS. First, the anti-tyrosinase activity of the SS extracted from these three silk varieties was assessed using mushroom tyrosinase. Further, AAS and PRS that showed anti-tyrosinase activity were selected to interpret the protective effect of SS against UVA and UVB radiation-induced hyperpigmentation. We pretreated mouse melanoma (B16F10) cells with SS and irradiated with different dosages of UVA and UVB radiations and evaluated the anti-melanogenesis activity of SS by determining the total melanin content, intracellular tyrosinase activity, and intracellular ROS generation.

6.2. Materials and Methods

6.2.1. Materials

Fetal bovine serum (FBS) and high glucose Dulbecco's modified Eagle's medium (DMEM) and were sourced from Gibco, ThermoFisher Scientific, USA. Sodium carbonate was sourced from SRL, India. MTT, mushroom tyrosinase, Triton X-100, L-DOPA, dichloro-dihydro-fluorescein diacetate (DCFH-DA), and Bradford's reagent were acquired from Sigma, USA. Trypsin-EDTA, 100X antibiotic-antimycotic solution, and kojic acid (KA) were procured from HiMedia, India. Sodium hydroxide and Dimethyl sulfoxide (DMSO) were obtained from Merck, India.

6.2.2. Isolation of silk sericin

Sericin was isolated from the cocoons of non-mulberry (AA and PR) and mulberry (BM) silk varieties using our established protocol (Kumar and Mandal, 2017). Cocoon pieces were cooked in 0.5 M Na_2CO_3 and the obtained protein solution was

dialyzed against double distilled water (dd. H_2O) for 48 h. Post-dialysis, the protein solution was lyophilized and conserved SS at -20 °C.

6.2.3. Determination of the anti-tyrosinase activity of silk sericin

The anti-tyrosinase activity of SS was determined using the modified protocol of Han *et al.* (2015). In brief, the enzyme solution was prepared by dissolving 100 U of mushroom tyrosinase in 1 mL of 20 mM phosphate buffer (pH 6.8) and 1.25 mM of L-DOPA was prepared in dd. H_2O. 40 µL of the enzyme was incubated with 20 µL of different concentration (0, 2, 4, 6, 8, and 10 mg/mL) of SS for 10 min. The reaction mixture was incubated with 20 µL of L-DOPA for 10 min and absorbance was recorded at 475 nm with a multiplate reader (Tecan, Infinite M200 PRO). Kojic acid (KA) was used as positive control. Anti-tyrosinase activity was measured using the following equation:

$$\text{Antityrosinase activity (\%)} = \left(\frac{\text{Test sample}}{\text{Control}}\right) \times 100 \quad (6.1)$$

6.2.4. *In vitro* biological studies

6.2.4.1. Cell culture

Mouse melanoma (B16F10) cell line was obtained from National Centre for Cell Science, Pune, India. B16F10 cells were cultured and maintained in high glucose DMEM added with 1X antibiotic-antimycotic solution and 10% FBS.

6.2.4.2. Cytocompatibility study

Cytocompatibility of the AAS and PRS was evaluated with the MTT assay. B16F10 cells were cultured in 96 well plates for 12 h at 37 °C and treated with 10 and 100 µg/mL of SS. Post 24 h of treatment, cells were incubated with MTT for 4 h at 37 °C. Post 4 h of incubation, formazan was solubilized in DMSO and the optical density was documented at 570 nm using the multiplate reader.

6.2.4.3. UV irradiation system

Before UV irradiation, cells were rinsed and covered with a thin layer of phosphate buffer saline (PBS) followed by UVA or UVB irradiation using UVA and UVB cross-linker (UVP, CL-1000L, UK) that consist of 5×8 W lamps with a maximum emission peak at 365 nm and 302 nm, respectively.

6.2.4.4. Cytotoxicity study

The cytotoxic effect of UVA and UVB radiation against B16F10 cells was evaluated with the MTT assay. B16F10 cells were seeded and cultured in 24 well plates

until they reached 80% confluency and irradiated with UVA (8 and 16 J/cm^2) and UVB (30, 60 and 120 mJ/cm^2). After 0, 1, 4, and 24 h of irradiation, MTT assay was performed.

6.2.4.5. Estimation of total melanin content

Total melanin content produced by melanocytes after UV irradiation was assessed using the modified protocol of Han *et al*. (2015). B16F10 cells were cultured in 24 well plates until they reached 80% confluence and irradiated with UVA (8 and 16 J/cm^2) and UVB (30, 60 and 120 mJ/cm^2) radiations. Cells were collected after for 0, 1, 4 and 24 h of irradiation and the cell pellets were solubilized in 9:1 ratio of 1 N NaOH and 10% DMSO for 1 h at 60 °C to dissolve melanin. 200 µL of cell lysates were placed in 96 well plates and absorbance was recorded at 415 nm using a multiplate reader. % of melanin produced by UV irradiated cells was estimated using the following equation:

$$\text{Cellular melanin (\%)} = \left(\frac{\text{Test sample}}{\text{Control}}\right) \times 100 \qquad (6.2)$$

6.2.4.6. Determination of melanin inhibitory activity of silk sericin

B16F10 cells were cultured in 6 well plates until they reached 60% and treated with 10 and 100 µg/mL of AAS, PRS, and KA for 24 h and irradiated with UVA (16 J/cm^2) and UVB (120 mJ/cm^2) radiations. Cells were trypsinized after 1 h of irradiation and the cell pellets were solubilized in 9:1 ratio of 1 N NaOH and 10% DMSO for 1 h at 60 °C. Post 1 h, 200 µL of cell lysates were placed in 96 well plates and optical density was measured at 415 nm using multiplate reader and % of melanin produced by UV irradiated cells were calculated.

6.2.4.7. Determination of intracellular tyrosinase activity

Intracellular tyrosinase activity was assessed using the protocol of Pan *et al*. (2012). In brief, B16F10 cells were cultured in 6 well plates until they reached 60% and treated with 10 and 100 µg/mL of AAS, PRS, and KA for 24 h. Cells were irradiated with UVA (8 J/cm^2) and UVB (120 mJ/cm^2) radiations and incubated for 1 h followed by three PBS washes and lysed in 1% Triton X-100 and centrifuged. The aliquots of the supernatant were used to measure the protein concentration using the Bradford assay. 20 µL of 5 mM L-DOPA was incubated with an equal protein concentration of samples for 45 min at 37 °C. Post incubation, absorbance was recorded at 475 nm using multiplate reader and % of melanin produced by intracellular tyrosinase was calculated.

6.2.4.8. Determination of antioxidant activity of silk sericin

ROS reducing activity of SS in UVA (8 J/cm^2) and UVB (120 mJ/cm^2) irradiated B16F10 cells were assessed using our established protocol (Kumar and Mandal, 2017). B16F10 cells were seeded in 96 well plates, cultured to 60% confluence and incubated with 10 and 100 µg/mL of SS or KA for 24 h. After incubation, cells were irradiated with UVA and UVB radiations followed the addition of media complemented with 10 µM of DCFH-DA and incubated for 30 min. Post incubation, cells were washed with PBS and covered with PBS and fluorescence intensity was recorded with multiplate reader at an excitation 488 nm and emission 525 nm.

6.3. Results

6.3.1. Anti-tyrosinase activity of silk sericin

Tyrosinase involves in the rate-limiting step of melanin synthesis. It catalyzes the hydroxylation of L-tyrosine to L-DOPA and further oxidizes L-DOPA to o-dopaquinone (precursor of melanin) (Parvez et al., 2006). Inhibition of L-tyrosinase activity plays a critical role in preventing melanin biosynthesis. Anti-tyrosinase activity of SS was assessed using mushroom tyrosinase. In comparison with control, incubation of mushroom tyrosinase with BMS significantly enhanced conversion of L-DOPA to o-dopaquinone, whereas, AAS and PRS inhibited the tyrosinase activity (**Fig.6.1**). 6 mg/mL of AAS and 10 mg/mL of PRS showed 50% inhibition of tyrosinase activity. We were looking for the SS variety that could possess anti-tyrosinase activity as well as inhibit UVA and UVB radiation-induced hyperpigmentation. Therefore, we have selected AAS and PRS to further study the anti-melanogenesis activity.

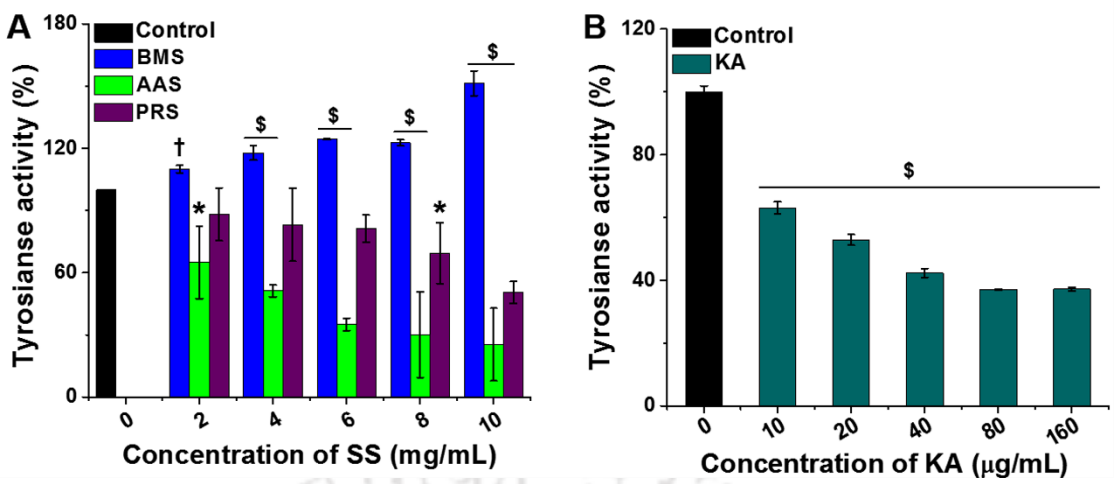

Fig.6.1. *The anti-tyrosinase of silk sericin was assessed by measuring the conversion of L-DOPA to o-dopaquinone by mushroom tyrosinase. Where mushroom tyrosinase incubated with (A) silk sericin and (B) kojic acid. ($p≤0.001 and *p≤0.01 compared with control)*

6.3.2. Cytocompatibility of silk sericin

Mitochondrial dehydrogenase of viable cells converts the water-soluble MTT to water-insoluble formazan. The viability of cells was determined by measuring the % of formazan formation. Cytocompatibility of SS was assessed by measuring the viability of cells by the MTT assay. **Fig.6.2** shows the % of the viability of B16F10 cells post incubating with SS. The viability of B16F10 cells significantly enhanced after incubating with 10 µg/mL (PRS) and 100 µg/mL (AAS and PRS) of SS than control.

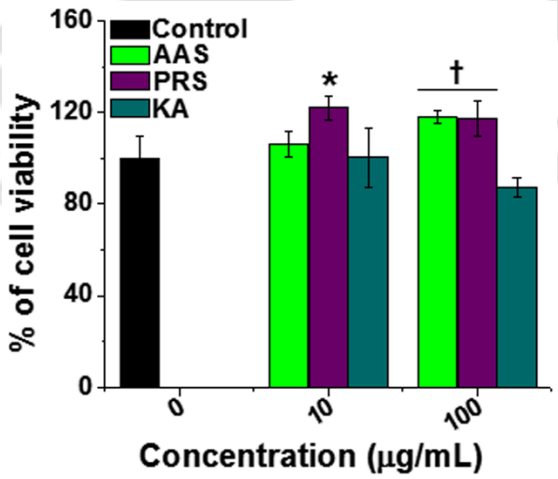

Fig.6.2. *The effect of silk sericin or kojic acid on the viability of B16F10 cells was evaluated with the MTT assay. (*p≤0.01 and †p≤0.05 compared with control cells)*

6.3.3. Cytotoxicity study

Oxidative stress induced in melanocytes by UV irradiation disrupts their cellular homeostasis, which leads to malignant transformation or compromises with viability (Denat et al., 2014). The cytotoxic effect of UV radiation against the viability of B16F10 cells was assessed using the MTT assay. In comparison with the viability of B16F10 cells after 0 h of UVA or UVB irradiation, the viability of UVA (8 J/cm^2) and UVB (30 mJ/cm^2) irradiated cells significantly enhanced after 24 h of incubation (**Fig.6.3**).

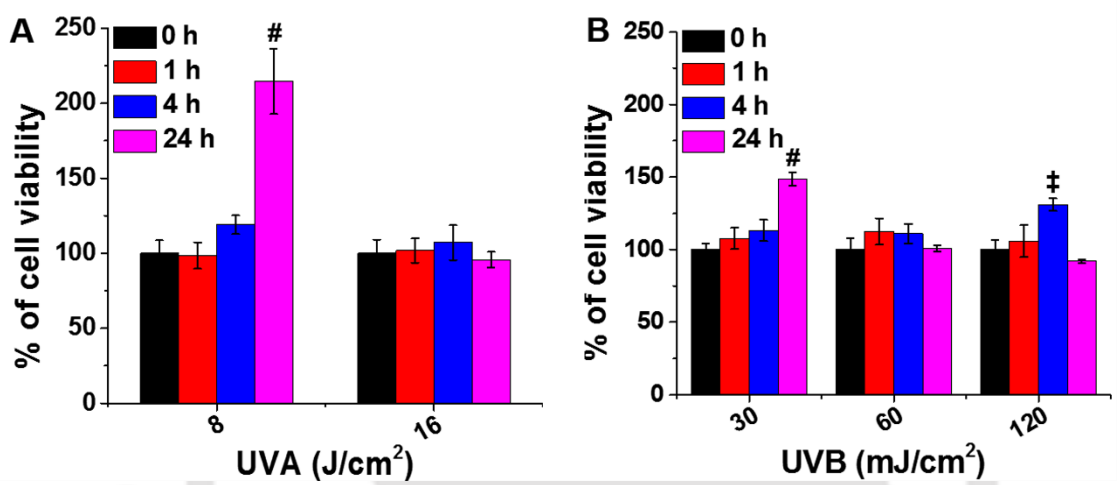

Fig.6.3. *The effect of (A) UVA and (B) UVB on the viability of B16F10 cells was evaluated using the MTT assay. (#p≤0.001 and ‡p≤0.05 compared to UV irradiated cells after 0 h)*

6.3.4. Total melanin content

Human and other animals produce melanin to protect the skin against UV radiation-induced damage (Yamaguchi et al., 2006). Melanin produced by B16F10 cells post UVA and UVB irradiation was assessed by measuring the total melanin produced by the melanocytes. **Fig.6.4 I** portray the % of melanin produced by B16F10 cells after UV irradiation, respectively. In comparison with B16F10 cells after 0 h of UV irradiation, B16F10 cells showed significantly high % of melanin content after 1 and 4 h of 8 and 16 J/cm^2 of UVA irradiation, however, melanin content was decreased after 24 h of UVA (8 J/cm^2) irradiation. Melanin content was significantly enhanced after 1 h (60 and 120 mJ/cm^2) and 4 h (30, 60, and 120 mJ/cm^2) of UVB irradiation than B16F10 cells after 0 h of UVB irradiation, while melanin amount was declined with time (24 h).

16 J/cm^2 of UVA and 120 mJ/cm^2 of UVB irradiation dosages were selected to evaluate the anti-melanogenesis activity of SS. However, 8 J/cm^2 of UVA radiations was selected to assess the intracellular tyrosinase activity and ROS levels.

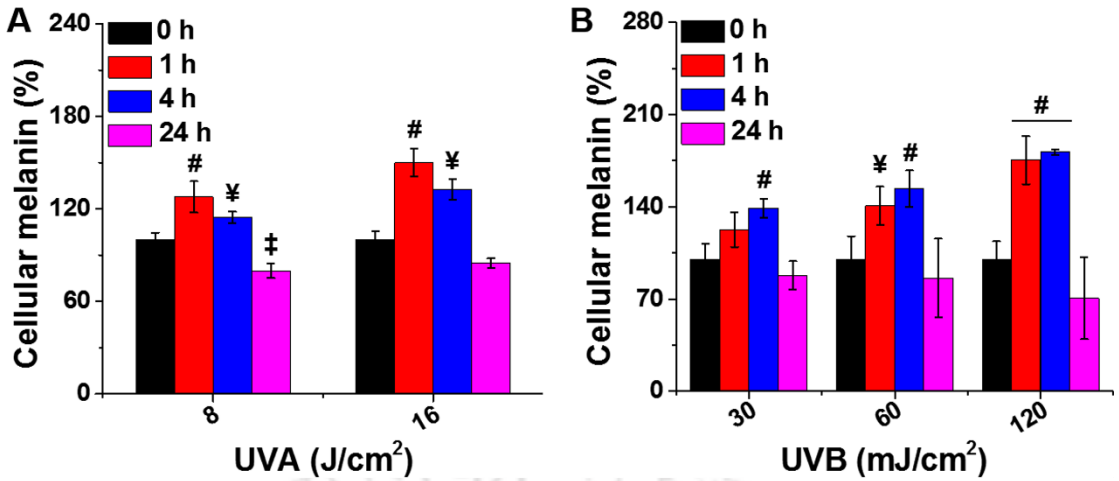

Fig.6.4. *The effect of (A) UVA and (B) UVB radiation on the production of melanin by B16F10 cells was assessed using 9:1 ratio of 1 N NaOH and 10% DMSO. (#p≤0.001, ¥p≤0.01, and ‡p≤0.05 compared to UV irradiated cells after 0 h)*

6.3.5. Anti-melanogenesis activity of silk sericin

ROS generated by UV irradiation stimulates the production of melanin by melanocytes (Alam et al., 2017; Lin and Fisher, 2007). However, supplementation of exogenous antioxidants scavenge the elevated levels of ROS and results in the downregulation of melanin production (Kim et al., 2008). Anti-melanogenesis activity of SS was assessed by determining the melanin produced by UV irradiated cells. **Fig.6.5** depicts the % of melanin produced by SS or KA pretreated cells after UVA (16 J/cm^2) and UVB (120 mJ/cm^2) irradiation. In comparison with control cells, UVA and UVB irradiation significantly enhanced melanin production in B16F10 cells, however, SS pretreatment significantly inhibited UV radiation-induced melanin production.

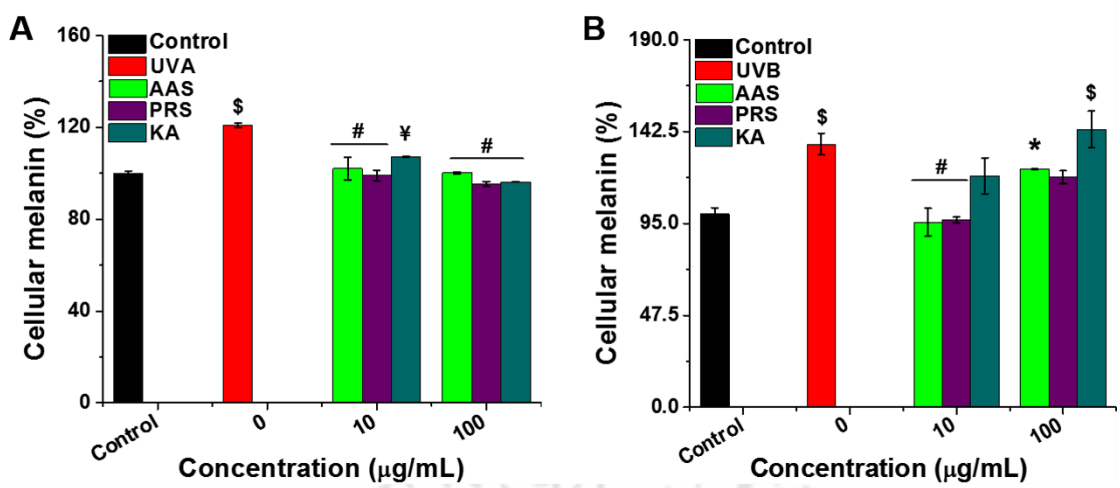

Fig.6.5. *Total melanin content produced by silk sericin or kojic acid pretreated B16F10 cells after (A) UVA and (B) UVB irradiation was assessed using 9:1 ratio of 1 N NaOH and 10% DMSO. ($p≤0.001 and *p≤0.01 compared with control cells; #p≤0.001 and ¥p≤0.01 compared with only UV irradiated cells)*

6.3.6. Determination of intracellular tyrosinase activity

ROS and reactive nitrogen species (RNS) generated by UV irradiation induce melanin production by upregulating intracellular tyrosinase at gene and protein levels in melanocytes (Dong et al., 2010). The effect of SS on the intracellular tyrosinase activity was determined by treating the cell lysate with L-DOPA. **Fig.6.6** illustrates the conversion of L-DOPA to o-dopaquinone after incubation with cell lysate. UVA and UVB irradiation significantly enhanced the intracellular tyrosinase activity in B16F10 cells than control cells. Cells treated with AAS and KA (10 µg/mL) before UVA and UVB irradiation significantly reduced tyrosinase activity than only UV irradiated cells. Whereas, PRS significantly inhibited intracellular tyrosinase activity in UVB irradiated B1610 cells.

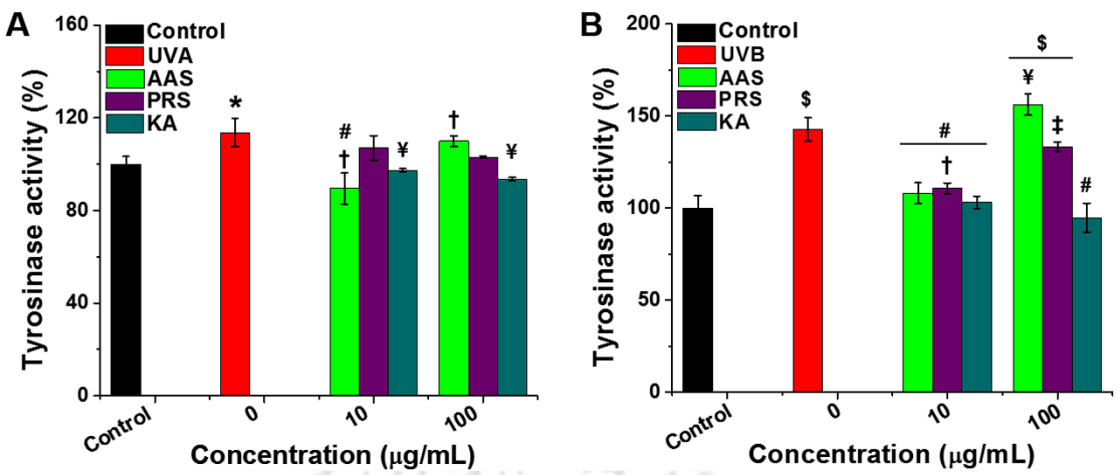

Fig.6.6. *Intracellular tyrosinase activity of silk sericin or kojic acid pretreated B16F10 cells after (A) UVA and (B) UVB irradiation was determined by measuring the o-dopaquinone formation. ($p≤0.001, *p≤0.01, and †p≤0.05 compared with control cells; #p≤0.001, ¥p≤0.01, and ‡ p≤0.05 compared with only UV irradiated cells)*

6.3.7. Determination of antioxidant activity of silk sericin

ROS elevated in melanocytes by UV irradiation triggers the melanin biosynthesis (Alam et al., 2017; Lin and Fisher, 2007). Antioxidants protect the cells from UV radiation-induced oxidative damage and downregulate the melanin production by reducing the elevated levels of ROS (Kim et al., 2008). Intracellular ROS reducing ability of SS was assessed using DCFH-DA. In comparison with control cells, UVA and UVB irradiation significantly elevated ROS levels in B16F10 cells. AAS and KA pretreatment significantly reduced the ROS levels in both UVA and UVB irradiated B16F10 cells, whereas PRS treatment reduced ROS levels in UVB irradiated cells **Fig.6.7**.

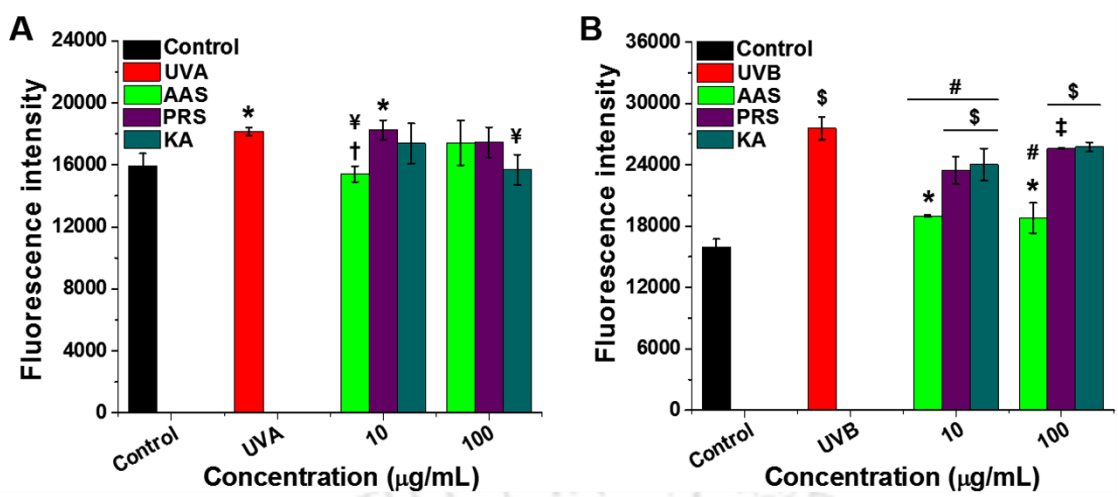

Fig.6.7. *The effect of silk sericin or kojic acid pretreatment on the intracellular ROS levels of B16F10 cells after (A) UVA and (B) UVB irradiation was evaluated using DCFH-DA. ($p≤0.001, *p≤0.01, and †p≤0.05 compared with control cells; #p≤0.001, ¥p≤0.01, and ‡ p≤0.05 compared with only UV irradiated cells)*

6.4. Discussion

ROS are by-products of aerobic metabolism act as secondary messengers in various signaling pathways (Glasauer and Chandel, 2014). However, excessive production of ROS leads to different pathological conditions; inflammation, aging, and cancer (Alfadda and Sallam, 2012; Davalli et al., 2016). Epidermal melanocytes of skin are highly vulnerable to ROS species. Excessive production of ROS overwhelms the endogenous antioxidants activity and stimulates melanin biosynthesis by triggering the upregulation of tyrosinase mRNA and protein expression (Denat et al., 2014). Overproduction of melanin leads to various skin disorders including melanoma skin cancer (Briganti et al., 2003; Cullen, 1998; Han et al., 2015; Urabe, 1998). Topical delivery of antioxidants or anti-tyrosinase compounds downregulates the melanin biosynthesis by scavenging such elevated levels of ROS or by inhibiting the tyrosinase activity (Alam et al., 2017; Garcia-Gavin et al., 2010; Jones et al., 2002). However, most of the anti-tyrosinase molecules (arbutin, hydroquinone, kojic acid, and corticosteroids) leads to adverse effects including cellular cytotoxicity along contact dermatitis, skin irritation, and poor enzyme inhibition (Alam et al., 2017; de Freitas et al., 2016; Garcia-Gavin et al., 2010; Jones et al., 2002). Therefore, there is a need to identify natural compounds which could be water soluble and possess antioxidant activity along with the anti-tyrosinase activity.

Silk sericin (SS), a globular protein produced by the silkworms is known to own free radical/reactive species (RS) reducing ability and anti-tyrosinase activity with other biological applications (Chlapanidas et al., 2013; Kumar and Mandal, 2017). These characteristics of SS depends on its electron donating and metal chelating groups of amino acid as well as polyphenols and flavonoids obtained during their isolation (Kumar and Mandal, 2017). The amino acid composition of SS and associated secondary metabolites varies based on the silk varieties, their food habitat and the peptides lengths produced respectively (Aramwit et al., 2010a; Kumar and Mandal, 2017). The anti-tyrosinase activity of SS extracted from the different strains of *Bombyx mori* has been studied. However, the anti-tyrosinase activity of different silk varieties (mulberry and non-mulberry) and their protective role against UV radiation-induced hyperpigmentation are yet to be investigated. In the present study, we explored the anti-tyrosinase activity and the protective role of SS isolated from the cocoons of *Philosamia ricini* (PR), *B. mori* (BM), and *Antheraea assamensis* (AA) against UVA and UVB radiation-induced hyperpigmentation. Further, skin care preparation was formulated using SS and their rheological properties were assessed.

Tyrosinases plays an important role in melanin synthesis by catalyzing the conversion of tyrosine to DOPA and further DOPA to o-dopaquinone (Parvez et al., 2006). It is a rate-limiting enzyme of melanin synthesis (Parvez et al., 2006). Inhibiting tyrosinase activity prevents the melanin biosynthesis. Secondary metabolites like polyphenols and flavonoids inhibit the enzyme activity by reducing the free radicals produced at the catalytic site of the enzyme or interacting with the co-factor of the tyrosinase (Kubo and Kinst-Hori, 1999; Xie et al., 2003). Amino acids like cysteine inhibit melanin biosynthesis by interacting with quinine (Dudley and Hotchkiss, 1989), whereas, arginine or valine containing peptides inhibits tyrosinase activity (Schurink et al., 2007). Anti-tyrosinase activity of AA sericin (AAS), BM sericin (BMS), PR sericin (PRS) evaluated using mushroom tyrosinase showed that AAS and PRS significantly inhibited mushroom tyrosinase activity, whereas, BMS enhanced its activity (**Fig.6.1**). Metal (copper and iron) chelating activity and the free radical reducing ability of amino acids (serine, threonine, aromatic amino acids) of SS and connected secondary metabolites might have inhibited the tyrosinase activity after incubating with AAS or PRS (Kato et al., 1998; Kubo and Kinst-Hori, 1999; Xie et al., 2003). However, the amino acids of BMS and associated metabolites might not able to chelate the co-factor of the enzyme and reduce the free radicals produced during the conversion of L-tyrosine

to L-DOPA. The L-tyrosine amino acid of BMS might have involved in the reaction and enhanced the tyrosinase activity (Aramwit et al., 2010a).

Chronic exposure of skin to UV radiations impairs the endogenous antioxidant defense mechanism and elevates the production of reactive oxygen species (ROS) (de Jager et al., 2017). Elevated levels of ROS species induced redox imbalance in melanocytes that lead to upregulation of tyrosinase, tyrosinase-related protein-1 (TRP-1), and TRP-2 (Alam et al., 2017; Cho et al., 2009). Upregulation of tyrosinase and TRP expression induces the melanin biosynthesis, which leads to the hyperpigmentation. Exposure of mouse melanoma (B16F10) cells to UVA and UVB radiations elevated their intracellular ROS levels (**Fig.6.7**), which leads to the melanin biosynthesis in melanocytes post 1 h of UV irradiation (**Fig.6.4**). Redox imbalance in melanocytes also leads to the cell senescence (Denat et al., 2014). B16F10 cells irradiated with UVA (16 J/cm^2) and UVB (60 and 120 mJ/cm^2) radiations did not show enhancement in their viability, which represents that UV radiation-induced cell death (**Fig.6.3**).

Topical delivery/supplementation of exogenous antioxidants protects the cells against UV radiation-induced oxidative damage by enhancing endogenous antioxidant activity and maintaining the redox balance of the cells (Katiyar, 2003). Maintaining ROS at basal levels prevents the upregulation of tyrosinase activity as well as oxidation of L-tyrosine to DOPA, and DOPA to dopaquinone that ultimately leads downregulation melanin biosynthesis (Denat et al., 2014; Panich, 2011). In comparison with only UV irradiated cells, AAS or PRS pretreated cells showed significantly low cellular melanin content (**Fig. 6.5**) and tyrosinase activity (**Fig.6.6**). AAS or PRS pretreatment reduced the UV radiation-induced ROS and maintained the redox balance of the cells, which downregulated the tyrosinase protein expression that resulted in the inhibition of melanin biosynthesis.

6.5. Significant Findings

The salient findings of this chapter are as follows:

1. AAS and PRS inhibited 50% of mushroom tyrosinase activity treatment.
2. AAS or PRS treatment prior to UV irradiation downregulated the melanin biosynthesis in B16F10 cells by downregulating elevated levels of ROS.
3. AAS pretreatment significantly downregulated tyrosinase expression in both UVA and UVB irradiated cells.

This chapter presents the inhibitory effect of SS on the tyrosinase activity and UVR-induced hyperpigmentation. In this chapter, AAS or PRS inhibited mushroom tyrosinase activity and downregulated melanin biosynthesis by scavenging UVR elevated ROS.

Results of all the five chapters displayed that SS extracted from the cocoons of AA showed potent AO activity along with other biological application as compared to the SS obtained from PR and BM. In the next chapter, we have formulated skin care preparation constituting AAS as a potent antioxidant.

Chapter 7

Formulation and Characterization of Skin Care Preparation Embedded with Silk Sericin

This chapter illustrates the formulation of AAS constituted skin care preparation and its characterization. Skin care preparation formulated using AAS as an ingredient is characterized for its flow properties using rheological studies.

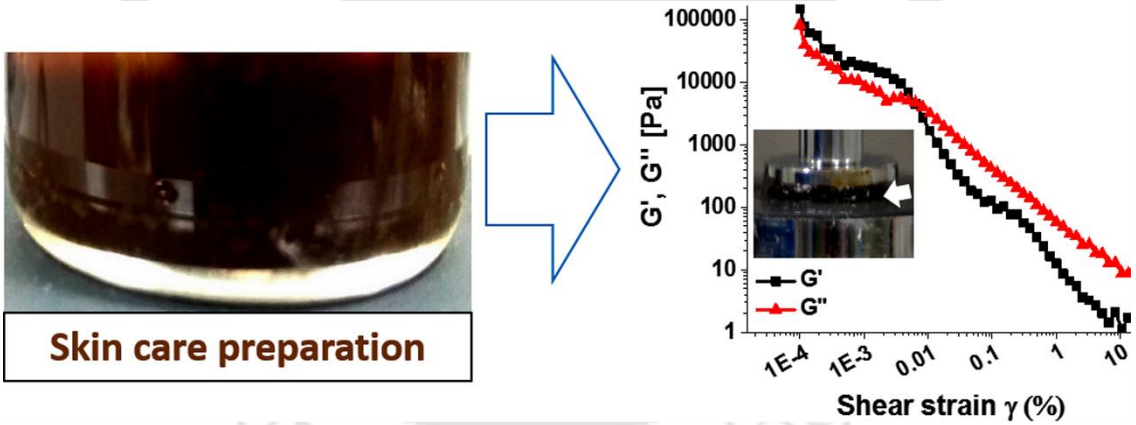

ABSTRACT

Oil-in-water emulsions are used as potential delivery vehicles to deliver low molecular antioxidants into deeper layers of the skin. In the present study, AAS used as an ingredient in the formulation of skin care preparation and characterized. Skin care preparation formulated using AAS was assessed for its rheological properties showed that addition of AAS into the basic skin care preparation reduced its linear viscoelastic range. Whereas, shear thinning and viscoelastic behavior of the preparation did not vary. Thus, our results validate that AAS constituted skin care preparation could be used in skin care cosmeceutics.

7.1. Introduction

The skin covers the entire body and provides physical protection to the underlining tissues and organs from the microbes, pollutants and ultraviolet radiation (UVR) and thermal factors (Costin and Hearing, 2007). However, prolonged exposure of skin to UVR depletes the endogenous defense system (enzymatic and non-enzymatic antioxidants) and enhances the production of reactive species (RS) (Martinez et al., 2017a; Xu et al., 2018). Elevated levels of RS induce redox imbalance in the epidermal and the dermal layers of the skin and causes inflammation, immunosuppression, oxidative damage, erythema, edema, photoaging and skin cancer (Gil and Kim, 2000; Rittié and Fisher, 2002). Therefore, preventing the depletion of the endogenous defense system and reducing the elevated levels of RS is necessary to overcome the UVR-induced skin damage.

Low molecular weight compounds (exogenous antioxidants) produced by the plants reduces the RS by donating their electrons or hydrogen and prevents the depletion of endogenous defense systems (Bosch et al., 2015; Svobodová and Vostálová, 2010). Topical delivery of such exogenous antioxidants showed a reduction in the elevated levels of RS and enhanced the endogenous defensive system. To deliver low molecular weight compounds efficiently into the deeper regions of the skin requires a delivery vehicle. Emulsions are the most suitable types of skin care formulations to deliver low molecular weight compounds into the skin due to their solubilizing capacity of both hydrophilic and lipophilic compounds (Zillich et al., 2015). Emulsions are the heterogeneous systems contains both oil and water phases, where one phase is stabilized by another phase. These systems are stabilized by an emulsifier (Zillich et al., 2015).

Silk sericin (SS) is a glycoprotein produced by the silkworms of Bombycidae and Saturniidae families (Dash et al., 2007). It plays an important role in cocoon formation by holding fibroin together and also protects the fibroin and pupa from UVR-induced oxidative damage (Kaur et al., 2013). SS extracted from the cocoons of *A. assamensis* (AA) showed better antioxidant activity along with other properties; enhancement of endogenous antioxidant activity, inhibition of cancer growth, lipid peroxidation, elastase and hyaluronidase activity than *Philosamaia ricini sericin* (PRS) and *Bombyx mori* sericin (BMS), respectively (Kumar et al., 2018; Kumar and Mandal, 2017, 2019). AA sericin (AAS) also showed a protective effect against UVA and UVB radiation-induced oxidative damage, photoaging, wrinkling, and hyperpigmentation. Topical delivery of such potential antioxidant molecule could be beneficial in protecting the human skin

against UVR-induced damage. Hence, there is a need to formulate AAS constituted skin care preparation and characterized their properties.

Here, we have formulated skin care preparation by embedding AAS in the emulsion and characterized the rheological properties.

7.2. Materials and Methods

7.2.1. Materials

Carnauba wax, paraffin wax and sorbitan monostearate were acquired from Sigma, USA. Cetyl alcohol, stearic acid, glycerin, 1, 2 propanediol, methyl 4-hydroxybenzoate, ethyl 4-hydroxybenzoate, and propylparaben were procured from HiMedia, India.

7.2.2. Formulation of silk sericin embedded preparation

The basic skin care preparation was formulated in the laboratory by addition of 5% (w/w) AAS. The components used for the formulation of skin care preparation are given in **Table 7.1**. Initially, both the aqueous and oil phases were separately heated at 70-80 °C and oil phase was added dropwise to the aqueous phase (Gilbert et al., 2013; Jarzycka et al., 2013). The reaction mixture was continuously stirred until the temperature reaches 30-40 °C, finally, preservatives were added and the reaction mixture was cooled to 20-25 °C. A blank preparation was formulated without AAS.

Table 7.1. *Composition of AAS embedded skin care preparation*

	Ingredients (INCI name)	**Content (%, W/W)**
Oil phase	Cetyl alcohol	6.0
	Carnauba wax	3.0
	Paraffin wax	2.0
	Sorbitan monostearate	2.0
	Almond oil	4.0
	Coconut oil	1.5
Aqueous phase	Glycerin	3.0
	1,2 Propandiol	3.0
	A. assamensis sericin	5.0
	Deionized water	69.5
Preservatives	Methyl paraben	0.18
	Propyl paraben	0.02
	Ethyl paraben	0.15
	2-Phenoxyethanol	0.15
	Stearic acid	0.5

7. 2.3. Rheology studies of the preparation

All the rheological properties of preparation were assessed using Anton Paar rheometer (Model: MCR302). The viscoelastic behavior of the AAS embedded skin care preparation was assessed using amplitude sweep (parallel plate with 25 mm diameter and the gap maintained between the plates was 1 mm). The amplitude sweep carried was out at a frequency of 1 rad/s with strain increasing from 0.01 to 1000%. The Linear Viscoelastic Range (LVER) obtained from the amplitude sweep and used for further

experiments. The time-dependent shear thinning behavior of the formulation was assessed using three interval thixotropy test (3iTT). The 3iTT test was carried out for 20 min by applying resting shear stress, of less than half the strain limit of the LVER, for a period of 120 s and a high shear stress condition for 120 s and then observing the behavior of the gel at rest for the remaining duration. The viscoelastic behavior of formulation was also evaluated using a frequency sweep test. The frequency sweep test was also carried out by applying the less than half the strain of the LVER obtained from the amplitude sweep. All the experiments were carried out at 25 °C.

7.3. Results

7.3.1. Rheology studies of the preparation

AAS has been selected to use as potential antioxidant molecules in the formulation of skin care preparation. 5% of AAS [topical delivery of 5% AAS using glycerol had protected the SKH-1 hairless female mouse against UVB radiation-induced oxidative damage (Kumar et al., 2018)] was used in the formulation and its rheological properties were assessed. The linear viscoelasticity of basic skin care preparation and AAS constituted skin care preparation was assessed using an amplitude sweep test. In comparison with the linear viscoelasticity of basic skin care preparation, AAS constituted skin care preparation showed less viscoelasticity (**Fig. 7.1 I).** The viscoelasticity and shear thinning of the basic skin care preparation and AAS constituted skin care preparation were assessed by applying shear stress selected less than half of the strain limit of the LVER obtained from the amplitude sweep. The viscoelasticity of the basic skin care preparation and AAS constituted skin care preparation using a frequency sweep test showed the preparations were stable with increasing angular frequency (**Fig.7.1 II**). The shear thinning properties of basic skin care preparation and AAS constituted skin care preparation was assessed using 3iTT test showed that the skin care preparation deforms when the shear strain was applied and retained to its form when the shear strain was withdrawn (**Fig.7.1 III).**

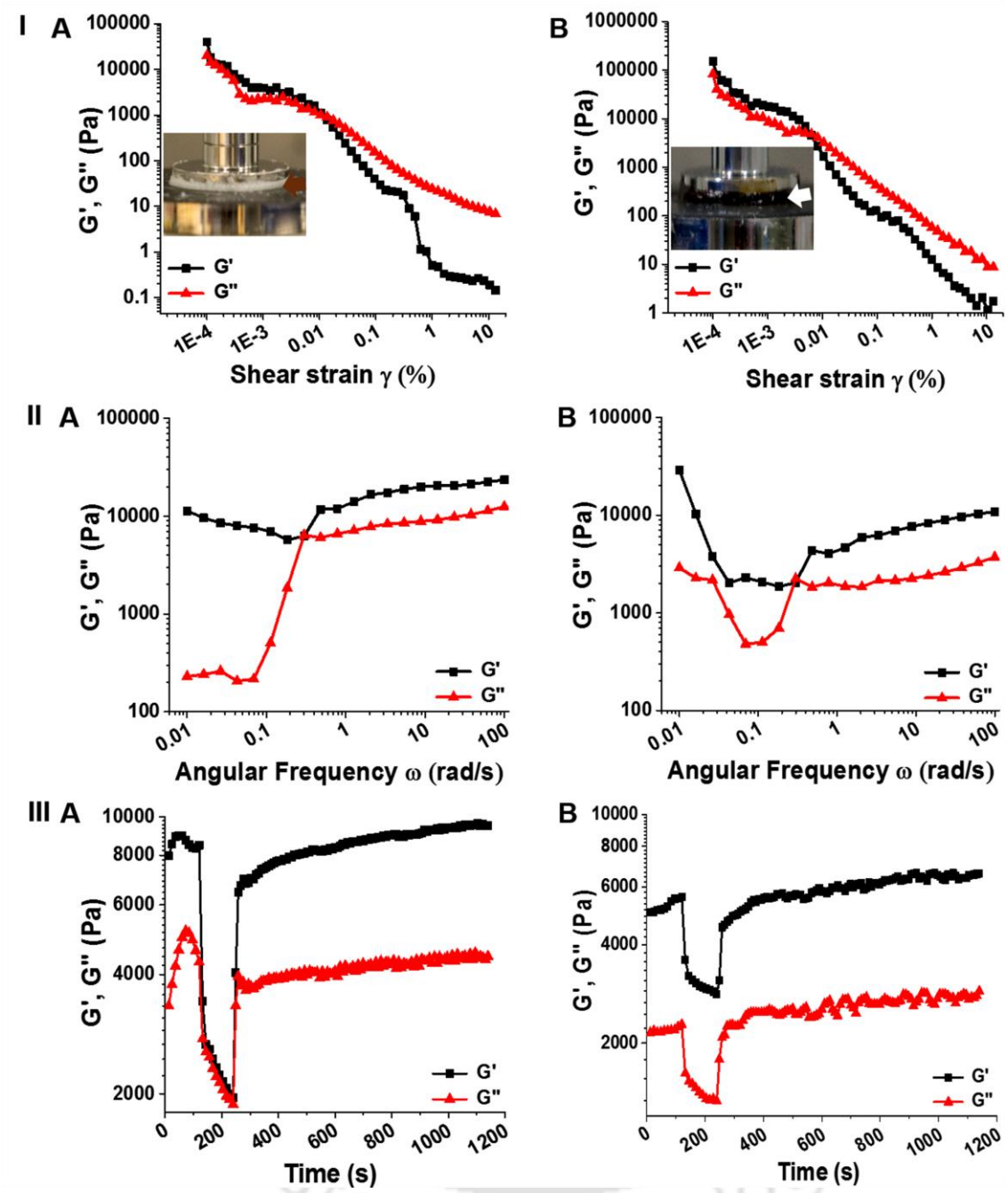

Fig.7.1. *The viscoelastic behavior of (A) basic preparation and (B) A. assamensis sericin constituted preparation was assessed using (I) amplitude sweep and (II) frequency sweep test. (III) Time-dependent shear thinning behavior of (A) basic preparation and (B) A. assamensis sericin constituted preparation was assessed using 3iTT test.*

7.4. Discussion

Emulsions (oil in water) are commonly used as vehicles for the topical delivery of potent antioxidants to protect the skin from pollutants and UVR-induced damage (Chappat, 1994; Gilbert et al., 2013). Rheological properties of the emulsions are very necessary to determine the flow properties of the formulations, which are required to predict their behavior while manufacturing and packaging (Tadros, 2004). In the present study, we have formulated a skin care preparation constituted with AAS and characterized its rheological properties.

AAS constituted skin care preparation showed less linear viscoelastic range than basic preparation. The shear thinning and viscoelastic behavior of the AAS embedded skin care preparation is similar to basic preparation. AAS is a hydrophilic protein polymer. Addition of AAS to skin care preparation might have shown less linear viscoelasticity due to its hydrophilic nature (**Fig.7.1 I**). However, AAS addition did not disturb the gel-like properties of the preparation (**Fig.7.1 II and III**).

7.5. Significant Findings

The salient findings of this chapter are as follows:

1. Addition of AAS as an ingredient during skin care preparation reduced linear viscoelastic range of the basic skin care preparation.
2. Shear thinning and viscoelastic behavior of the preparation did not vary with the addition of AAS in basic skin care preparation.

Based on the results obtained by the rheological studies incorporation of AAS did not change the flow properties of the gel. The prepared AAS containing emulsion could be used to deliver the AAS topically for protecting the skin against pollutants and UVR-induced skin damage.

SUMMARY AND FUTURE PERSPECTIVE

SUMMARY AND FUTURE PERSPECTIVE

The endogenous defensive system protects skin from pollutants and UVR-induced damage. However, chronic exposure of skin to UVRs causes the depletion of the endogenous defensive system and elevates the generation of RS, which leads to various skin disorders. Researchers focused on the topical delivery of exogenous LMWMs to protect the skin against pollutants and UVR-induced damage. However, most of the LMWMs are unable to penetrate through the stratum corneum of the epidermis and also get oxidized irreversibly when exposed to air and UVRs. Some of the LMWMs also cause skin diseases including dermatitis. Therefore, there is a need of a potent AO which could protect the skin from the pollutants and UVR-induced skin damage without causing adverse effects. In this context, the present investigation reports the usage of AAS as an ingredient in skin care preparation, which could protect the skin against oxidative damage, cancer, and UVR-induced photodamage, aging, wrinkling, and hyperpigmentation while preventing dehydration. The significant advancement of the study and the future prospects associated with it are described in the following section:

(1) Sericin was randomly cleaved into different length peptides by physical and chemical extraction methods, which generated peptides of molecular weight ranging from 10 to 220 kDa. Based on the extraction methods the secondary structural conformation of SS and associated secondary metabolites varied, which affected its DPPH scavenging activity and biochemical functions. SS extracted using autoclaving (for AA), alkali-degradation (for AA, BM, and PR) and conventional (for PR) methods protected the L929 cells from H_2O_2 induced oxidative damage by enhancing CAT activity and reducing ROS levels. In order to find out the most potent silk variety alkali-degraded BMS, PRS and AAS were taken further to evaluate their other properties important for skin protection.

(2) At higher concentration (4 mg/mL), alkali-degraded BMS, AAS, and PRS acted as pro-oxidant and elevated the intracellular ROS levels in human cancer cells. Redox imbalance-induced in cancer cells by SS treatment triggered apoptotic cell death by upregulating p53 and dysregulating of Bax and Bcl-2 gene expression. AAS treatment

also inhibited SOD activity. SS treatment induced fatal effect to the cancer cells with marginal effect towards normal cells.

(3) SS treatment prior to UVA and UVB irradiations reduced the apoptotic death of human keratinocytes by scavenging the elevated levels of ROS, arresting the cells at sub-G1 phases and preventing mitochondrial membrane depolarization. SS downregulated pro-inflammatory cytokines (IL-6 and IL-8), upregulated p53 and reduced the dysregulation of Bax and Bcl-2 gene expression in UV irradiated cells. AAS showed a better protective effect against UVR-induced HaCaT cell death than PRS and BMS. Topical delivery of AAS protected SKH-1 hairless mice against UVB radiation-induced skin damage by scavenging elevated levels of ROS and preventing the oxidation of endogenous antioxidants.

(4) AAS and PRS post-treatment showed a protective effect against UVR-induced aging and wrinkling by downregulating MMPs expression in human dermal fibroblast and keratinocyte cells. AAS also inhibited the elastase and hyaluronidase activity. AAS showed better activity than PRS and BMS.

(5) AAS and PRS inhibited mushroom tyrosinase activity and prevented the UVR-induced hyperpigmentation by scavenging the elevated levels of ROS and inhibiting tyrosinase activity (except PRS treated prior to UVA-irradiated cells) of mouse melanoma cells.

(6) SS extracted from the cocoons of AA showed potent AO activity, which was used as an ingredient in skin care preparation. AAS addition reduced the linear viscoelastic range of the basic skin care preparation, however, the flow properties of the gel did not change.

(7) In the near future, AAS may be topically delivered using skin care preparations and assessed for its protective effect against UVR-induced skin aging, wrinkling, and hyperpigmentation using *in vivo* studies.

(8) In the near future, the anti-tumor activity of AAS may be assessed using *in vivo* models.

(9) Post *in vivo* assessment, the AAS constituted skin care preparation could be evaluated through clinical studies and then used for manufacturing a multifunctional skin care cosmetic.

(10) Alkali-degraded AAS may also be used for evaluating its hair and nail care applications.

In summary, exploring the properties of SS extracted from the cocoons of different silk varieties have been useful to identify a potent AO activity possessing silk variety that could protect the skin from pollutants and UVR-induced damage. AAS extracted using alkali-degradation showed better anti-tumor, anti-elastase, and anti-hyaluronidase activity and showed a better protective effect against UVR-induced skin damage, aging, and hyperpigmentation than PRS and BMS. AAS was used as an ingredient in skin care preparation. Moreover, this work could provide an opportunity to develop a value-added product from the textile industrial by-products and also helpful in reducing environmental contamination.

Bibliography

1. Adams, J.M., and Cory, S. (1998). The Bcl-2 protein family: arbiters of cell survival. Science 281, 1322-1326.
2. Afaq, F., Adhami, V.M., and Ahmad, N. (2003). Prevention of short-term ultraviolet B radiation-mediated damages by resveratrol in SKH-1 hairless mice☆. Toxicology and applied pharmacology 186, 28-37.
3. Afaq, F., Malik, A., Syed, D., Maes, D., Matsui, M.S., and Mukhtar, H. (2005). Pomegranate fruit extract modulates UV-B–mediated phosphorylation of mitogen-activated protein kinases and activation of nuclear factor kappa B in normal human epidermal keratinocytes. Photochemistry and photobiology 81, 38-45.
4. Afaq, F., and Mukhtar, H. (2001). Effects of solar radiation on cutaneous detoxification pathways. Journal of Photochemistry and photobiology B: biology 63, 61-69.
5. Agar, N., and Young, A.R. (2005). Melanogenesis: a photoprotective response to DNA damage? Mutation Research/Fundamental and Molecular Mechanisms of Mutagenesis 571, 121-132.
6. Agarwal, R., Katiyar, S.K., Khan, S.G., and Mukhtar, H. (1993). Protection against ultraviolet B radiation-induced effects in the skin of SKH-1 hairless mice by a polyphenolic fraction isolated from green tea. Photochemistry and photobiology 58, 695-700.
7. Ahmad, R., Kamra, A., and Hasnain, S.E. (2004). Fibroin silk proteins from the nonmulberry silkworm Philosamia ricini are biochemically and immunochemically distinct from those of the mulberry silkworm Bombyx mori. DNA and cell biology 23, 149-154.
8. Akowuah, G., Ismail, Z., Norhayati, I., and Sadikun, A. (2005). The effects of different extraction solvents of varying polarities on polyphenols of Orthosiphon stamineus and evaluation of the free radical-scavenging activity. Food chemistry 93, 311-317.
9. Al-Duais, M., Müller, L., Böhm, V., and Jetschke, G. (2009). Antioxidant capacity and total phenolics of Cyphostemma digitatum before and after processing: use of different assays. European food research and technology 228, 813-821.

10. Al-Naama, L.M., Hassan, M.A.K., and Mehdi, J.K. (2015). Association of erythrocytes antioxidant enzymes and their cofactors with markers of oxidative stress in patients with sickle cell anemia. Qatar medical journal 2015, 14.
11. Alam, M.B., Bajpai, V.K., Lee, J., Zhao, P., Byeon, J.-H., Ra, J.S., Majumder, R., Lee, J.S., Yoon, J.I., and Rather, I.A. (2017). Inhibition of melanogenesis by jineol from Scolopendra subspinipes mutilans via MAP-Kinase mediated MITF downregulation and the proteasomal degradation of tyrosinase. Scientific reports 7, 45858.
12. Alam, S., Pal, A., Singh, D., and Ansari, K.M. (2018). Topical application of Nexrutine inhibits ultraviolet B-induced cutaneous inflammatory responses in SKH-1 hairless mouse. Photodermatology, photoimmunology and photomedicine 34, 82-90.
13. Albright, A., and Stern, J. (1998). Adipose tissue, encyclopedia of sports medicine and science. Internet society for sport science.
14. Alfadda, A.A., and Sallam, R.M. (2012). Reactive oxygen species in health and disease. BioMed research international 2012.
15. Allemann, I.B., and Baumann, L. (2008). Antioxidants used in skin care formulations. Skin therapy Letter 13, 5-9.
16. Alonso, C., Martí, M., Barba, C., Carrer, V., Rubio, L., and Coderch, L. (2017). Skin permeation and antioxidant efficacy of topically applied resveratrol. Archives of dermatological research 309, 423-431.
17. Amaro-Ortiz, A., Yan, B., and D'Orazio, J. (2014). Ultraviolet radiation, aging and the skin: prevention of damage by topical cAMP manipulation. Molecules 19, 6202-6219.
18. Angel, P., Szabowski, A., and Schorpp-Kistner, M. (2001). Function and regulation of AP-1 subunits in skin physiology and pathology. Oncogene 20, 2413.
19. Antille, C., Tran, C., Sorg, O., Carraux, P., Didierjean, L., and Saurat, J.-H. (2003). Vitamin A exerts a photoprotective action in skin by absorbing ultraviolet B radiation. Journal of investigative dermatology 121, 1163-1167.
20. Antille, C., Tran, C., Sorg, O., and Saurat, J.H. (2004). Topical β-carotene is converted to retinyl esters in human skin ex vivo and mouse skin in vivo. Experimental dermatology 13, 558-561.

21. Antolovich, M., Prenzler, P.D., Patsalides, E., McDonald, S., and Robards, K. (2002). Methods for testing antioxidant activity. Analyst 127, 183-198.
22. Aprioku, J.S. (2013). Pharmacology of free radicals and the impact of reactive oxygen species on the testis. Journal of reproduction and infertility 14, 158.
23. Aramwit, P., Damrongsakkul, S., Kanokpanont, S., and Srichana, T. (2010a). Properties and antityrosinase activity of sericin from various extraction methods. Biotechnology and applied biochemistry 55, 91-98.
24. Aramwit, P., Kanokpanont, S., Nakpheng, T., and Srichana, T. (2010b). The effect of sericin from various extraction methods on cell viability and collagen production. International journal of molecular sciences 11, 2200-2211.
25. Aramwit, P., and Sangcakul, A. (2007). The effects of sericin cream on wound healing in rats. Bioscience, biotechnology, and biochemistry 71, 2473-2477.
26. Aramwit, P., Siritientong, T., Kanokpanont, S., and Srichana, T. (2010). Formulation and characterization of silk sericin–PVA scaffold crosslinked with genipin. International journal of biological macromolecules 47, 668-675.
27. Aramwit, P., Siritientong, T., and Srichana, T. (2012). Potential applications of silk sericin, a natural protein from textile industry by-products. Waste management and research 30, 217-224.
28. Aricioglu, A., Bozkurt, M., Balabanli, B., Kilinc, M., Nazaroglu, N.K., and Turkozkan, N. (2001). Changes in zinc levels and superoxide dismutase activities in the skin of acute, ultraviolet-B-irradiated mice after treatment with ginkgo biloba extract. Biological trace element research 80, 175-179.
29. Assefa, Z., Van Laethem, A., Garmyn, M., and Agostinis, P. (2005). Ultraviolet radiation-induced apoptosis in keratinocytes: on the role of cytosolic factors. Biochimica et biophysica acta (BBA)-Reviews on cancer 1755, 90-106.
30. Avram, A.S., Avram, M.M., and James, W.D. (2005). Subcutaneous fat in normal and diseased states: 2. Anatomy and physiology of white and brown adipose tissue. Journal of the American academy of dermatology 53, 671-683.
31. Bae, J.Y., Choi, J.S., Choi, Y.J., Shin, S.Y., Kang, S.W., Han, S.J., and Kang, Y.H. (2008). (−) Epigallocatechin gallate hampers collagen destruction and collagenase activation in ultraviolet-B-irradiated human dermal fibroblasts: involvement of mitogen-activated protein kinase. Food and chemical toxicology 46, 1298-1307.

32. Bashir, M.M., Sharma, M.R., and Werth, V.P. (2009a). TNF-alpha production in the skin. Archives of dermatological research 301, 87-91.
33. Bashir, M.M., Sharma, M.R., and Werth, V.P. (2009b). UVB and proinflammatory cytokines synergistically activate TNF-alpha production in keratinocytes through enhanced gene transcription. The Journal of investigative dermatology 129, 994-1001.
34. Batista, L.F., Kaina, B., Meneghini, R., and Menck, C.F. (2009). How DNA lesions are turned into powerful killing structures: insights from UV-induced apoptosis. Mutation research/reviews in mutation research 681, 197-208.
35. Baylin, S.B., and Ohm, J.E. (2006). Epigenetic gene silencing in cancer - a mechanism for early oncogenic pathway addiction? Nature reviews cancer 6, 107-116.
36. Bayon, Y., Ortiz, M.A., Lopez-Hernandez, F.J., Gao, F., Karin, M., Pfahl, M., and Piedrafita, F.J. (2003). Inhibition of IκB kinase by a new class of retinoid-related anticancer agents that induce apoptosis. Molecular and cellular biology 23, 1061-1074.
37. Bienert, G.P., Schjoerring, J.K., and Jahn, T.P. (2006). Membrane transport of hydrogen peroxide. Biochimica et biophysica acta (BBA) - Biomembranes 1758, 994-1003.
38. Birben, E., Sahiner, U.M., Sackesen, C., Erzurum, S., and Kalayci, O. (2012). Oxidative Stress and Antioxidant Defense. The world allergy organization journal 5, 9-19.
39. Bissett, D., Chatterjee, R., and Hannon, D. (1990). Photoprotective effect of superoxide-scavenging antioxidants against ultraviolet radiation-induced chronic skin damage in the hairless mouse. Photodermatology, photoimmunology and photomedicine 7, 56-62.
40. Black, A.K., Greaves, M., Hensby, C., and Plummer, N. (1978). Increased prostaglandins E2 and F2alpha in human skin at 6 and 24 h after ultraviolet B irradiation (290− 320 nm). British journal of clinical pharmacology 5, 431-436.
41. Bosch, R., Philips, N., Suárez-Pérez, J., Juarranz, A., Devmurari, A., Chalensouk-Khaosaat, J., and González, S. (2015). Mechanisms of photoaging and cutaneous photocarcinogenesis, and photoprotective strategies with phytochemicals. Antioxidants 4, 248-268.

42. Bralley, E., Greenspan, P., Hargrove, J.L., and Hartle, D.K. (2008). Inhibition of hyaluronidase activity by select sorghum brans. Journal of medicinal food 11, 307-312.
43. Brand, M.D. (2010). The sites and topology of mitochondrial superoxide production. Experimental gerontology 45, 466-472.
44. Brás, N.r.F., Gonçalves, R., Mateus, N., Fernandes, P.A., Ramos, M.J.o., and de Freitas, V. (2010). Inhibition of pancreatic elastase by polyphenolic compounds. Journal of agricultural and food chemistry 58, 10668-10676.
45. Brash, D.E., Rudolph, J.A., Simon, J.A., Lin, A., McKenna, G.J., Baden, H.P., Halperin, A.J., and Ponten, J. (1991). A role for sunlight in skin cancer: UV-induced p53 mutations in squamous cell carcinoma. Proceedings of the National academy of sciences 88, 10124-10128.
46. Brenneisen, P., Sies, H., and Scharffetter-Kochanek, K. (2002). Ultraviolet-B irradiation and matrix metalloproteinases: from induction via signaling to initial events. Annals of the New York academy of sciences 973, 31-43.
47. Brenner, M., and Hearing, V.J. (2008). The protective role of melanin against UV damage in human skin. Photochemistry and photobiology 84, 539-549.
48. Briganti, S., Camera, E., and Picardo, M. (2003). Chemical and instrumental approaches to treat hyperpigmentation. Pigment cell and melanoma research 16, 101-110.
49. Brigelius-Flohe, R. (2006). Glutathione peroxidases and redox-regulated transcription factors. Biological chemistry 387, 1329-1335.
50. Burke, K. (2005). Cosmeceuticals. Nutritional antioxidants, Edited by Zoe Diana Draclos 18, 125-131.
51. Burke, K.E., Clive, J., Combs, G.F., Commisso, J., Keen, C.L., and Nakamura, R.M. (2000). Effects of topical and oral vitamin E on pigmentation and skin cancer induced by ultraviolet irradiation in Skh: 2 hairless mice. Nutrition and cancer 38, 87-97.
52. Burr, S., and Penzer, R. (2005). Promoting skin health. Nursing standard 19.
53. Butkhup, L., Jeenphakdee, M., Jorjong, S., Samappito, S., Samappito, W., and Butimal, J. (2012). Phenolic composition and antioxidant activity of Thai and Eri silk sericins. Food science and biotechnology 21, 389-398.
54. Cadenas, E. (2004). Mitochondrial free radical production and cell signaling. Molecular aspects of medicine 25, 17-26.

55. Cairns, R.A., Harris, I.S., and Mak, T.W. (2011). Regulation of cancer cell metabolism. Nature reviews cancer11, 85-95.
56. Cao, J., Schulte, J., Knight, A., Leslie, N.R., Zagozdzon, A., Bronson, R., Manevich, Y., Beeson, C., and Neumann, C.A. (2009). Prdx1 inhibits tumorigenesis via regulating PTEN/AKT activity. The EMBO journal 28, 1505-1517.
57. Chan, A.C. (1993). Partners in defense, vitamin E and vitamin C. Canadian journal of physiology and pharmacology 71, 725-731.
58. Chan, A.C., Chow, C.K., and Chiu, D. (1999). Interaction of antioxidants and their implication in genetic anemia. Proceedings of the society for experimental biology and medicine 222, 274-282.
59. Chappat, M. (1994). Some applications of emulsions. Colloids and Surfaces A: Physicochemical and engineering aspects 91, 57-77.
60. Chatterjee, A. (2013). Reduced glutathione: a radioprotector or a modulator of DNA-repair activity? Nutrients 5, 525-542.
61. Chen, L., Hu, J.Y., and Wang, S.Q. (2012). The role of antioxidants in photoprotection: a critical review. Journal of the American academy of dermatology 67, 1013-1024.
62. Chen, W., Barthelman, M., Martinez, J., Alberts, D., and Gensler, H.L. (1997). Inhibition of cyclobutane pyrimidine dimer formation in epidermal p53 gene of UV-irradiated mice by α-tocopherol. Nutrition and cancer 29, 205-211.
63. Chiang, H.M., Lin, T.J., Chiu, C.Y., Chang, C.W., Hsu, K.C., Fan, P.C., and Wen, K.C. (2011). Coffea arabica extract and its constituents prevent photoaging by suppressing MMPs expression and MAP kinase pathway. Food and chemical toxicology 49, 309-318.
64. Chidambara Murthy, K.N., Jayaprakasha, G.K., and Singh, R.P. (2002). Studies on antioxidant activity of pomegranate (Punica granatum) peel extract using in vivo models. Journal of agricultural and food chemistry 50, 4791-4795.
65. Chipuk, J.E., Kuwana, T., Bouchier-Hayes, L., Droin, N.M., Newmeyer, D.D., Schuler, M., and Green, D.R. (2004). Direct activation of Bax by p53 mediates mitochondrial membrane permeabilization and apoptosis. Science 303, 1010-1014.
66. Chlapanidas, T., Faragò, S., Lucconi, G., Perteghella, S., Galuzzi, M., Mantelli, M., Avanzini, M.A., Tosca, M.C., Marazzi, M., and Vigo, D. (2013). Sericins

exhibit ROS-scavenging, anti-tyrosinase, anti-elastase, and in vitro immunomodulatory activities. International journal of biological macromolecules 58, 47-56.

67. Cho, H.S., Kwak, D.H., Choi, I.S., Park, H.K., Kang, S.J., Yoo, H.S., Lee, M.S., Oh, K.W., and Hong, J.T. (2009). Inhibitory effect of proanthocyanidin on ultraviolet B irradiation-induced melanogenesis. Journal of toxicology and environmental health, part A 72, 1475-1483.
68. Chung, J.H., Seo, J.Y., Lee, M.K., Eun, H.C., Lee, J.H., Kang, S., Fisher, G.J., and Voorhees, J.J. (2002). Ultraviolet modulation of human macrophage metalloelastase in human skin in vivo. Journal of investigative dermatology 119, 507-512.
69. Chung, K.Y., Agarwal, A., Uitto, J., and Mauviel, A. (1996). An AP-1 binding sequence is essential for regulation of the human 2 (I) collagen (COL1A2) promoter activity by transforming growth factor. Journal of biological chemistry 271, 3272-3278.
70. Costin, G.E., and Hearing, V.J. (2007). Human skin pigmentation: melanocytes modulate skin color in response to stress. The FASEB Journal 21, 976-994.
71. Cotelle, N. (2001). Role of flavonoids in oxidative stress. Current topics in medicinal chemistry 1, 569-590.
72. Csoka, A.B., Frost, G.I., and Stern, R. (2001). The six hyaluronidase-like genes in the human and mouse genomes. Matrix biology 20, 499-508.
73. Cullen, M. (1998). Genetic epidermal syndromes: disorders characterized by lentigines. The pigmentary system: physiology and pathophysiology, 760-766.
74. D'Orazio, J., Jarrett, S., Amaro-Ortiz, A., and Scott, T. (2013). UV radiation and the skin. International journal of molecular sciences 14, 12222-12248.
75. da Silvaa, T.L., da Silva Juniora, A.C., Ribanib, M., Vieiraa, M.L.G., and da Silva, M.G. (2014). Evaluation of molecular weight distribution of sericin in solutions concentrated via precipitation by ethanol and precipitation by freezing/thawing. Chemical engineering 38, 103-108.
76. Dai, G., Freudenberger, T., Zipper, P., Melchior, A., Grether-Beck, S., Rabausch, B., de Groot, J., Twarock, S., Hanenberg, H., Homey, B., et al. (2007). Chronic Ultraviolet B Irradiation Causes Loss of Hyaluronic Acid from Mouse Dermis Because of Down-Regulation of Hyaluronic Acid Synthases. The American journal of pathology 171, 1451-1461.

77. Dai, J., Ma, H., Fan, J., Li, Y., Wang, J., Ni, H., Xia, G., and Chen, S. (2011). Crude polysaccharide from an anti-UVB cell clone of Bupleurum scorzonerifolium protect HaCaT cells against UVB-induced oxidative stress. Cytotechnology 63, 599-607.
78. Dai, J., and Mumper, R.J. (2010). Plant phenolics: extraction, analysis and their antioxidant and anticancer properties. Molecules 15, 7313-7352.
79. Darr, D., Dunston, S., Faust, H., and Pinnell, S. (1996). Effectiveness of Antioxidants (Vitamin C and E) With and. Acta Derm Vcnereol (Stockh) 76, 264-268.
80. Darvin, M.E., Richter, H., Ahlberg, S., Haag, S.F., Meinke, M.C., Le Quintrec, D., Doucet, O., and Lademann, J. (2014). Influence of sun exposure on the cutaneous collagen/elastin fibers and carotenoids: negative effects can be reduced by application of sunscreen. Journal of biophotonics 7, 735-743.
81. Darwiche, N., Bazzi, H., El-Touni, L., Abou-Lteif, G., Doueiri, R., Hatoum, A., Maalouf, S., and Gali-Muhtasib, H. (2005). Regulation of ultraviolet B radiation-mediated activation of AP1 signaling by retinoids in primary keratinocytes. Radiation research 163, 296-306.
82. Das, M., Ansari, K.M., Dhawan, A., Shukla, Y., and Khanna, S.K. (2005). Correlation of DNA damage in epidemic dropsy patients to carcinogenic potential of argemone oil and isolated sanguinarine alkaloid in mice. International journal of cancer 117, 709-717.
83. Dash, R., Ghosh, S.K., Kaplan, D.L., and Kundu, S. (2007). Purification and biochemical characterization of a 70 kDa sericin from tropical tasar silkworm, Antheraea mylitta. Comparative biochemistry and physiology part B: Biochemistry and molecular biology 147, 129-134.
84. Dash, R., Mandal, M., Ghosh, S.K., and Kundu, S. (2008). Silk sericin protein of tropical tasar silkworm inhibits UVB-induced apoptosis in human skin keratinocytes. Molecular and cellular biochemistry 311, 111-119.
85. Davalli, P., Mitic, T., Caporali, A., Lauriola, A., and D'Arca, D. (2016). ROS, Cell Senescence, and Novel Molecular Mechanisms in Aging and Age-Related Diseases. Oxidative medicine and cellular longevity 2016, 3565127.
86. de Freitas, M.M., Fontes, P.R., Souza, P.M., Fagg, C.W., Guerra, E.N.S., de Medeiros Nóbrega, Y.K., Silveira, D., Fonseca-Bazzo, Y., Simeoni, L.A., and Homem-de-Mello, M. (2016). Extracts of Morus nigra L. leaves standardized in

chlorogenic acid, rutin and isoquercitrin: tyrosinase inhibition and cytotoxicity. PloS one 11, e0163130.

87. de Jager, T.L., Cockrell, A.E., and Du Plessis, S.S. (2017). Ultraviolet Light Induced Generation of Reactive Oxygen Species. Advances in experimental medicine and biology 996, 15-23.
88. Debnath, T., Park, S.R., Kim, D.H., Jo, J.E., and Lim, B.O. (2013). Anti-oxidant and anti-inflammatory activities of Inonotus obliquus and germinated brown rice extracts. Molecules 18, 9293-9304.
89. Denat, L., Kadekaro, A.L., Marrot, L., Leachman, S., and Abdel-Malek, Z.A. (2014). Melanocytes as Instigators and Victims of Oxidative Stress. The journal of investigative dermatology 134, 1512-1518.
90. Deponte, M. (2013). Glutathione catalysis and the reaction mechanisms of glutathione-dependent enzymes. Biochimica et biophysica acta (BBA) - General subjects 1830, 3217-3266.
91. Derrickson, B. (2009). Principles of anatomy and physiology: Organization, support and movement, and control systems of the human body (John Wiley & Sons).
92. Devi, R., Deori, M., and Devi, D. (2011). Evaluation of antioxidant activities of silk protein sericin secreted by silkworm Antheraea assamensis (Lepidoptera: Saturniidae). Journal of pharmacy research 4, 4688-4691.
93. Dinkova-Kostova, A.T. (2008). Phytochemicals as protectors against ultraviolet radiation: versatility of effects and mechanisms. Planta medica 74, 1548-1559.
94. Dispersyn, G., Nuydens, R., Connors, R., Borgers, M., and Geerts, H. (1999). Bcl-2 protects against FCCP-induced apoptosis and mitochondrial membrane potential depolarization in PC12 cells. Biochimica et biophysica acta 5, 2-3.
95. Dong, Y., Cao, J., Wang, H., Zhang, J., Zhu, Z., Bai, R., Hao, H., He, X., Fan, R., and Dong, C. (2010). Nitric oxide enhances the sensitivity of alpaca melanocytes to respond to α-melanocyte-stimulating hormone by up-regulating melanocortin-1 receptor. Biochemical and biophysical research communications 396, 849-853.
96. Dudley, E.D., and Hotchkiss, J.H. (1989). Cysteine as an inhibitor of polyphenol oxidase. Journal of food biochemistry 13, 65-75.

97. Dunaway, S., Odin, R., Zhou, L., Ji, L., Zhang, Y., and Kadekaro, A.L. (2018). Natural Antioxidants: Multiple Mechanisms to Protect Skin From Solar Radiation. Frontiers in pharmacology 9.
98. During, A., Dawson, H.D., and Harrison, E.H. (2005). Carotenoid transport is decreased and expression of the lipid transporters SR-BI, NPC1L1, and ABCA1 is downregulated in Caco-2 cells treated with ezetimibe. The journal of nutrition 135, 2305-2312.
99. Egbert, M., Ruetze, M., Sattler, M., Wenck, H., Gallinat, S., Lucius, R., and Weise, J. (2014). The matricellular protein periostin contributes to proper collagen function and is downregulated during skin aging. Journal of dermatological science 73, 40-48.
100. Elmets, C.A., Singh, D., Tubesing, K., Matsui, M., Katiyar, S., and Mukhtar, H. (2001). Cutaneous photoprotection from ultraviolet injury by green tea polyphenols. Journal of the American academy of dermatology 44, 425-432.
101. Engel, W., and Hoppe, U. (1988). Aqueous hair preparations containing sericin and pelarogenic acids. Ger Offen DE 3603595 A1, 4.
102. Ersel, M., Uyanikgil, Y., Akarca, F.K., Ozcete, E., Altunci, Y.A., Karabey, F., Cavusoglu, T., Meral, A., Yigitturk, G., and Cetin, E.O. (2016). Effects of silk sericin on incision wound healing in a dorsal skin flap wound healing rat model. Medical science monitor: international medical journal of experimental and clinical research 22, 1064.
103. Fan, J.B., WU, L.P., Chen, L.S., Mao, X.Y., and Ren, F.Z. (2009). Antioxidant activities of silk sericin from silkworm Bombyx mori. Journal of food biochemistry 33, 74-88.
104. Fang, J.Y., Hung, C.F., Hwang, T.L., and Wong, W.W. (2006). Transdermal delivery of tea catechins by electrically assisted methods. Skin pharmacology and physiology 19, 28-37.
105. Fang, J., Seki, T., and Maeda, H. (2009). Therapeutic strategies by modulating oxygen stress in cancer and inflammation. Advanced drug delivery reviews 61, 290-302.
106. Fanjul, A., Dawson, M.I., Hobbs, P.D., Jong, L., Cameron, J.F., Harlev, E., Graupner, G., Lu, X.P., and Pfahl, M. (1994). A new class of retinoids with selective inhibition of AP-1 inhibits proliferation. Nature 372, 107.

107. Farhat, Z., Browne, R.W., Bonner, M.R., Tian, L., Deng, F., Swanson, M., and Mu, L. (2018). How do glutathione antioxidant enzymes and total antioxidant status respond to air pollution exposure? Environment international 112, 287-293.
108. Farris, P.K. (2014). Cosmeceutical vitamins: vitamin C. Cosmeceuticals E-Book: Procedures in cosmetic dermatology Series, 37.
109. Fazekas, Z., Gao, D., Saladi, R.N., Lu, Y., Lebwohl, M., and Wei, H. (2003). Protective effects of lycopene against ultraviolet B-induced photodamage. Nutrition and cancer 47, 181-187.
110. Fernández-García, E. (2014). Skin protection against UV light by dietary antioxidants. Food and function 5, 1994-2003.
111. Ferreira, P.M., Monteiro, L.S., Coban, T., and Suzen, S. (2009). Comparative effect of N-substituted dehydroamino acids and α-tocopherol on rat liver lipid peroxidation activities. Journal of enzyme inhibition and medicinal chemistry 24, 967-971.
112. Fisher, G.J., Datta, S.C., Talwar, H.S., Wang, Z.Q., Varani, J., Kang, S., and Voorhees, J.J. (1996). Molecular basis of sun-induced premature skin ageing and retinoid antagonism. Nature 379, 335.
113. Fisher, G.J., Kang, S., Varani, J., Bata-Csorgo, Z., Wan, Y., Datta, S., and Voorhees, J.J. (2002). Mechanisms of photoaging and chronological skin aging. Archives of dermatology 138, 1462-1470.
114. Fu, S., Wu, H., Zhang, H., Lian, C.G., and Lu, Q. (2017). DNA methylation/hydroxymethylation in melanoma. Oncotarget 8, 78163.
115. Garcia-Gavin, J., Gonzalez-Vilas, D., Fernandez-Redondo, V., and Toribio, J. (2010). Pigmented contact dermatitis due to kojic acid. A paradoxical side effect of a skin lightener. Contact dermatitis 62, 63-64.
116. Garg, T.K., and Chang, J.Y. (2004). 15-deoxy-delta 12, 14-Prostaglandin J2 prevents reactive oxygen species generation and mitochondrial membrane depolarization induced by oxidative stress. BMC pharmacology 4, 6.
117. Gensler, H.L., and Magdaleno, M. (1991). Topical vitamin E inhibition of immunosuppression and tumorigenesis induced by ultraviolet irradiation. Nutrition and cancer 15, 97-106.
118. Gensler, H.L., Timmermann, B.N., Valcic, S., Wächter, G.A., Dorr, R., Dvorakova, K., and Alberts, D.S. (1996). Prevention of photocarcinogenesis by

topical administration of pure epigallocatechin gallate isolated from green tea. Nutrition and cancer 26, 325-335.

119. Gil, E.M., and Kim, T.H. (2000). UV-induced immune suppression and sunscreen. Photodermatology, photoimmunology and photomedicine 16, 101-110.
120. Gil, M.I., Tomás-Barberán, F.A., Hess-Pierce, B., Holcroft, D.M., and Kader, A.A. (2000). Antioxidant activity of pomegranate juice and its relationship with phenolic composition and processing. Journal of agricultural and food chemistry 48, 4581-4589.
121. Gilbert, L., Picard, C., Savary, G., and Grisel, M. (2013). Rheological and textural characterization of cosmetic emulsions containing natural and synthetic polymers: relationships between both data. Colloids and surfaces A: physicochemical and engineering aspects 421, 150-163.
122. Gilchrest, B.A. (1989). Skin aging and photoaging: an overview. Journal of the American academy of dermatology 21, 610-613.
123. Gimenes, M.L., Silva, V.R., Vieira, M.G., Silva, M.G., and Scheer, A.P. (2014). High molecular sericin from Bombyx mori cocoons: Extraction and recovering by ultrafiltration. International journal of chemical engineering and applications 5, 266.
124. Glasauer, A., and Chandel, N.S. (2014). Targeting antioxidants for cancer therapy. Biochemical pharmacology 92, 90-101.
125. Gloster, H.M., and Neal, K. (2006). Skin cancer in skin of color. Journal of the American academy of dermatology 55, 741-760.
126. Godic, A., Poljšak, B., Adamic, M., and Dahmane, R. (2014). The role of antioxidants in skin cancer prevention and treatment. Oxidative medicine and cellular longevity 2014, 860479.
127. Gorrini, C., Harris, I.S., and Mak, T.W. (2013). Modulation of oxidative stress as an anticancer strategy. Nature reviews drug discovery 12, 931-947.
128. Gough, D., and Cotter, T. (2011). Hydrogen peroxide: a Jekyll and Hyde signalling molecule. Cell death and disease 2, e213.
129. Griffiths, C.E., Kang, S., Ellis, C.N., Kim, K.J., Finkel, L.J., Ortiz-Ferrer, L.C., White, G.M., Hamilton, T.A., and Voorhees, J.J. (1995). Two concentrations of topical tretinoin (retinoic acid) cause similar improvement of photoaging but

different degrees of irritation: A double-blind, vehicle-controlled comparison of 0.1% and 0.025% tretinoin creams. Archives of dermatology 131, 1037-1044.

130. Grünenfelder, J., Miniati, D.N., Murata, S., Falk, V., Hoyt, E.G., Kown, M., Koransky, M.L., and Robbins, R.C. (2001). Upregulation of Bcl-2 through caspase-3 inhibition ameliorates ischemia/reperfusion injury in rat cardiac allografts. Circulation 104, I-202-I-206.
131. Habold, C., Poehlmann, A., Bajbouj, K., Hartig, R., Korkmaz, K.S., Roessner, A., and Schneider-Stock, R. (2008). Trichostatin A causes p53 to switch oxidative-damaged colorectal cancer cells from cell cycle arrest into apoptosis. Journal of cellular and molecular medicine 12, 607-621.
132. Haigis, M.C., and Yankner, B.A. (2010). The aging stress response. Molecular cell 40, 333-344.
133. Halliday, G.M., Robertson, B.O., and Barnetson, R.S.T.C. (2000). Topical Retinoic Acid Enhances, and a Dark Tan Protects, from Subedemal Solar-Simulated Photocarcinogenesis. Journal of investigative dermatology 114, 923-927.
134. Halliwell, B. (2007). Biochemistry of oxidative stress. Biochemical society transactions 35, 1147-1150.
135. Han, E., Chang, B., Kim, D., Cho, H., and Kim, S. (2015). Melanogenesis inhibitory effect of aerial part of Pueraria thunbergiana in vitro and in vivo. Archives of dermatological research 307, 57-72.
136. Hanahan, D., and Weinberg, R.A. (2011). Hallmarks of cancer: the next generation. Cell 144, 646-674.
137. Hashem, M., Jun, K.Y., Lee, E., Lim, S., Choo, H.Y.P., and Kwon, Y. (2008). A rapid and sensitive screening system for human type I collagen with the aim of discovering potent anti-aging or anti-fibrotic compounds. Molecules and cells (Springer Science & Business Media BV) 26.
138. Hata, O. (1987). Cosmetics containing sericin hydrolysates. Jpn Kokai Tokkyo Koho Jap 62036308 A2, 7.
139. Hawk, J., Murphy, G., and Holden, C. (1988). The presence of neutrophils in human cutaneous ultraviolet-B inflammation. British journal of dermatology 118, 27-30.

140. Haywood, R., Rogge, F., and Lee, M. (2008). Protein, lipid, and DNA radicals to measure skin UVA damage and modulation by melanin. Free radical biology and medicine 44, 990-1000.
141. Heck, D.E., Vetrano, A.M., Mariano, T.M., and Laskin, J.D. (2003). UVB light stimulates production of reactive oxygen species unexpected role for catalase. Journal of biological chemistry 278, 22432-22436.
142. Hellemans, L., Corstjens, H., Neven, A., Declercq, L., and Maes, D. (2003). Antioxidant enzyme activity in human stratum corneum shows seasonal variation with an age-dependent recovery. Journal of investigative dermatology 120, 434-439.
143. Hemann, M.T., and Lowe, S.W. (2006). The p53-Bcl-2 connection. Cell death and differentiation 13, 1256-1259.
144. Hodnick, W.F., MllosavljeviĆ, E.B., Nelson, J.H., and Pardini, R.S. (1988). Electrochemistry of flavonoids: relationships between redox potentials, inhibition of mitochondrial respiration, and production of oxygen radicals by flavonoids. Biochemical pharmacology 37, 2607-2611.
145. Homsy, R., Pelletier-Lebon, P., Tixier, J.-M., Godeau, G., Robert, L., and Hornebeck, W. (1988). Characterization of human skin fibroblasts elastase activity. Journal of investigative dermatology 91, 472-477.
146. Hoppe, U., Koerbaecher, K., and Roeckl, M. (1984). Hair and bath preparations containing sericin. Ger Offen DE 3233388 A1, 15.
147. Hou, W., Gao, W., Wang, D., Liu, Q., Zheng, S., and Wang, Y. (2015). The protecting effect of deoxyschisandrin and schisandrin B on HaCaT cells against UVB-induced damage. PLoS One 10, e0127177.
148. Humbert, P.G., Haftek, M., Creidi, P., Lapière, C., Nusgens, B., Richard, A., Schmitt, D., Rougier, A., and Zahouani, H. (2003). Topical ascorbic acid on photoaged skin. Clinical, topographical and ultrastructural evaluation: double-blind study vs. placebo. Experimental dermatology 12, 237-244.
149. Hunter, D., and Frumkin, A. (1991). Adverse reactions to vitamin E and aloe vera preparations after dermabrasion and chemical peel. Cutis 47, 193-196.
150. Imokawa, G. (2009). Mechanism of UVB-induced wrinkling of the skin: Paracrine cytokine linkage between keratinocytes and fibroblasts leading to the stimulation of elastase. Journal of investigative dermatology symposium proceedings 14, 36-43.

151. Jarzycka, A., Lewińska, A., Gancarz, R., and Wilk, K.A. (2013). Assessment of extracts of Helichrysum arenarium, Crataegus monogyna, Sambucus nigra in photoprotective UVA and UVB; photostability in cosmetic emulsions. Journal of Photochemistry and photobiology B: biology 128, 50-57.
152. Jena, K., Pandey, J.P., Kumari, R., Sinha, A.K., Gupta, V.P., and Singh, G.P. (2018). Tasar silk fiber waste sericin: New source for anti-elastase, anti-tyrosinase and anti-oxidant compounds. International Journal of Biological Macromolecules 114, 1102-1108.
153. Jones, K., Hughes, J., Hong, M., Jia, Q., and Orndorff, S. (2002). Modulation of melanogenesis by aloesin: a competitive inhibitor of tyrosinase. Pigment cell research 15, 335-340.
154. Jung, Y.R., Kim, D.H., Kim, S.R., An, H.J., Lee, E.K., Tanaka, T., Kim, N.D., Yokozawa, T., Park, J.N., and Chung, H.Y. (2014). Anti-wrinkle effect of magnesium lithospermate B from Salvia miltiorrhiza BUNGE: inhibition of MMPs via NF-kB signaling. PLoS One 9, e102689.
155. Jurkiewicz, B.A., Bissett, D.L., and Buettner, G.R. (1995). Effect of topically applied tocopherol on ultraviolet radiation-mediated free radical damage in skin. Journal of investigative dermatology 104, 484-488.
156. Kaewkorn, W., Limpeanchob, N., Tiyaboonchai, W., Pongcharoen, S., and Sutheerawattananonda, M. (2012). Effects of silk sericin on the proliferation and apoptosis of colon cancer cells. Biological research 45, 45-50.
157. Kagan, V., Witt, E., Goldman, R., Scita, G., and Packer, L. (1992). Ultraviolet light-induced generation of vitamin E radicals and their recycling. A possible photosensitizing effect of vitamin E in skin. Free radical research communications 16, 51-64.
158. Kang, J.S., Kim, H.N., Kim, J.E., Mun, G.H., Kim, Y.S., Cho, D., Shin, D.H., Hwang, Y.I., and Lee, W.J. (2007). Regulation of UVB-induced IL-8 and MCP-1 production in skin keratinocytes by increasing vitamin C uptake via the redistribution of SVCT-1 from the cytosol to the membrane. Journal of investigative dermatology 127, 698-706.
159. Kanitakis, J. (2002). Anatomy, histology and immunohistochemistry of normal human skin. European journal of dermatology: EJD 12, 390-399; quiz 400-391.

160. Katiyar, S.K. (2003). Skin photoprotection by green tea: antioxidant and immunomodulatory effects. Current Drug Targets-Immune, Endocrine & Metabolic Disorders 3, 234-242.
161. Katiyar, S.K., Afaq, F., Perez, A., and Mukhtar, H. (2001). Green tea polyphenol (–)-epigallocatechin-3-gallate treatment of human skin inhibits ultraviolet radiation-induced oxidative stress. Carcinogenesis 22, 287-294.
162. Katiyar, S.K., Elmets, C.A., Agarwal, R., and Mukhtar, H. (1995). Protection against ultraviolet-B radiation-induced local and systemic suppression of contact hypersensitivity and edema responses in C3H/HeN mice by green tea polyphenols. Photochemistry and photobiology 62, 855-861.
163. Katiyar, S.K., Perez, A., and Mukhtar, H. (2000). Green tea polyphenol treatment to human skin prevents formation of ultraviolet light B-induced pyrimidine dimers in DNA. Clinical cancer research 6, 3864-3869.
164. Katiyar, S.K., Singh, T., Prasad, R., Sun, Q., and Vaid, M. (2012). Epigenetic alterations in ultraviolet radiation-induced skin carcinogenesis: interaction of bioactive dietary components on epigenetic targets. Photochemistry and photobiology 88, 1066-1074.
165. Kato, N., Sato, S., Yamanaka, A., Yamada, H., Fuwa, N., and Nomura, M. (1998). Silk protein, sericin, inhibits lipid peroxidation and tyrosinase activity. Bioscience, biotechnology, and biochemistry 62, 145-147.
166. Kaur, J., Rajkhowa, R., Afrin, T., Tsuzuki, T., and Wang, X. (2014). Facts and myths of antibacterial properties of silk. Biopolymers 101, 237-245.
167. Kaur, J., Rajkhowa, R., Tsuzuki, T., Millington, K., Zhang, J., and Wang, X. (2013). Photoprotection by silk cocoons. Biomacromolecules 14, 3660-3667.
168. Kawashima, A., Sekizawa, A., Koide, K., Hasegawa, J., Satoh, K., Arakaki, T., Takenaka, S., and Matsuoka, R. (2015). Vitamin C Induces the Reduction of Oxidative Stress and Paradoxically Stimulates the Apoptotic Gene Expression in Extravillous Trophoblasts Derived From First-Trimester Tissue. Reproductive sciences 22, 783-790.
169. Kim, J., Hwang, J.S., Cho, Y.K., Han, Y., Jeon, Y.J., and Yang, K.H. (2001). Protective effects of (–)-epigallocatechin-3-gallate on UVA-and UVB-induced skin damage. Skin pharmacology and physiology 14, 11-19.

170. Kim, Y., and He, Y.Y. (2014). Ultraviolet radiation-induced non-melanoma skin cancer: Regulation of DNA damage repair and inflammation. Genes and diseases 1, 188-198.
171. Kim, Y.J., Kang, K.S., and Yokozawa, T. (2008). The anti-melanogenic effect of pycnogenol by its anti-oxidative actions. Food and chemical toxicology 46, 2466-2471.
172. Kirikawa, M., Kasaharu, T., Kishida, K., and Akiyama, D. (2000). Silk protein micropowders for coating with excellent feeling, antistaticity and moisture absorbability and releasability and there manufacture. Jpn Kokai Tokkyo Koho Jap 2000044598 A2, 8.
173. Kohen, R., and Gati, I. (2000). Skin low molecular weight antioxidants and their role in aging and in oxidative stress. Toxicology 148, 149-157.
174. Kojo, S. (2004). Vitamin C: basic metabolism and its function as an index of oxidative stress. Current medicinal chemistry 11, 1041-1064.
175. Kolarsick, P.A., Kolarsick, M.A., and Goodwin, C. (2011). Anatomy and physiology of the skin. Journal of the Dermatology Nurses' Association 3, 203-213.
176. Kondo, S. (2000). The roles of cytokines in photoaging. Journal of dermatological science 23, S30-S36.
177. Konwarh, R., Gogoi, B., Philip, R., Laskar, M., and Karak, N. (2011). Biomimetic preparation of polymer-supported free radical scavenging, cytocompatible and antimicrobial “green” silver nanoparticles using aqueous extract of Citrus sinensis peel. Colloids and surfaces B: biointerfaces 84, 338-345.
178. Krol, E., Kramer-Stickland, K.A., and Liebler, D.C. (2000). Photoprotective actions of topically applied vitamin E. Drug metabolism reviews 32, 413-420.
179. Krutmann, J., Bouloc, A., Sore, G., Bernard, B.A., and Passeron, T. (2017). The skin aging exposome. Journal of Dermatological Science 85, 152-161.
180. Kubatka, P., Kapinová, A., Kello, M., Kruzliak, P., Kajo, K., Výbohová, D., Mahmood, S., Murin, R., Viera, T., and Mojžiš, J. (2016). Fruit peel polyphenols demonstrate substantial anti-tumour effects in the model of breast cancer. European journal of nutrition 55, 955-965.

181. Kubo, I., and Kinst-Hori, I. (1999). Flavonols from saffron flower: tyrosinase inhibitory activity and inhibition mechanism. Journal of agricultural and food chemistry 47, 4121-4125.
182. Kulms, D., and Schwarz, T. (2000). Molecular mechanisms of UV-induced apoptosis. Photodermatology, photoimmunology and photomedicine 16, 195-201.
183. Kulms, D., Zeise, E., Pöppelmann, B., and Schwarz, T. (2002). DNA damage, death receptor activation and reactive oxygen species contribute to ultraviolet radiation-induced apoptosis in an essential and independent way. Oncogene 21, 5844.
184. Kumar, J.P., Alam, S., Jain, A.K., Ansari, K.M., and Mandal, B.B. (2018). Protective Activity of Silk Sericin against UV Radiation-Induced Skin Damage by Downregulating Oxidative Stress. ACS applied bio materials 1, 2120-2132.
185. Kumar, J.P., Bhardwaj, N., and Mandal, B.B. (2016). Cross-linked silk sericin–gelatin 2D and 3D matrices for prospective tissue engineering applications. RSC Advances 6, 105125-105136.
186. Kumar, J.P., Konwarh, R., Kumar, M., Gangrade, A., and Mandal, B.B. (2017). Potential Nanomedicine Applications of Multifunctional Carbon Nanoparticles Developed Using Green Technology. ACS sustainable chemistry and Engineering 6, 1235-1245.
187. Kumar, J.P., and Mandal, B.B. (2017). Antioxidant potential of mulberry and non-mulberry silk sericin and its implications in biomedicine. Free radical biology and medicine 108, 803-818.
188. Kumar, J.P., and Mandal, B.B. (2019). Silk sericin induced pro-oxidative stress leads to apoptosis in human cancer cells. Food and chemical toxicology 123, 275-287.
189. Kumar, R., Das, M., and Ansari, K.M. (2012). Nexrutine® inhibits tumorigenesis in mouse skin and induces apoptotic cell death in human squamous carcinoma A431 and human melanoma A375 cells. Carcinogenesis 33, 1909-1918.
190. Kundu, S., Kundu, B., Talukdar, S., Bano, S., Nayak, S., Kundu, J., Mandal, B.B., Bhardwaj, N., Botlagunta, M., and Dash, B.C. (2012). Nonmulberry silk biopolymers. Biopolymers 97, 455-467.

191. Kundu, S.C., Dash, B.C., Dash, R., and Kaplan, D.L. (2008). Natural protective glue protein, sericin bioengineered by silkworms: potential for biomedical and biotechnological applications. Progress in polymer science 33, 998-1012.
192. Kurioka, A., Kurioka, F., and Yamazaki, M. (2004). Characterization of sericin powder prepared from citric acid-degraded sericin polypeptides of the silkworm, Bombyx Mori. Bioscience, biotechnology, and biochemistry 68, 774-780.
193. Kurioka, A., and Yamazaki, M. (2002). Purification and identification of flavonoids from the yellow green cocoon shell (Sasamayu) of the silkworm, Bombyx mori. Bioscience, biotechnology, and biochemistry 66, 1396-1399.
194. Kurutas, E.B. (2016). The importance of antioxidants which play the role in cellular response against oxidative/nitrosative stress: current state. Nutrition journal 15, 71-71.
195. Lademann, J., Schanzer, S., Meinke, M., Sterry, W., and Darvin, M.E. (2011). Interaction between carotenoids and free radicals in human skin. Skin pharmacology and physiology 24, 238-244.
196. Langton, A., Sherratt, M., Griffiths, C., and Watson, R. (2010). A new wrinkle on old skin: the role of elastic fibres in skin ageing. International journal of cosmetic science 32, 330-339.
197. Lautier, D., Luscher, P., and Tyrrell, R.M. (1992). Endogenous glutathione levels modulate both constitutive and UVA radiation/hydrogen peroxide inducible expression of the human heme oxygenase gene. Carcinogenesis 13, 227-232.
198. Leccia, M.T., Yaar, M., Allen, N., Gleason, M., and Gilchrest, B. (2001). Solar simulated irradiation modulates gene expression and activity of antioxidant enzymes in cultured human dermal fibroblasts. Experimental dermatology 10, 272-279.
199. Lee, H., Lee, J.Y., Song, K.C., Kim, J., Park, J.H., Chun, K.H., and Hwang, G.S. (2012). Protective effect of processed Panax ginseng, sun ginseng on UVB-irradiated human skin keratinocyte and human dermal fibroblast. Journal of ginseng research 36, 68.
200. Lee, S.R., Yang, K.S., Kwon, J., Lee, C., Jeong, W., and Rhee, S.G. (2002). Reversible inactivation of the tumor suppressor PTEN by H2O2. Journal of biological chemistry 277, 20336-20342.

201. Lee, W.L., Huang, J.Y., and Shyur, L.F. (2013). Phytoagents for cancer management: regulation of nucleic acid oxidation, ROS, and related mechanisms. Oxidative medicine and cellular longevity 2013, 925804.
202. Lenormand, H., Tranchepain, F., Deschrevel, B., and Vincent, J.C. (2009). The hyaluronan–protein complexes at low ionic strength: How the hyaluronidase activity is controlled by the bovine serum albumin. Matrix Biology 28, 365-372.
203. León-González, A.J., Auger, C., and Schini-Kerth, V.B. (2015). Pro-oxidant activity of polyphenols and its implication on cancer chemoprevention and chemotherapy. Biochemical pharmacology 98, 371-380.
204. Lephart, E.D., and Andrus, M.B. (2017). Human skin gene expression: natural (trans) resveratrol versus five resveratrol analogs for dermal applications. Experimental biology and medicine 242, 1482-1489.
205. Lephart, E.D., Sommerfeldt, J.M., and Andrus, M.B. (2014). Resveratrol: influences on gene expression in human skin. Journal of functional foods 10, 377-384.
206. Leyden, J., Grove, G., and Zerweck, C. (2004). Facial tolerability of topical retinoid therapy. Journal of drugs in dermatology: JDD 3, 641-651.
207. Li, H., Xu, J., Liu, Y., Ai, S., Qin, F., Li, Z., Zhang, H., and Huang, Z. (2011). Antioxidant and moisture-retention activities of the polysaccharide from Nostoc commune. Carbohydrate polymers 83, 1821-1827.
208. Li, M., Lin, X.f., Lu, J., Zhou, B.R., and Luo, D. (2016). Hesperidin ameliorates UV radiation-induced skin damage by abrogation of oxidative stress and inflammatory in HaCaT cells. Journal of photochemistry and photobiology B: biology 165, 240-245.
209. Li, P.F., Dietz, R., and Von Harsdorf, R. (1999). p53 regulates mitochondrial membrane potential through reactive oxygen species and induces cytochrome c-independent apoptosis blocked by Bcl-2. The EMBO journal 18, 6027-6036.
210. Liang, B., Peng, L., Li, R., Li, H., Mo, Z., Dai, X., Jiang, N., Liu, Q., Zhang, E., and Deng, H. (2018). Lycium barbarum polysaccharide protects HSF cells against ultraviolet-induced damage through the activation of Nrf2. Cellular and molecular biology letters 23, 18.
211. Liang, Y., Yan, C., and Schor, N.F. (2001). Apoptosis in the absence of caspase 3. Oncogene 20, 6570-6578.

212. Lin, J.Y., Selim, M.A., Shea, C.R., Grichnik, J.M., Omar, M.M., Monteiro-Riviere, N.A., and Pinnell, S.R. (2003). UV photoprotection by combination topical antioxidants vitamin C and vitamin E. Journal of the American academy of dermatology 48, 866-874.
213. Lin, J.Y., and Fisher, D.E. (2007). Melanocyte biology and skin pigmentation. Nature 445, 843.
214. Liu, M., Dhanwada, K.R., Birt, D.F., Hecht, S., and Pelling, J.C. (1994). Increase in p53 protein half-life in mouse keratinocytes following UV-B irradiation. Carcinogenesis 15, 1089-1092.
215. Lopez-Torres, M., Thiele, J., Shindo, Y., Han, D., and Packer, L. (1998). Topical application of alpha-tocopherol modulates the antioxidant network and diminishes ultraviolet-induced oxidative damage in murine skin. The British journal of dermatology 138, 207-215.
216. Maia Campos, P.M., Gonçalves, G.M., and Gaspar, L.R. (2008). In vitro antioxidant activity and in vivo efficacy of topical formulations containing vitamin C and its derivatives studied by non-invasive methods. Skin Research and Technology 14, 376-380.
217. Makimura, M., Hirasawa, M., Kobayashi, K., Indo, J., Sakanaka, S., Taguchi, T., and Otake, S. (1993). Inhibitory effect of tea catechins on collagenase activity. Journal of periodontology 64, 630-636.
218. Mandal, B.B., Ghosh, B., and Kundu, S. (2011). Non-mulberry silk sericin/poly (vinyl alcohol) hydrogel matrices for potential biotechnological applications. International journal of biological macromolecules 49, 125-133.
219. Martinez, R., Fattori, V., Saito, P., Melo, C., Borghi, S., Pinto, I., Bussmann, A., Baracat, M., Georgetti, S., and Verri Jr, W. (2018). Lipoxin A4 inhibits UV radiation-induced skin inflammation and oxidative stress in mice. Journal of dermatological science.
220. Martinez, R.M., Pinho-Ribeiro, F.A., Steffen, V.S., Caviglione, C.V., Fattori, V., Bussmann, A.J., Bottura, C., Fonseca, M.J., Vignoli, J.A., and Baracat, M.M. (2017a). trans-Chalcone, a flavonoid precursor, inhibits UV-induced skin inflammation and oxidative stress in mice by targeting NADPH oxidase and cytokine production. Photochemical & Photobiological Sciences 16, 1162-1173.
221. Martinez, R.M., Pinho-Ribeiro, F.A., Vale, D.L., Steffen, V.S., Vicentini, F.T., Vignoli, J.A., Baracat, M.M., Georgetti, S.R., Verri Jr, W.A., and Casagrande, R.

(2017b). Trans-chalcone added in topical formulation inhibits skin inflammation and oxidative stress in a model of ultraviolet B radiation skin damage in hairless mice. Journal of Photochemistry and Photobiology B: Biology 171, 139-146.

222. Marzulli, F.N., and Maibach, H.I. (1984). Permeability and reactivity of skin as related to age. J Soc Cosmet Chem 35, 95-102.
223. Masella, R., Di Benedetto, R., Varì, R., Filesi, C., and Giovannini, C. (2005). Novel mechanisms of natural antioxidant compounds in biological systems: involvement of glutathione and glutathione-related enzymes. The Journal of nutritional biochemistry 16, 577-586.
224. Matsuda, S., Shibayama, H., Hisama, M., Ohtsuki, M., and Iwaki, M. (2008). Inhibitory effects of a novel ascorbic derivative, disodium isostearyl 2-O-L-ascorbyl phosphate on melanogenesis. Chemical and Pharmaceutical Bulletin 56, 292-297.
225. McCord, J.M., and Fridovich, I. (1988). Superoxide dismutase: the first twenty years (1968–1988). Free Radical Biology and Medicine 5, 363-369.
226. McDaniel, D., Neudecker, B., DiNardo, J., Lewis, J., and Maibach, H. (2005a). Clinical efficacy assessment in photodamaged skin of 0.5% and 1.0% idebenone. Journal of cosmetic dermatology 4, 167-173.
227. McDaniel, D., Neudecker, B., DiNardo, J., Lewis, J., and Maibach, H. (2005b). Idebenone: a new antioxidant–Part I. Relative assessment of oxidative stress protection capacity compared to commonly known antioxidants. Journal of cosmetic dermatology 4, 10-17.
228. McKay, B.C., Becerril, C., and Ljungman, M. (2001). P53 plays a protective role against UV-and cisplatin-induced apoptosis in transcription-coupled repair proficient fibroblasts. Oncogene 20, 6805.
229. McLafferty, E., Hendry, C., and Farley, A. (2012). The integumentary system: anatomy, physiology and function of skin. Nursing standard (through 2013) 27, 35.
230. Mink, P.J., Scrafford, C.G., Barraj, L.M., Harnack, L., Hong, C.P., Nettleton, J.A., and Jacobs, D.R. (2007). Flavonoid intake and cardiovascular disease mortality: a prospective study in postmenopausal women. The American journal of clinical nutrition 85, 895-909.
231. Mohania, D., Chandel, S., Kumar, P., Verma, V., Digvijay, K., Tripathi, D., Choudhury, K., Mitten, S.K., and Shah, D. (2017). Ultraviolet radiations: skin

defense-damage mechanism. In ultraviolet light in human health, diseases and environment (Springer), pp. 71-87.

232. Mondal, M. (2007). The silk proteins, sericin and fibroin in silkworm, Bombyx mori Linn.,-a review. Caspian journal of environmental sciences 5, 63-76.
233. Monteiro-Riviere, N.A. (1996). Anatomical factors affecting barrier function. Dermatotoxicology 5, 3-17.
234. Montenegro, L. (2014). Nanocarriers for skin delivery of cosmetic antioxidants. Journal of Pharmacy & Pharmacognosy Research 2.
235. Mrass, P., Rendl, M., Mildner, M., Gruber, F., Lengauer, B., Ballaun, C., Eckhart, L., and Tschachler, E. (2004). Retinoic acid increases the expression of p53 and proapoptotic caspases and sensitizes keratinocytes to apoptosis: a possible explanation for tumor preventive action of retinoids. Cancer research 64, 6542-6548.
236. Nagai, N., Murao, T., Ito, Y., Okamoto, N., and Sasaki, M. (2009). Enhancing effects of sericin on corneal wound healing in rat debrided corneal epithelium. Biological and Pharmaceutical Bulletin 32, 933-936.
237. Nagura, M., Ohnishi, R., Gitoh, Y., and Ohkoshi, Y. (2001). Structures and physical properties of cross-linked sericin membranes. Journal of Insect Biotechnology and Sericology 70, 149-153.
238. Nair, R., and Maseeh, A. (2012). Vitamin D: The "sunshine" vitamin. Journal of pharmacology & pharmacotherapeutics 3, 118-126.
239. Nakamura, T., Pinnell, S.R., Darr, D., Kurimoto, I., Itami, S., Yoshikawa, K., and Streilein, J.W. (1997). Vitamin C abrogates the deleterious effects of UVB radiation on cutaneous immunity by a mechanism that does not depend on TNF-α. Journal of Investigative Dermatology 109, 20-24.
240. Nayama, S., Takehana, M., Kanke, M., Itoh, S., Ogata, E., and Kobayashi, S. (1999). Protective effects of sodium-L-ascorbyl-2 phosphate on the development of UVB-induced damage in cultured mouse skin. Biological and pharmaceutical bulletin 22, 1301-1305.
241. Nema, N.K., Maity, N., Sarkar, B., and Mukherjee, P.K. (2011). Cucumis sativus fruit-potential antioxidant, anti-hyaluronidase, and anti-elastase agent. Archives of dermatological research 303, 247-252.
242. Neog, K., Das, A., Unni, B., Ahmed, G., and Rajan, R. (2011). Studies on secondary metabolites of som (Persea bombycina Kost), a primary host plant of

Muga silkworm (Antheraea assamensis Helfer). International J Pharmaceutical Science and Research 3, 1441-1447.

243. Nichols, J.A., and Katiyar, S.K. (2010). Skin photoprotection by natural polyphenols: anti-inflammatory, antioxidant and DNA repair mechanisms. Archives of dermatological research 302, 71-83.
244. Nicolaou, A., Pilkington, S.M., and Rhodes, L.E. (2011). Ultraviolet-radiation induced skin inflammation: dissecting the role of bioactive lipids. Chemistry and Physics of Lipids 164, 535-543.
245. Nishimura, N., Tohyama, C., Satoh, M., Nishimura, H., and Reeve, V. (1999). Defective immune response and severe skin damage following UVB irradiation in interleukin-6-deficient mice. Immunology 97, 77.
246. Ogawa, A., and Yamada, H. (1999). Antiaging cosmetic containing sericin or hydrolysates and saccharomyces extracts. Jpn Kokai Tokkyo Koho Jap 11193210 A2, 9.
247. Oresajo, C., Stephens, T., Hino, P.D., Law, R.M., Yatskayer, M., Foltis, P., Pillai, S., and Pinnell, S.R. (2008). Protective effects of a topical antioxidant mixture containing vitamin C, ferulic acid, and phloretin against ultraviolet-induced photodamage in human skin. Journal of cosmetic dermatology 7, 290-297.
248. Oroian, M., and Escriche, I. (2015). Antioxidants: Characterization, natural sources, extraction and analysis. Food Research International 74, 10-36.
249. OyetakinWhite, P., Tribout, H., and Baron, E. (2012). Protective mechanisms of green tea polyphenols in skin. Oxidative medicine and cellular longevity 2012.
250. Padamwar, M., and Pawar, A. (2004). Silk sericin and its applications: A review.
251. Padamwar, M.N., Pawar, A.P., Daithankar, A.V., and Mahadik, K. (2005). Silk sericin as a moisturizer: an in vivo study. Journal of cosmetic dermatology 4, 250-257.
252. Padayatty, S.J., Katz, A., Wang, Y., Eck, P., Kwon, O., Lee, J.H., Chen, S., Corpe, C., Dutta, A., Dutta, S.K., et al. (2003). Vitamin C as an antioxidant: evaluation of its role in disease prevention. J Am Coll Nutr 22, 18-35.
253. Palanivel, K., Kanimozhi, V., Kadalmani, B., and Akbarsha, M.A. (2014). Verrucarin A Induces Apoptosis Through ROS-Mediated EGFR/MAPK/Akt Signaling Pathways in MDA-MB-231 Breast Cancer Cells. Journal of cellular biochemistry 115, 2022-2032.

254. Pan, T., Zhu, J., Hwu, W.J., and Jankovic, J. (2012). The role of alpha-synuclein in melanin synthesis in melanoma and dopaminergic neuronal cells. PLoS One 7, e45183.
255. Panich, U. (2011). Antioxidant Defense and UV-Induced Melanogenesis: Implications for Melanoma Prevention. In Current Management of Malignant Melanoma (InTech).
256. Papakonstantinou, E., Roth, M., and Karakiulakis, G. (2012). Hyaluronic acid: A key molecule in skin aging. Dermato-endocrinology 4, 253-258.
257. Paravicini, T.M., and Touyz, R.M. (2006). Redox signaling in hypertension. Cardiovasc Res 71, 247-258.
258. Park, E.J., and M Pezzuto, J. (2012). Flavonoids in cancer prevention. Anti-Cancer Agents in Medicinal Chemistry (Formerly Current Medicinal Chemistry-Anti-Cancer Agents) 12, 836-851.
259. Park, H.H., Lee, S., Son, H.-Y., Park, S.B., Kim, M.S., Choi, E.J., Singh, T.S., Ha, J.H., Lee, M.G., and Kim, J.E. (2008). Flavonoids inhibit histamine release and expression of proinflammatory cytokines in mast cells. Archives of pharmacal research 31, 1303-1311.
260. Park, W.H. (2013). The effects of exogenous H2O2 on cell death, reactive oxygen species and glutathione levels in calf pulmonary artery and human umbilical vein endothelial cells. International journal of molecular medicine 31, 471-476.
261. Parvez, S., Kang, M., Chung, H.S., Cho, C., Hong, M.C., Shin, M.K., and Bae, H. (2006). Survey and mechanism of skin depigmenting and lightening agents. Phytotherapy research 20, 921-934.
262. Pattison, D.I., Rahmanto, A.S., and Davies, M.J. (2012). Photo-oxidation of proteins. Photochemical and photobiological sciences 11, 38-53.
263. Pearson, P., Lewis, S.A., Britton, J., Young, I.S., and Fogarty, A. (2006). The pro-oxidant activity of high-dose vitamin E supplements in vivo. BioDrugs 20, 271-273.
264. Perrenoud, D., Homberger, H.P., Auderset, P., Emmenegger, R., Frenk, E., Saurat, J.H., Hauser, C., and Group, S.C.D.R. (1994). An epidemic outbreak of papular and follicular contact dermatitis to tocopheryl linoleate in cosmetics. Dermatology 189, 225-233.
265. Pietta, P.G. (2000). Flavonoids as antioxidants. Journal of natural products 63, 1035-1042.

266. Pillai, S., Oresajo, C., and Hayward, J. (2005). Ultraviolet radiation and skin aging: roles of reactive oxygen species, inflammation and protease activation, and strategies for prevention of inflammation-induced matrix degradation–a review. International journal of cosmetic science 27, 17-34.
267. Pinnell, S.R., Yang, H., Omar, M., Riviere, N.M., DeBuys, H.V., Walker, L.C., Wang, Y., and Levine, M. (2001). Topical L-ascorbic acid: percutaneous absorption studies. Dermatologic surgery 27, 137-142.
268. Pittayapruek, P., Meephansan, J., Prapapan, O., Komine, M., and Ohtsuki, M. (2016). Role of Matrix Metalloproteinases in photoaging and photocarcinogenesis. International journal of molecular sciences 17, 868.
269. Podda, M., Traber, M.G., Weber, C., Yan, L.J., and Packer, L. (1998). UV-irradiation depletes antioxidants and causes oxidative damage in a model of human skin. Free radical biology and medicine 24, 55-65.
270. Poljsak, B., Šuput, D., and Milisav, I. (2013). Achieving the balance between ROS and antioxidants: when to use the synthetic antioxidants. Oxidative medicine and cellular longevity 2013.
271. Pozarowski, P., and Darzynkiewicz, Z. (2004). Analysis of cell cycle by flow cytometry. Checkpoint Controls and Cancer: Volume 2: Activation and regulation protocols, 301-311.
272. Pringle, F., and Penzer, R. (2002). Normal skin: its function and care (Oxford: Butterworth Heinimann).
273. Pullar, J.M., Carr, A.C., and Vissers, M.C.M. (2017). The Roles of Vitamin C in Skin Health. Nutrients 9, 866.
274. Quan, T., Qin, Z., Xu, Y., He, T., Kang, S., Voorhees, J.J., and Fisher, G.J. (2010). Ultraviolet irradiation induces CYR61/CCN1, a mediator of collagen homeostasis, through activation of transcription factor AP-1 in human skin fibroblasts. Journal of investigative dermatology 130, 1697-1706.
275. Rakkestad, K.E., Skaar, I., Ansteinsson, V.E., Solhaug, A., Holme, J.A., Pestka, J.J., Samuelsen, J.T., Dahlman, H.J., Hongslo, J.K., and Becher, R. (2010). DNA damage and DNA damage responses in THP-1 monocytes after exposure to spores of either S. chartarum or A. versicolor or to T-2 toxin. Toxicological sciences, kfq045.
276. Ramasamy, K., Shanmugam, M., Balupillai, A., Govindhasamy, K., Gunaseelan, S., Muthusamy, G., Robert, B.M., and Nagarajan, R.P. (2017). Ultraviolet

radiation-induced carcinogenesis: Mechanisms and experimental models. Journal of Radiation and Cancer Research 8, 4.

277. Ramos-e-Silva, M., Celem, L.R., Ramos-e-Silva, S., and Fucci-da-Costa, A.P. (2013). Anti-aging cosmetics: Facts and controversies. Clinics in dermatology 31, 750-758.
278. Rangi, A., and Jajpura, L. (2015). The biopolymer sericin: extraction and applications. Journal of textile science and engineering 5, 1-5.
279. Reguera, S., Zamora-Camacho, F.J., Melero, E., Garcia-Mesa, S., Trenzado, C.E., Cabrerizo, M.J., Sanz, A., and Moreno-Rueda, G. (2015). Ultraviolet radiation does not increase oxidative stress in the lizard Psammodromus algirus along an elevational gradient. Comparative biochemistry and physiology part A: molecular & integrative physiology 183, 20-26
280. Rhie, G.E., Shin, M.H., Seo, J.Y., Choi, W.W., Cho, K.H., Kim, K.H., Park, K.C., Eun, H.C., and Chung, J.H. (2001). Aging- and Photoaging-Dependent Changes of Enzymic and Nonenzymic Antioxidants in the Epidermis and Dermis of Human Skin In Vivo. Journal of investigative dermatology 117, 1212-1217.
281. Rhodes, L., Belgi, G., Parslew, R., McLoughlin, L., Clough, G., and Friedmann, P. (2001). Ultraviolet-B-induced erythema is mediated by nitric oxide and prostaglandin E2 in combination. Journal of investigative dermatology 117, 880-885.
282. Rittié, L., and Fisher, G.J. (2002). UV-light-induced signal cascades and skin aging. Ageing research reviews 1, 705-720.
283. Robinson, E., and Werth, V. (2015). The role of cytokines in the pathogenesis of cutaneous lupus erythematosus. Cytokine 73, 326-334.
284. Sangwong, G., Sumida, M., and Sutthikhum, V. (2016). Antioxidant activity of chemically and enzymatically modified sericin extracted from cocoons of Bombyx mori. Biocatalysis and Agricultural Biotechnology 5, 155-161.
285. Sakamoto, K., and Yamakishi, K. (2000). Sericin containing cleaning composition. Jpn Kokai Tokkyo Koho Japan A 2.
286. Sárdy, M. (2009). Role of matrix metalloproteinases in skin ageing. Connective tissue research 50, 132-138.
287. Sarovart, S., Sudatis, B., Meesilpa, P., Grady, B.P., and Magaraphan, R. (2003). The use of sericin as an antioxidant and antimicrobial for polluted air treatment. Reviews on advanced materials science 5, 193-198.

288. Sasaki, H., Akamatsu, H., and Horio, T. (1997). Effects of a single exposure to UVB radiation on the activities and protein levels of copper-zinc and manganese superoxide dismutase in cultured human keratinocytes. Photochemistry and Photobiology 65, 707-713.
289. Sasseville, D., Moreau, L., and Al-Sowaidi, M. (2007). Allergic contact dermatitis to idebenone used as an antioxidant in an anti-wrinkle cream. Contact dermatitis 56, 117-118.
290. Saurat, J.H., Sorg, O., and Didierjean, L. (1999). New concepts for delivery of topical retinoid activity to human skin. In Retinoids (Springer), pp. 521-538.
291. Savini, I., D'Angelo, I., Ranalli, M., Melino, G., and Avigliano, L. (1999). Ascorbic acid maintenance in HaCaT revents radical formation and apoptosis by UV-B. Free radical biology and medicine 26, 1172-1180.
292. Scharffetter–Kochanek, K., Brenneisen, P., Wenk, J., Herrmann, G., Ma, W., Kuhr, L., Meewes, C., and Wlaschek, M. (2000). Photoaging of the skin from phenotype to mechanisms. Experimental gerontology 35, 307-316.
293. Schmitt, W. (1992). Skin-care products. In chemistry and technology of the cosmetics and toiletries industry (Springer), pp. 104-148.
294. Schurink, M., van Berkel, W.J., Wichers, H.J., and Boeriu, C.G. (2007). Novel peptides with tyrosinase inhibitory activity. Peptides 28, 485-495.
295. Sharaf, A., and Nigm, S. (1964). The oestrogenic activity of pomegranate seed oil. Journal of endocrinology 29, 91-92.
296. Sharma, P., Jha, A.B., Dubey, R.S., and Pessarakli, M. (2012). Reactive oxygen species, oxidative damage, and antioxidative defense mechanism in plants under stressful conditions. Journal of botany 2012.
297. Sharma, S., Singh, L., and Singh, S. (2013). A review on medicinal plants having antioxidant potential. Indian journal of research in pharmacy and biotechnology 1, 404.
298. Sharma, S.D., Meeran, S.M., and Katiyar, S.K. (2007). Dietary grape seed proanthocyanidins inhibit UVB-induced oxidative stress and activation of mitogen-activated protein kinases and nuclear factor-κB signaling in in vivo SKH-1 hairless mice. Molecular cancer therapeutics 6, 995-1005.

299. Sharma, S.K., and Le Maguer, M. (1996). Kinetics of lycopene degradation in tomato pulp solids under different processing and storage conditions. Food Research International 29, 309-315.
300. Shindo, Y., Witt, E., Han, D., Epstein, W., and Packer, L. (1994a). Enzymic and non-enzymic antioxidants in epidermis and dermis of human skin. Journal of investigative dermatology 102, 122-124.
301. Shindo, Y., Witt, E., Han, D., and Packer, L. (1994b). Dose-response effects of acute ultraviolet irradiation on antioxidants and molecular markers of oxidation in murine epidermis and dermis. Journal of investigative dermatology 102, 470-475.
302. Shindo, Y., Witt, E., Han, D., Tzeng, B., Aziz, T., Nguyen, L., and Packer, L. (1994c). Recovery of antioxidants and reduction in lipid hydroperoxides in murine epidermis and dermis after acute ultraviolet radiation exposure. Photodermatology, photoimmunology & photomedicine 10, 183-191.
303. Shindo, Y., Witt, E., and Packer, L. (1993). Antioxidant Defense Mechanisms in Murine Epidermis and Dermis and Their Responses to Ultraviolet Light. Journal of investigative dermatology 100, 260-265.
304. Shukla, V., Mishra, S.K., and Pant, H.C. (2011). Oxidative stress in neurodegeneration. Advances in pharmacological sciences 2011.
305. Silva, S.A.M.e., Michniak-Kohn, B., and Leonardi, G.R. (2017). An overview about oxidation in clinical practice of skin aging. Anais brasileiros de dermatologia 92, 367-374.
306. Singh, N.P., McCoy, M.T., Tice, R.R., and Schneider, E.L. (1988). A simple technique for quantitation of low levels of DNA damage in individual cells. Experimental cell research 175, 184-191.
307. Siritienthong, T., Ratanavaraporn, J., and Aramwit, P. (2012). Development of ethyl alcohol-precipitated silk sericin/polyvinyl alcohol scaffolds for accelerated healing of full-thickness wounds. International journal of pharmaceutics 439, 175-186.
308. Somasagara, R.R., Hegde, M., Chiruvella, K.K., Musini, A., Choudhary, B., and Raghavan, S.C. (2012). Extracts of strawberry fruits induce intrinsic pathway of apoptosis in breast cancer cells and inhibits tumor progression in mice. PloS one 7, e47021.

309. Song, T.Y., Chen, C.H., Yang, N.C., and Fu, C.S. (2009). The correlation of in vitro mushroom tyrosinase activity with cellular tyrosinase activity and melanin formation in melanoma cells A2058. Journal of food and drug analysis 17.
310. Sorg, O., Iran, C., Carraux, P., Grand, D., Hügin, A., Didierjean, L., and Saurat, J.H. (2005). Spectral Properties of Topical Retinoids Prevent DNA Damage and Apoptosis After Acute UV-B Exposure in Hairless Mice¶. Photochemistry and photobiology 81, 830-836.
311. Sorg, O., and Saurat, J.H. (2014). Topical retinoids in skin ageing: a focused update with reference to sun-induced epidermal vitamin A deficiency. Dermatology 228, 314-325.
312. Stahl, W., and Sies, H. (1996). Lycopene: a biologically important carotenoid for humans? Archives of biochemistry and biophysics 336, 1-9.
313. Stamatas, G.N., Zmudzka, B.Z., Kollias, N., and Beer, J.Z. (2004). Non-invasive measurements of skin pigmentation in situ. Pigment Cell Research 17, 618-626.
314. Steenvoorden, D.P., and van Henegouwen, G.M.B. (1997). The use of endogenous antioxidants to improve photoprotection. Journal of Photochemistry and photobiology B: biology 41, 1-10.
315. Stewart, M.S., Cameron, G.S., and Pence, B.C. (1996). Antioxidant nutrients protect against UVB-induced oxidative damage to DNA of mouse keratinocytes in culture. Journal of investigative dermatology 106, 1086-1089.
316. Stojiljković, D., Pavlović, D., and Arsić, I. (2014). Oxidative Stress, Skin Aging and Antioxidant Therapy/Oksidacioni Stres, Starenje Kože I Antioksidaciona Terapija. Acta facultatis medicae naissensis 31, 207-217.
317. Story, E.N., Kopec, R.E., Schwartz, S.J., and Harris, G.K. (2010). An update on the health effects of tomato lycopene. Annual review of food science and technology 1, 189-210.
318. Strickland, I., Rhodes, L.E., Flanagan, B.F., and Friedmann, P.S. (1997). TNF-α and IL-8 are upregulated in the epidermis of normal human skin after UVB exposure: correlation with neutrophil accumulation and E-selectin expression. Journal of investigative dermatology 108, 763-768.
319. Sun, Y. (1990). Free radicals, antioxidant enzymes, and carcinogenesis. Free radical biology and medicine 8, 583-599.

320. Suzuki, N., Fujimura, A., Nagai, T., Mizumoto, I., Itami, T., Hatate, H., Nozawa, T., Kato, N., Nomoto, T., and Yoda, B. (2004). Antioxidative activity of animal and vegetable dietary fibers. Biofactors 21, 329-333.
321. Svobodová, A., and Vostálová, J. (2010). Solar radiation induced skin damage: review of protective and preventive options. International journal of radiation biology 86, 999-1030.
322. Svobodova, A., Zdarilova, A., Maliskova, J., Mikulkova, H., Walterova, D., and Vostalova, J. (2007). Attenuation of UVA-induced damage to human keratinocytes by silymarin. Journal of dermatological science 46, 21-30.
323. Syed, D.N., Malik, A., Hadi, N., Sarfaraz, S., Afaq, F., and Mukhtar, H. (2006). Photochemopreventive effect of pomegranate fruit extract on UVA-mediated activation of cellular pathways in normal human epidermal keratinocytes. Photochemistry and photobiology 82, 398-405.
324. Tadić, V.M., Dobrić, S., Marković, G.M., Đorđević, S.M., Arsić, I.A., Menković, N.a.R., and Stević, T. (2008). Anti-inflammatory, gastroprotective, free-radical-scavenging, and antimicrobial activities of hawthorn berries ethanol extract. Journal of agricultural and food chemistry 56, 7700-7709.
325. Tadros, T. (2004). Application of rheology for assessment and prediction of the long-term physical stability of emulsions. Advances in colloid and interface science 108, 227-258.
326. Takahashi, H., Hashimoto, Y., Aoki, N., Kinouchi, M., Ishida-Yamamoto, A., and Iizuka, H. (2000). Copper, zinc–superoxide dismutase protects from ultraviolet B-induced apoptosis of SV40-transformed human keratinocytes: the protection is associated with the increased levels of antioxidant enzymes. Journal of dermatological science 23, 12-21.
327. Takai, D., and Jones, P.A. (2003). The CpG island searcher: a new WWW resource. In silico biology 3, 235-240.
328. Takasu, Y., Yamada, H., and Tsubouchi, K. (2002). Isolation of three main sericin components from the cocoon of the silkworm, Bombyx mori. Bioscience, biotechnology, and biochemistry 66, 2715-2718.
329. Takechi, T., Wada, R., Fukuda, T., Harada, K., and Takamura, H. (2014). Antioxidant activities of two sericin proteins extracted from cocoon of silkworm (Bombyx mori) measured by DPPH, chemiluminescence, ORAC and ESR methods. Biomedical reports 2, 364-369.

330. Tamura, Y., Nakajima, K.I., Nagayasu, K.I., and Takabayashi, C. (2002). Flavonoid 5-glucosides from the cocoon shell of the silkworm, Bombyx mori. Phytochemistry 59, 275-278.
331. Tan, B.L., Norhaizan, M.E., and Winnie-Pui-Pui Liew, H.S. (2018). Antioxidant and Oxidative Stress: A Mutual Interplay in Age-Related Diseases. Frontiers in pharmacology 9.
332. Telang, P.S. (2013). Vitamin C in dermatology. Indian dermatology online journal 4, 143.
333. Terada, S., Nishimura, T., Sasaki, M., Yamada, H., and Miki, M. (2002). Sericin, a protein derived from silkworms, accelerates the proliferation of several mammalian cell lines including a hybridoma. Cytotechnology 40, 3-12.
334. Teramoto, H., Kakazu, A., and Asakura, T. (2006). Native structure and degradation pattern of silk sericin studied by 13C NMR spectroscopy. Macromolecules 39, 6-8.
335. Teunissen, M.B., Piskin, G., di Nuzzo, S., Sylva-Steenland, R.M., de Rie, M.A., and Bos, J.D. (2002). Ultraviolet B radiation induces a transient appearance of IL-4+ neutrophils, which support the development of Th2 responses. The journal of immunology 168, 3732-3739.
336. Thiele, J.J., Traber, M.G., and Packer, L. (1998). Depletion of human stratum corneum vitamin E: an early and sensitive in vivo marker of UV induced photo-oxidation. Journal of investigative dermatology 110, 756-761.
337. Thiesen, L.C., Baccarin, T., Fischer-Muller, A.F., Meyre-Silva, C., Couto, A.G., Bresolin, T.M.B., and Santin, J.R. (2017). Photochemoprotective effects against UVA and UVB irradiation and photosafety assessment of Litchi chinensis leaves extract. Journal of Photochemistry and photobiology B: biology 167, 200-207.
338. Thody, A.J., Higgins, E.M., Wakamatsu, K., Ito, S., Burchill, S.A., and Marks, J.M. (1991). Pheomelanin as well as eumelanin is present in human epidermis. Journal of investigative dermatology 97, 340-344.
339. Thring, T.S., Hili, P., and Naughton, D.P. (2009). Anti-collagenase, anti-elastase and anti-oxidant activities of extracts from 21 plants. BMC complementary and alternative medicine 9, 27.
340. Tokutake, S. (1980). Isolation of the smallest component of silk protein. Biochemical journal 187, 413-417.

341. Traber, M.G., and Atkinson, J. (2007). Vitamin E, Antioxidant and Nothing More. Free radical biology and medicine 43, 4-15.
342. Trachootham, D., Alexandre, J., and Huang, P. (2009). Targeting cancer cells by ROS-mediated mechanisms: a radical therapeutic approach? Nature reviews drug discovery 8, 579-591.
343. Traikovich, S.S. (1999). Use of topical ascorbic acid and its effects on photodamaged skin topography. Archives of otolaryngology–head & neck surgery 125, 1091-1098.
344. Tran, C., Sorg, O., Carraux, P., Didierjean, L., and Saurat, J.H. (2001). Topical Delivery of Retinoids Counteracts the UVB-induced Epidermal Vitamin A Depletion in Hairless Mouse. Photochemistry and photobiology 73, 425-431.
345. Tsubouchi, K., Igarashi, Y., Takasu, Y., and Yamada, H. (2005). Sericin enhances attachment of cultured human skin fibroblasts. Bioscience, biotechnology, and biochemistry 69, 403-405.
346. Tsuji, N., Moriwaki, S., Suzuki, Y., Takema, Y., and Imokawa, G. (2001). The role of elastases secreted by fibroblasts in wrinkle formation: implication through selective inhibition of elastase activity. Photochemistry and Photobiology 74, 283-290.
347. Tsuruoka, H., Khovidhunkit, W., Brown, B.E., Fluhr, J.W., Elias, P.M., and Feingold, K.R. (2002). Scavenger Receptor Class B Type I Is Expressed in Cultured Keratinocytes and Epidermis regulation in response to changes in cholesterol homeostasis and barrier requirements. Journal of biological chemistry 277, 2916-2922.
348. Tyrrell, R.M. (1996). Activation of mammalian gene expression by the UV component of sunlight–from models to reality. Bioessays 18, 139-148.
349. Urabe, K. (1998). Mixed epidermal and dermal hypermelanoses. The pigmentary system: physiology and pathophysiology, 909-911.
350. Vaithanomsat, P., and Kitpreechavanich, V. (2008). Sericin separation from silk degumming wastewater. Separation and purification technology 59, 129-133.
351. van Bennekum, A., Werder, M., Thuahnai, S.T., Han, C.H., Duong, P., Williams, D.L., Wettstein, P., Schulthess, G., Phillips, M.C., and Hauser, H. (2005). Class B scavenger receptor-mediated intestinal absorption of dietary β-carotene and cholesterol. Biochemistry 44, 4517-4525.

352. Vayalil, P.K., Mittal, A., Hara, Y., Elmets, C.A., and Katiyar, S.K. (2004). Green tea polyphenols prevent ultraviolet light-induced oxidative damage and matrix metalloproteinases expression in mouse skin. Journal of investigative dermatology 122, 1480-1487.
353. Venza, M., Visalli, M., Beninati, C., De Gaetano, G.V., Teti, D., and Venza, I. (2015). Cellular mechanisms of oxidative stress and action in melanoma. Oxidative medicine and cellular longevity 2015.
354. Verschooten, L., Claerhout, S., Van Laethem, A., Agostinis, P., and Garmyn, M. (2006). New strategies of photoprotection. Photochemistry and photobiology 82, 1016-1023.
355. Vilela, F.M., Oliveira, F.M., Vicentini, F.T., Casagrande, R., Verri Jr, W.A., Cunha, T.M., and Fonseca, M.J. (2016). Commercial sunscreen formulations: UVB irradiation stability and effect on UVB irradiation-induced skin oxidative stress and inflammation. Journal of photochemistry and photobiology B: biology 163, 413-420.
356. Wang, Z.Y., Agarwal, R., Bickers, D.R., and Mukhtar, H. (1991). Protection against ultraviolet B radiation-induced photocarcinogenesis in hairless mice by green tea polyphenols. Carcinogenesis 12, 1527-1530.
357. Warren, J.B. (1994). Nitric oxide and human skin blood flow responses to acetylcholine and ultraviolet light. The FASEB journal 8, 247-251.
358. Warren, R., Gartstein, V., Kligman, A.M., Montagna, W., Allendorf, R.A., and Ridder, G.M. (1991). Age, sunlight, and facial skin: a histologic and quantitative study. Journal of the American academy of dermatology 25, 751-760.
359. Weber, S.U., Thiele, J.J., Packer, L., and Cross, C.E. (1999). Vitamin C, uric acid, and glutathione gradients in murine stratum corneum and their susceptibility to ozone exposure. Journal of investigative dermatology 113, 1128-1132.
360. Weinberg, F., and Chandel, N.S. (2009). Reactive oxygen species-dependent signaling regulates cancer. Cellular and molecular life sciences 66, 3663.
361. Weinberg, F., Hamanaka, R., Wheaton, W.W., Weinberg, S., Joseph, J., Lopez, M., Kalyanaraman, B., Mutlu, G.M., Budinger, G.S., and Chandel, N.S. (2010). Mitochondrial metabolism and ROS generation are essential for Kras-mediated tumorigenicity. Proceedings of the national academy of sciences 107, 8788-8793.

362. Weydert, C.J., and Cullen, J.J. (2010). Measurement of superoxide dismutase, catalase and glutathione peroxidase in cultured cells and tissue. Nature protocols 5, 51-66.
363. Winterbourn, C.C. (2016). Revisiting the reactions of superoxide with glutathione and other thiols. Archives of biochemistry and biophysics 595, 68-71.
364. Wiswedel, I., Keilhoff, G., Dorner, L., Navarro, A., Bockelmann, R., Bonnekoh, B., Gardemann, A., and Gollnick, H. (2007). UVB irradiation-induced impairment of keratinocytes and adaptive responses to oxidative stress. Free radical research 41, 1017-1027.
365. Wolff, S., Erster, S., Palacios, G., and Moll, U.M. (2008). p53's mitochondrial translocation and MOMP action is independent of Puma and Bax and severely disrupts mitochondrial membrane integrity. Cell research 18, 733-744.
366. Wood, S.M., Mastaloudis, A.F., Hester, S.N., Gray, R., Kern, D., Namkoong, J., and Draelos, Z.D. (2017). Protective effects of a novel nutritional and phytonutrient blend on ultraviolet radiation-induced skin damage and inflammatory response through aging defense mechanisms. Journal of cosmetic dermatology 16, 491-499.
367. Wright, J.R., Colby, H.D., and Miles, P.R. (1981). Cytosolic factors which affect microsomal lipid peroxidation in lung and liver. Archives of biochemistry and biophysics 206, 296-304.
368. Xiang, J., Wan, C., Guo, R., and Guo, D. (2016). Is Hydrogen Peroxide a Suitable Apoptosis Inducer for All Cell Types? BioMed research international 2016, 7343965.
369. Xie, L.P., Chen, Q.X., Huang, H., Wang, H.Z., and Zhang, R.Q. (2003). Inhibitory effects of some flavonoids on the activity of mushroom tyrosinase. Biochemistry (Moscow) 68, 487-491.
370. Xu, P., Zhang, M., Wang, X., Yan, Y., Chen, Y., Wu, W., Zhang, L., and Zhang, L. (2018). Antioxidative Effect of Quetiapine on Acute Ultraviolet-B-Induced Skin and HaCaT Cell Damage. International journal of molecular sciences 19, 953.

371. Yaar, M., and Gilchrest, B.A. (2007). Photoageing: mechanism, prevention and therapy. British journal of dermatology 157, 874-887.
372. Yamada, H., Fuha, Y., Yuri, O., Obayashi, M., and Arashima, T. (1998). Collagen formation promoters containing sericin or its hydrolyzates and antiaging cosmetics. Jpn Kokai Tokkyo Koho, JP 10226653 A2, 8.
373. Yamada, H., and Tsubouchi, K. (2001). Characterization of silk proteins in the cocoon fibers of Cricula trifenestrata. International journal of wild silkmoth and silk (Japan).
374. Yamada, H., Yamasaki, K., and Zozaki, K. (2001a). Nail cosmetics containing sericin. PCT Int Appl WO 2001015660 A1, 15.
375. Yamada, H., Yamazuki, K., and Nozaki, K. (2001b). Skin moisturizing and conditioning cosmetics containing sericin and saccharides. Jpn Kokai Tokkyo Koho Jap 2001064148 A2, 6.
376. Yamada, H., and Yuri, O. (1998). Sericin coated powders for cosmetics. Jpn Kokai Tokkyo Koho Jap 10226626 A2, 9.
377. Yamaguchi, Y., Takahashi, K., Zmudzka, B.Z., Kornhauser, A., Miller, S.A., Tadokoro, T., Berens, W., Beer, J.Z., and Hearing, V.J. (2006). Human skin responses to UV radiation: pigment in the upper epidermis protects against DNA damage in the lower epidermis and facilitates apoptosis. The FASEB journal 20, 1486-1488.
378. Yasuda, N., Yamada, H., and Nomura, M. (1998). Sericin from silk as dermatitis inhibitor. Paper presented at: Chemical Abstracts.
379. Yin, Y., Li, W., Son, Y.O., Sun, L., Lu, J., Kim, D., Wang, X., Yao, H., Wang, L., and Pratheeshkumar, P. (2013). Quercitrin protects skin from UVB-induced oxidative damage. Toxicology and applied pharmacology 269, 89-99.
380. Yokohira, M., Yamakawa, K., Saoo, K., Matsuda, Y., Hosokawa, K., Hashimoto, N., Kuno, T., and Imaida, K. (2008). Antioxidant effects of flavonoids used as food additives (purple corn color, enzymatically modified isoquercitrin, and isoquercitrin) on liver carcinogenesis in a rat medium-term bioassay. Journal of food science 73, C561-C568.
381. Yoshioka, M., Segawa, A., Veda, A., and Omi, S. (2001). UV absorbing compositions containing fine capsules. Jpn Kokai Tokkyo Koho Jap2001049233 A2, 14.

382. Yue, Y., Zhou, H., Liu, G., Li, Y., Yan, Z., and Duan, M. (2010). The advantages of a novel CoQ10 delivery system in skin photo-protection. International journal of pharmaceutics 392, 57-63.
383. Zhang, Y.Q. (2002). Applications of natural silk protein sericin in biomaterials. Biotechnology advances 20, 91-100.
384. Zhaorigetu, S., Yanaka, N., Sasaki, M., Watanabe, H., and Kato, N. (2003). Inhibitory effects of silk protein, sericin on UVB-induced acute damage and tumor promotion by reducing oxidative stress in the skin of hairless mouse. Journal of photochemistry and photobiology B: biology 71, 11-17.
385. Zhong, X., Zeng, M., Bian, H., Zhong, C., and Xiao, F. (2017). An evaluation of the protective role of vitamin C in reactive oxygen species-induced hepatotoxicity due to hexavalent chromium in vitro and in vivo. Journal of occupational medicine and toxicology 12, 15.
386. Zhu, C., Hu, W., Wu, H., and Hu, X. (2014). No evident dose-response relationship between cellular ROS level and its cytotoxicity–a paradoxical issue in ROS-based cancer therapy. Scientific reports 4, 5029.
387. Zhu, M., and Bowden, G.T. (2004). Molecular Mechanism (s) for UV-B Irradiation-Induced Glutathione Depletion in Cultured Human Keratinocytes¶. Photochemistry and Photobiology 80, 191-196.
388. Ziegler, A., Jonason, A.S., Leffellt, D.J., Simon, J.A., Sharma, H.W., Kimmelman, J., Remington, L., Jacks, T., and Brash, D.E. (1994). Sunburn and p53 in the onset of skin cancer. Nature 372, 773.
389. Zillich, O., Schweiggert-Weisz, U., Eisner, P., and Kerscher, M. (2015). Polyphenols as active ingredients for cosmetic products. International journal of cosmetic science 37, 455-464.
390. Zorov, D.B., Juhaszova, M., and Sollott, S.J. (2014). Mitochondrial Reactive Oxygen Species (ROS) and ROS-Induced ROS Release. Physiological Reviews 94, 909-950.
391. Züge, L., Silva, V., Hamerski, F., Ribani, M., Gimenes, M., and Scheer, A. (2017). Emulsifying properties of sericin obtained from hot water degumming process. Journal of Food Process Engineering 40, e12267.

APPENDIX

APPENDIX

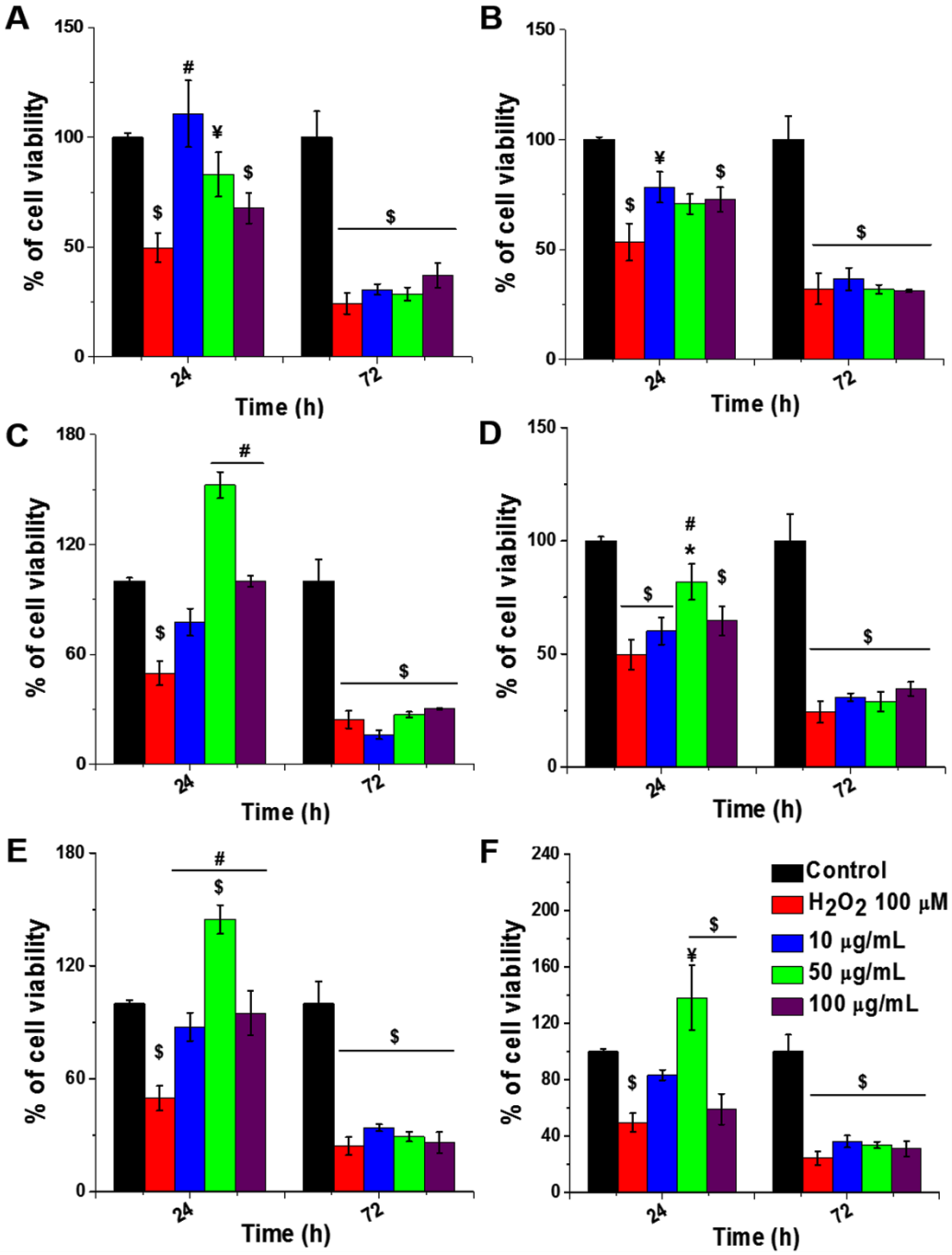

Fig.A2.1. *Protective effect of SS against H_2O_2 induced oxidative damage and promotion of cellular viability on L929 cells by MTT assay. Cells were pretreated with sericin extracts where (A) conventionally extracted BMS, (B) autoclaved BMS, (C) acid-degraded PRS, (D) conventionally extracted AAS (E) Vit. C, and (F) arbutin. ($p≤0.001 and *p≤0.01 in comparison with control; #p≤0.001 and ¥p≤0.01 in comparison with SS untreated cells).*

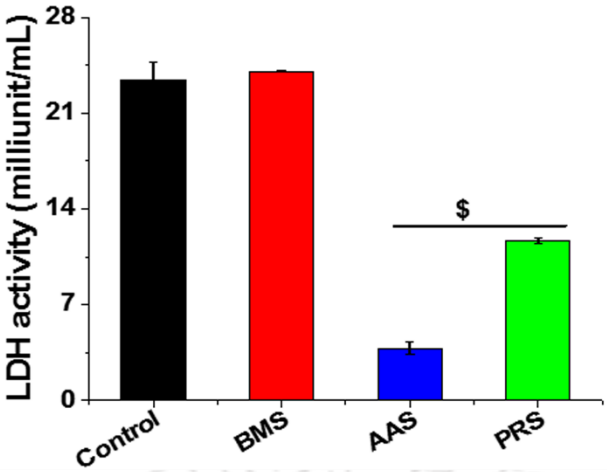

Fig.A3.1. *Cellular membrane integrity of silk sericin treated HaCaT cells was assessed by determining their LDH activity using LDH assay. ($p≤0.001 in comparison with control).*

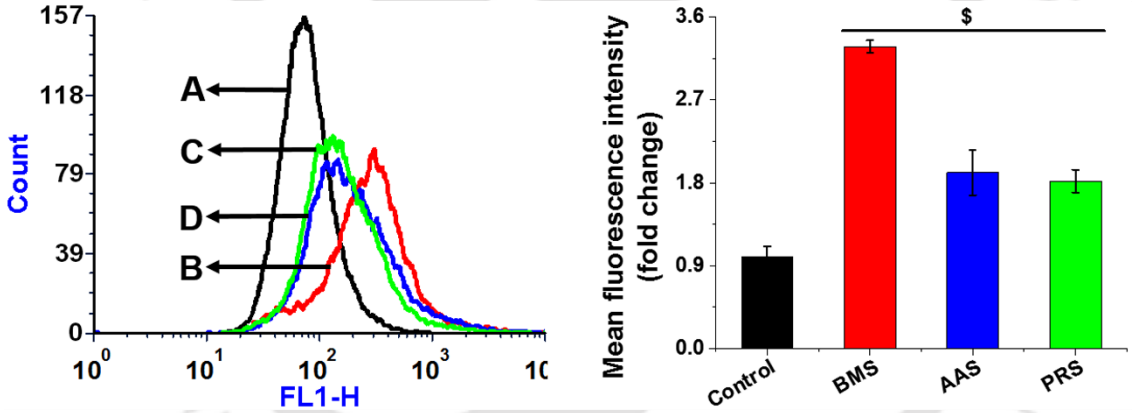

Fig.A3.2. *The effect of silk sericin on the intracellular ROS levels of HaCaT cells was assessed using DCFH-DA; where (A) control, (B) BMS, (C) PRS and (D) AAS treated cells. ($p≤0.001 in comparison with control)*

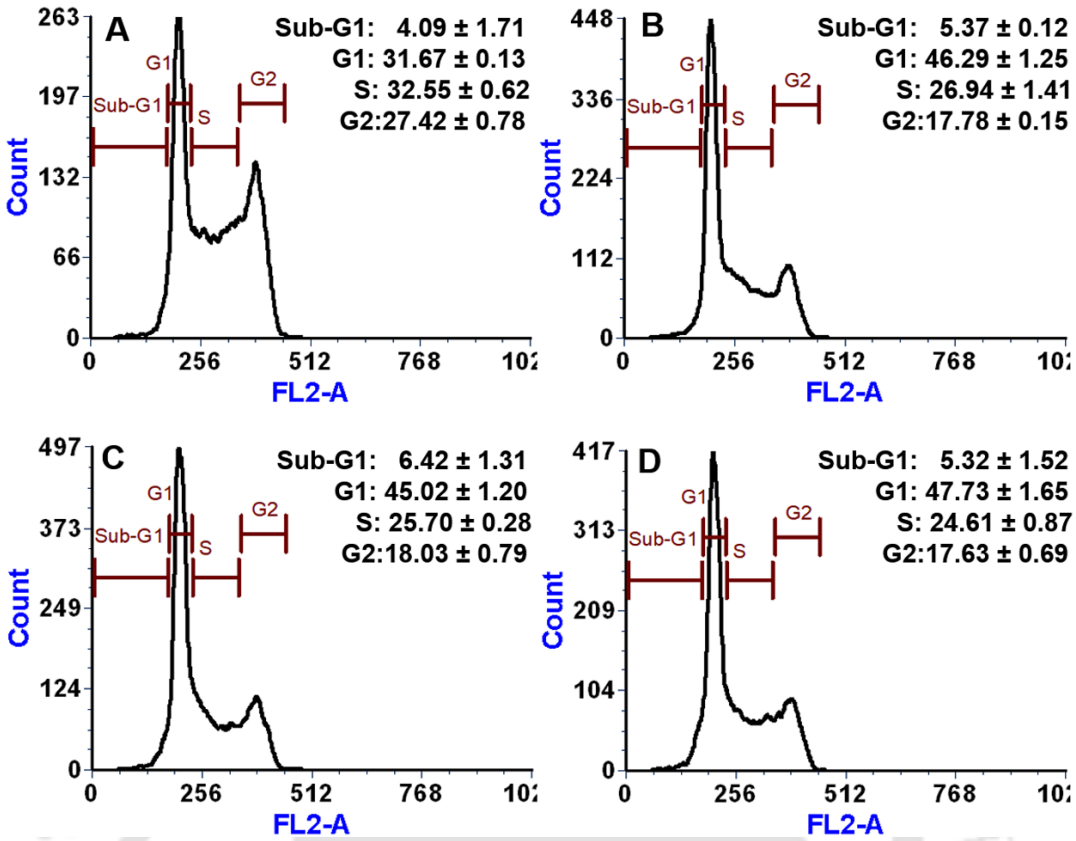

Fig.A3.3. *Cell cycle of silk sericin treated HaCaT cells was assessed using PI: Where (A) control, (B) BMS, (C) PRS and (D) AAS treated cells. Data are expressed as mean ± S.D (n=3).*

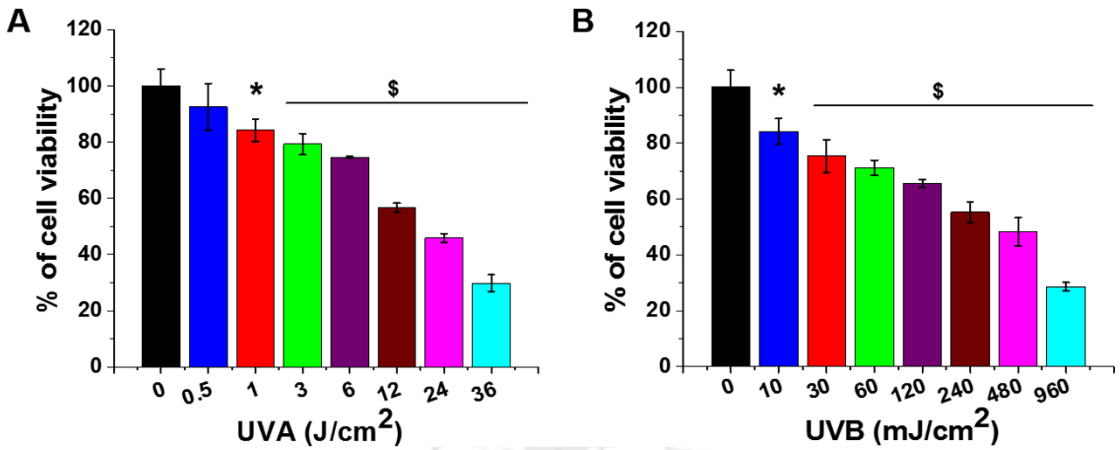

Fig.A4.1. *The effect of (A) UVA and (B) UVB radiations on the viability of HaCaT cells was assessed using the MTT assay. ($p≤0.001 and *p≤0.01 in comparison with control cells)*

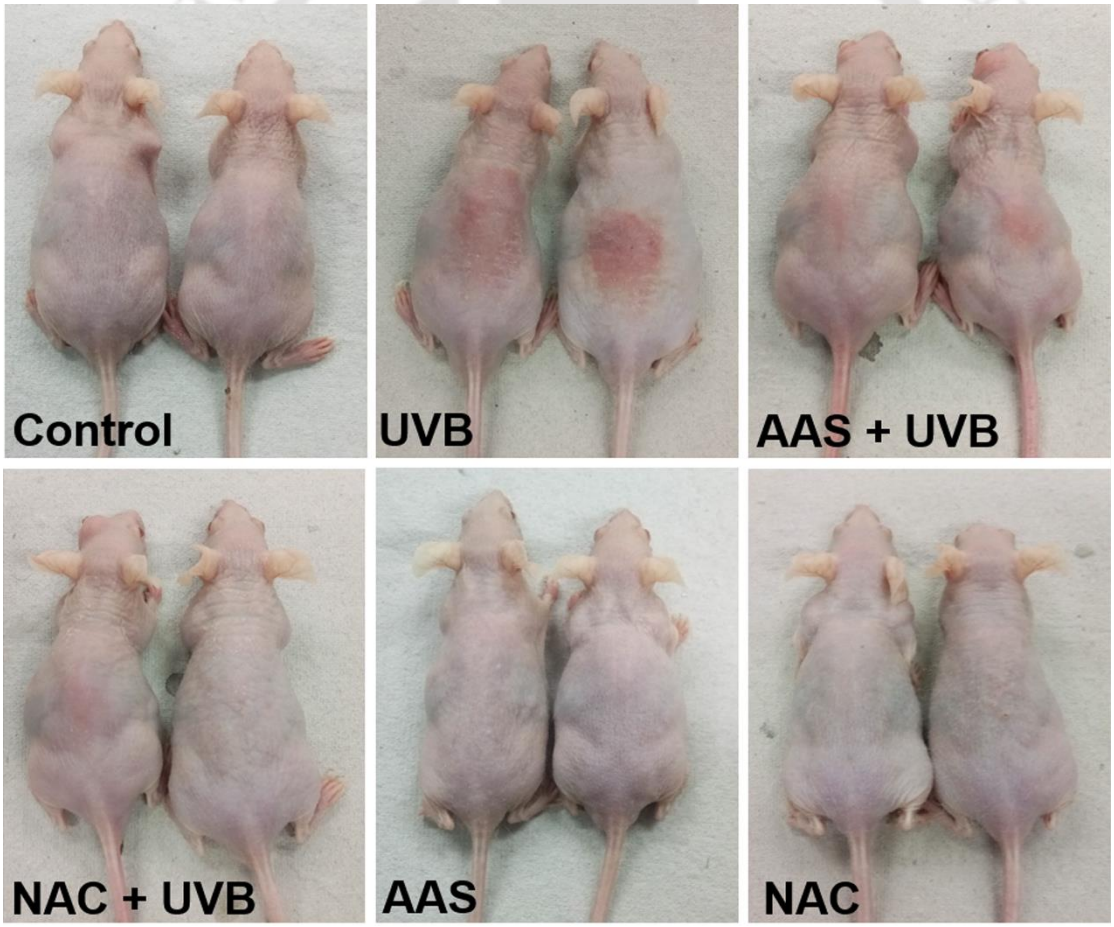

Fig.A4.2. *Pictorial representation of SKH-1 hairless mice that were protected by AAS against UVB-induced edema and sunburn.*

LIST OF PUBLICATIONS

List of Publications

Patents from Ph.D. Thesis:

1. Biman B. Mandal and **Jadi Praveen Kumar**. "Silk Sericin for Skin Care Application and its Process of Preparation". (*Indian Patent application No. 201831026915*)

Journal Publications from Ph.D. Thesis:

1. **Jadi Praveen Kumar** and Biman B. Mandal. "Antioxidant Potential of Mulberry and Non-Mulberry Silk Sericin and its Implications in Biomedicine". *Free Radical Biology & Medicine*, 108 (2017): 803-818. IF 6.020
2. **Jadi Praveen Kumar** and Biman B. Mandal. "Silk Sericin Induced Pro-oxidative Stress Leads to Apoptosis in Human Cancer Cells". *Food and Chemical Toxicology*, 123 (2019): 275-287. IF 3.97
3. **Jadi Praveen Kumar**, Shamshad Alam, Abhishek Kumar Jain, Kausar Mahmood Ansari, and Biman B. Mandal. "Protective Activity of Silk Sericin against UV Radiation-induced Skin Damage by Downregulating Oxidative Stress". *ACS Applied Bio Materials*, 1 (2018): 2120-2132.
4. **Jadi Praveen Kumar** and Biman B. Mandal. "Inhibitory Role of Silk Cocoon Extract on Elastase, Hyaluronidase and UV Radiation-Induced Matrix Metalloproteinases Expression in Human Dermal Fibroblast and Keratinocytes". *Photochemical & Photobiological Sciences*, 18 (2019): 1259-1274. IF 2.90
5. **Jadi Praveen Kumar** and Biman B. Mandal. "Inhibitory Effect of Silk Sericin against Ultraviolet-induced Hyperpigmentation and its Potential use in Cosmeceutics". *Photochemical & Photobiological Sciences* (Revision submitted)

Journal Publications from Other Collaborative Research Projects:

1. **Jadi Praveen Kumar**, Nandana Bhardwaj, and Biman B. Mandal. "Cross-linked Silk Sericin–Gelatin 2D and 3D Matrices for Prospective Tissue Engineering Applications". *RSC Advances*, 6 (2016): 105125-105136. IF 2.936
2. **Jadi Praveen Kumar**, Rocktotpal Konwarh, Manishekhar Kumar, Ankit Gangrade, and Biman B Mandal. "Potential Nanomedicine Applications of

Multifunctional Carbon Nanoparticles Developed Using Green Technology". *ACS Sustainable Chemistry and Engineering*, 6 (2017): 1235-1245. IF 6.140

3. Ashish A Prabhu, **Jadi Praveen Kumar**, Biman B. Mandal, and V. Venkata Dasu. "Process Engineering Strategy for Enhanced Production of Recombinant Human Interferon Gamma (rhIFN-γ) and Exploring the Antitumor Activity for Potential Biomedical Applications". (Under communication). (**# Equal contribution**)
4. Prerak Gupta, Manishekhar Kumar, Nandana Bhardwaj, **Jadi Praveen Kumar**, CS Krishnamurthy, Samit Kumar Nandi, and Biman B. Mandal. "Mimicking Form and Function of Native Small Diameter Vascular Conduits Using Mulberry and Non-Mulberry Patterned Silk Films." *ACS Applied Materials & Interfaces*, 8 (2016): 15874-15888. IF 8.09
5. Ashish A. Prabhu, Anwesha Purkayastha, Bapi Mandal, **Jadi Praveen Kumar**, Biman B. Mandal, and Venkata Dasu Veeranki. "A Novel Reverse Micellar Purification Strategy for Histidine Tagged Human Interferon Gamma (hIFN-γ) Protein from *Pichia pastoris*". *International Journal of Biological Macromolecules* 107 (2018): 2512-2524. IF 3.90
6. Shreya Mehrotra, Dimple Chouhan, Rocktotpal Konwarh, Manishekhar Kumar, **Praveen Kumar Jadi**, and Biman B. Mandal. "Comprehensive Review on Silk at Nanoscale for Regenerative Medicine and Allied Applications". *ACS Biomaterials Science and Engineering*, 5 (2019): 2054-2078. IF 4.43

Book Chapters:

1. Yogendra Pratap Singh, Shreya Mehrotra, **Jadi Praveen Kumar,** Bibhas Kumar Bhunia, Nandana Bhardwaj, and Biman B Mandal. Tissue Engineering Therapies for Ocular Regeneration. *Biomaterials and Nanotechnology for Tissue Engineering* (2016):173

Conference Proceedings:

1. **Jadi Praveen Kumar** and Biman B. Mandal. "Antioxidant Potency of North-East Indian Silkworm Cocoon Based Sericin: Effect of Extraction Protocols". *Advances in Polymer Science & Technology (APST-2015) National Conference, IASST,* Guwahati, India, March 13, 2015. (**Poster**)

2. **Jadi Praveen Kumar** and Biman B. Mandal. "Exploring Anticancer Properties of Silk Sericin Extracted from the Cocoons of North-East Silk Varieties". *International Conference on Perspectives of Cell Signaling and Molecular Medicine*, Bose Institute, Kolkata, India, January 8-10, 2017. (**Poster**)
3. **Jadi Praveen Kumar** and Biman B. Mandal. "Protective Effect of Silk Sericin against UVA and UVB-induced Photo-damage and Photo-aging". *Indo-Japan Bilateral Symposium on Future Perspective of Bioresource Utilization in North-East India*, IIT Guwahati, Guwahati, India, February 1-4, 2018. (**Poster**)
4. **Jadi Praveen Kumar** and Biman B. Mandal. "Oxidative Stress Induced by Silk Sericin Triggers Apoptosis in Human Cancer Cell Lines". *Research conclave*, IIT Guwahati, Guwahati, India, March 8-11, 2018. (**Poster**)
5. Prerak Gupta, Manishekhar Kumar, Nandana Bhardwaj, **Jadi Praveen Kumar**, C. S. Krishnamurthy, Samit K. Nandi, and Biman B. Mandal. Bioengineered Silk Vascular Grafts for Coronary Artery Bypass Surgery. *European cells & materials*, 2016; 31:231. IF 4.00 (**Published abstract**)
6. **Jadi Praveen Kumar**, Rocktotpal Konwarh, Manishekhar Kumar, Ankit Gangrade, and Biman B. Mandal. "Green Technology Derived Carbon Nanoparticles for Anticancer Drug Delivery". *International Conference on Advanced Nanomaterials and Nanotechnology (ICANN)*, IIT Guwahati, Guwahati, India, December 18-21, 2017. (**Poster**)
7. **Jadi Praveen Kumar**, Rocktotpal Konwarh and Biman B. Mandal. Preparation of Novel Carbonaceous Nanoparticle using Yoghurt Drink (Lassi) for Anticancer Drug Delivery Application. *International Conference on Advances in Biological Systems and Materials Science in NanoWorld (ABSMSNW)*. Indian Institute of Technology, Banaras Hindu University, Varanasi. February 19-23, 2017. (**Oral**)
8. **Jadi Praveen Kumar**, Rocktotpal Konwarh, and Biman B. Mandal. Exploring the Intrinsic Fluorescence Properties of Fibroin and Sericin, Extracted from Silk Varieties Endemic to North East India. *Research Conclave*, Indian Institute of Technology Guwahati, Guwahati. March 16-19, 2017. (**Poster**)